Mapping The Microscale Variability of Microphytobenthos

Development Of A Hyperspectral Imaging Method

Arjun Chennu

Doctoral Dissertation

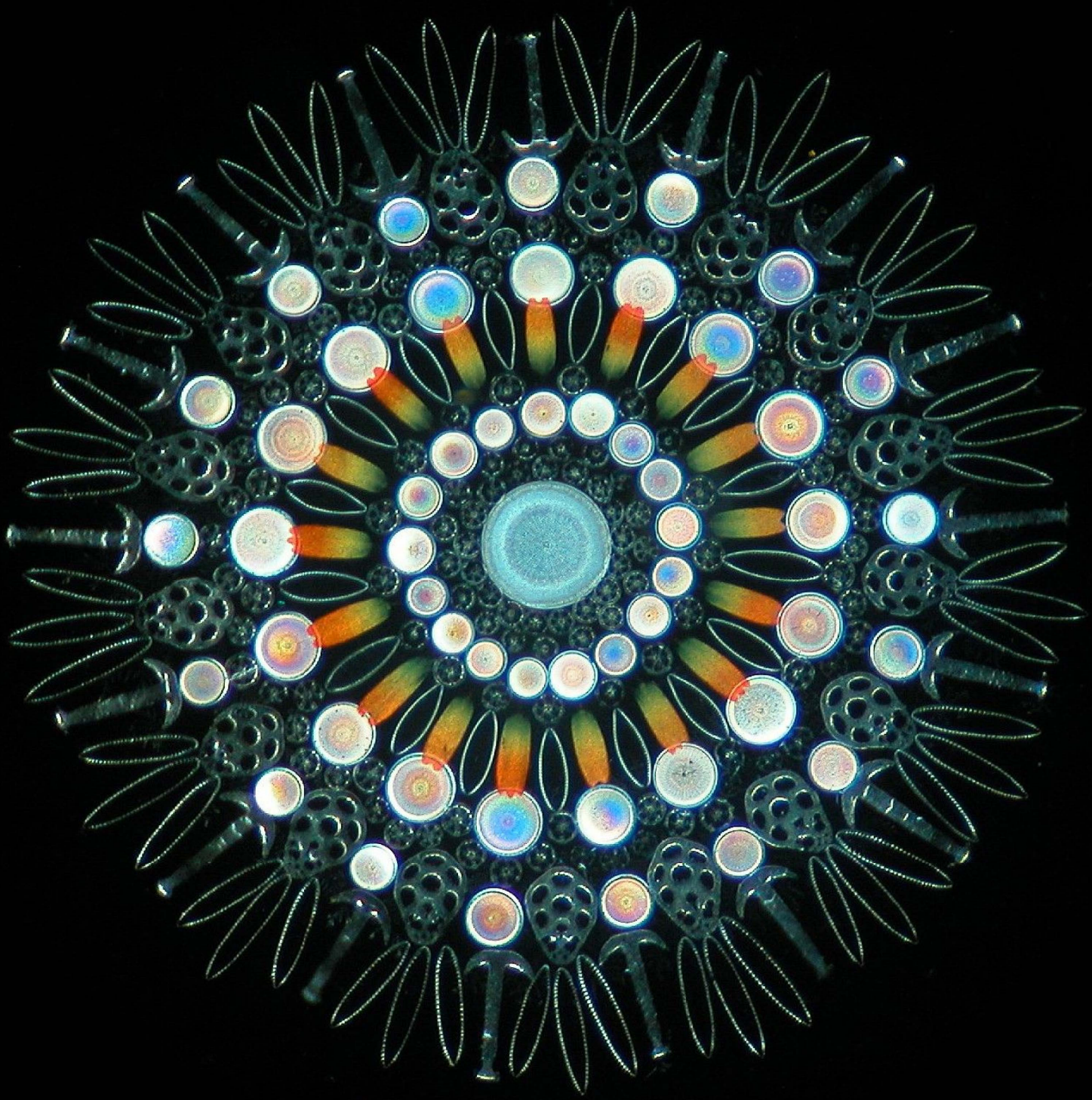

MAPPING THE MICROSCALE VARIABILITY OF MICROPHYTOBENTHOS

DEVELOPMENT OF A HYPERSPECTRAL IMAGING METHOD

DOCTORAL DISSERTATION
BY

ARJUN CHENNU

UNIVERSITY OF BREMEN

DECEMBER 2013

version: Final

Produced on February 27, 2014

Mapping the microscale variability of microphytobenthos: Development of a hyperspectral imaging method

Images for front and back covers were kindly donated by Howard Lynk. Imaged from 19th century microscope slides of arranged diatoms and other microbes.

MAPPING THE MICROSCALE VARIABILITY OF MICROPHYTOBENTHOS

DEVELOPMENT OF A HYPERSPECTRAL IMAGING METHOD

DISSERTATION

ZUR ERLANGUNG DES DOKTORGRADES
DER NATURWISSENSCHAFTEN
— DR.RER.NAT. —

AM FACHBEREICH GEOWISSENSCHAFTEN
DER UNIVERSITÄT BREMEN

VORGELEGT VON

ARJUN CHENNU

BREMEN, DECEMBER 2013

The presented work was conducted from January 2010 to December 2013 at the Max Planck Institute for Marine Microbiology, Bremen as a part of the Marie Curie Initial Training Network "SENSEnet".

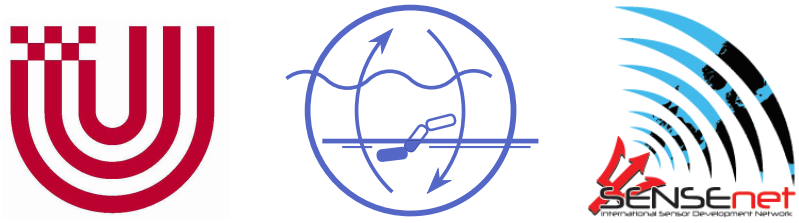

1. Gutachterin: Prof. Dr. Antje Boetius
2. Gutachter: Prof. Dr. Kai-Uwe Hinrichs

Colloquium date: February 17, 2014

DECLARATION

ERKLÄRUNG GEMÄSS §6 ABS. 5 DER PROMOTIONSORDNUNG DER UNIVERSITÄT BREMEN FÜR DIE MATHEMATISCHEN, NATUR- UND INGENIEURWISSENSCHAFTLICHEN FACHBEREICHE.

Hiermit versichere ich, dass ich die vorliegende Arbeit

1. ohne unerlaubte fremde Hilfe angefertigt habe,
2. keine anderen als die von mir im Text angegebenen Quellen und Hilfsmittel benutzt habe, und
3. die den benutzten Werken wörtlich oder inhaltlich entnommen Stellen als solche kenntlich gemacht habe.

Bremen, den 30.12.2013

Arjun Chennu

DEDICATED TO THE KINDNESS OF STRANGERS

AND THE UNSUNG HEROISM OF OPEN SOURCE SOFTWARE

I have had my results for a long time, but I do not yet know how to arrive at them.
— Karl Friederich Gauss

ABSTRACT

Microphytobenthos (MPB) is a grouping of microbial benthic phototrophs that inhabit the sediments of coastal regions with a biogeographic distribution extending to both polar regions. The significance of their photosynthetic productivity and their role as ecosystem engineers was only recently recognized, and has prompted much study into the analysis of their physiology, abundance and function. The spatio-temporal organization of MPB communities is important to record and analyze in order to further our understanding of photosynthetic marine ecology. However, measuring the abundance of MPB in natural habitats poses technical challenges due to the cryptic and delineated nature of the microbenthic environment. This has resulted in poor global coverage of existing datasets, inconsistent measurement protocols, high variability and contradictory results across various studies. However there are clear indications that MPB distributions exhibit profuse spatio-temporal variability on the scale of milli- to centimeters, which corresponds to the spatial span of their proximal habitats. It has been documented that this "microscale" variability in MPB distributions escapes detection by most traditional measurement techniques, and is the likely source of the anomalies between studies. Furthermore, modern understanding of ecology suggests that the analysis of large-scale patterns must integrate the effect of small-scale processes that operate within the region. Such analysis for MPB is largely missing due to the inability of current methods to capture the MPB distributions with high spatial and temporal resolution, which would allow for an understanding of the operant ecological processes of control. This doctoral study identifies a methodological gap in our ability to measure *in situ* MPB distributions at the microscale and attempts to rectify it through the development of a field instrument and measurement protocol that utilize hyperspectral imaging technology. The ecological applications of the novel ability to measure and visualize full-field patterns of MPB distribution with a high temporal resolution are explored in subsequent studies.

Chapter 1 provides a general introduction to the realm of benthic photosynthesis. The significance of MPB to the function and production of marine ecosystems is outlined. Then a brief review of the multifarious ecological factors that are known to affect the spatio-temporal variability of MPB communities is provided. The analysis of this variability is encumbered by current methods of measuring MPB production or abundance, which are reviewed thereafter. The lack of a method and an instrument for measuring the *in situ* microscale distribution and dynamics of MPB is identified, and the motivation of the doctoral study to develop a hyperspectral imaging method is elaborated.

Chapter 2 details the development of an *in situ* hyperspectral imaging instrument that was used to assess the microscale distributions of MPB with high spatial, temporal and spectral resolutions. To establish a quantitative method, the measurement technique was calibrated and validated for a variety of natural sediment types. The sensitivity of the method to the sub-millimeter vertical distribution of MPB in the surficial sediment was demonstrated and a quantitative model derived for the estimation of diel vertical migration of MPB. Applications of the system for *in situ* measurements and compilation of dense spatio-temporal profiles of MPB were demonstrated, with discussion about the implications for interpretation of previous studies.

Chapter 3 presents the study of the ecological interaction in which, by using the hyperspectral imaging method in a variety of natural and artificial settings, it was shown that the hydraulic activity of a marine worm in the sediment depth causes fertilization of MPB at the sediment surface. This established the case for the worm "gardening" a major component of its dietary base and generating profoundly heterogeneous spatial distributions of MPB in sediments inhabited by these worms.

Chapter 4 documents the resurrection of cyanobacteria in desiccated microbial mats upon rehydration. Hyperspectral imaging provided a synoptic view to monitor the different layers of the mat, which indicated rapid resynthesis of Chlorophyll *a* within minutes of rehydration with subsequent migration of cyanobacterial filaments to the sediment surface. Other measurements confirmed the same along with reactivation of photosynthetic activity within minutes. The mechanism and the ecological implications for such an adaptation in desiccation-prone cyanobacteria are discussed.

Chapter 5 presents the abstract of a co-author study of growth rates, using hyperspectral imaging, of subtidal MPB assemblages from temperate and Arctic sites in response to temperature and nutrient treatments.

Chapter 6 discusses the achievements of the doctoral research in terms of the technical achievements of the system developed, the ecological insights gained due to the application of the new method and the limitations of the technique. Additionally, possible future adaptations and avenues of research are outlined.

Appendix A presents the conceptual background to spectral imaging, and explains the characteristics of spectral imaging systems that are relevant for capturing high-resolution data.

ZUSAMMENFASSUNG

Mikrophytobenthos (MPB) ist eine Gruppierung mikrobieller, benthischer phototropher Organismen, welche die Sedimente der Küstenregionen bewohnen und deren biogeographische Ausbreitung sich von Pol zu Pol erstreckt. Die Bedeutung ihrer photosynthetischen Produktivität und ihre Rolle als "Ökosystem-Ingenieure" sind erst kürzlich erkannt worden und regten zahlreiche Studien zur Erforschung ihrer Physiologie, Abundanz und Funktion an. Um unser Verständnis der photosynthetischen marinen Ökologie zu vertiefen, ist es wichtig die räumliche und zeitliche Organisation der MPB Gemeinschaften aufzuzeichnen und zu analysieren. Das Messen der Abundanz von MPB im natürlichen Habitat stellt jedoch auf Grund der kryptischen Natur des mikrobenthischen Lebensraumes eine technische Herausforderung dar. Dies führte zu einer geringen globalen Verteilung bisher erhobener Datensätze, zu uneinheitlichen Messprotokollen, hoher Variabilität und zu widersprüchlichen Ergebnissen zwischen verschiedenen Studien. Es gibt jedoch Hinweise, dass die Verteilung des MPB zahlreiche zeitlich-räumliche Variablität in der Größenordnung von Millimetern bis Zentimetern aufweist, die mit ihren unmittelbaren Habitaten korrelieren. Es wurde gezeigt, dass diese Mikroskala-Variabilität in der MPB Verteilung oftmals von den traditionellen Messtechniken nicht erfasst wird und dass sie vermutlich die Ursache für die Unstimmigkeiten zwischen den verschiedenen Studien ist. Zudem empfiehlt ein modernes Verständnis der Ökologie, dass bei der Analyse von großskaligen Strukturen die Effekte kleinskaliger, regional spezifischer Prozesse zu integrieren sind. Dieser Ansatz fehlt jedoch bislang weitestgehend bei der Untersuchung von MPB, da gegenwärtige Methoden es nicht erlauben die MPB Verteilung mit hoher räumlicher und zeitlicher Auflösung zu erfassen, welche ein Verständnis der wirksamen vorherrschenden ökologischen Prozesse ermöglichen würde. Diese Doktorarbeit deckt die methodische Lücke in der Messung der *in situ* Verteilung von MPB im mikroskaligen Bereich auf und versucht diese Lücke durch die Entwicklung eines Feldinstrumentes sowie eines entsprechenden Messprotokolls, welches sich der Technologie des „Hyperspectral Imaging“ bedient, zu schließen. Die ökologischen Anwendungsbereiche dieser neuartigen Möglichkeit der Messung und Visualisierung von Vollfeldmustern der MPB Verteilung mit hoher zeitlicher Auflösung werden in nachfolgenden Studien untersucht.

KAPITEL 1 gibt eine generelle Einleitung in das Gebiet der benthischen Photosynthese. Die Bedeutung von MPB für die Funktion und Produktion mariner Ökosysteme wird herausgearbeitet. Anschließend wird eine kurze Übersicht der vielseitigen ökologischen Faktoren gegeben, die die zeitliche und räumliche Variabilität von MPB Gemeinschaften beein-

flussen. Des Weiteren wird diskutiert wie die Erfassung der Variabilität durch die gegenwärtigen für die Messung von MPB Produktion und Abundanz zur Verfügung stehenden Methoden beeinflusst wird. Das Fehlen einer Methode und eines Instrumentes für das Messen der mikroskaligen *in situ* Verteilung und Dynamik von MPB wird identifiziert und die Motivation der Doktorarbeit, ein hyperspektrales Messsystem zu entwickeln, herausgearbeitet.

KAPITEL 2 bespricht im Detail die Entwicklung eines *in situ* Hyperspectral Imaging Instrumentes, welches eingesetzt wurde, um die mikroskalige Verteilung von MPB in hoher zeitlicher und räumlicher Auflösung zu erfassen. Der quantitative Aspekt der Methode wurde in einer Reihe natürlicher Sedimenttypen kalibriert und validiert. Die Genauigkeit der Methode unterhalb der Millimeter-Auflösung in der Vertikalverteilung von MPB in Oberflächensedimenten wurde demonstriert und ein quantitatives Model für das Abschätzen der tagesperiodischen vertikalen Migration von MPB abgeleitet. Anwendungen des Systems für *in situ* Messungen und das Zusammentragen zeitlich-räumlicher Profilen von MPB einschließlich einer Diskussion über Anwendungsmöglichkeiten bezüglich der Interpretation vorangegangener Studien werden gezeigt.

KAPITEL 3 präsentiert die Studie zu der ökologischen Interaktion, in welcher mit der Hyperspectral Imaging Methode in unterschiedlichen natürlichen und künstlichen Ansätzen gezeigt wurde, dass die hydraulische Aktivität mariner Würmer in tieferen Sedimenten zu einer Düngung des MPB an der Sedimentoberfläche führt. Diese Studie zeigt den Fall des "gärtnernden Wurmes", der sich den Hauptteil seiner Nahrungsgrundlage selbst gärtnert und dabei eine hochgradig heterogene räumliche Verteilung von MPB im Sediment schafft.

KAPITEL 4 dokumentiert das Regenerieren von Cyanobakterien in ausgetrockneten mikrobiellen Matten nach Rehydratation. Hyperspectral Imaging ermöglicht die Visualisierung der verschiedenen Schichten der Matte, welche eine rasche Regeneration von Chlorophyll *a* innerhalb von Minuten nach Rehydratation sowie eine anschließende Migration der Cyanobakterien-Filamente an die Sedimentoberfläche zeigten. Weitere Messungen bestätigten diese Beobachtung sowie die Reaktivierung der photosynthetischen Aktivität innerhalb von Minuten. Die Mechanismen und die ökologische Relevanz einer solchen Adaptation von Cyanobakterien an Austrocknungsperioden werden diskutiert.

KAPITEL 5 präsentiert die Zusammenfassung einer Ko-Autoren Studie, die mit Hilfe von Hyperspectral Imaging Wachstumsraten in subtidalen MPB Gemeinschaften von einem temperierten und einem arktischen Standort in Reaktion auf Temperatur- und Nährstoffbehandlungen bestimmt hat.

KAPITEL 6 diskutiert die Leistungen der Doktorarbeit im Hinblick auf die technischen Erfolge des entwickelten Systems, die ökologischen Einblicke, die nach der Anwendung der neuen Methode gewonnen wurden, sowie ihre technische Limitierungen. Des Weiteren werden mögliche Anpassungen in der Zukunft und Wege innerhalb der Wissenschaft dargestellt.

ANHANG A präsentiert den konzeptionellen Hintergrund zur spektralen Abbildung und erklärt die Charakteristika von spektralen Abbildungssystemen, welche relevant sind um hochauflösende Daten zu erfassen.

CURRICULUM VITÆ

ARJUN CHENNU

Max Planck Institute
for Marine Microbiology
Celsiusstr. 1, Bremen
28359 Germany

achennu@mpi-bremen.de
arjun.chennu@gmail.com
+49 421 2028 832

EDUCATION

2010–2013	EARLY STAGE RESEARCHER – MARIE CURIE FELLOW
(expected)	Initial Training Network: SENSEnet
	Doctoral candidate at Universität Bremen
	Max Planck Institute for Marine Microbiology, Germany
2006–2008	ERASMUS MUNDUS MASTER OF SCIENCE IN PHOTONICS
	Belgium: Gent Universiteit and Vrije Universiteit Brussels
	Scotland: University of St. Andrews and Heriot-Watt
2002–2006	BACHELOR OF TECHNOLOGY IN ENGINEERING PHYSICS
	Indian Institute of Technology, Madras
2000–2002	ALL INDIA SECONDARY SCHOOL EXAM FOR SCIENCE
	Central Board of Secondary Education, India

COURSES & CERTIFICATIONS

2012	European Scientific Diver
	Italian Association of Scientific Divers, Italy
2012	Marine: Personal survival techniques STCW 95
	Warsash Maritime Academy, Southampton, UK
2011	Scientific writing for natural scientists
	Universität Bremen, Bremen, Germany
2010	Aquatic microbial and molecular ecology
	University of Southern Denmark, Odense, Denmark
2009	NAUI Assistant Instructor and Dive Master
	DiveIndia, Havelock, India

PUBLICATIONS

2013	The gardening lugworm: bioadvection by *Arenicola marina* and its fertilizing effect on the microphytobenthos at the sediment surface. In: *Limnology and Oceanography* (in review)
2013	Hyperspectral imaging of the microscale distribution and dynamics of microphytobenthos in intertidal sediments. In: *Limnology and Oceanography: Methods* 11, pp. 511–528. DOI: 10.4319/lom.2013.11.511
2006	Statistics of single-electron signals in electron-multiplying charge-coupled devices. In: *Electron Devices, IEEE Transactions* 53.4, pp.618–622. DOI: 10.1109/TED.2006.870572

CONFERENCES & WORKSHOPS

Feb 2013	American Society of Limnology & Oceanography New Orleans, USA (oral presentation)
Apr 2012	European Geophysical Union Vienna, Austria (oral presentation)
Sep 2011	Use of in situ sensor technology in marine research Delivered training on hyperspectral imaging Sylt, Germany (SENSEnet field workshop)
Jun 2011	Trophic significance of microbial biofilms on tidal flats La Rochelle, France (oral presentation)
Jul 2010	European Science Open Forum Turin, Italy (poster presentation)

SHIP EXPERIENCE

2012	RRS James Clark Ross, British Antarctic Survey
2010	RV Thomas G. Thompson, NEPTUNEcanada

RESEARCH EXPERIENCE

2012	SUBTIDAL HYPERSPECTRAL IMAGING Observatoire Océanologique de Banyuls-sur-mer, France
2010–2011	MICROSENSOR SETUP ON BENTHIC CRAWLER NEPTUNEcanada, Canada and Jacobs University, Germany
2007–2008	OPTICAL COHERENCE TOMOGRAPHY M.Sc. project, University of St. Andrews, Scotland
2007	OPTICAL NEUROIMAGING Dept. of Neurologie, Charité Hospital, Germany
2005	LOW-LIGHT IMAGING University of Queensland, Australia
2004	QUANTUM THEORY MODELING Technische Universität Chemnitz, Germany

AWARDS & GRANTS

2010–2012	EU Marie Curie fellowship as Early Stage Researcher
2008	'Great distinction' award for M.Sc. performance
2006–2008	EU Erasmus Mundus fellowship for graduate course
2002–2006	Institute scholarship at IIT Madras for undergraduate course
2002	Top score (0.1 percentile) in Mathematics in All India Senior Secondary School Exam

ACKNOWLEDGMENTS

I am grateful for the quality of advice and steadfastness of support I have received during the course of my doctoral work. It is best to dispel the illusion at the outset that this was an individual task, for I have leant upon the shoulders of many experts and friends in preparing this doctoral research thesis.

Foremost, I would like to thank Lubos Polerecky for his guidance as a direct supervisor of my scientific work. I have learnt a great deal from working with him, and my hope is that I have imbibed at least some of his unrelenting scrutiny and guarded skepticism that make him such a good scientist. I am pleased to have had the opportunity to learn from our very instructive (and fun) field expeditions and manuscript discussions. I hope that some of the lessons in precision and brevity I have gathered from him show through in my dissertation.

I would like to thank Dirk de Beer, my group leader, for the generous support I received from him during the course of my research. As often as I laid my varied scientific demands before him, he surprised me with his open-minded and pragmatic guidance for pursuing diverse avenues of interest, whether it be collaborations, technical ambitions, or educational courses. I am thankful for the many helpful discussions, fun diversions and of course, financial support I have had from him.

Of the many wonderful co-workers that make MPI Bremen the professional yet friendly workplace that it is, a special mention of thanks is reserved for the three magicians of the electrical workshop: Paul Färber, Volker Meyer and Harald Osmers. Their cheerful disposition and expert solutions always brought a smile to my face, even as we puzzled over circuits and O-rings. Paul Färber was the reason several of my technical solutions were realistic, rather than idealistic, and worked. I'm thankful for all that I have learned about the design of underwater instrumentation from him and Georg Herz from the mechanical workshop. I also would like to thank Carsten John, Ulrike Tiejten and Heike Wojack for their proficient administrative support throughout the years. Bernd Stickfort, with his quiet efficiency, has been of great help in my literature research.

I am happy to have shared my research time in the "Microsensor club, not group" with some very fine and fun colleagues. Mohammad Al-Najjar sets the bar higher for patient and helpful co-workers everywhere, and I thank him for the enjoyable times we shared — peering at sub-millimeter biofilms, discussing evolution or swabbing up hummus-filled dinners. Duygu Sevilgen and Ines Heisterkamp have the charm to have transformed every project we ever shared into a fun-filled and diversionary memory, whether it be watching mud grow or fishing for krill in

Antarctica or practicing headstands after football. I remember with equal relish many moments of work and leisure shared with Anna Behrendt, Inigo Müller, Martin Glas, Stefan Häusler, Judith Klatt, Felix Janssen, Danny Ionescu and Hannah Brocke. A big thanks to all for creating a friendly and interesting workgroup. Naturally, a special thanks to the laboratory technicians for their steady supply of smiling assistance and microsensor wizardry.

Two collaborators during this project have been particularly special in their impact they have had on my project, knowledge and vision about many aspects of marine ecology. Nils Volkenborn has, with characteristic charm, shown me the joy and expertise of being "a worm guy" and made grueling field work so much more bearable. Katell Guizien cheerfully hosted me for some adventurous attempts at subtidal deployment, and was never flustered at the logistical challenge each day brought. I'm thankful for the kind and friendly hospitality I received from both of them in their scientific as well as personal abodes. I have also received help and useful advice from several professors and scientists around the world: Michael Kühl, Frank Wenzhöfer, Sarah Woodin, David Wethey, Mairi Best and Nadine Le Bris. Particularly, the interest and support shown by Antje Boetius, Kai-Uwe Hinrichs and Hildegard Westphal to evaluate my dissertation.

I feel obliged to express my appreciation for the research and education initiatives by the European Commission, which provided me some wonderful opportunities to pursue my scientific education at excellent universities across Europe. The Erasmus Mundus fellowship (EMMP) provided a great grounding in optical physics, which served well during my doctoral work, and the chance to have interacted with inspiring teachers such as Prof. Roel Baets and Prof. Thomas Krauss. The SENSEnet Initial Training Network, part of the Marie Curie Actions, provided funding and support for my doctoral work and the latitude to refocus my research towards marine ecology.

I have many personal friends and kind strangers to thank who have, in their own ways, shaped my attitude towards my life and work over the last years. In particular some discussions with Niveditha Menon, Vandit Kalia, Drs. Shailaja and Gopalan Parathasarthy from India which helped me in "shopping for a different life". I also thank many Bremen friends for providing the social distraction necessary to lubricate a long research task.

I feel lucky to have a family that has given me great support through the understanding of my mother while her sons are off in faraway lands pursuing their educations and the wise guidance of my brother. Most of all, I am indebted to my charming wife Sabine Tardé Chennu. I cannot express with words how grateful I am for her patient affection and unflinching optimism through the shared, and sometimes long, journey of this research project, our life in Bremen and beyond. She has been and remains the steadying shoulder at the background of it all.

CONTENTS

LIST OF FIGURES

LIST OF TABLES

Part I

INTRODUCTION

1

PHOTOSYNTHESIS IN THE CRYPTIC MICROBENTHOS

The majority of the ecosystems of the Earth's biosphere derive their operational energy from the Sun as the primary source. This occurs through the engagement of a photochemical process known as photosynthesis, which is used by various organisms to transform the light energy of the Sun into chemical bond energy, which is stored, consumed and propagated along the various trophic levels of the ecosystem (Falkowski and Raven, 1996). Photosynthesis is one of the few extant biological mechanisms for the reduction of inorganic carbon for incorporation into organic molecules, and generally occurs in the presence of light and water, and is mediated by specifically adapted biomolecules known as photopigments. The photosynthetic process, especially the common variant involving the release of oxygen molecules, has been fundamental in the co-evolution of the atmosphere and biota of the modern Earth (Bekker et al., 2004; Knoll, 2003), and continues to be the primal source of energy for the carbon-based biological economy of the Earth (Field et al., 1998).

Photosynthetic production, or primary production, has a direct and significant effect on the geological carbon cycle of the Earth. Net primary production of an ecosystem is generally defined as the amount of photosynthetically fixed carbon that is available to the first heterotrophic level (Lindeman, 1942) and an estimated 104.9 petagrams of carbon are photosynthetically fixed annually in both marine and terrestrial domains across the globe (Field et al., 1998). This has many significant geochemical and meteorological consequences, the most topical being the removal of enormous amounts of carbon dioxide, an important greenhouse gas, from the atmosphere which is considered a key regulator of global climate change. As can be inferred from the global distribution map in Figure 1.1, photosynthetic organisms, also known as *phototrophs*, thrive in nearly all latitudes of the Earth and consist of all terrestrial plants (such as trees, grass, ferns, etc.), aquatic plants (such as sea-grass, kelp, etc.) as well as numerous species of algae, microalgae and bacteria. Due to the abundance of excellent literature (Falkowski and Raven (1996) and references therein) on the various biological, chemical and paleological aspects of photosynthesis, they will not be elaborated up on in this thesis. The focus from hereon will be photosynthesis in the benthic domain.

1.1 THE FERTILE MICROBENTHIC GARDEN

The bottom of lakes, seas or oceans, called *benthos* (meaning "depths of the sea" in Greek), represent a major ecosystem space of the biosphere

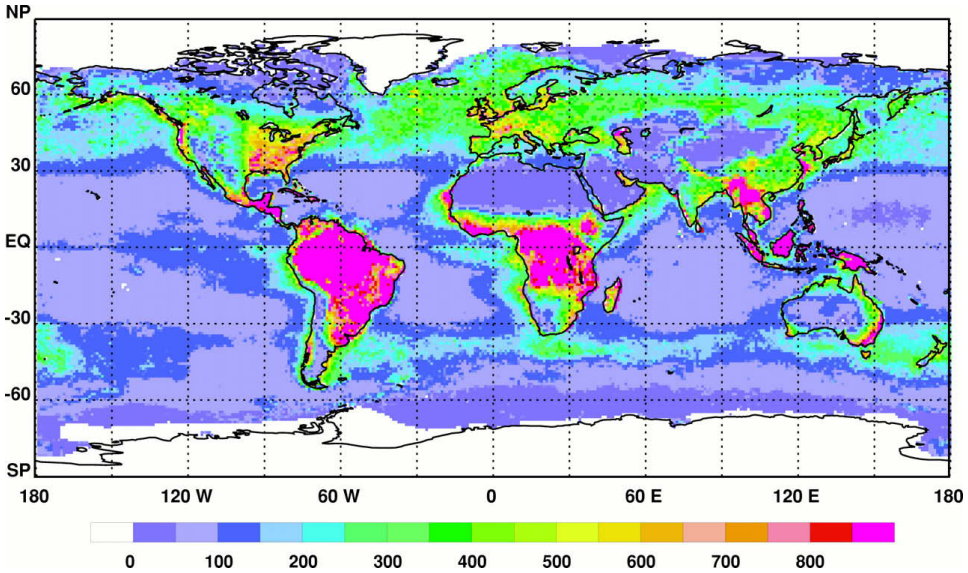

Figure 1.1: Global distribution of net primary production estimated from satellite data averaged over 1978–1983 (oceanic) and 1982–1990 (terrestrial). The total global production is 104.9×10^{15}g of C year^{-1}, comprising of 46.2% of marine and 53.8% of terrestrial contributions. Adapted from Field et al. (1998).

on Earth, since benthic habitats occur in a great variety of settings, from high-altitude lakes to the estuaries and tidal flats of coastal regions to the sea-mounts and hydrothermal vents of the deep sea floor. Forming the interface between the overlying water column and the bottom sediment, benthic ecosystems are zones of intricate interaction of various physical, chemical, biological and geological agents that operate over scales ranging from the micro-environments of the interstitial porespaces to the wide-scale interchange regions of coastal or deep-sea terrain (Boudreau and Jørgensen, 2001; McCave, 1976). Accordingly, the structure and function of benthic ecosystems emerge from a tight interplay between the physics of the sediment-water environment, the geochemical exchange with the water column, and the biology of the numerous species of microorganisms and macrofauna that inhabit the substratum (Jones et al., 1994; Levinton, 1995). In this setting, microbes are the biological agents that form a vital link between the worlds of organic and inorganic chemistry, and the micro-environments they thrive in are often zones of carefully balanced availabilities and demands. Understanding the function of benthic ecosystems requires careful unraveling of the complex and nested relationships, at the *operant spatial and temporal scales*, between its inhabitants and the environment. This perspective serves as an effective intellectual scalpel to examine the phenomenon of benthic photosynthesis.

Hereon, "photosynthesis" generally refers to oxygenic photosynthesis.

Photosynthesis in the benthic domain has the same primary requirements: sufficient light, water and nutrients, and therefore faces the same paradigm of operation as in the aquatic or terrestrial domains, but with a distinctively different set of limitations. Terrestrial phototrophs generally have more than necessary light irradiation from the Sun, necessitating

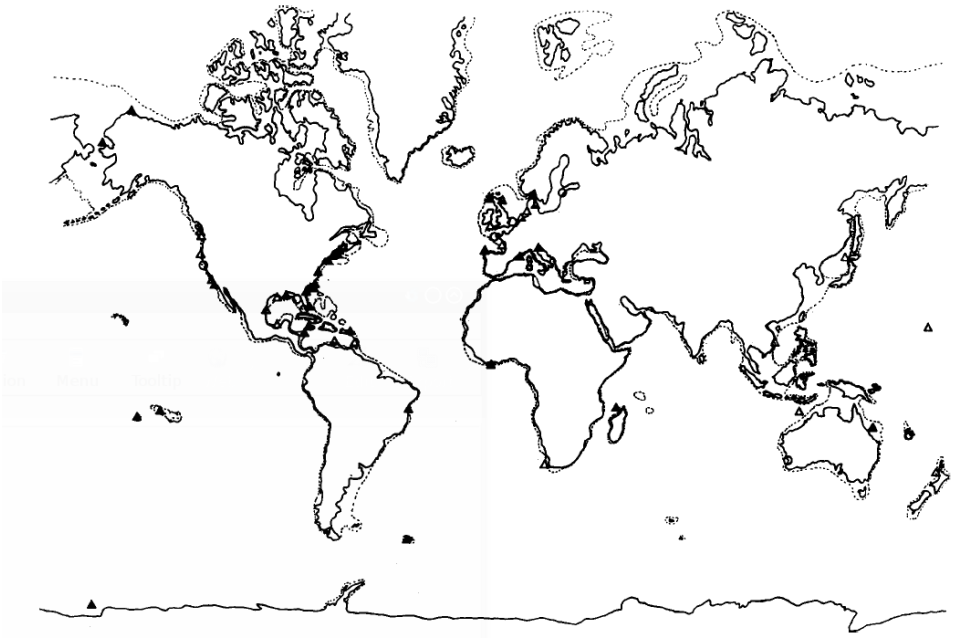

Figure 1.2: Map from Cahoon (1999) showing the locations of studies which measured microphytobenthic production (empty triangles), biomass (empty circles) or both (filled triangles). The neritic zone is (dashed line for 200m isobath) grossly undersampled. Overall less than 100 *in situ* measurements of MPB abundance were available in 2006, of which 4 were in the large, shallow Arctic seas and overall only 10 were at water depth >5m (Glud, 2006).

the development of elaborate photo-protective apparatus, but are essentially limited by the availability of water for nutrient transport to carry out primary production. Aquatic phototrophs, such as phytoplankton, which live in the photic zone of the water column, have sufficient light and water for photosynthesis but are generally limited by the availability of nutrients (Hecky and Kilham, 1988). Benthic phototrophs live at the sediment-water interface, which is a region at the nexus of benthic nutrient supply (from remineralization), the overlying water column and sufficient albeit attenuated light intensity, which is the primary limitation for performing photosynthesis (Cahoon, 1999). Therefore, many ecological aspects of benthic phototrophs derive from the dynamics of the light climate, transport properties, sediment stability and geochemistry that are particular to the benthic boundary layer (Boudreau and Jørgensen, 2001).

Nevertheless, coastal and continental shelf ecosystems are disproportionately fertile in terms of primary production: with just over 7% of the total ocean area, their waters are estimated to contribute 20% of the total annual oceanic production (Figure 1.1; Longhurst et al., 1995). This estimate does not include the contribution of benthic microbial photosynthesis which has been conservatively estimated, despite the paucity of global field datasets (Figure 1.2), to add 2–4 % (0.5 Pg C yr^{-1}) to the primary production of the oceans (Cahoon, 1999). Additionally, a considerable portion of the pelagic primary production in coastal areas could be ascribed

to benthic phototrophs that, due to resuspension, spend extended periods of time in the water-column (Guarini and Blanchard, 1998), with possible effects extending down to continental shelf sediments (Cahoon et al., 1994). The global significance of benthic primary production is reviewed in detail by Cahoon (1999). To motivate the focus of this doctoral dissertation, some significant ecological of benthic primary production are discussed below.

Microphytobenthos generally refers to the biotic phototrophic component of the microbenthos, which is defined here as the narrow region close to the sediment-water interface, approximately the photic zone of the benthos.

In contrast to the terrestrial domain, the majority of benthic and aquatic primary production is performed by microorganisms. Microphytobenthos (MPB) is an artificial grouping, consisting of diatoms, cyanobacteria, dinoflagellates, chlorophytes, euglenoids and other groups of photosynthetic microorganisms that live in the very top layers of the benthos (MacIntyre et al., 1996). Also known as benthic microalgae, it has historically been an understudied component of marine phototrophy but the importance of its contribution as a "secret garden" to the primary production and ecology of marine ecosystems is being increasingly recognized (Cahoon, 1999; MacIntyre et al., 1996; Miller et al., 1996). This is particularly so in shallow-water systems, such as estuaries, tidal flats or lagoons, where the biomass and production of MPB frequently equal or exceed that of the (relatively well-documented) water-column (Barranguet et al., 1998; Cahoon et al., 1999; Underwood and Kromkamp, 1999).

Microphytobenthic communities (MPBC) are found, with varying taxonomic compositions, in nearly the entire biogeographic range of the planet and across a wide variety of environments. The primary habitats for MPBC are in coastal and neritic (<200 m water depth) ecosystems, such as in intertidal and subtidal mud/sand flats and waters, rocky shores, estuaries, lagoons, coral reefs and sea-grass beds (Cahoon, 1999; MacIntyre et al., 1996). MPBC are also found in several land-based ecosystems such as in lakes (alpine, hypersaline, grassland), salt flats, thermal springs and cryptobiotic desert crusts (Eldridge and Greene, 1994). Their latitudinal range includes both polar regions, with occurrences of MPBC reported in sea-ice algae, cryoconite structures in glaciers, in Antarctic lakes as well as in the Arctic cold deserts. In several of the above environments, the MPBC form laminated microbial communities known as microbial mats, which are self-sufficient ecosystems with purely microbial biota, that are thought be the oldest preserved habitats of Earth (Walter et al., 1980). Furthermore, the deep-sea floor has generally been considered to be bereft of photosynthetic organisms (due to the absence of sufficient light), but recent reports indicated detection of photoactivty (Beatty et al., 2005) and recovery of active photosynthetic biomass (Boetius et al., 2013) from the deep-sea floor.

1.2 VARIABILITY OF MICROPHYTOBENTHIC COMMUNITIES

The spatio-temporal organization of communities is a prominent factor in the function of ecosystems (Levin, 1992). Despite the great variety of

habitats in which MPBC thrive, it is possible to note some common features between these habitats that are characteristic of benthic ecosystems. Being at the interface of two media of very different permeabilities, both in terms of hydrodynamics and light conditions, benthic ecosystems generally feature strong vertical gradients that are also temporally dynamic. These physico-chemical gradients often operate at the spatial scale of the organisms and generate microbial and chemical zonations at millimeter and sub-millimeter scales, as in the well-documented case of microbial mats (Franks and Stolz, 2009) or cohesive mudflats (Yallop et al., 1994). The microbes in the microbenthos respond in various ways to these delineated gradients and, in turn, affect the nature of the benthic substrate and exhibit profuse spatio-temporal variability of biomass and production on all measured scales (Chapman et al., 2010; Guarini and Blanchard, 1998; Seuront and Leterme, 2006). Therefore, it is important to understand the interplay between MPBC and the microbenthic environment in order to develop an overview of the complex and nested set of ecological interactions that generate the profuse microscale variability of MPBC distributions. Some important sources of this spatio-temporal variability are briefly reviewed below to highlight the variety of them, and the degree of uncertainty induced in interpretations of MPBC distributions.

Although technically a misnomer, "microscale" has been used frequently to refer to the fine spatial scale that characterizes microbial habitats, despite the fact that the emergent patterns can span millimeters or centimeters.

1.2.1 *Taxis and migration*

A primary example of an evolved adaptation of various MPBC to the steep gradients of the microbenthic environment is the ability to vertically migrate within the sediment (MacIntyre et al., 1996), in a variety of habitats such as desert crusts, tidal flats and hypersaline microbial mats. Even though such migratory response in MPBC is considered to be endogenous in some habitats such as tidal flats, it can be regarded as a general form of motility by taxis. The diel light and tidal cycles are the primary drivers of a vertical migration rhythm in tidal-flat and estuarine diatoms (Palmer and Round, 1967; Paterson, 1986; Round, 1979). Diel migratory rhythms can also be observed in hypersaline mats, and although the light cycle has precedence in both cases, the migratory patterns cannot be explained as a pure light-based response (Garcia-Pichel et al., 1994; Mitbavkar and Anil, 2004). The migratory rhythm that coincides with tidal emersion is likely an avoidance behavior against re-suspension due to an incoming tide (Heckman, 1985) or grazing pressure (Montagna, 1984), whereas the coincidence with diel light cycle serves to optimize the position of the MPBC within the narrow (0.1–3 mm) photic zone of benthic substrates and thereby maximize photosynthetic potential (Al-Najjar et al., 2012). The specifics of the migratory rhythm seem to be site and taxon dependent, with no universally valid set of cues that trigger taxis in estuarine diatoms (Consalvey et al., 2004).

Taxis, which is Greek for "arrangement", is formally defined as an innate behavioral migratory response of an organism to a directional stimulus.

Several forms of taxis as avoidance behavior have been observed in MPBC, particularly cyanobacteria (Stal, 1995). Cyanobacteria inhabiting

hot springs, freshwater or shallow marine habitats migrate deeper into the sediment on exposure to high ultraviolet radiation, as well as develop sunscreen or protective sheath pigments such as scytonemin (Bebout and Garcia-Pichel, 1995; Castenholz and Garcia-Pichel, 2002). Cyanobacteria have also been demonstrated to respond to salinity gradients (Kohls et al., 2010) in hypersaline environments, and desiccation in hydrated desert crusts (Pringault and Garcia-Pichel, 2004). Therefore, the adaptation to motility in MPBC is a manifestation of the drive to optimize their survival function or photosynthetic production in a highly dynamic and delineated microbenthic environment. This is a prime source of the microscale temporal and spatial variability of MBPC distributions, and is addressed in some detail in Chapters 2, 3 and 4.

1.2.2 *Seasonality*

The effect of the seasonal variations in the physico-chemical properties of benthic ecosystems due to the changes in solar irradiance, temperature and meteorological forces, on MPBC distributions has been studied mostly in temperate seas (Asmus, 1982; Underwood and Paterson, 1993), with few reports in polar (Gilbert, 1991; Glud et al., 2002; Howard-Williams et al., 1989) or tropical (Mitbavkar and Anil, 2002; Underwood, 2002) ecosystems. MPBC abundance and distributions in the field are known to be influenced by a multitude of seasonally-modulated drivers: resurgence of resuspension feeders (Coma et al., 2002), nitrogen fixation (Pinckney et al., 1995), temperature (Spilmont et al., 2006), carbon remineralization rates (Therkildsen and Lomstein, 1993), bentho-pelagic coupling (Ubertini et al., 2012; Xinling et al., 2006), etc. Despite some general trends, there is contradictory proof regarding the direct seasonal control of MPB abundance, with some studies identifying higher biomass in the summer (De Jonge and Beusekom, 1995; Underwood and Kromkamp, 1999), while others reporting the opposite (Brito et al., 2013; Koh et al., 2007) or no seasonal patterns (Brotas et al., 1995; Underwood, 1994). The spatio-temporal variability in MPB abundance due to seasonal variations must be studied at the scale of the ecosystem, while integrating the small-scale variability that has been shown to account for a significant portion of the measured variability (Brito et al., 2009a; MacIntyre et al., 1996).

1.2.3 *Light climate*

Despite the great variety of habitats in which MPBC thrive, their abundance and activity corresponds closely to the availability of photosynthetically active radiation. The light flux transmitted down to the benthos is a function of the incident flux, clarity, depth and absorption characteristics of the water-column (Jerlov, 1976; Kirk, 1994). The basic pattern of variation in the incident flux is the diel rhythm of the solar cycle,

and a significant seasonal variation, particularly in polar regions. Some other factors that influence the optical properties of the water are: tidal or runoff load and frequency (Wetsteyn and Kromkamp, 1994), particulate size, suspended concentrations of chromophoric dissolved organic matter (Green and Blough, 1994) or other pigmented communities (De Jonge and Beusekom, 1995). Furthermore, the sediment substrate itself imposes, due to intense scattering and absorption, a very steep spatial gradient in the light intensity (Kühl and Jørgensen, 1994; Kühl et al., 1994; Lassen et al., 1992). The optical scattering properties of the sediment are closely related to the sediment grain-size, and this strongly affects the extent of light penetration (0.2–5 mm) into different sediment types. The cumulative effect of these diverse variations renders the benthic light climate highly variable, down to near-zero levels of available light within a few hundred microns of the surface, which implies that MPBC in the neritic zone must be able to adapt to a very wide range of available light fluxes (Kromkamp et al., 1995; Nozais et al., 2001). Indeed this is evidenced in the wide variety of photosynthesis-vs-irradiance curves observed in various MPBC measurements (Blanchard and Montagna, 1992; MacIntyre et al., 1997; Al-Najjar et al., 2012; Pinckney and Zingmark, 1991; Preez et al., 1990; Underwood, 2002). The theoretical minimum light intensity required to sustain photosynthetic growth is estimated to be 0.1% of the incident flux (Falkowski, 1988), and in several cases, photosynthetic activity in MPBC has been detected close to or at this physiological limit (Kromkamp and Peene, 1995; Palmisano et al., 1985; Vopel and Hawes, 2006). Apart from the available light intensity, the spectral quality of the light is also of significance due to the very specific absorption characteristics of the photopigments. In clear waters with long optical paths, the spectral attenuation due to the water column can significantly deplete the intensity of longer (red and infrared) wavelengths, which could lead to chromatic adaptation or taxonomic shifts, but more study is needed to confirm this phenomenon for MPBC (Dring and Lüning, 1983; Falkowski and LaRoche, 1991).

1.2.4 *Sediment substrate and stability*

In many studies of coastal MPBC distributions, the large-scale spatial variability has been found to be closely linked to the properties of the sediment substrate (Cahoon et al., 1999; Davis and McIntire, 1983; Krejci and Lowe, 1986), with similar species of diatoms found in both intertidal and subtidal areas. The macroscopic properties of the sediment substrate, such as porosity, permeability, tortuosity, photic depth, cohesiveness etc. derive from both abiotic (grain-sizes, organic matter, etc.) and biotic (biofilm formation, burrows, etc.) features of the benthos (Paterson, 1994). Round (1971) considered the sediment structure as a primary basis for classifying diatoms: epilithic (on rock substrata), epipelic (on mud), epipsammic (on sand), endopelic (inside sediment) and endolithic (inside rock) to list a few. Due to these associations, MPBC distributions correlate with the spa-

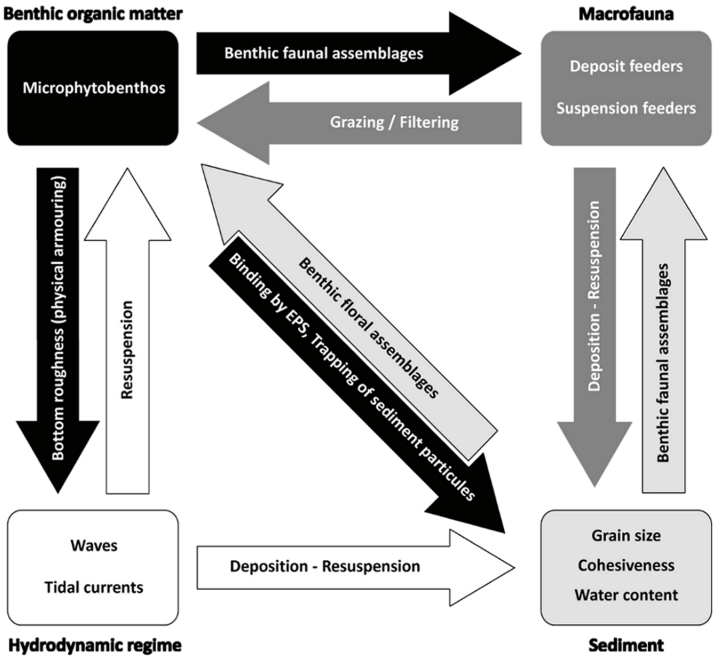

Figure 1.3: A schematic indicating the interplay of the factors involved in sediment stabilization and resuspension of microphytobenthos. Adapted from Ubertini et al. (2012).

tial variability in the sediment structure on ecosystem scales, with muddy sediments generally colonized by diatoms, and sandy sediments hosting a greater diversity of taxa such as cyanobacteria and euglenids (Jesus et al., 2009; Underwood and Barnett, 2006).

The erodibility (or cohesiveness) of the sediment bed is a critical factor for MPB ecosystems since the sediment bed provides the major shelter space for resident MPBC, and non-cohesive sediments represent higher mortality to MPBC due to cell damage by sediment abrasion (Delgado et al., 1991). MPBC in erodible sediments naturally face higher temporal variability based on the frequency of resuspension into the water-column due to tidal, wind or wave action. Due to the dense concentrations of MPB cells at the sediment surface, the erosion of even the top few millimeters of the sediment can result in the majority or all of the water-column phototrophs to be from MPBC (Brito et al., 2010; De Jonge and Beusekom, 1995; Underwood and Paterson, 1993). Some MPB taxa prefer a "tychopelagic" lifestyle that alternates between planktonic and benthic modes (Cahoon et al., 1994). Such adaptations blur the previously-held distinctions between the benthos and the water-column, and establishes the need to consider resuspension as a basic source of variability and function of estuarine ecosystems (Cahoon, 1999; MacIntyre et al., 1996).

As indicated in Figure 1.3, MPBC themselves greatly increase the cohesiveness of the sediment, aided by the secretion of an organic matrix of polymeric substances (Paterson, 1994; Stal, 2010), which is considered to be an adaptation against resuspension. Modification of the cohesiveness

of the sediment by MPBC increases the habitability and productivity of sandy sediments (Boudreau et al., 2001) and furthermore has profound effects on various aspects of the ecosystem, such as boundary-layer nutrient fluxes (Cabrita and Brotas, 2000), macrofaunal assemblages (Huang and Boney, 1984) and trophic stability (Kang et al., 2006). Through the formation of stabilizing biofilms (Stal, 2010), MPBC are considered ecosystem engineers with "keystone species" implications for conservation strategies (Boogert et al., 2006; Daborn et al., 1993). Therefore, the general parameters of bentho-pelagic coupling and sediment bed properties are important factors in the spatio-temporal variability of MPBC distributions (Brito et al., 2010; Ubertini et al., 2012).

1.2.5 *Nutrient fluxes*

The high concentration of MPB cells at the sediment surface invokes a need for transport of a large amount of nutrients to the sediment-water interface. The stabilization of sediment (see Sediment substrate and stability) improves the access of MPB to nutrients in two ways: low but steady nutrient uptake from the steady advection of overlying water (Adey, 1987), and through changes in the thickness of the diffusive boundary-layer to improve nutrient uptake (Rodgers and Harvey, 1976). Additionally, a large store of organic matter usually lies deeper within the sediment, which is remineralized into porewater solutes and emerges at the surface either through diffusive or advective transport, driven by waves (Precht et al., 2004; Precht and Huettel, 2003) or macrofaunal activity (Volkenborn et al., 2010; Wethey et al., 2008). The uptake of nutrients by MPB is regulated by the diel light cycle and seasonality (Bertuzzi and Bruckler, 1996; Reay et al., 1995), and can be large enough to create limiting conditions for phytoplankton (Armitage and Fong, 2004). Overall, the presence and activity of MPBC modify the nutrient fluxes at the sediment-water interface and in the water column at both local and regional scales (Cabrita and Brotas, 2000).

Complimentarily, changes in the nutrient economy of an ecosystem, such as eutrophication, or river run-off or glacier melt, in turn affects the health and abundance of MPBC. Gradients in salinity, silt particulate matter or nutrient concentrations, as is the norm in estuaries, are drivers of variability in the abundance and the community composition of MPB (Grinham et al., 2011; Underwood et al., 1998). Although MPBC respond to increased nutrient loading or eutrophication, there is generally a lag due to the buffering effect of a nutrient-rich sediment (Jonge et al., 1996). Diatoms also possess the ability to alter their metabolism to be able to survive persistent unfavorable conditions, such as the respiration of nitrate to survive anoxia (Kamp et al., 2011), which ties in to their involvement in the nitrogen cycling of estuaries (Rysgaard et al., 1995). There is also evidence that environmental shifts in the nutrient supply lead to significant changes in the species composition and spatial structure of MPB biofilms

due to the dynamics of nutrient uptake and resource competition (Larson and Passy, 2012). A specific example of MPBC response to macrofauna-driven nutrient flux is documented in Chapter 3.

1.2.6 *Trophic and competitive interactions*

Grazing and resource pressure by higher trophic levels is recognized to be a significant factor in the spatio-temporal variability of distributions of MPBC species, even over geological time scales (Garrett, 1970). A variety of micro-, meio- and macro-fauna, such as ciliates, forminifera, copepods and polychaete worms graze on MPBC directly, while macroalgal mats compete with MPBC for light and nutrients (Sundbäck and McGlathery, 2013). Due to the large difference between the growth rates of grazers and MPB cells, there has been some interest in studying the small-scale spatio-temporal correlations between the population dynamics of both (Azovsky et al., 2004; Buffan-Dubau and Carman, 2000; Pinckney and Sandulli, 1990). The general result has been that, despite the existence of a strong grazing relationship, the spatial correlations between microalgal and meiofaunal abundances seem to be weak and confounded by a variety of factors. MPBC are also associated with other trophic interactions, such as stimulated growth rates due to feeding (Skov et al., 2010), selective grazing of taxa (Azovsky et al., 2005), deterrence of habitat recruitment (Wennhage and Pihl, 1994), seasonal and depth dependence of grazing (Sundbäck et al., 1996). Therefore, the trophic supply of MPB extends beyond the usually assumed "small food web" and includes benthic macrofaunal species, which further underscores the importance of MPBC as a fundament of the marine food web. The variety of grazing pressures and non-competitive resource pressures must be considered as one of the sources of microscale variability of MPBC distributions.

1.3 MEASURING MICROPHYTOBENTHOS

Given the multiple scales of spatial and temporal variability of MPBC, empirical measurements of their abundance, distribution, physiological status or dynamics must be designed to capture the important interactions that are relevant for developing accurate models of MPB ecology (Blanchard et al., 2001; Guarini and Blanchard, 1998; Guarini et al., 2000), so that they may be integrated into existing models of aquatic phototrophy. The most common techniques for measuring MPBC production and distribution are introduced here.

1.3.1 *Primary production estimation*

The effects of MPBC on the biogeochemistry of ecosystems has generally been assessed by measuring the primary production of the communities. Although there is no standardized procedure for quantifying MPB production, most studies have either measured the flux of dissolved oxygen or the uptake of isotopic (^{14}C) substrate, as these are rather direct indications of the process of oxygenic photosynthesis (Cahoon, 1999). Primary production estimation from the measurement of oxygen flux is carried out by using some variation of the light-dark method, where flux in the dark is added to that in the light to sum up the contributions of respiration and photosynthesis. The oxygen measurements are usually performed using incubation chambers or micro-electrodes. The chamber-based methods have generally suffered from under-replication, and in combination with limited resolution tend to underestimate MPB production (Fenchel and Glud, 2000). On the other hand, micro-electrodes have enabled very fine-scaled profiling of the oxygen fluxes around the sediment-water interface and revolutionized our view of the microbial world since their introduction in the 1970s (Revsbech and Jørgensen, 1986; Revsbech et al., 1983), but estimation of areal rates have proved difficult due to the extremely limited horizontal resolution (Glud, 2006). Planar optodes are a recent development (Glud et al., 2002; Polerecky et al., 2005) that provide sufficiently high spatial and temporal resolutions, but generally require invasive treatment of the sediment, which is likely problematic for *in situ* use (but see the adaptation by Kühl et al. (2001)). While the isotope uptake method has provided greater sensitivity and the possibility to measure without an overlying water-column, it needs the uniform introduction of labeled medium across the entire sediment-water interface and provides no distinction between gross and net photosynthetic production (Cahoon, 1999). These methodological limitations have posed significant difficulties in extending field studies to larger ecosystem-scale measurements.

1.3.2 *Biomass estimation*

Considering the limitations of measuring primary production (see above), there has been a general shift towards quantifying MPB biomass instead of production, since the relationship between photosynthetic biomass and production is reliably linear. There has been interest in the identification and quantification of MPB cells in sediment since the 18th century, when taxonomic investigations were initially conducted using microscopes. The direct method of counting cells, still applicable to optical microscopy today, is very laborious due to the great density of cells in MPBC, further confounded by the diversity of other particles, in the sediment. As already noted by Haeckel (1890), the application of direct microscopy, although very useful for identification, cannot be completed without "ruin of body and mind" for estimating biomass. Modern methods of optical microscopy,

particularly confocal laser scanning microscopy, have eased the required effort through spectral or spatial filtering of the desired optical signal (Neu et al., 2010; Sinclair et al., 2006). However, microscopy is not generally conducive to *in situ* measurements due to the requirement of large infrastructure and sample preparation, although some modern adaptations have been reported. For example, an epifluorescence microscope was used to detect the fluorescent response of photopigments in the deep Antarctic ice-sheets for possible signs of life in extreme environments (Storrie-Lombardi and Sattler, 2009).

The most common method of quantifying MPB biomass is in terms of Chlorophyll *a* (Chl *a*) concentration, since it is a photopigment common to nearly all phototrophs and serves as a useful proxy for estimating MPB biomass (Bale and Kenny, 2007). The chlorophyll-to-carbon ratio is generally unknown, and is known to vary with the physiological status or acclimation of the MPBC cells (Cloern et al., 1995; Geider, 1987), and must be accounted for to avoid a systematic error in estimation of biomass. With no standard procedure yet in place for determining Chlorophyll *a* in MPBC, it has been determined through several complimentary methods. The most accurate, and also expensive, is through pigment extraction followed by high-performance liquid chromatography (HPLC). This technique is very good at differentiating between the various pigments and degradation products and allows for quantification by comparison against available pigment standards (Brotas and Plante-Cuny, 2003; Jeffrey et al., 1999). A more rapid and analogous method is the spectrophotometric determination of the optical density of the extractants, and subsequent quantification of Chl *a* concentration through the use of derived spectrometric equations for Chl *a* (Lorenzen, 1967). The virtually indistinguishable spectral signatures of the degradation products (pheophytins, chlorophyllides and pheophorbides) of Chlorophyll *a* has prompted improvements of the protocols (Whitney and Darley, 1979). This method remains the standard choice when Chlorophyll *a* is the sole pigment of interest and large number of samples need to be rapidly processed (Brotas et al., 2007), although the values obtained are somewhat lower than from HPLC (Cahoon, 1999; Grinham et al., 2011). General drawbacks of the pigment extraction strategy are that it entails (destructive) sampling of the sediment substrate, large physical effort, and chemical extraction of the photopigments from the samples. It also suffers from inconsistent sampling protocols of sediments. As reported by Grinham et al. (2007), past studies differed over many methodological parameters, with the critical one of sediment sampling-depth varying between 1–20 mm. These different sample depths certainly represent, depending upon the sediment substrate, different fractions of active and degraded Chlorophyll *a*. This greatly impacts ecological interpretations, such as the estimation of specific production for a given community. Similarly, the use of large or small diameter sampling cores and number of replicate samples have varied, which has been shown to result in undersampling and mis-estimation of the microscale distribution and variability of MPB communities (MacIntyre et al., 1996; Spilmont et al., 2011).

1.3.3 *Optical methods*

The ease and versatility of optical measurements have attracted considerable interest in the development of spectrometric or fluorometric techniques that can exploit modern high-throughput electronics for scaling up the spatio-temporal ranges and resolutions of MPB biomass estimation. The "upwelling" or reflected light from a benthic substrate, such as a biofilm, contains spectroscopic information about the constituent photopigments of the biofilm, due to absorption, scattering and fluorescence interactions. The non-invasive and versatile modalities of optical measurements have enabled the development of several methods with complementary strengths and applications for the quantification of MPB biomass.

1.3.3.1 *Fluorometry*

A popular fluorometric method is pulsed-amplitude modulation (PAM), which uses pulses of light to saturate the light-harvesting complexes of the photosystems of the cells and subsequently measures the fluorescent emission of the complex (Consalvey et al., 2005; Schreiber et al., 1994). The relative ratio between the minimum fluorescence and variable fluorescence due light-saturation of dark-adapted cells is an indicator of the maximum light-utilization efficiency of the photosystem. This provides a means of quantifying the 'openness' (or readiness) of the light-harvesting apparatus of the cells to engage in photosynthesis (Consalvey et al., 2005). Therefore, PAM fluorometry can be used to infer the level of potential photosynthetic activity that a group of cells is capable at a given time, and provides a mechanistic filter between active and senescent Chl *a*. Since the invention of the first PAM fluorometer (Schreiber, 1986), several improvements in the measurement protocols, such as single-turnover or multiple-turnover pulses, have been incorporated into many commercial fluorometers (Consalvey et al., 2005; Schreiber, 2004). Another fluorometric method, invented about the same time and developed parallel to the PAM method, is fast-repetition rate fluorometry (Falkowski et al., 1986). This technique utilizes a series of short (microsecond) illumination pulses called flashlets to generate fluorescent transients, which can be flexibly combined to evoke the responses of both single and multiple turnover pulse illuminations and produce a robust characterization of the photoactivity of the cells (Kolber and Falkowski, 1993). Fluorometric methods continue to be actively developed (Serôdio et al., 2013).

Fluorescence techniques have a long history of use in benthic studies for biomass estimation or to study the vertical migration of benthic diatoms more than a century ago (Fauvel and Bohn, 1907). However, improvements in instrumentation and knowledge of the photochemical mechanisms of pigments have led to renewed interest in the assessment of the physiology and migratory behavior of marine MPB communities (Cartaxana and Serôdio, 2008; Serôdio et al., 2012; Serôdio et al., 1997), as well

as desert communities (Bowker et al., 2002). The minimum fluorescence signal has been reported to correlate linearly with Chlorophyll *a* concentration and, despite dependence on temperature and variability between sediment substrates, has been used a proxy for MPB biomass (Honeywill et al., 2002; Jesus et al., 2005; Serôdio et al., 1997). The probing depth of PAM fluorometry within the sediment has attracted some discussion, with estimates between 150–300 µm depending on the granulometry of the substrate (Consalvey et al., 2004; Kromkamp et al., 1998). The weak intensity of fluorescence emission means that the probing depth is generally lesser than the photic depth measured for visible light. This has been used to advantage for assessing the vertical migration of MPBC with a fine-scaled, but essentially unknown, vertical spatial resolution. Other aspects of MPBC such as physiological status, photosynthesis production and down-regulation rate have been inferred from fluorometric measurements, however many confounding factors such as migration and variable response have yet to be resolved (Consalvey et al., 2005; Perkins et al., 2010). One methodological requirement of fluorometry of natural MPBC assemblages is the requirement for dark-adaptation of the sediment for 10–15 minutes to measure the maximum variable fluorescence, which limits the temporal resolution of measurements. The requirement for dark-adaptation can present a drawback for field-based measurements, and the duration of dark-adaptation also seems to entail short-term response in MPB cells, which recommends caution against a strong interpretation of quantitative biomass measurement (Consalvey et al., 2005; Perkins et al., 2010).

Overall, the emergence of fluorometry as a tool for non-destructive and rapid assessment of the biomass, physiological status and photoactivity of natural assemblages of MPBC has considerably added to our knowledge about the dynamic microbenthos (Kromkamp et al., 2006). While fluorometric measurements provide unique insights into the small-scale spatial and temporal properties as well as the taxonomic composition of MPBC (Aberle et al., 2006), scaling up the measurements to ecosystem levels, such as through airborne measurements, remain difficult (Forster and Kromkamp, 2006; Forster and Jesus, 2006). This is because the technique is essentially a single-point single-wavelength measurement, and requires sampling at different locations in the region of interest. Repeated sampling of the small-scale (2 cm) distribution of MPBC has revealed that much finer resolutions are necessary to capture the microscale spatial heterogeneity of natural MPBC (Jesus et al., 2005).

1.3.3.2 *Spectral imaging*

The combination of spectroscopic analysis and imaging, called spectral imaging, is a complementary and powerful technique for the analysis of complex and dynamic systems such as MPB habitats. A modern form of spectral imaging for the assessment of microscale variability of MPB is the topic of this doctoral dissertation and is presented in detail below.

1.4 HYPERSPECTRAL IMAGING

Spectral imaging refers to the combination of two well-established fields of physics: optical imaging and radiative spectroscopy. Imaging involves the capture of light field reflected or emitted by an object to create a consistent representation of its size, shape or configuration. Spectroscopy is the study of the spectral signatures of light-matter interactions, which arises due to the interaction of photons with the band structure of the electrons in the material, and can be broadly classified into the types: absorption, emission and scattering. Therefore, spectral imaging is a technique where the light used for imaging is captured with spectral resolution at every spatial location in the image, which provides a spectrum associated with each picture element (pixel) of the image. The analysis of spectral images allows one to correlate spectroscopic information (like identity, state or function) with spatial information (like location, shape or size) — providing the means to generate zonation maps of functional parameters. The ability to delineate such information across spatial regions is a prime asset in the task of deconstructing the structure and functional relationships of complex systems. Therefore, the fine sensitivity of spectroscopy to various light-matter interactions and the non-invasive modality of optical imaging provide spectral imaging with great analytic versatility and render it an incisive tool for diagnosis and mapping of complex and heterogeneous systems (Garini et al., 2006; Goetz, 1992).

Details about the concepts and characteristics of spectral imaging systems are given in Appendix A.

Hyperspectral imaging systems are those that capture spectral information in narrow contiguous bands over a certain spectral range and therefore provide a quasi-continuous, and often dense, sampling of the optical spectrum at each imaged location of the target. The development of the diffraction grating as a precise yet compact dispersion element has led to the emergence of hyperspectral imaging systems that measure several hundred contiguous bands, covering more than the entire visual span. Such data throughput is equivalent to the simultaneous measurement of hundreds of images of the same target each at a different wavelength. Hyperspectral images (Figure 1.4), sometimes referred to as hypercubes, are rich datasets that provide a greater scope for spectral analysis than previously used multispectral images, which contained sparse and discontiguous spectral samples. Therefore, the last couple of decades has seen widespread adoption of hyperspectral technology in a variety of disciplines ranging from microscopic studies (Sinclair et al., 2006) to Earth observation systems such as remote sensing satellites (Cloutis, 1996). Hyperspectral analysis of reflectance spectra has been used for a variety of studies, such as to estimate suspended particles in lakes and coastal waters (Carder et al., 1993; Hamilton et al., 1993), vegetation (Rouse et al., 1973; Sabol et al., 1996), atmospheric pollutants (Spinetti et al., 2008), etc.

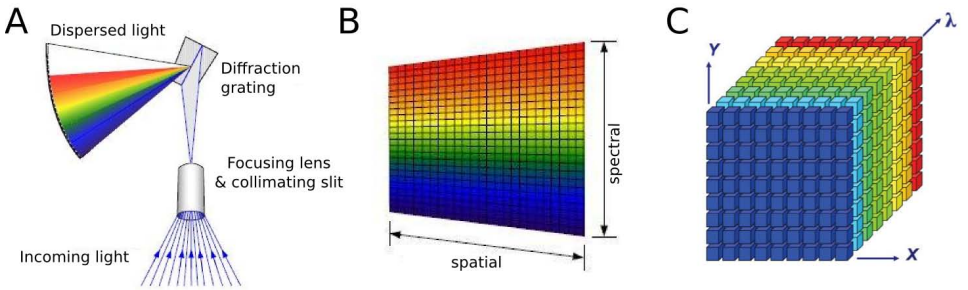

Figure 1.4: Schematic of the compilation of a hyperspectral image captured with a line-detector imager. (A) The incoming light is focused and collimated before being passed through a narrow linear slit. This linear beam of light is dispersed into the constituent spectra by a diffraction grating. (B) The dispersed light from each location of the line-of-view is captured across an array of detectors of the imager, such that each captured frame has one spatial and one spectral dimension. (C) The compilation of several such frames as the imager is moved across the target results in a hyperspectral image, which is a 3D (x, y, λ) dataset that consists of a 2D (x, y) spatial image at a variety of wavelengths (λ). Modified after Garini et al. (2006).

1.4.1 *Assessment of microphytobenthic communities*

The use of hyperspectral imaging for the assessment of MPB is based on the spectral analysis of the light back-scattered from the sediment/sample that contains a natural assemblage of MPB cells. The light back-scattered after interaction with the sediment substrate contains the spectral imprints of the photopigments and chromophores in the biofilm, as well as the scattering and absorption imprints due to the sediment grains and porewater. Generally, the photosynthetic biomass is estimated as the concentration of Chlorophyll *a* detectable through spectral analysis of the recorded light, and forms the basis for both remote sensing and microscale methods for MPB assessment (Hakvoort et al., 1997). MPB cells of different taxa contain specific accessory photopigments, such as phycobilins, carotenoids, xanthins, etc., which have characteristic spectral signatures, some of which overlap closely with those of Chl *a*. Therefore, the reflected spectra from MPB communities are a mix of the various components of the assemblage, and deconvolving the relative abundance of the different pigments serves as a taxonomical marker for the community composition (Gieskes, 1991).

The concentration of Chl *a* (or any pigment) is generally quantified through the calculation of a spectral index designed to estimate the relative contribution of the pigment absorption to the overall reflectance spectrum. Indices calculated from spectra captured in similar light settings are generally comparable, but absolute concentration of the photopigment must be determined by a complementary measurement through pigment extraction (Jeffrey, 1997; Porra et al., 1989). A variety of spectral indices have been applied for assessing MPB in field or lab measurements, with varying degrees of success (Barillé et al., 2011; Murphy et al., 2005). The accuracy of

the predictive power of spectral indices has been very variable, and is indicative of either the sub-optimal design of the index or of systematic problems in measuring the extracted pigment. The former problem is perhaps a historical artifact since many commonly used spectral indices are simple arithmetic ratios inherited from the analysis of sparse multi-spectral datasets. The availability of hyperspectral resolution has underscored the inadequacy of simple ratio-based methods at accurate predictions of MPB biomass, and has prompted a search for more sophisticated approaches using spectral peak areas (Carrère et al., 2004), derivative analysis (Murphy et al., 2005), or non-linear inversion of spectra (Barillé et al., 2007; Combe et al., 2005). The latter problem of systematic errors in the sampled measurements of pigment concentrations is likely due to inconsistent sampling protocols in the various studies (Grinham et al., 2007).

A general problem for spectroscopic estimation of MPB in natural sediments is the large degree of substrate dependence, which significantly alters the shape of the reflected spectrum irrespective of the Chl *a* content (Barillé et al., 2011; Murphy et al., 2005). This is related to the great multiplicity of scattering events within sediment biofilms (Kühl and Jørgensen, 1994), which can create a 10–fold difference in the photic depth between muddy and sandy sediments. Naturally, this confounds the interpretation of the measurement of extracted pigment since the sediments are often sampled to a designated (and differing between studies) depth that generally doesn't correspond to the photic depth (Grinham et al., 2007). Therefore, the interest to resolve the substrate dependence and a variety of targets (photopigments) of interest in measuring field distributions of MPB have led to the promising development of optical models of microphytobenthic biofilms (Kazemipour et al., 2011). The modeling effort is towards combining the spectra of artificial biofilms of pure cultures in the lab and estimating the effect of the sediment substrate from measured reflectance (Kazemipour et al., 2012) in order to derive an estimate of the *in situ* biomass from remote sensing hyperspectral images. Clearer validation of the applicability of these models is pending, but promotes confidence in the ability to use remote sensing for the large-scale estimation of MPB biomass. A variety of other features of interest of the benthic habitat are accessible through remote hyperspectral imaging (Adam et al., 2009; Dehouck et al., 2012) and the comprehensive review by Méléder et al. (2010) covers the details related to MPB biomass estimation.

Hyperspectral imaging has also been used to analyze MPB distributions at the microscopic scale, through the use of a modular imaging system developed by Polerecky et al. (2009a). The system allows the discrimination of a variety of photopigments through the use of fluorometry either under a microscope or high-magnification optics, or through reflective macroscopic imaging of samples (Kühl and Polerecky, 2008; Polerecky et al., 2009a). This application of hyperspectral imaging is an excellent tool for the study of the role that spatial structure plays in the functional organization of heterogeneous ecosystems, such as microbial mats (Bachar et al., 2008; Kohls et al., 2010), stromatolites (Farías et al., 2013) and biofilms

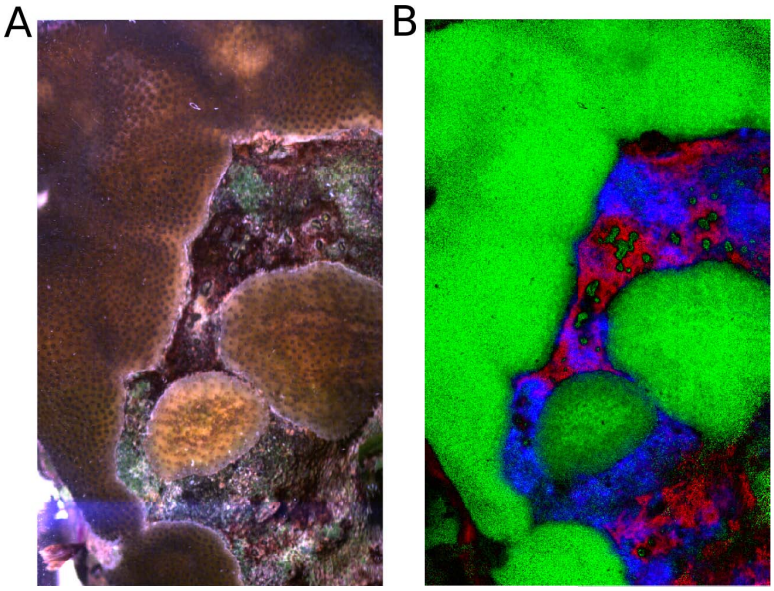

Figure 1.5: Hyperspectral reflectance imaging of a coral organism incubated in the laboratory was performed by the system described in Polerecky et al. (2009a). The true-color image (A) approximates the visual present to the naked eye, whereas the false-color map (B) combines quantified spectral maps of zooxanthallae (green), phycoerithrin (red) and bacteriochlorophyll *a*. Measurement was performed under a halogen lamp with the coral organism removed from water for a few minutes. Estimation of the photopigment concentration was done through derivative analysis of the hyperspectral image. (Images courtesy of Lubos Polerecky)

(Ionescu et al., 2012). The system has also been used to monitor biofilm growth in the laboratory (Polerecky et al., 2009b). Although mostly limited to laboratory-based measurements of samples, an exemplary study of a coral organism using this system amply demonstrates the power of microscale hyperspectral imaging for the study of benthic ecology. The hyperspectral image of the coral surface was analyzed for spectral signatures of the expected phototrophs: the symbiotic zooxanthallae and the invasive microalgal species that was known to be part of a coral-algal phase shift. However, the hyperspectral resolution of the measurement allowed the identification of a third characteristic photopigment which signified the presence of a previously unindicated phototroph. Apart from enabling serendipity in spectral analysis of natural assemblages, the measurement allowed the mapping the relative concentrations of the various photopigments (Figure 1.5). This revealed that the spatial distribution of the photopigments corresponded to the health of the coral tissue, and was structured in a complex and interleaved pattern that would be quite impossible to visualize by traditional methods of pigment evaluation. Similar analysis was performed for the assessment of coral-algal phase shift in a field sampling study (Barott et al., 2009). This demonstrates the potential of using hyperspectral imaging at high spatial resolutions with its non-

invasive modality and spectral versatility to enable incisive analyses of the spatio-temporal structure of microbenthic communities.

1.4.2 *Current limitations*

The adoption of hyperspectral imaging technology for benthic studies has been primarily focused towards the remote sensing domain. The spatial resolution of the currently available spaceborne imagers are 50–150m, while airborne imagers allow resolutions of 5–30m (Kaufmann et al., 2012). Barring the spatial resolution, the scanning range of the remote sensing imagers provide the possibility to cover large areas of coastal region with relative ease. Remote sensing visibility depends upon clear skies, which has been a general hindrance in repeatedly measuring a particular location. Nevertheless, the relatively long optical path of the light through the layers of the atmosphere, and possible water cover of shallow beds, further complicates the spectral analysis of the light reflected from the variety of sediment substrates and necessitates a range of complex corrections to account for them. Most of the studies (see above) that analyzed the suitability of remote sensing through complementary field measurements have performed "ground-truthing" either using sediment sampling with cores or a field spectroradiometer. Neither of these methods delivers detailed information about the spatial structure of the MPB distributions at the level of field measurements (1–1000 mm), which is known to be a scale of strong spatial and temporal variability for MPB communities (see Section 1.2). On the other hand, the modular optical imaging system developed by Polerecky et al. (2009a) has a limited scanning range and is unsuitable for *in situ* measurements or field deployments. Therefore, there is currently no reasonable technique to "scale down" the remote sensing measurements from an aerial or satellite imager to the millimeter-to-meter mesoscale of MPB habitats which corresponds to the spatial scale of the operant control mechanisms that are likely to affect MPB communities (Azovsky, 2000).

Another limitation of the current methodologies, as highlighted by Cahoon (1999), is the assessment of subtidal MPB biomass. This is evident from the paucity of subtidal datasets of MPB biomass (Glud, 2006). Remote sensing imagers have limited scope of measurement for subtidal habitats of the neritic zone due to the vagaries of weather, turbidity and solar radiation. Underwater imaging has the potential to overcome these problems and provide the much-needed empirical input on MPB abundance in shallow ecosystems. However, despite the improvements in underwater imaging technology (Kocak et al., 2008), there are currently no available underwater hyperspectral imagers that are commonly available for benthic studies.

1.5 MOTIVATION OF THE DOCTORAL THESIS

As has been outlined so far, microphytobenthic communities thrive in nearly all latitudes and longitudes of our planet and perform photosynthetic primary production. They form the fundament of the marine food web in many habitats, and their activity directly, or indirectly, impacts many ecosystem parameters and functions. Despite a small areal footprint on the world's oceans, MPB habitats are disproportionately productive. Their contribution to the carbon cycle and primary production is globally significant, and has been previously unrecognized. The under-estimation of their impact continues, in part due to the paucity of globally-distributed *in situ* datasets (Figure 1.2) and large variability in previous measures of their production or abundance (Cahoon, 1999; MacIntyre et al., 1996).

The spatio-temporal organization of a community is a prominent issue in ecology, and it has been argued that the analysis of large-scale patterns must integrate effects occurring at smaller scales (Levin, 1992; Underwood et al., 2000). Given their ecological significance as the autotrophic base of many marine food webs, particularly in polar regions which face imminent perturbation due to global climate change, it is a pressing need to be able to record, analyze and understand the processes that control the abundance and activity of MPB communities. Miller et al. (1996) advocated a reductionist approach to disentangle the complex relationships of the microbenthic ecosystem and called for the study of "first-order interactions" with the ecosystem that directly affect the MPB distribution. The particularities of microbenthic habitats, characterized by steep physical, chemical and biological gradients, generate profuse spatio-temporal heterogeneity at all measured scales in MPB distributions (Chapman et al., 2010). Variability in growth rates and abundance is to be expected on the scale of the body-size of an organism (Azovsky, 2000; Azovsky et al., 2004), and there is clear evidence of sub-millimeter scale spatial heterogeneity in MPB distributions (Jesus et al., 2005; Seuront and Leterme, 2006). The observed large-scale and seasonal variability in MPB distributions generally lacks causative explanations (Brito et al., 2009b; Chapman et al., 2010; Underwood, 1994), and there is reason to believe that this is due to systematic under-sampling of the spatio-temporal heterogeneity of MPB distributions (Cahoon, 1999). Traditional methods of measuring MPB distribution, such as sediment sampling (Spilmont et al., 2011) or fluorometry (Jesus et al., 2005), lack the spatial and temporal resolutions to capture the MPB distribution in sufficient detail so that the natural scales of variability may "emerge from the data" (Chapman et al., 2010).

Therefore, there is an unfilled void in the methodology for assessing the microscale distribution and dynamics of MPB communities, which allows swift measurement of the microstructure over a spatial range conducive to the analysis of relevant "first-order interactions" and to elaborate the context for secondary and tertiary dependencies (Jones and Callaway, 2007). The methodological void seems linked to the unavailability of suit-

able instrumentation that allows hyperspectral imaging to be conducted in the often dynamic and demanding conditions of intertidal and subtidal field sites. Hyperspectral imaging technology adapted for field-based and underwater use has the potential to fill that void as it offers a natural extension of the spatial resolutions of remote sensing imagers (meter-to-kilometer) down to the microscale (millimeters-to-meter), with the possibility to propagate the small-scale patterns of variation into the large-scale analysis of ecosystems. The non-invasive technique and the sensitivity to a range of photopigments would also allow the study of the evolution of the microscale patterns over diel and seasonal cycles.

In combination, these motivate the technical and scientific objectives of this doctoral project: to develop a field-instrument for *in situ* hyperspectral imaging of microbenthos, and to develop a methodology that exploits this technology for recording the microscale spatial and temporal dynamics of microphytobenthic communities. This would provide novel empirical data that will be useful to study the sources of the microscale variability, and elucidate some of the operant ecological processes that regulate the abundance and function of the phototrophic fundament of the fertile, delineated and dynamic microbenthos of the vast neritic regions.

1.6 REFERENCES

Aberle, N., M. Beutler, C. Moldaenke, and K. H. Wiltshire (2006). "'Spectral fingerprinting' for specific algal groups on sediments in situ: a new sensor." In: *Archive für Hydrobiologie* 167.1, pp. 575–592. DOI: 10.1127/0003-9136/2006/0167-0575 (cited on page 16).

Adam, S., J. Monbaliu, and E. A. Toorman (2009). "Quantification of biophysical intertidal sediment properties using hyperspectral measurements." In: *Remote sensing for a changing Europe. Proceedings of the 28th Symposium of the European Association of Remote Sensing Laboratories, Istanbul, Turkey, 2-5 June 2008.* IOS Press, pp. 340–347 (cited on page 19).

Adey, W. H. (1987). "Food-production in low-nutrient seas." English. In: *Bioscience* 37.5, 340–348. DOI: 10.2307/1310690 (cited on page 11).

Armitage, A. R. and P. Fong (2004). "Upward cascading effects of nutrients: shifts in a benthic microalgal community and a negative herbivore response." English. In: *Oecologia* 139.4, pp. 560–567. DOI: 10.1007/s00442-004-1530-6 (cited on page 11).

Asmus, R. (1982). "Field measurements on seasonal variation of the activity of primary producers on a sandy tidal flat in the northern Wadden sea." In: *Netherlands Journal of Sea Research* 16, pp. 389–402. DOI: 10.1016/0077-7579(82)90045-X (cited on page 8).

Azovsky, A. (2000). "Concept of scale in marine ecology: linking the words or the worlds." In: *Web Ecol* 1, pp. 28–34. DOI: 10.5194/we-1-28-2000 (cited on pages 21 sq.).

Azovsky, A., E. Chertoprood, M. Saburova, and I. Polikarpov (2004). "Spatio-temporal variability of micro- and meiobenthic communities in a White Sea intertidal sandflat." In: *Estuarine, Coastal and Shelf Science* 60.4, pp. 663–671. DOI: 10.1016/j.ecss.2004.03.005 (cited on pages 12, 22).

Azovsky, A., M. Saburova, E. Chertoprood, and I. Polikarpov (2005). "Selective feeding of littoral harpacticoids on diatom algae: hungry gourmands?" English. In: *Marine Biology* 148.2, pp. 327–337. DOI: 10.1007/s00227-005-0086-2 (cited on page 12).

Bachar, A., L. Polerecky, J. P. Fischer, K. Vamvakopoulos, D. de Beer, and H. M. Jonkers (2008). "Two-dimensional mapping of photopigment distribution and activity of *Chloroflexus*-like bacteria in a hypersaline microbial mat." In: *FEMS microbiology ecology* 65.3, pp. 434–48. DOI: 10.1111/j.1574-6941.2008.00534.x (cited on page 19).

Bale, A. J. and A. J. Kenny (2007). "Sediment Analysis and Seabed Characterization." In: *Methods for the Study of Marine Benthos*. Third. Blackwell Science Ltd. Chap. 2, pp. 43–86. DOI: 10.1002/9780470995129.ch2 (cited on page 14).

Barillé, L., V. Méléder, and J. Combe (2007). "Comparative analysis of field and laboratory spectral reflectances of benthic diatoms with a modified Gaussian model approach." In: *Journal of Experimental Marine Biology and Ecology* 343.2, pp. 197–209. DOI: 10.1016/j.jembe.2006.11.013 (cited on page 19).

Barillé, L., J.-L. Mouget, V. Méléder, P. Rosa, and B. Jesus (2011). "Spectral response of benthic diatoms with different sediment backgrounds." In: *Remote sensing of Environment* 115.4, pp. 1034–1042. DOI: 10.1016/j.rse.2010.12.008 (cited on pages 18 sq.).

Barott, K., J. Smith, E. Dinsdale, and M. Hatay (2009). "Hyperspectral and physiological analyses of coral-algal interactions." In: *PLoS One* 4.11, e8043. DOI: 10.1371/journal.pone.0008043 (cited on page 20).

Barranguet, C., J. Kromkamp, and J. Peene (1998). "Factors controlling primary production and photosynthetic characteristics of intertidal microphytobenthos." In: *Marine Ecology Progress Series* 173, pp. 117–126. DOI: 10.3354/meps173117 (cited on page 6).

Beatty, J. T., J. Overmann, M. T. Lince, A. K. Manske, A. S. Lang, R. E. Blankenship, C. L. Van Dover, T. A. Martinson, and F. G. Plumley (2005). "An obligately photosynthetic bacterial anaerobe from a deep-sea hydrothermal vent." In: *Proceedings of the National Academy of Sciences* 102.26, pp. 9306–9310. DOI: 10.1073/pnas.0503674102 (cited on page 6).

Bebout, B. M. and F. Garcia-Pichel (1995). "UV B-Induced Vertical Migrations of Cyanobacteria in a Microbial Mat." In: *Applied and environmental microbiology* 61.12, pp. 4215–4222 (cited on page 8).

Bekker, A., H. D. Holland, P.-L. Wang, D. Rumble, H. J. Stein, J. L. Hannah, L. L. Coetzee, and N. J. Beukes (2004). "Dating the rise of atmospheric oxygen." In: *Nature* 427.6970, pp. 117–120. DOI: 10.1038/nature02260 (cited on page 3).

Bertuzzi, P. and L. Bruckler (1996). "A scaling based estimation of soil unsaturated hydraulic properties at a field scale." English. In: *Irrigation Science* 17.1, 23–30. DOI: 10.1007/s002710050018 (cited on page 11).

Blanchard, G. F., J.-M. Guarini, F. Orvain, and P.-G. Sauriau (2001). "Dynamic behaviour of benthic microalgal biomass in intertidal mudflats." In: *Journal of Experimental Marine Biology and Ecology* 264.1, pp. 85–100. DOI: 10.1016/S0022-0981(01)00312-4 (cited on page 12).

Blanchard, G. F. and P. A. Montagna (1992). "Photosynthetic response of natural assemblages of marine benthic microalgae to short- and long-term variations of incident irradiance in Baffin Bay, Texas." In: *Journal of Phycology* 28.1, pp. 7–14. DOI: 10.1111/j.0022-3646.1992.00007.x (cited on page 9).

Boetius, A., S. Albrecht, K. Bakker, C. Bienhold, J. Felden, M. Fernández-Méndez, S. Hendricks, C. Katlein, C. Lalande, T. Krumpen, M. Nicolaus, I. Peeken, B. Rabe, A. Rogacheva, E. Rybakova, R. Somavilla, F. Wenzhöfer, and R. P. A.-3.-S. S. Party (2013). "Export of Algal Biomass from the Melting Arctic Sea Ice." In: *Science* 339.6126, pp. 1430–1432. DOI: 10.1126/science.1231346 (cited on page 6).

Boogert, N. J., D. M. Paterson, and K. N. Laland (2006). "The Implications of Niche Construction and Ecosystem Engineering for Conservation Biology." In: *BioScience* 56.7, pp. 570–578. DOI: 10.1641/0006-3568(2006)56[570:TIONCA]2.0.CO;2 (cited on page 11).

Boudreau, B. P. and B. B. Jørgensen (2001). *The Benthic Boundary Layer: Transport Processes and Biogeochemistry*. Oxford University Press (cited on pages 4 sq.).

Boudreau, B. P., M. Huettel, S. Forster, R. A. Jahnke, A. McLachlan, J. J. Middelburg, P. Nielsen, F. Sansone, G. Taghon, W. Van Raaphorst, I. Webster, J. M. Weslawski, P. Wiberg, and B. Sundby (2001). "Permeable marine sediments: overturning an old paradigm." In: *Eos, Transactions American Geophysical Union* 82.11, pp. 133–136. DOI: 10.1029/EO082i011p00133-01 (cited on page 11).

Bowker, M. A., S. C. Reed, J. Belnap, and S. L. Phillips (2002). "Temporal variation in community composition, pigmentation, and F_v/F_m of desert cyanobacterial soil crusts." In: *Microbial ecology* 43.1, pp. 13–25. DOI: 10.1007/s00248-001-1013-9 (cited on page 16).

Brito, A., A. Newton, P. Tett, and T. Fernandes (2009a). "Development of an optimal methodology for the extraction of microphytobenthic chlorophyll." In: *Journal of International Environmental Application and Science* 4.1, pp. 42–54 (cited on page 8).

Brito, A. C., I. Benyoucef, B. Jesus, V. Brotas, P. Gernez, C. R. Mendes, P. Launeau, M. P. Dias, and L. Barillé (2013). "Seasonality of microphytobenthos revealed by remote-sensing in a South European estuary." In: *Continental Shelf Research* 66, pp. 83–91. DOI: 10.1016/j.csr.2013.07.004 (cited on page 8).

Brito, A., A. Newton, P. Tett, and T. F. Fernandes (2009b). "Temporal and spatial variability of microphytobenthos in a shallow lagoon: Ria Formosa (Portugal)." In: *Estuarine, Coastal and Shelf Science* 83.1, pp. 67–76. DOI: 10.1016/j.ecss.2009.03.023 (cited on page 22).

— (2010). "Sediment and water nutrients and microalgae in a coastal shallow lagoon, Ria Formosa (Portugal): Implications for the Water Framework Directive." In: *Journal of Environmental Monitoring* 12.1, pp. 318–328. DOI: 10.1039/b909429f (cited on pages 10 sq.).

Brotas, V., T. Cabrita, A. Portugal, J. Serôdio, and F. Catarino (1995). "Spatio-temporal distribution of the microphytobenthic biomass in intertidal flats of Tagus Estuary (Portugal)." In: *Hydrobiologia* 300-301.1, pp. 93–104. DOI: 10.1007/BF00024451 (cited on page 8).

Brotas, V., C. R. Mendes, and P. Cartaxana (2007). "Microphytobenthic biomass assessment by pigment analysis: comparison of spectrophotometry and High Performance Liquid Chromatography methods." In: *Hydrobiologia* 587.1, pp. 19–24. DOI: 10.1007/s10750-007-0680-z (cited on page 14).

Brotas, V. and M.-R. Plante-Cuny (2003). "The use of HPLC pigment analysis to study microphytobenthos communities." In: *Acta Oecologica* 24, Supplement 1. Proceedings of the Plankton Symposium, Espinho, Portugal, S109–S115. DOI: 10.1016/S1146-609X(03)00013-4 (cited on page 14).

Buffan-Dubau, E. and K. R. Carman (2000). "Diel feeding behavior of meiofauna and their relationships with microalgal resources." In: *Limnology and Oceanography* 45.2, pp. 381–395. DOI: 10.4319/lo.2000.45.2.0381 (cited on page 12).

Cabrita, M. and V. Brotas (2000). "Seasonal variation in denitrification and dissolved nitrogen fluxes in intertidal sediments of the Tagus estuary, Portugal." In: *Marine Ecology Progress Series* 202, pp. 51–65. DOI: 10.3354/meps202051 (cited on page 11).

Cahoon, L. B. (1999). "The role of benthic microalgae in neritic ecosystems." In: *Oceanography and Marine Biology, An Annual Review*. Ed. by A. Ansell, R. Gibson, and M. Barnes. Vol. 37. Aberdeen University Press, pp. 47–86 (cited on pages 5 sq., 10, 13 sq., 21 sq.).

Cahoon, L. B., R. A. Laws, and C. J. Thomas (1994). "Viable diatoms and chlorophylla in continental slope sediments off Cape Hatteras, North Carolina." In: *Deep Sea Research Part II: Topical Studies in Oceanography*

41.4-6, pp. 767–782. DOI: 10.1016/0967-0645(94)90047-7 (cited on pages 6, 10).

Cahoon, L., J. Nearhoof, and C. Tilton (1999). "Sediment grain size effect on benthic microalgal biomass in shallow aquatic ecosystems." In: *Estuaries* 22.3, pp. 735–741. DOI: /10.2307/1353106 (cited on pages 6, 9).

Carder, K. L., P. Reinersman, R. F. Chen, F. Muller-Karger, C. Davies, and M. K. Hamilton (1993). "AVIRIS calibration and application in coastal oceanic environments." In: *Remote Sensing of Environment* 44.2-3, pp. 205–216. DOI: 10.1016/0034-4257(93)90016-Q (cited on page 17).

Carrère, V., N. Spilmont, and D. Davoult (2004). "Comparison of simple techniques for estimating Chlorophyll *a* concentration in the intertidal zone using high spectral-resolution field-spectrometer data." In: *Marine Ecology Progress Series* 274, pp. 31–40. DOI: 10.3354/meps274031 (cited on page 19).

Cartaxana, P. and J. Serôdio (2008). "Inhibiting diatom motility: a new tool for the study of the photophysiology of intertidal microphytobenthic biofilms." In: *Limnology and Oceanography: Methods* 6, pp. 466–476. DOI: 10.4319/lom.2008.6.466 (cited on page 15).

Castenholz, R. W. and F. Garcia-Pichel (2002). "Cyanobacterial responses to UV-radiation." In: *The ecology of cyanobacteria*. Springer, pp. 591–611. DOI: 10.1007/0-306-46855-7_21 (cited on page 8).

Chapman, M., T. Tolhurst, R. Murphy, and A. Underwood (2010). "Complex and inconsistent patterns of variation in benthos, micro-algae and sediment over multiple spatial scales." In: *Marine Ecology Progress Series* 398, pp. 33–47. DOI: 10.3354/meps08328 (cited on pages 7, 22).

Cloern, J. E., C. Grenz, and L. Vidergar-lucas (1995). "An empirical model of the phytoplankton chlorophyll:carbon ratio – the conversion factor between productivity and growth rate." In: *Limnology and Oceanography* 40.7, pp. 1313–1321. DOI: 10.4319/lo.1995.40.7.1313 (cited on page 14).

Cloutis, E. A. (1996). "Review Article Hyperspectral geological remote sensing: evaluation of analytical techniques." In: *International Journal of Remote Sensing* 17.12, pp. 2215–2242. DOI: 10.1080/01431169608948770 (cited on page 17).

Coma, R., M. Ribes, J.-M. Gili, and M. Zabala (2002). "Seasonality of in situ respiration rate in three temperate benthic suspension feeders." In: *Limnology and Oceanography* 47.1, pp. 324–331. DOI: 10.4319/lo.2002.47.1.0324 (cited on page 8).

Combe, J. P., P. Launeau, V. Carrere, D. Despan, V. Meleder, L. Barille, and C. Sotin (2005). "Mapping microphytobenthos biomass by non-linear inversion of visible-infrared hyperspectral images." In: *Remote sensing*

of Environment 98.4, pp. 371–387. DOI: 10.1016/j.rse.2005.07.010 (cited on page 19).

Consalvey, M., D. Paterson, and G. Underwood (2004). "The ups and downs of life in a benthic biofilm: migration of benthic diatoms." In: *Diatom Research* 18, pp. 181–202. DOI: 10.1080/0269249X.2004.9705870 (cited on pages 7, 16).

Consalvey, M., R. G. Perkins, and D. M. Paterson (2005). "PAM fluorescence: a beginners guide for benthic diatomists." In: *Diatom Research* 20.1, pp. 1–22. DOI: 10.1080/0269249X.2005.9705619 (cited on pages 15 sq.).

Daborn, G., C. Amos, and M. Brylinsky (1993). "An ecological cascade effect: migratory birds affect stability of intertidal sediments." In: *Limnology and Oceanography* 38.1, pp. 225–231. DOI: 10.4319/lo.1993.38.1.0225 (cited on page 11).

Davis, M. W. and C. D. McIntire (1983). "Effects of physical gradients on the production dynamics of sediment-associated algae." In: *Marine Ecology Progress Series* 13, pp. 103–114 (cited on page 9).

De Jonge, V. N. and J. E. E. van Beusekom (1995). "Wind- and tide-induced resuspension of sediment and microphytobenthos from tidal flats in the Ems estuary." In: *Limnology and Oceanography* 40.4, pp. 766–778. DOI: 10.4319/lo.1995.40.4.0776 (cited on pages 8–10).

Dehouck, A., V. Lafon, B. Lubac, S. Kervella, D. Bru, M. Schmeltz, and A. Roubache (2012). "Hyperspectral field database in support to coastal wetland mapping." In: *Geoscience and Remote Sensing Symposium (IGARSS), 2012 IEEE International*, pp. 2649–2652. DOI: 10.1109/IGARSS.2012.6350384 (cited on page 19).

Delgado, M., V. De Jonge, and H. Peletier (1991). "Effect of sand movement on the growth of benthic diatoms." In: *Journal of Experimental Marine Biology and Ecology* 145.2, pp. 221–231. DOI: 10.1016/0022-0981(91)90177-X (cited on page 10).

Dring, M. J. and K. Lüning (1983). *Photomorphogenesis of Marine Macroalgae*. Springer-Verlag, pp. 545–568. DOI: 10.1007/978-3-642-68918-5_21 (cited on page 9).

Eldridge, D. and R. Greene (1994). "Microbiotic soil crusts — a review of their roles in soil and ecological processes in the rangelands of Australia." In: *Soil Research* 32.West 1990, pp. 389–415. DOI: 10.1071/SR9940389 (cited on page 6).

Falkowski, P. G. (1988). "Theoretical calculation of the depth of the euphotic zone in the sea." In: *Biogeochemical cycling and fluxes between the deep euphotic zone and other oceanic realms*. Ed. by C. Agegian. Rockville, MD: National Undersea Research Program Report No. 88-1, pp. 47–60 (cited on page 9).

Falkowski, P. G. and J. LaRoche (1991). "Acclimation to spectral irradiance in algae." In: *Journal of Phycology* 27.1, pp. 8–14. DOI: 10.1111/j.0022-3646.1991.00008.x (cited on page 9).

Falkowski, P. G., K. Wyman, A. C. Ley, and D. C. Mauzerall (1986). "Relationship of steady-state photosynthesis to fluorescence in eucaryotic algae." In: *Biochimica et Biophysica Acta - Bioenergetics* 849.2, pp. 183–192. DOI: 10.1016/0005-2728(86)90024-1 (cited on page 15).

Falkowski, P. and J. Raven (1996). *Aquatic Photosynthesis*. Malden, Massachussetts: Blackwell Publishers (cited on page 3).

Farías, M. E., N. Rascovan, D. M. Toneatti, V. H. Albarracín, M. R. Flores, D. G. Poiré, M. M. Collavino, O. M. Aguilar, M. P. Vazquez, and L. Polerecky (2013). "The discovery of stromatolites developing at 3570 m above sea level in a high-altitude volcanic lake Socompa, Argentinean Andes." In: *PloS one* 8.1, e53497. DOI: 10.1371/journal.pone.0053497 (cited on page 19).

Fauvel, P. and G. Bohn (1907). "Le Rythme des marées chez les Diatomées littorales." In: *Compte Rendu des Seances de la Societé* 62, pp. 121–123 (cited on page 15).

Fenchel, T. and R. N. Glud (2000). "Benthic primary production and O_2-CO_2 dynamics in a shallow-water sediment: Spatial and temporal heterogeneity." In: *Ophelia* 53.2, pp. 159–171. DOI: 10.1080/00785236.2000.10409446 (cited on page 13).

Field, C. B., M. J. Behrenfeld, J. T. Randerson, and P. Falkowski (1998). "Primary production of the biosphere: Integrating terrestrial and oceanic components." In: *Science* 281.5374, pp. 237–240. DOI: 10.1126/science.281.5374.237 (cited on pages 3 sq.).

Forster, R. and J. Kromkamp (2006). "Estimating benthic primary production: scaling up from point measurements to the whole estuary." In: *Functioning of microphytobenthos in estuaries: Proceedings of the Colloquium, Amsterdam, 21-23 August 2003*. Royal Netherlands Academy of Arts and Sciences, pp. 109–120 (cited on page 16).

Forster, R. and B. Jesus (2006). "Field spectroscopy of estuarine intertidal habitats." In: *International Journal of Remote Sensing* 27.17, pp. 3657–3669. DOI: 10.1080/01431160500500367 (cited on page 16).

Franks, J. and J. F. Stolz (2009). "Flat laminated microbial mat communities." In: *Earth-Science Reviews* 96.3, pp. 163–172. DOI: 10.1016/j.earscirev.2008.10.004 (cited on page 7).

Garcia-Pichel, F., M. Mechling, and R. W. Castenholz (1994). "Diel migrations of microorganisms within a benthic, hypersaline mat community." In: *Applied and environmental microbiology* 60.5, pp. 1500–1511 (cited on page 7).

Garini, Y., I. T. Young, and G. McNamara (2006). "Spectral imaging: principles and applications." In: *Cytometry Part A* 69.8, pp. 735–47. DOI: 10.1002/cyto.a.20311 (cited on pages 17 sq.).

Garrett, P. (1970). "Phanerozoic stromatolites: Noncompetitive ecologic restriction by grazing and burrowing animals." In: *Science* 169.3941, pp. 171–173. DOI: 10.1126/science.169.3941.171 (cited on page 12).

Geider, R. J. (1987). "Light and temperature dependence of the carbon to Chlorophyll *a* ratio in microalgae and cyanobacteria: implications for physiology and growth of phytoplankton." In: *New Phytologist* 106.1, pp. 1–34. DOI: 10.1111/j.1469-8137.1987.tb04788.x (cited on page 14).

Gieskes, W. W. C. (1991). "Particle Analysis in Oceanography." In: ed. by S. Demers. Springer Verlag. Chap. Algal pigment fingerprints: clue to taxon-specific abundance, productivity and degradation of phytoplankton in seas and oceans, pp. 61–99 (cited on page 18).

Gilbert, N. (1991). "Microphytobenthic seasonality in near-shore marine sediments at Signy Island, South Orkney Islands, Antarctica." In: *Estuarine, Coastal and Shelf Science* 33.1, pp. 89–104. DOI: http://dx.doi.org/10.1016/0272-7714(91)90072-J (cited on page 8).

Glud, R. N. (2006). "Microscale techniques to measure photosynthesis: A mini-review." In: *Functioning of microphytobenthos in estuaries: Proceedings of the Colloquium, Amsterdam, 21-23 August 2003*. Ed. by J. C. Kromkamp. Vol. 103. Royal Netherlands Academy of Arts and Sciences, pp. 123–140 (cited on pages 5, 13, 21).

Glud, R. N., M. Kühl, F. Wenzhöfer F, and S. Rysgaard (2002). "Benthic diatoms of a high Arctic fjord (Young Sound, NE Greenland): importance for ecosystem primary production." In: *Marine Ecology Progress Series* 238, pp. 15–29. DOI: 10.3354/meps238015 (cited on pages 8, 13).

Goetz, A. F. H. (1992). "Imaging spectrometry for Earth observation." In: *Episodes* 15, pp. 1–14 (cited on page 17).

Green, S. A. and N. V. Blough (1994). "Optical absorption and fluorescence properties of chromophoric dissolved organic matter in natural waters." In: *Limnology and Oceanography* 39.8, pp. 1903–1916. DOI: 10.4319/lo.1994.39.8.1903 (cited on page 9).

Grinham, A., D. Gale, and J. Udy (2011). "Impact of sediment type, light and nutrient availability on benthic diatom communities of a large estuarine bay: Moreton Bay, Australia." In: *Journal of Paleolimnology* 46.4, pp. 511–523. DOI: 10.1007/s10933-010-9407-7 (cited on pages 11, 14).

Grinham, A. R., T. J. Carruthers, P. L. Fisher, J. W. Udy, and W. C. Dennison (2007). "Accurately measuring the abundance of benthic microalgae in spatially variable habitats." In: *Limnology and Oceanography: Methods* 5, pp. 119–125. DOI: 10.4319/lom.2007.5.119 (cited on pages 14, 19).

Guarini, J.-M. and G. Blanchard (1998). "Dynamics of spatial patterns of microphytobenthic biomass: inferences from a geostatistical analysis of two comprehensive surveys in Marennes-Oléron Bay (France)." In: *Marine Ecology Progress Series* 166, pp. 131–141. DOI: 10.3354/meps166131 (cited on pages 6 sq., 12).

Guarini, J.-M., G. F. Blanchard, P. H. Gros, D. Gouleau, and C. Bacher (2000). "Dynamic model of the short-term variability of microphytobenthic biomass on temperate intertidal mudflats." In: *Marine Ecology-Progress Series* 195, pp. 291–303. DOI: 10.3354/meps195291 (cited on page 12).

Haeckel, E. (1890). "Plankton-Studien, vergleichende Untersuchangen aber die Bedeutung und Zusamnensetzung der Pelagischen Fauna und Flora." In: *Plankton-Studien, vergleichende Untersuchangen aber die Bedeutung und Zusamnensetzung der Pelagischen Fauna und Flora.* pages (cited on page 13).

Hakvoort, H., K. Heymann, C. Stein, and D. Murphy (1997). "In-situ optical measurements of sediment type and phytobenthos of tidal flats: a basis for imaging remote sensing spectroscopy." In: *Ocean Dynamics* 49.2-3, pp. 367–373. DOI: 10.1007/BF02764045 (cited on page 18).

Hamilton, M. K., C. O. Davies, W. J. Rhea, S. H. Pilorz, and K. L. Carder (1993). "Estimating chlorophyll content and bathymetry of Lake Tahoe using AVIRIS data." In: *Remote Sensing of Environment* 44.2-3, pp. 217–230 (cited on page 17).

Heckman, C. W. (1985). "The development of vertical migration patterns in the sediments of estuaries as a strategy for algae to resist drift with tidal currents." In: *Internationale Revue der gesamten Hydrobiologie und Hydrographie* 70.1, pp. 151–164. DOI: 10.1002/iroh.19850700112 (cited on page 7).

Hecky, R. E. and P. Kilham (1988). "Nutrient limitation of phytoplankton in freshwater and marine environments: A review of recent evidence on the effects of enrichment." In: *Limnology and Oceanography* 33.4-2, pp. 796–822. DOI: 10.4319/lo.1988.33.4_part_2.0796 (cited on page 5).

Honeywill, C., D. Paterson, and S. Hagerthey (2002). "Determination of microphytobenthic biomass using pulse-amplitude modulated minimum fluorescence." In: *European Journal of Phycology* 37.4, pp. 485–492. DOI: 10.1017/S0967026202003888 (cited on page 16).

Howard-Williams, C., R. Pridmore, M. Downes, and W. Vincent (1989). "Microbial biomass, photosynthesis and chlorophyll a related pigments in the ponds of the McMurdo Ice Shelf, Antarctica." In: *Antarctic Science* 1.02, pp. 125–131. DOI: 10.1017/S0954102089000192 (cited on page 8).

Huang, R. and A. Boney (1984). "Growth interactions between littoral diatoms and juvenile marine algae." In: *Journal of Experimental Marine Biology and Ecology* 81.1, pp. 21–45. DOI: 10.1016/0022-0981(84)90222-3 (cited on page 11).

Ionescu, D., C. Siebert, L. Polerecky, Y. Y. Munwes, C. Lott, S. Häusler, M. Bižić-Ionescu, C. Quast, J. Peplies, F. O. Glöckner, A. Ramette, T. Rödiger, T. Dittmar, A. Oren, S. Geyer, H.-J. Stärk, M. Sauter, T. Licha, J. B. Laronne, and D. de Beer (2012). "Microbial and chemical characterization of underwater fresh water springs in the Dead Sea." In: *PloS one* 7.6, e38319. DOI: 10.1371/journal.pone.0038319 (cited on page 20).

Jeffrey, S. W. (1997). "Application of pigment method to oceanography." In: *Phytoplankton pigments in oceanography. Monographs on oceanographic methodology*. Ed. by S. W. Jeffrey, R. F. C. Mantoura, and W. S. W. Paris, UNESCO publishing (cited on page 18).

Jeffrey, S. W., S. W. Wright, and M. Zapata (1999). "Recent advances in HPLC pigment analysis of phytoplankton." In: *Marine and Freshwater Research* 50.8, p. 879. DOI: 10.1071/MF99109 (cited on page 14).

Jerlov, N. G. (1976). *Marine optics*. Elsevier (cited on page 8).

Jesus, B., V. Brotas, M. Marani, and D. Paterson (2005). "Spatial dynamics of microphytobenthos determined by PAM fluorescence." In: *Estuarine, Coastal and Shelf Science* 65.1-2, pp. 30–42. DOI: 10.1016/j.ecss.2005.05.005 (cited on pages 16, 22).

Jesus, B., V. Brotas, L. Ribeiro, C. Mendes, P. Cartaxana, and D. Paterson (2009). "Adaptations of microphytobenthos assemblages to sediment type and tidal position." In: *Continental Shelf Research* 29.13, pp. 1624–1634. DOI: 10.1016/j.csr.2009.05.006 (cited on page 10).

Jones, C. G. and R. M. Callaway (2007). "The third party." In: *Journal Of Vegetation Science* 18.6, 771–776. DOI: 10.1111/j.1654-1103.2007.tb02593.x (cited on page 22).

Jones, C. G., J. H. Lawton, and M. Shachak (1994). "Organisms as Ecosystem Engineers." In: *Oikos* 69.3, p. 373. DOI: 10.2307/3545850 (cited on page 4).

Jonge, V. de, J. Bakker, and M. Stralen (1996). "Recent changes in the contributions of river Rhine and North Sea to the eutrophication of the western Dutch Wadden Sea." English. In: *Netherland Journal of Aquatic Ecology* 30.1, pp. 27–39. DOI: 10.1007/BF02092145 (cited on page 11).

Kamp, A., D. de Beer, J. L. Nitsch, G. Lavik, and P. Stief (2011). "Diatoms respire nitrate to survive dark and anoxic conditions." In: *Proceedings of the National Academy of Sciences* 108.14, pp. 5649–5654. DOI: 10.1073/pnas.1015744108 (cited on page 11).

Kang, C.-K., Y.-W. Lee, E. J. Choy, J.-K. Shin, I.-S. Seo, and J.-S. Hong (2006). "Microphytobenthos seasonality determines growth and reproduction in intertidal bivalves." English. In: *Marine Ecology Progress Series* 315, 113–127. DOI: 10.3354/meps315113 (cited on page 11).

Kaufmann, H., S. Förster, H. Wulf, K. Segl, L. Guanter, M. Bochow, U. Heiden, A. Müller, W. Heldens, T. Schneiderhan, P. Leitão, S. van der Linden, P. Hostert, J. Hill, H. Buddenbaum, W. Mauser, T. Hank, H. Krasemann, R. Röttgers, N. Oppelt, and B. Heim (2012). *Science Plan of the Environmental Mapping and Analysis Program (EnMAP)*. Tech. rep. Potsdam: Deutsches GeoForschungsZentrum GFZ (cited on page 21).

Kazemipour, F., P. Launeau, and V. Méléder (2012). "Microphytobenthos biomass mapping using the optical model of diatom biofilms: Application to hyperspectral images of Bourgneuf Bay." In: *Remote Sensing of Environment* 127, pp. 1–13. DOI: 10.1016/j.rse.2012.08.016 (cited on page 19).

Kazemipour, F., V. Méléder, and P. Launeau (2011). "Optical properties of microphytobenthic biofilms (MPBOM): Biomass retrieval implication." In: *Journal of Quantitative Spectroscopy and Radiative Transfer* 112.1, pp. 131–142. DOI: 10.1016/j.jqsrt.2010.08.029 (cited on page 19).

Kirk, J. T. O. (1994). *Light and photosynthesis in aquatic ecosystems*. Cambridge university press (cited on page 8).

Knoll, A. H. (2003). "The geological consequences of evolution." In: *Geobiology* 1.1, pp. 3–14. DOI: 10.1046/j.1472-4669.2003.00002.x (cited on page 3).

Kocak, D. M., F. R. Dalgleish, F. M. Caimi, and Y. Y. Schechner (2008). "A focus on recent developments and trends in underwater imaging." In: *Marine Technology Society Journal* 42.1, pp. 52–67. DOI: doi:10.4031/002533208786861209 (cited on page 21).

Koh, C.-H., J. S. Khim, H. Araki, H. Yamanishi, and K. Koga (2007). "Within-day and seasonal patterns of microphytobenthos biomass determined by co-measurement of sediment and water column chlorophylls in the intertidal mudflat of Nanaura, Saga, Ariake Sea, Japan." In: *Estuarine, Coastal and Shelf Science* 72.1-2, pp. 42–52. DOI: 10.1016/j.ecss.2006.10.005 (cited on page 8).

Kohls, K., R. M. M. Abed, L. Polerecky, M. Weber, and D. de Beer (2010). "Halotaxis of cyanobacteria in an intertidal hypersaline microbial mat." In: *Environmental microbiology* 12.3, pp. 567–75. DOI: 10.1111/j.1462-2920.2009.02095.x (cited on pages 8, 19).

Kolber, Z. and P. G. Falkowski (1993). "Use of active fluorescence to estimate phytoplankton photosynthesis in situ." In: *Limnology and Oceanography* 38.8, pp. 1646–1665. DOI: 10.4319/lo.1993.38.8.1646 (cited on page 15).

Krejci, M. and R. Lowe (1986). "Importance of sand grain mineralogy and topography in determining micro-spatial distribution of epipsammic diatoms." In: *Journal of the North American Benthological Society* 5.3, pp. 211–220 (cited on page 9).

Kromkamp, J. C., J. de Brouwer, G. F. Blanchard, R. M. Forster, and V. Créach, eds. (2006). *Functioning of microphytobenthos in estuaries*. Amsterdam: Royal Netherlands Academy of Arts and Sciences (cited on page 16).

Kromkamp, J. and J. Peene (1995). "Possibility of net phytoplankton primary production in the turbid Schelde Estuary (SW Netherlands)." In: *Marine Ecology Progress Series* 121, pp. 249–259. DOI: 10.3354/meps121249 (cited on page 9).

Kromkamp, J., J. Peene, P. Rijswijk, A. Sandee, and N. Goosen (1995). "Nutrients, light and primary production by phytoplankton and microphytobenthos in the eutrophic, turbid Westerschelde estuary (The Netherlands)." In: *Hydrobiologia* 311.1-3, pp. 9–19. DOI: 10.1007/BF00008567 (cited on page 9).

Kromkamp, J., C. Barranguet, and J. Peene (1998). "Determination of microphytobenthos PSII quantum efficiency and photosynthetic activity by means of variable chlorophyll fluorescence." In: *Marine Ecology Progress Series* 162, pp. 45–55. DOI: 10.3354/meps162045 (cited on page 16).

Kühl, M., R. N. Glud, J. Borum, R. Roberts, and S. Rysgaard (2001). "Photosynthetic performance of surface-associated algae below sea ice as measured with a pulse amplitude-modulated (PAM) fluorometer and O2 microsensors." In: *Marine Ecology Progress Series* 223, pp. 1–14. DOI: 10.3354/meps223001 (cited on page 13).

Kühl, M. and B. B. Jørgensen (1994). "The light field of microbenthic communities: radiance distribution and microscale optics of sandy coastal sediments." In: *Limnology and Oceanography* 39.6, pp. 1368–1398. DOI: 10.4319/lo.1994.39.6.1368 (cited on pages 9, 19).

Kühl, M., C. Lassen, and B. B. Jørgensen (1994). "Light penetration and light intensity in sandy marine sediments measured with irradiance and scalar irradiance fiberoptic microprobes Rid A-1977-2009." In: *Marine Ecology Progress Series* 1.2, pp. 139–148 (cited on page 9).

Kühl, M. and L. Polerecky (2008). "Functional and structural imaging of phototrophic microbial communities and symbioses." In: *Aquatic Microbial Ecology* 53, pp. 99–118. DOI: doi:10.3354/ame01224 (cited on page 19).

Larson, C. A. and S. I. Passy (2012). "Taxonomic and functional composition of the algal benthos exhibits similar successional trends in response to nutrient supply and current velocity." In: *FEMS Microbiology*

Ecology 80.2, pp. 352–362. DOI: 10.1111/j.1574-6941.2012.01302.x (cited on page 12).

Lassen, C., H. Ploug, and B. B. Jørgensen (1992). "Microalgal photosynthesis and spectral scalar irradiance in coastal marine sediments of Limfjorden, Denmark." In: *Limnology and Oceanography* 37.4, pp. 760–772. DOI: 10.4319/lo.1992.37.4.0760 (cited on page 9).

Levin, S. (1992). "The problem of pattern and scale in ecology: the Robert H. MacArthur award lecture." In: *Ecology* 73.6, pp. 1943–1967. DOI: 10.2307/1941447 (cited on pages 6, 22).

Levinton, J. (1995). "Bioturbators as ecosystem engineers: Control of the sediment fabric, inter-individual interactions, and material fluxes." English. In: *Linking Species & Ecosystems*. Ed. by C. G. Jones and J. H. Lawton. Springer US, pp. 29–36. DOI: 10.1007/978-1-4615-1773-3_3 (cited on page 4).

Lindeman, R. L. (1942). "The trophic-dynamic aspect of ecology." In: *Ecology* 23.4, pp. 399–417. DOI: 10.2307/1930126 (cited on page 3).

Longhurst, A., S. Sathyendranath, T. Platt, and C. Caverhill (1995). "An estimate of global primary production in the ocean from satellite radiometer data." In: *Journal of Plankton Research* 17.6, pp. 1245–1271. DOI: 10.1093/plankt/17.6.1245 (cited on page 5).

Lorenzen, C. (1967). "Determination of chlorophyll and pheo-pigments: spectrophotometric equations." In: *Limnology and Oceanography* 12.2, pp. 343–346. DOI: 10.4319/lo.1967.12.2.0343 (cited on page 14).

MacIntyre, H., R. Geider, and D. Miller (1996). "Microphytobenthos: The ecological role of the "secret garden" of unvegetated, shallow-water marine habitats. I. Distribution, abundance and primary production." In: *Estuaries and Coasts* 19.2, pp. 186–201. DOI: 10.2307/1352224 (cited on pages 6–8, 10, 14, 22).

MacIntyre, J., J. Cullen, and A. Cembella (1997). "Vertical migration, nutrition and toxicity in the dinoflagellate *Alexandrium tamarense*." In: *Marine Ecology Progress Series* 148, pp. 201–216. DOI: 10.3354/meps148201 (cited on page 9).

McCave, I. N. (1976). *The Benthic Boundary Layer*. Ed. by I. N. McCave. Springer US. DOI: 10.1007/978-1-4615-8747-7 (cited on page 4).

Méléder, V., P. Launeau, L. Barillé, and J.-P. Combe (2010). "Hyperspectral imaging for mapping microphytobenthos in coastal areas." In: *Geomatic Solutions For Coastal Environments*. Ed. by M. Maanan and M. Robin. Nova Science Publishers Inc., pp. 71–139 (cited on page 19).

Miller, D., R. Geider, and H. MacIntyre (1996). "Microphytobenthos: the ecological role of the "secret garden" of unvegetated, shallow-water marine habitats. II. Role in sediment stability and shallow-water food

webs." In: *Estuaries and Coasts* 19.2A, pp. 202–212. DOI: 10.2307/1352225 (cited on pages 6, 22).

Mitbavkar, S. and A. C. Anil (2002). "Diatoms of the microphytobenthic community: population structure in a tropical intertidal sand flat." In: *Marine Biology* 140.1, pp. 41–57. DOI: 10.1007/s002270100686 (cited on page 8).

— (2004). "Vertical migratory rhythms of benthic diatoms in a tropical intertidal sand flat: influence of irradiance and tides." In: *Marine Biology* 145.1, pp. 9–20. DOI: 10.1007/s00227-004-1300-3 (cited on page 7).

Montagna, P. A. (1984). "In situ measurement of meiobenthic grazing rates on sediment bacteria and edaphic diatoms." In: *Marine Ecology Progress Series* 18.1, pp. 119–130 (cited on page 7).

Murphy, R. J., T. J. Tolhurst, M. G. Chapman, and A. J. Underwood (2005). "Estimation of surface chlorophyll-a on an emersed mudflat using field spectrometry: accuracy of ratios and derivative-based approaches." In: *International Journal of Remote Sensing* 26.9, pp. 1835–1859. DOI: 10.1080/01431160512331326530 (cited on pages 18 sq.).

Al-Najjar, M. A. A., D. de Beer, M. Kühl, and L. Polerecky (2012). "Light utilization efficiency in photosynthetic microbial mats." In: *Environmental Microbiology* 14.4, pp. 982–92. DOI: 10.1111/j.1462-2920.2011.02676.x (cited on pages 7, 9).

Neu, T. R., B. Manz, F. Volke, J. J. Dynes, A. P. Hitchcock, and J. R. Lawrence (2010). "Advanced imaging techniques for assessment of structure, composition and function in biofilm systems." In: *FEMS microbiology ecology* 72.1, pp. 1–21. DOI: 10.1111/j.1574-6941.2010.00837.x (cited on page 14).

Nozais, C., R. Perissinotto, and S. Mundree (2001). "Annual cycle of microalgal biomass in a South African temporarily-open estuary: nutrient versus light limitation." In: *Marine Ecology Progress Series* 223, pp. 39–48. DOI: doi:10.3354/meps223039 (cited on page 9).

Palmer, J. D. and F. E. Round (1967). "Persistent, vertical-migration rhythms in benthic microflora. VI. The tidal and diurnal nature of the rhythm in the diatom *Hantzschia virgata*." In: *The Biological Bulletin* 132.1, pp. 44–55. DOI: 10.1017/S0025315400017641 (cited on page 7).

Palmisano, A. C., J. B. SooHoo, and C. W. Sullivan (1985). "Photosynthesis-irradiance relationships in sea ice microalgae from McMurdo Sound, Antarctica." In: *Journal of Phycology* 21.3, pp. 341–346. DOI: 10.1111/j.0022-3646.1985.00341.x (cited on page 9).

Paterson, D. M. (1986). "The migratory behaviour of diatom assemblages in a laboratory tidal micro-ecosystem examined by low temperature scanning electron microscopy." In: *Diatom Research* 1.2, pp. 227–239. DOI: 10.1080/0269249X.1986.9704971 (cited on page 7).

Paterson, D. M. (1994). "Microbiological mediation of sediment structure and behaviour." English. In: *Microbial Mats*. Ed. by L. Stal and P. Caumette. Vol. 35. NATO ASI Series. Springer Berlin Heidelberg, pp. 97–109. DOI: 10.1007/978-3-642-78991-5_11 (cited on pages 9 sq.).

Perkins, R., J. Kromkamp, J. Serôdio, J. Lavaud, B. Jesus, J. Mouget, S. Lefebvre, and R. Forster (2010). "The application of variable chlorophyll fluorescence to microphytobenthic biofilms." English. In: *Chlorophyll a Fluorescence in Aquatic Sciences: Methods and Applications*. Ed. by D. J. Suggett, O. Prášil, and M. A. Borowitzka. Vol. 4. Developments in Applied Phycology. Springer Netherlands, pp. 237–275. DOI: 10.1007/978-90-481-9268-7_12 (cited on page 16).

Pinckney, J. and R. Sandulli (1990). "Spatial autocorrelation analysis of meiofaunal and microalgal populations on an intertidal sandflat: Scale linkage between consumers and resources." In: *Estuarine, Coastal and Shelf Science* 30.4, pp. 341–353. DOI: 10.1016/0272-7714(90)90002-9 (cited on page 12).

Pinckney, J. and R. Zingmark (1991). "Effects of tidal stage and sun angles on intertidal benthic microalgal productivity." In: *Marine Ecology Progress Series* 76, pp. 81–89. DOI: 10.3354/meps076081 (cited on page 9).

Pinckney, J. L., H. Paerl, and M. Fitzpatrick (1995). "Impacts of seasonality and nutrients on microbial mat community structure and function." In: *Marine Ecology Progress Series* 123, p. 207. DOI: 10.3354/meps123207 (cited on page 8).

Polerecky, L., A. Bissett, M. Al-Najjar, P. Färber, H. Osmers, P. A. Suci, P. Stoodley, and D. de Beer (2009a). "Modular spectral imaging (MOSI) system for discrimination of pigments in cells and microbial communities." In: *Applied and Environmental Microbiology* 75.3, pp. 1–9. DOI: 10.1128/AEM.00819-08 (cited on pages 19–21).

Polerecky, L., U. Franke, U. Werner, B. Grunwald, and D. de Beer (2005). "High spatial resolution measurement of oxygen consumption rates in permeable sediments." In: *Limnology and Oceanography: Methods* 3, pp. 75–85. DOI: 10.4319/lom.2005.3.75 (cited on page 13).

Polerecky, L., J. M. Klatt, M. A. A. Al-Najjar, and D. de Beer (2009b). "Hyper-spectral imaging of biofilm growth dynamics." In: *Hyperspectral Image and Signal Processing: Evolution in Remote Sensing. WHISPERS '09.* Pp. 1–4 (cited on page 20).

Porra, R. J., W. A. Thompson, and P. E. Kriedemann (1989). "Determination of accurate extinction coefficients and simultaneous equations for assaying chlorophylls a and b extracted with four different solvents: verification of the concentration of chlorophyll standards by atomic absorption spectroscopy." In: *Biochimica et Biophysica Acta* 975, pp. 384–394 (cited on page 18).

Precht, E., U. Franke, L. Polerecky, and M. Huettel (2004). "Oxygen dynamics in permeable sediments with wave-driven pore water exchange." In: *Limnology and Oceanography* 49.3, pp. 693–705. DOI: 10.4319/lo.2004.49.3.0693 (cited on page 11).

Precht, E. and M. Huettel (2003). "Advective pore-water exchange driven by surface gravity waves and its ecological implications." In: *Limnology and Oceanography* 48.4, pp. 1674–1684. DOI: 10.4319/lo.2003.48.4.1674 (cited on page 11).

Preez, D. R. du, E. E. Campbell, and G. C. Bate (1990). "Photoinhibition of photosynthesis in the surf diatom, *Anaulus australis Drebes et Schulz*." In: *Botanica Marina* 33.6, pp. 539–544. DOI: 10.1515/botm.1990.33.6.539 (cited on page 9).

Pringault, O. and F. Garcia-Pichel (2004). "Hydrotaxis of cyanobacteria in desert crusts." In: *Microbial ecology* 47.4, pp. 366–73. DOI: 10.1007/s00248-002-0107-3 (cited on page 8).

Reay, W. G., D. l. Gallagher, and G. M. Simmons (1995). "Sediment-water column oxygen and nutrient fluxes in nearshore environments of the lower Delmarva Peninsula, USA." In: *Marine Ecology Progress Series* 118.1-3, 215–227. DOI: 10.3354/meps118215 (cited on page 11).

Revsbech, N. P. and B. B. Jørgensen (1986). "Microelectrodes: their use in microbial ecology." In: *Advances in Microbial Ecology* 9, pp. 293–352. DOI: 10.1007/978-1-4757-0611-6_7 (cited on page 13).

Revsbech, N. P., B. B. Jørgensen, T. H. Blackburn, and Y. Cohen (1983). "Microelectrode studies of the photosynthesis and O_2, H_2S, and pH profiles of a microbial mat." In: *Limnology and Oceanography* 28.6, pp. 1062–1074. DOI: 10.4319/lo.1983.28.6.1062 (cited on page 13).

Rodgers, J. H. and R. S. Harvey (1976). "The effect of current on periphytic productivity as determined using carbon-14." In: *Journal of the American Water Resources Association* 12.6, pp. 1109–1118. DOI: 10.1111/j.1752-1688.1976.tb00247.x (cited on page 11).

Round, F. E. (1971). "Benthic marine diatoms." In: *Oceanography and Marine Biology: an annual review*. Vol. 9. Aberdeen University Press, pp. 83–139 (cited on page 9).

Round, F. E. (1979). "A diatom assemblage living below the surface of intertidal sand flats." In: *Marine Biology* 54.3, pp. 219–223. DOI: 10.1007/BF00395784 (cited on page 7).

Rouse, J. W., R. H. Haas, S. J. A, and D. D. W (1973). "Monitoring vegetation systems in the Great Plains with ERTS." In: *Proceedings of the third ERTS Symposium*. Vol. 1. SP-351. Washington DC: NASA (cited on page 17).

Rysgaard, S., P. Christensen, L. Nielsen, et al. (1995). "Seasonal variation in nitrification and denitrification in estuarine sediment colonized

by benthic microalgae and bioturbating infauna." In: *Marine Ecology Progress Series* 126.1, pp. 111–121. DOI: 10.3354/meps126111 (cited on page 11).

Sabol, D. E., M. Smith, J. B. Adams, A. R. Gillespie, and C. J. Tucker (1996). "Monitoring forest regrowth using a multi-platform time series." In: *Summaries of the 6 annual JPL Airborne Earth Science Workshop*. Vol. 1. JPL Pub: 96-4. AVIRIS Workshop, Jet Propulsion Laboratory, California Institute of Technology, Pasadena, California, pp. 203–208 (cited on page 17).

Schreiber, U. (1986). "Detection of rapid induction kinetics with a new type of high-frequency modulated chlorophyll fluorometer." English. In: *Current Topics In Photosynthesis*. Ed. by J. Amesz, A. Hoff, and H. Gorkum. Springer Netherlands, pp. 259–270. DOI: 10.1007/978-94-009-4412-1_24 (cited on page 15).

Schreiber, U., W. Bilger, and C. Neubauer (1994). "Chlorophyll fluorescence as a nonintrusive indicator for rapid assessment of in vivo photosynthesis." In: *Ecophysiology Of Photosynthesis*. Springer, pp. 49–70. DOI: 10.1007/978-3-642-79354-7_3 (cited on page 15).

Schreiber, U. (2004). "Pulse-amplitude-modulation (PAM)) fluorometry and saturation pulse method: an overview." In: *Chlorophyll a Fluorescence*. Ed. by G. Papageorgiou and Govindjee. Vol. 19. Advances in Photosynthesis and Respiration. Springer Netherlands, pp. 279–319. DOI: 10.1007/978-1-4020-3218-9_11 (cited on page 15).

Serôdio, J., J. Ezequiel, A. Barnett, V. Méléder, M. Laviale, and J. Lavaud (2012). "Efficiency of photoprotection in microphytobenthos: role of vertical migration and the xanthophyll cycle against photoinhibition." In: *Aquatic Microbial Ecology* 67.2, pp. 161–175. DOI: 10.3354/ame01591 (cited on page 15).

Serôdio, J., J. Ezequiel, J. Frommlet, M. Laviale, and J. Lavaud (2013). "A method for the rapid generation of nonsequential light-response curves of chlorophyll fluorescence." In: *Plant Physiology* 163.3, pp. 1089–1102. DOI: 10.1104/pp.113.225243 (cited on page 15).

Serôdio, J., J. Marques da Silva, and F. Catarino (1997). "Non-destructive tracing of migratory rhythms of intertidal benthic microalgae using in vivo chlorophyll a fluorescence." In: *Journal of Phycology* 33.3, pp. 542–553. DOI: 10.1111/j.0022-3646.1997.00542.x (cited on pages 15 sq.).

Seuront, L. and S. Leterme (2006). "Microscale patchiness in microphytobenthos distributions: evidence for a critical state." In: *Functioning Of Microphytobenthos In Estuaries*. Ed. by J. C. Kromkamp, J. de Brouwer, G. F. Blanchard, R. M. Forster, and V. Créach. Royal Netherlands Academy of Arts and Sciences, pp. 167–186 (cited on pages 7, 22).

Sinclair, M. B., D. M. Haaland, J. A. Timlin, and H. D. Jones (2006). "Hyperspectral confocal microscope." In: *Applied Optics* 45.24, pp. 6283–6291. DOI: 10.1364/AO.45.006283 (cited on pages 14, 17).

Skov, M., M. Volkelt-Igoe, S. Hawkins, B. Jesus, R. Thompson, and C. Doncaster (2010). "Past and present grazing boosts the photo-autotrophic biomass of biofilms." In: *Marine Ecology Progress Series* 401, pp. 101–111. DOI: 10.3354/meps08481 (cited on page 12).

Spilmont, N., D. Davoult, and A. Migné (2006). "Benthic primary production during emersion: In situ measurements and potential primary production in the Seine Estuary (English Channel, France)." In: *Marine pollution bulletin* 53.1-4, pp. 49–55. DOI: 10.1016/j.marpolbul.2005.09.016 (cited on page 8).

Spilmont, N., L. Seuront, T. Meziane, and D. T. Welsh (2011). "There's more to the picture than meets the eye: Sampling microphytobenthos in a heterogeneous environment." In: *Estuarine, Coastal and Shelf Science* 95.4, pp. 470–476. DOI: 10.1016/j.ecss.2011.10.021 (cited on pages 14, 22).

Spinetti, C., V. Carrère, F. Buongirono, A. Jefferson Sutton, and E. Tamar (2008). "Carbon dioxide of Pu'u'O'o volcanic plume at Kilauea retrieved by AVIRIS hyperspectral data," in: *Remote Sensing of Environment* 112, pp. 3192–3199. DOI: 10.1016/j.rse.2008.03.010 (cited on page 17).

Stal, L. J. (1995). "Physiological ecology of cyanobacteria in microbial mats and other communities." In: *New Phytologist* 131, pp. 1–32. DOI: 10.1111/j.1469-8137.1995.tb03051.x (cited on page 7).

— (2010). "Microphytobenthos as a biogeomorphological force in intertidal sediment stabilization." In: *Ecological Engineering* 36.2, pp. 236–245. DOI: 10.1016/j.ecoleng.2008.12.032 (cited on pages 10 sq.).

Storrie-Lombardi, M. C. and B. Sattler (2009). "Laser-induced fluorescence emission (LIFE): in situ nondestructive detection of microbial life in the ice covers of Antarctic lakes." In: *Astrobiology* 9.7, pp. 659–672. DOI: 10.1089/ast.2009.0351 (cited on page 14).

Sundbäck, K. and K. McGlathery (2013). "Interactions between benthic macroalgal and microalgal mats." In: *Interactions Between Macro- and Microorganisms in Marine Sediments*. American Geophysical Union, pp. 7–29. DOI: 10.1029/CE060p0007 (cited on page 12).

Sundbäck, K., P. Nilsson, C. Nilsson, and B. Jönsson (1996). "Balance between autotrophic and heterotrophic components and processes in microbenthic communities of sandy sediments: a field study." In: *Estuarine, Coastal and Shelf Science* 43.6, pp. 689–706. DOI: 10.1006/ecss.1996.0097 (cited on page 12).

Therkildsen, M. S. and B. A. Lomstein (1993). "Seasonal variation in net benthic C-mineralization in a shallow estuary." In: *FEMS Microbiology Ecology* 12.2, pp. 131–142 (cited on page 8).

Ubertini, M., S. Lefebvre, A. Gangnery, K. Grangeré, R. Le Gendre, and F. Orvain (2012). "Spatial variability of benthic-pelagic coupling in an estuary ecosystem: consequences for microphytobenthos resuspension phenomenon." In: *PLoS ONE* 7.8, e44155. DOI: 10.1371/journal.pone.0044155 (cited on pages 8, 10 sq.).

Underwood, A. J., M. G. Chapman, and S. D. Connell (2000). "Observations in ecology: you can't make progress on processes without understanding the patterns." In: *Journal of Experimental Marine Biology and Ecology* 250.1-2, pp. 97–115. DOI: 10.1016/S0022-0981(00)00181-7 (cited on page 22).

Underwood, G. J. C. and M. Barnett (2006). "What determines species composition in microphytobenthic biofilms?" In: *Functioning Of Microphytobenthos In Estuaries*. Ed. by J. C. Kromkamp. Vol. 103. Proceedings of the Colloquium, Amsterdam, 21-23 August 2003. Royal Netherlands Academy of Arts and Sciences, pp. 123–140 (cited on page 10).

Underwood, G. and J. Kromkamp (1999). "Primary production by phytoplankton and microphytobenthos in estuaries." In: *Estuaries*. Ed. by D. Nedwell and D. Raffaelli. Vol. 29. Advances in Ecological Research. Academic Press, pp. 93–153. DOI: 10.1016/S0065-2504(08)60192-0 (cited on pages 6, 8).

Underwood, G. (2002). "Adaptations of tropical marine microphytobenthic assemblages along a gradient of light and nutrient availability in Suva Lagoon, Fiji." In: *European Journal of Phycology* 37.3, pp. 449–462. DOI: 10.1017/S0967026202003785 (cited on pages 8 sq.).

Underwood, G. J. C. (1994). "Seasonal and spatial variation in epipelic diatom assemblages in the Severn estuary." In: *Diatom Research* 9.2, pp. 451–472. DOI: 10.1080/0269249X.1994.9705319 (cited on pages 8, 22).

Underwood, G. J. C. and D. M. Paterson (1993). "Seasonal changes in diatom biomass, sediment stability and biogenic stabilization in the Severn Estuary." In: *Journal of the Marine Biological Association of the United Kingdom* 73.04, p. 871. DOI: 10.1017/S0025315400034780 (cited on pages 8, 10).

Underwood, G., J. Phillips, and K. Saunders (1998). "Distribution of estuarine benthic diatom species along salinity and nutrient gradients." In: *European Journal of Phycology* 33.2, pp. 173–183. DOI: 10.1080/09670269810001736673 (cited on page 11).

Volkenborn, N., L. Polerecky, D. S. Wethey, and S. A. Woodin (2010). "Oscillatory porewater bioadvection in marine sediments induced by hydraulic activities of *Arenicola marina*." In: *Limnology and Oceanography*

55.3, pp. 1231–1247. DOI: 10.4319/lo.2010.55.3.1231 (cited on page 11).

Vopel, K. and I. Hawes (2006). "Photosynthetic performance of benthic microbial mats in Lake Hoare, Antarctica." In: *Limnology and Oceanography* 51.4, pp. 1801–1812. DOI: 10.4319/lo.2006.51.4.1801 (cited on page 9).

Walter, M. R., R. Buick, and J. S. R. Dunlop (1980). "Stromatolites 3,400–3,500 Myr old from the North Pole area, Western Australia." In: *Nature* 284.5755, pp. 443–445. DOI: 10.1038/284443a0 (cited on page 6).

Wennhage, H. and L. Pihl (1994). "Substratum selection by juvenile plaice *Pleuronectes platessa L.*: Impact of benthic microalgae and filamentous macroalgae." In: *Netherlands Journal of Sea Research* 32.3-4, pp. 343–351. DOI: 10.1016/0077-7579(94)90011-6 (cited on page 12).

Wethey, D. S., S. A. Woodin, N. Volkenborn, and K. Reise (2008). "Porewater advection by hydraulic activities of lugworms, *Arenicola marina*: A field, laboratory and modeling study." In: *Journal of Marine Research* 66.2, pp. 255–273. DOI: 10.1357/002224008785837121 (cited on page 11).

Wetsteyn, L. P. M. J. and J. C. Kromkamp (1994). "Turbidity, nutrients and phytoplankton primary production in the Oosterschelde (The Netherlands) before, during and after a large-scale coastal engineering project (1980–1990)." In: *Hydrobiologia* 282-283.1, pp. 61–78. DOI: 10.1007/BF00024622 (cited on page 9).

Whitney, D. E. and W. M. Darley (1979). "A method for the determination of chlorophyll a in samples containing degradation products." In: *Limnology and Oceanography* 24.1, pp. 183–186. DOI: 10.4319/lo.1979.24.1.0183 (cited on page 14).

Xinling, Z., W. Zengmao, L. Jie, Y. Guangyao, Z. Zhinan, and G. Shanhong (2006). "Modeling study of seasonal variation of the pelagic-benthic ecosystem characteristics of the Bohai Sea." English. In: *Journal of Ocean University of China* 5.1, pp. 21–28. DOI: 10.1007/BF02919368 (cited on page 8).

Yallop, M. L., B. de Winder, D. M. Paterson, and L. J. Stal (1994). "Comparative structure, primary production and biogenic stabilization of cohesive and non-cohesive marine sediments inhabited by microphytobenthos." In: *Estuarine, Coastal and Shelf Science* 39.6, pp. 565–582. DOI: 10.1016/S0272-7714(06)80010-7 (cited on page 7).

Part II

DOCTORAL RESEARCH

OVERVIEW OF CHAPTERS

The doctoral dissertation is a cumulative thesis consisting of the complete versions of three manuscripts prepared for publication in international journals (Chapters 2, 3 and 4) and the abstract of a manuscript in preparation (Chapter 5). Of these, one is already published, one is under review, one is ready for submission and one is in preparation.

Chapter 2 – HYPERSPECTRAL IMAGING OF THE MICROSCALE DISTRIBUTION AND DYNAMICS OF MICROPHYTOBENTHOS IN INTERTIDAL SEDIMENTS

Arjun Chennu, Paul Färber, Nils Volkenborn, Mohammad A.A. Al-Najjar, Felix Janssen, Dirk de Beer and Lubos Polerecky

See Author contributions

Published in *Limnology and Oceanography: Methods* 2013, vol. 11, pp. 511–528.

Chapter 3 – THE GARDENING LUGWORM: BIOADVECTION BY ARENICOLA MARINA AND ITS FERTILIZING EFFECT ON MICROPHYTOBENTHOS AT THE SEDIMENT SURFACE

Arjun Chennu, Nils Volkenborn, Dirk de Beer, David S. Wethey, Sarah A. Woodin and Lubos Polerecky

See Author contributions

Submitted to *Limnology and Oceanography*, November 2013

Chapter 4 – CYANOBACTERIA RESURRECTED: RAPID REACTIVATION OF PHOTOSYNTHESIS UPON REHYDRATION OF DESICCATED MICROBIAL MATS

Arjun Chennu, Alistair Grinham and Mohammad A.A. Al-Najjar

See Author contributions

Prepared for submission to *Environmental Microbiology*

Chapter 5 – WILL AN UPWARD SHIFT OF THE TEMPERATURE BASELINE CHANGE BIOMASS GROWTH OF SUB-ARCTIC (SVALBARD, KONGSFJORDEN) AND TEMPERATE (NORTH SEA, HELGOLAND) MICROPHYTOBENTHOS COMMUNITIES? A QUANTITATIVE PILOT-STUDY

Duygu S. Sevilgen, Arjun Chennu and Tom Brey

See Author contributions

In preparation for *Polar Biology*

2

HYPERSPECTRAL IMAGING OF THE MICROSCALE DISTRIBUTION AND DYNAMICS OF MICROPHYTOBENTHOS IN INTERTIDAL SEDIMENTS

Arjun Chennu[1], Paul Färber[1], Nils Volkenborn[2,3], Mohammad A.A. Al-Najjar[1,4], Felix Janssen[1,5], Dirk de Beer[1] and Lubos Polerecky[1,6]

See Author contributions

MANUSCRIPT STATUS

Published as A. Chennu et al. (2013). "Hyperspectral imaging of the microscale distribution and dynamics of microphytobenthos in intertidal sediments." In: *Limnology and Oceanography: Methods* 11, pp. 511–528. DOI: 10.4319/lom.2013.11.511

2.1 ABSTRACT

We describe a novel, field-deployable hyperspectral imaging system, called Hypersub, that allows non-invasive *in situ* mapping of the microphytobenthos (MPB) biomass distribution with a high spatial (sub-millimeter) and temporal (minutes) resolution over areas of 1×1 m. The biomass is derived from a log-transformed and near-infrared corrected reflectance hyperspectral index, which exhibits a linear relationship (R^2>0.97) with the Chlorophyll *a* (Chl *a*) concentration in the euphotic zone of the sediment and depends on the sediment grain size. Deployments of the system revealed that due to factors such as sediment topography, bioturbation and grazing, the distribution of MPB in intertidal sediments is remarkably heterogeneous, with Chl *a* concentrations varying laterally by up to 400% of the average value over a distance of 1 cm. Furthermore, due to tidal cycling and diel light variability, MPB concentrations in the top 1 mm of sediments are very dynamic, changing by 40–80% over a few hours due to

1 Max Planck Institute for Marine Microbiology, Celsiusstrasse 1, Bremen 28359, Germany
2 Dept. of Biological Sciences, University of South Carolina, Columbia SC 29208, USA
3 IFREMER, Laboratory of Benthic Ecology, Technopole Brest BP70, Plouzane, France
4 Red Sea Research Center, King Abdullah University of Science and Technology, Saudi Arabia
5 Alfred Wegener Institute for Polar and Marine Research, Am Handelshafen 12, 27570 Bremerhaven, Germany
6 Dept. of Earth Sciences - Geochemistry, Utrecht University, Budapestlaan 4, 3584 CD Utrecht, The Netherlands

vertical migration. We argue that the high-resolution hyperspectral imaging method overcomes the inadequate resolution of traditional methods based on sedimentary Chlorophyll *a* extraction, and thus helps improve our understanding of the processes that control benthic primary production in coastal sediments.

2.2 INTRODUCTION

Microphytobenthos (MPB), consisting of benthic phototrophs such as microalgae, cyanobacteria and dinoflagellates, is the fundament of the trophic food web in coastal ecosystems. In shallow-water environments, such as intertidal flats and estuaries, MPB represents a considerable portion of the autotrophic biomass, accounting for up to 50% of the primary (MacIntyre et al., 1996; Nozais et al., 2001; Spilmont et al., 2006). MPB is the predominant food source for many deposit-feeding organisms, and the activity and distribution of MPB profoundly affect nutrient fluxes across the sediment-water interface, sediment geochemistry, as well as sediment morphology and stability (Miller et al., 1996; Montagna et al., 1995; Stal, 2010; Sundbäck et al., 1991).

The spatio-temporal organization of a community is a prominent issue in ecology. Levin (1992) argued that analysis of large-scale (regional) patterns must integrate effects occurring at smaller scales. Generally, the distribution of MPB is affected by both abiotic processes (e.g., nutrient availability, hydrodynamic exposure, sediment type) and biotic processes (e.g., grazing, competition) through a complex network of interactions. In their reductionist approach to benthic ecology, Miller et al. (1996) argued that studies of interactions with a direct effect on the MPB distribution (so called "isolated first-order interactions") are required to disentangle the complex relationships between the sediment bed, infaunal organisms and the water column, and for a comprehensive picture of shallow-water ecosystems to emerge. The small scale of perception (which relates to the body size) and short generation times of the organisms are thought to lead to a high degree of spatio-temporal variability for MPB (Azovsky et al., 2004), and several studies emphasized the importance of gathering quantitative data on MPB distributions at a sub-millimeter scale (Murphy et al., 2008; Seuront et al., 2002; Underwood et al., 2000), which is in the range of perception of the MPB organisms. However, most previous work was generally unable to resolve the spatial variability in MPB distributions below the decimeter range (5–10 cm) (Moreno and Niell, 2004; Seuront and Leterme, 2006; Spilmont et al., 2011).

MPB biomass is considered a basic environmental descriptor in benthic studies (Bale and Kenny, 2007), and is estimated through the measurement of Chlorophyll *a* (Chl *a*) concentrations in surficial sediments. This is typically done by collecting sediment cores from the field site and measuring absorbance or autofluorescence of Chl *a* extracted from the sediment

using a solvent (Lorenzen, 1967; Whitney and Darley, 1979). This procedure, although time-consuming and labor-intensive, has been widely used to estimate the spatial structure and temporal dynamics of MPB biomass (Brito et al., 2009b; Guarini and Blanchard, 1998; Spilmont et al., 2011). A troubling feature of this method has been the lack of standardization of the protocol involved, such as sampling core diameter, sampling depth, the number of replicates, or the extraction solvent, which makes it challenging to compare results of different studies (Brito et al., 2009a; Grinham et al., 2007). A further disadvantage of the method is that it is destructive and does not allow repetitive measurements at the same location.

Recently, optical methods have been explored as alternatives to extractive methods for Chl *a* quantification in sediments. They provide the potential to measure rapidly enough to capture the MPB biomass distribution within the relevant spatial (mm) and temporal (min) scale, and have the additional advantage of being essentially non-invasive (reviewed by Kühl and Polerecky (2008)).

One approach of optical Chl *a* quantification in sediments is based on the measurement of in vivo auto-fluorescence. Although this approach offers high sensitivity and high signal-to-noise ratio (Serôdio et al., 1997), it is encumbered by practical difficulties such as the requirement of dark (or low-light) adaptation of the measured MPB community Honeywill et al. (2002), Jesus et al. (2005), and Jesus et al. (2006).

An alternative approach for optical Chl *a* quantification in sediments is reflectance spectrometry, which is based on the measurement of light back-scattered from the sediment at wavelengths around 675 nm, i.e., the wavelength of maximal *in vivo* Chl *a* absorption (Hakvoort et al., 1997). One implementation of this approach uses a spectrometer with hyperspectral resolution to collect light back-scattered from several square centimeters of the sediment's surface (Forster and Jesus, 2006; Kromkamp et al., 2006). Although successfully applied in the field, the fact that this approach is essentially a single-point measurement makes it impractical for achieving a sub-millimeter spatial resolution across larger areas. To improve the spatial resolution, Murphy et al. (2005, 2009) used color-infrared cameras for the detection of back-scattered light in three wavelength bands, including near-infrared light. Although this imaging approach decreased the spatial resolution to about 0.5 mm, the lack of spectral resolution is an impediment to the spectrometric analysis of the sediment reflectance, which undergoes subtle variations depending on the sediment type or the MPB composition, and may therefore influence the interpretation of results (Barillé et al., 2011; Kazemipour et al., 2011).

The capture of back-scattered light with simultaneously high spatial and spectral resolution has been enabled by using hyperspectral cameras. As shown by Polerecky et al. (2009a), this approach can be used for pigment identification, localization and relative quantification on scales ranging from single cells to whole microbial communities. This versatility is achieved by simply changing the optical arrangement (i.e., microscope vs.

different types of lenses) in front of the camera. This system greatly facilitated studies on the structure and composition of benthic photosynthetic microbial communities such as microbial mats (Bachar et al., 2008; Kohls et al., 2010; Al-Najjar et al., 2012), biofilms (Ionescu et al., 2012; Kühl and Polerecky, 2008; Polerecky et al., 2009b) or modern stromatolites (Farías et al., 2013). However, hyperspectral imaging at a high (sub-millimeter) spatial resolution has so far been limited to laboratory-based measurements across relatively small areas (few squared centimeters).

This study describes a novel hyperspectral imaging system for *in situ* quantification of pigments in benthic ecosystems. The system, called Hypersub, is an adaptation of the system developed by Polerecky et al. (2009a), and enables field-based, remotely-operable and underwater spectral reflectance measurements with sub-millimeter resolution over areas of about one squared-meter. The hyperspectral resolution (~1 nm) enables a variety of spectrometric analyses, including the quantification of the concentration of Chlorophyll *a* and other photopigments in sediments. We used artificial biofilms for the calibration and validation of the system against a well-established method based on pigment extraction and spectrophotometry. We then used Hypersub to study the spatio-temporal variations of Chl *a* in surficial sediments of intertidal sandflats, such as those associated with sediment topography, sediment bioturbation, and vertical migration of MPB linked to tidal and diel light cycles.

2.3 MATERIALS AND PROCEDURES

2.3.1 *Hardware Components*

The primary components of the submersible hyperspectral imaging system Hypersub are two imagers, imaging optics and control electronics, all enclosed in an underwater housing mounted on a mechanical sledge (Figure 2.1A–B). Additional components include a pair of halogen lamps (BLV Whitestar 5000–6500 K) for supplementary illumination, a motorized sledge for moving the cameras across the imaged area, and an on-board battery pack. The mechanical sledge is driven along a threaded stainless-steel rail by a motor that can also be used underwater, and allows scanning across a distance of 1 m at a maximal velocity of about 3 mm s^{-1}. Combined with the view of the imaging optics, the maximum size of the scanning area is about 1×1 m.

The first imager, a hyperspectral camera (PIKA-II; Resonon Inc.), is used to resolve and capture back-reflected light in 480 spectral bands (bandwidth of ~1 nm) across the range of wavelengths from blue (400 nm) to near-infrared (900 nm). The imager is a line camera that directs incoming light from each spectral band onto a measuring line of 640 pixels, which can be considered as the "line of view". The second imager (Guppy; Allied Vision Technologies GmbH) is a standard monochrome

camera and is used to record the scanned region as gray-scale images of visible light intensity. Both imagers provide a firewire port (IEEE 1394) as the electronic interface to the control system, which is also used to transfer the acquired image data to a storage device. These components are sealed inside an underwater housing (rated to a depth of 75 m) with an optical window (PMMA) that transmits across the spectral range of the imagers. Once the underwater housing is sealed, the necessary adjustments to the zoom, aperture and focus of the objective lenses (Fujinon Inc. or Pentax Inc.) are done via a custom-built electronic control circuit.

Polymethyl methacrylate (PMMA) is a transparent thermo-plastic used as a shatter resistant alternative to glass.

The control electronics comprises a single-board computer (PC/104; Kontron AG), which runs a Linux operating system (Ubuntu 10.04) and provides interfaces for firewire, ethernet and serial communication. The firewire ports are used to control image acquisition, the serial ports are used to control the motor, lenses and the halogen lamps, and the ethernet port allows for network operations (Figure 2.1C). The battery pack for Hypersub consists of three rechargeable lithium-polymer cells (12 V 16 Ah; Headway Headquarters LLC; 40160SE). This allows to support an active measurement time of 3–4 hours (including illumination by the halogen lamps). Since one scan typically requires about 10 minutes, this allows for acquisition of about 15-20 hyperspectral scans. With the use of timer-circuits, all devices can be powered off between measurements, which allows extension of the overall deployment time to about 1 week. The electronics housing also contains a circuit that can draw electricity from an external power source and recharge the on-board battery pack, allowing for extended field deployments. Effectively, Hypersub can be operated with the only external dependencies being a 12–24 V recharging power supply and an ethernet connection for communication.

The external dependencies of Hypersub are the same for underwater operation.

2.3.2 *Measurement Software*

A custom-built software (Sinkraft), which runs on the Hypersub computer, establishes a network platform for the various devices to communicate and interact. Sinkraft is written in Python (`www.python.org`) and makes use of several free software libraries. It follows a modular design that reflects the modular design of the hardware (Figure 2.1C). Each device is associated with a TCP server that provides a communication interface with clients (e.g., another device or a user within the local network) to perform device-specific operations. This enables real-time remote operations at the device-level, as well as autonomous operation through text scripts that embody a measurement protocol (see Table 2.1).

While measuring, the frames acquired from the imagers are sequentially stored in a 16-bit binary file on the storage disk. Additionally, the binary file is accompanied by a meta-data file that contains information about the data file structure, wavelengths, time of measurement and motor

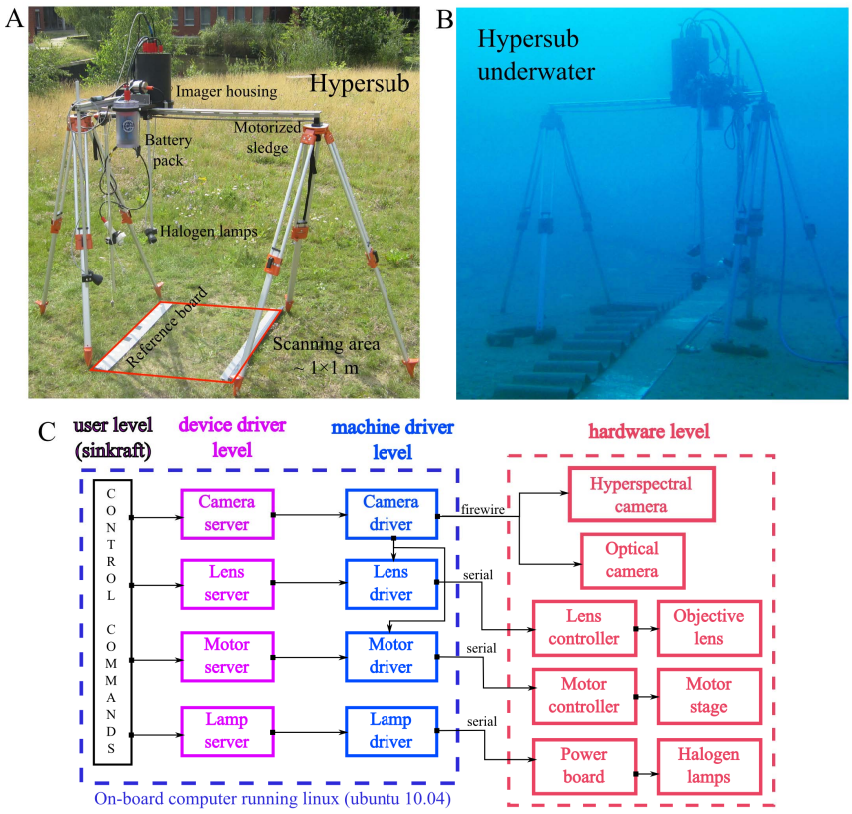

Figure 2.1: Photographs of Hypersub, the novel submersible hyperspectral imaging system, showing the primary components mounted on a motorized sledge. A schematic diagram of the hardware and software architecture of the system is shown in panel C.

SINKRAFT COMMANDS [a]	ACTION PERFORMED [b]
`@manager act start @ipower; @ipower set ports 1; @self sleep 2;`	`# start the power module to power other devices and wait 2 seconds for hardware initialization`
`@manager act start @hscam @hslens @optcam @optlens @motor @lamps @timer;`	`# now start all other devices`
`@motor set lims -20 1010; act abspos !! 0;`	`# set motor scanning limits in mm. Then, move motor to start (0) position; wait until arrival (!!)`
`@lamps set ports 1;`	`# switch on lamps`
`@hscam set fps 7.5; @optcam set fps 15;`	`# set frame-rates of hs-imager and gray-scale imager`
`@hscam act autoexpose; act autofocus; @optcam act autoexpose; act autofocus;`	`# perform auto-exposure and auto-focusing with imagers`
`@hscam set scan $name=hsi $filename=hs_scan $logmotor=@motor; @optcam set scan $name=vis $triggertime=10 $filename=vis_scan $logmotor=@motor;`	`# define scan parameters for both imagers. Files are sequentially numbered on repetition`
`@optcam act startscan vis; @self pause 0.1; @hscam act startscan hsi; @self pause 0.1;`	`# start frame acquisition by both imagers`
`@motor act relmm !! 1000;`	`# move motor by 1000 mm, blocking further execution of the script until the distance has been traversed`
`@hscam act stopscan hsi; @optcam act stopscan vis;`	`# stop frame acquisition after motor movement`
`@lamps set ports 0; @motor act abspos !! 0;`	`# scanning completed. Switch off lamps and move to start position before power off`
`@timer set reltimealarm 121; @manager act stop all; act systemhalt 60;`	`# set a wake-alarm to restart the system after 121 minutes, and execute power-off after 60 seconds`

Table 2.1: An example of a protocol script for conducting a hyperspectral scan with the Sinkraft software used in Hypersub.

a The various devices or subsystems of Hypersub are referenced through device tokens such as @hscam, @optcam, @motor, etc. Semicolon is used for separation of commands.

b The # character marks the beginning of text used for documentation.

positions for each frame. Formatting of both files complies with common hyperspectral imaging standards[7].

2.3.3 *Measurement Procedure*

A hyperspectral scan is performed by mounting the imagers facing the object (e.g., sediment surface), and acquiring image frames as the sledge is moved along the rail (Figure 2.1A). Before acquiring images, several optical adjustments have to be performed. First a region-of-interest is selected using an interactive viewer of the line-of-view and field-of-view seen by the hyperspectral and direct imagers, respectively. Optionally, the halogen lamps can be switched on if the ambient illumination is insufficient. Subsequently, the exposure is adjusted to ensure optimal dynamic range of the detected light intensity across the entire spectral range of sensitivity, which is done by adjusting the shutter duration of the imagers and the aperture size of the objectives. Finally, the focus of the objectives is adjusted to optimize sharpness of a spatial feature (artificially introduced, if not present) seen by the cameras.

Spectral referencing is necessary because the imager on Hypersub is not radiometrically calibrated.

An important step during optical adjustments is to include a spectral reference board along the top or bottom edge of the imaged area (Figure 2.1A). The pixels recorded as the hyperspectral imager scans across the reference board are used in subsequent data processing (see Hyperspectral Data Analysis) to calculate the spectral reflectance from the captured intensities of the back-scattered light. In principle the reference board can be made of any diffusely reflecting material with a flat reflectance spectrum in the wavelength region 400–900 nm, even if its reflectance is lower than 100%. In this study we used white or gray plastic (PVC), which were checked against a reflectance standard (DLC DL-0510) to have a flat reflectance spectrum in the range 400–900 nm. The reference boards were prepared with a matte surface finish to eliminate specular reflection.

After the initial optical adjustments, the acquisition scan is initiated by a command to the motor to move the sledge at a constant velocity and, simultaneously, by a command to the imagers to acquire and record frames at a predefined frame-rate (typically 4 fps). During the scan, the position of the motorized sledge is recorded along with the time-stamp of each frame to allow accurate spatial reconstruction of the scanned area. To improve the signal-to-noise ratio of the acquired images, averaging of frames or binning of spectral bands can be optionally applied. An example of the protocol scripts used in this study are shown in Table 2.1.

7 see http://www.exelisvis.com/docs/ENVIHeaderFiles.html

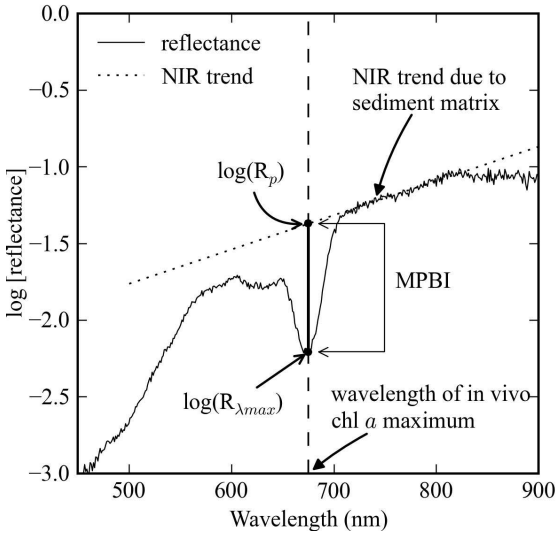

Figure 2.2: A typical example of reflectance spectrum of intertidal sediment with a MPB biofilm, with a graphical representation of the spectrometric index (MPBI) used for the quantification of the MPB biomass in terms of the sedimentary Chl *a* concentration.

2.3.4 *Hyperspectral Data Analysis*

Hyperspectral measurements generate a rich multi-dimensional dataset, and require special software for processing and analysis. Based on previous ideas on hyperspectral analysis (Polerecky et al., 2009a), a custom analysis software was developed using Python. The software, called HyPurveyor, provides an interactive view of the hyperspectral data in both its spatial and spectral dimensions, and can be used to create contextual maps of arbitrary, user-defined spectral indices. Additionally, tools for spatial context analysis or image analysis are also available. All data presented in this study were analyzed using HyPurveyor.

2.3.5 *Spectral-index for quantification of benthic Chlorophyll a*

A typical reflectance spectrum of sediment covered with a microphytobenthic biofilm contains a pronounced valley at around $\lambda_{max} = 675$ nm due to *in vivo* absorption maximum of Chl *a*, and an approximately linear trend in the near-infrared (NIR) region due to the combined effects of absorption and scattering by the sediment-seawater matrix (Figure 2.2; see also Barillé et al., 2011; Murphy et al., 2005). To account for these specific features, we calculated a hyperspectral microphytobenthos index (MPBI) as

$$\mathrm{MPBI} = \log(R_p) - \log(R_{\lambda max}) \qquad (2\text{–}i)$$

where $R_{\lambda max}$ is the measured reflectance at λ_{max} and R_p is the value of the fitted linear trend in the NIR range (720-800 nm) extrapolated to λ_{max}

(Figure 2.2). By using the extrapolated value R_p, the index effectively incorporates a form of "continuum correction" that is used to remove the effects of the sediment substrate on the overall shape of the reflectance spectrum (Clark and Roush, 1984; Kokaly and Clark, 1999). Furthermore, by incorporating logarithmic transformation of the reflectance ratio $R_p/R_{\lambda max}$, the index accounts for the exponentially decreasing light intensity within an MPB biofilm, which results in a linear relationship between the MPBI and Chl *a* concentrations in the biofilms (see Assessment), as opposed to the saturated exponential relationship found for spectral indices that are not log-transformed (Barillé et al., 2011; Carrère et al., 2004).

Using HyPurveyor, the calculation of MPBI was done in each pixel of the spatial image. To minimize the influence of the sensor noise, the $R_{\lambda max}$ value was calculated from the fit of the reflectance spectrum around λ_{max} by a third-order polynomial rather than from the reflectance measured in a single band. By implementing a calibration, the hyperspectral MPBI values were then converted to Chl *a* concentrations and displayed as color-coded images.

2.3.6 *Preparation of artificial biofilms for calibration and validation*

Calibration and validation of the hyperspectral imaging system for Chl *a* quantification in sediments were done using artificial biofilms prepared by mixing natural sediment grains with diatoms from a laboratory culture. Sediments were collected from various intertidal sites in the North Sea and sorted by sieving into 4 grain-size groups: <63 µm, 63–125 µm, 125–250 µm and 250–355 µm. These groups roughly represent muddy (0–125 µm) and sandy (125–355 µm) sediments. The sorted sediment grains were then boiled with hydrogen peroxide (90%) at 65°C to remove any dissolved organic content, and dried again in an oven at 80°C. Concentrated diatom suspensions (species *Amphora Coffeaeformis*) were prepared by centrifugation of the diatom culture in the exponential growth phase. Subsequently, the suspensions were added into the sediment at various concentrations and mixed with a low-gelling agar (1.5% wt.) at temperature of 40°C. While still fluid, the mixture was cast into plastic molds (20×10×1 mm) and left to cool for about a minute, resulting in 1-mm-thick solidified sediment biofilms. Additionally, reference "biofilms" with no added diatoms were also prepared. The biofilm thickness of 1 mm was chosen to match the typical penetration depth of light in natural marine sediments (see Discussion).

Scanning of the calibration and validation biofilms took around 10–15 minutes and was done while the biofilms were submersed in seawater. Because the solidified agar prevented diatom migration, the initially homogeneous diatom distribution in the biofilms was maintained homogeneous throughout the measurements. Immediately after scanning, the biofilms were subjected to 90% acetone, sonicated for 2 minutes in tubes

and placed at -20°C overnight to extract the intracellular Chl *a*. For each tube, the absorption spectrum of the filtered extractant was measured (USB4000; Ocean Optics Inc.) and the Chl *a* concentration therein was calculated based on spectrophotometric comparison with a standard (C5753; Sigma-Aldrich Co.). This value was subsequently multiplied by the known volume of the extractant to obtain the Chl *a* content in the biofilm.

2.3.7 *Quantification of benthic Chl a*

Chlorophyll *a* contents in the calibration and validation biofilms were normalized to the biofilm's porewater volume. Consequently, all Chl *a* concentrations in this study are reported in "micrograms of Chlorophyll *a* per milliliter of porewater" (μg Chl *a* ml^{-1}PW). This choice of normalization, although not used in benthic studies, better reflects the fact that it is the porewater where the MPB cells reside, interact with light and thus contribute to primary productivity. Additionally, it has an advantage that it allows a more straight-forward comparison between the concentrations of photosynthetically active biomass in pelagic and benthic ecosystems (the pelagic Chl *a* concentrations are typically reported per liter of water). In benthic studies, sedimentary Chl *a* concentrations are typically reported in units normalized to sediment weight (μg Chl *a* per g of wet or dry sediment weight) or to sediment area (μg Chl *a* per m^2 of sediment). The conversion between our volume-normalized Chl *a* concentrations and those normalized to the sediment weight or area is straight-forward: [μg Chl *a* g^{-1} dry wt.] = [μg Chl *a* ml^{-1}PW] × (φ / ρ_{DS}), [μg Chl *a* g^{-1} wet wt.] = [μg Chl *a* ml^{-1}PW]×φ/($\rho_{DS} + \varphi \times \rho_{PW}$), and [mg Chl *a* m^{-2}] = [μg Chl *a* ml^{-1}PW] ×φ × d, where φ is the sediment porosity, ρ_{DS} is the bulk density of dry sediment (g ml^{-1}), ρ_{PW} is the porewater density (g ml^{-1}), and d (in mm) is the depth range for which the areal Chlorophyll *a* concentration is reported (d=1 mm in this study). To achieve brevity, the following text will omit "Chl *a*" and "dry wt." in the units of Chlorophyll *a* concentrations, with "g" always referring to sediment dry weight.

2.4 ASSESSMENT

2.4.1 *Calibration and validation of the method using artificial biofilms*

To calibrate the hyperspectral method, artificial MPB biofilms with variable but spatially homogeneous Chl *a* concentrations were scanned with Hypersub and the MPBI values obtained for each sample, using (2–i), were averaged over all measured pixels. The values were subsequently corrected for an offset, $MPBI_0$, measured in biofilms prepared from the same sediments but with no diatoms added, and plotted against the porewater volume-specific Chl *a* concentrations determined through extraction.

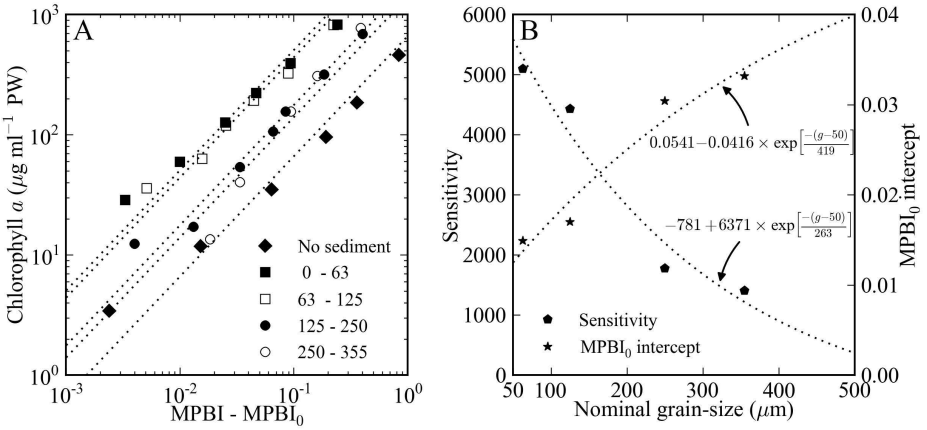

Figure 2.3: Calibration plots (panel A) of the hyperspectral microphytobenthic index (MPBI) versus the concentration of Chl *a* in artificially prepared mixtures of MPB and sediment. Dotted lines show least-square fits with a line given by (2–i). The values of the parameters S and $MPBI_0$ for the studied sediment types (see legend) are given in Table 2.2 and depend on the nominal grain-size as shown in panel B.

NOMINAL GRAIN-SIZE	SENSITIVITY	$MPBI_0$ INTERCEPT	CORRELATION COEFFICIENT
micrometer	μg Chl *a* ml^{-1} PW		
0	665	0.002	0.9904
1–63	5094	0.015	0.9980
63–125	4432	0.017	0.9862
125–250	1776	0.030	0.9728
250–355	1407	0.033	0.9913

Table 2.2: Parameters of calibration (Equation 2–ii) between the hyperspectral microphytobenthic index, MPBI, and porewater Chl *a* concentrations.

The relationship between the Chl *a* concentrations and the offset-corrected MPBI values was very well ($R^2 > 0.97$) described by a linear model

$$\text{Chl } a\,[\mu\text{g ml}^{-1}\,PW] = S \times (\text{MPBI} - \text{MPBI}_0) \qquad (2\text{–ii})$$

Linearity was maintained for Chl *a* concentrations from 4 to 820 µg Chl *a* ml^{-1}PW, with a lower accuracy below 10 µg Chl *a* ml^{-1}PW and no systematic deviations towards the upper end of concentrations (Figure 2.3). Assuming sediment porosity of 0.4, the range of linear response corresponds to 0.016–3.3×10^5 mg m^{-3} of sediment volume. Thus, the system is able to quantify MPB biomass over a wide range of concentrations that are typically found in natural MPB biofilms (0.03–7×10^5 mg m^{-3}; Krause-Jensen and Sand-Jensen, 1998).

An important finding of the calibration step is that the sensitivity (or slope) of the calibration, S, as well as the zero-chlorophyll offset, $MPBI_0$, depend strongly on the sediment grain-size (Table 2.2; Figure 2.3). This is, most likely, due to the close coupling between the geometrical characteristics of the sediment (grain-size and packing) and its light scattering properties (see Discussion). The fact that the $MPBI_0$ offset is non-zero indicates that the linear continuum correction in the MPBI calculation did not fully account for the effect of the sediment matrix on the reflectance spectrum. The reason for this is unclear, but could be due to the slightly non-linear absorption of the agar-solidified sediment matrix in the wavelength range of 675–800 nm.

For the studied sediment type (silicate intertidal sediment), empirical functions that describe the dependencies of the calibration sensitivity, S, and of the offset, $MPBI_0$, on the grain-size are given in Figure 2.3B. Using these functions, one can estimate a potential error that can be made if the prediction of the sedimentary Chl *a* concentration is done without reliable information about the sediment grain-size. For example, for an MPBI value of 0.1, the Chl *a* concentration predicted for a fine muddy sediment (grain sizes <63 µm) would be 433 µg Chl *a* ml^{-1}PW, whereas it would be about 4-fold lower for a coarse sandy sediment (grain sizes 250–355 µm). This demonstrates that the knowledge of sediment characteristics is very important for accurate quantification of the Chl *a* concentration in sediments based on the measurement of spectral reflectance, in agreement with conclusions reached in previous studies (Murphy et al., 2005; Spilmont et al., 2011).

To validate the method and assess its predictive power, independent measurements were performed on a different set of biofilms prepared from the same sediment and diatoms, and the Chl *a* concentrations predicted from the measured MPBI were compared against those obtained through extraction. Both Chl *a* concentrations followed well a 1:1 line (Figure 2.4A). However, Chl *a* values for some samples differed by up to 40% (on average by about ±20%), and this difference varied depending on the grain-size of the sediment used (whiskers in Figure 2.4B). This shows that even with careful biofilm preparation and measurements, Chl *a* concentrations ob-

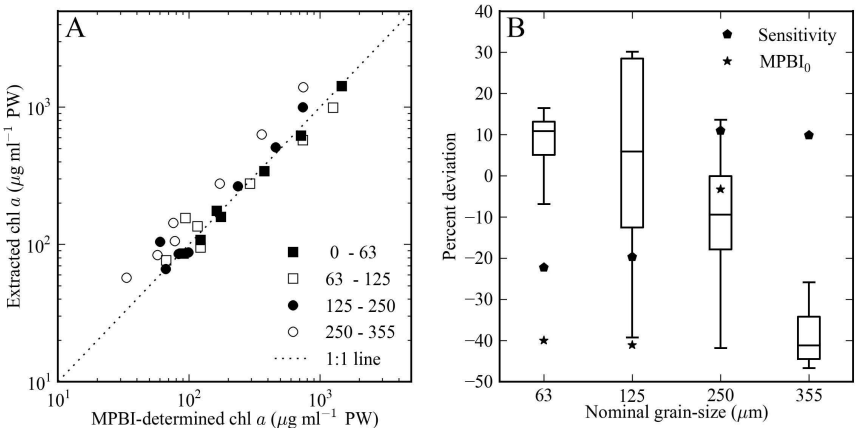

Figure 2.4: Validation of the hyperspectral imaging method for Chl *a* quantification in MPB biofilms. (A) Chlorophyll *a* concentrations calculated from the measured MPBI using calibration parameters shown in Figure 2.3 versus those measured via spectrophotometric analysis of extracted pigments. (B) The box-whisker plot shows percentage deviations between the calculated and measured Chl *a* concentrations, as derived from data shown in panel A, with boxes spanning the upper and lower quartiles, horizontal lines indicating the median, and whiskers extending to the full range of values. Filled symbols show the percentage deviation of the calibration parameters (S and $MPBI_0$) determined from the independently prepared "validation" and "calibration" biofilms.

tained by the hyperspectral and extraction-based method may differ by several tens of percent, similar to results obtained by others (Carrère et al., 2004; Murphy et al., 2009). It is likely that this phenomenon is linked to the small differences in the size distribution and especially the compaction of grains in each individually prepared biofilm, which affect the hyperspectral signal by influencing the scattering properties of the sediment (see Discussion). This is consistent with the relatively strong dependence of the calibration parameters on the nominal grain-size (Figure 2.3B), and further supported by the fact that calibration parameters derived for the "validation biofilms" differed by as much as 40% from those derived for the calibration biofilms (see filled symbols in Figure 2.4B) although both sets of biofilms were prepared from the same sediments and diatoms.

These relatively large discrepancies imply that the calibration shown in Table 2 and Figure 3 cannot be applied universally for all sediments. Instead, both the slope S of the calibration line and the zero-chlorophyll offset $MPBI_0$ must be obtained individually for each studied sediment to allow accurate prediction of Chl *a* concentrations. Moreover, hyperspectral reflectance imaging should be accompanied by parallel measurements of the grain-size distribution if the latter characteristic of the studied sediment is expected to vary significantly within the imaged area.

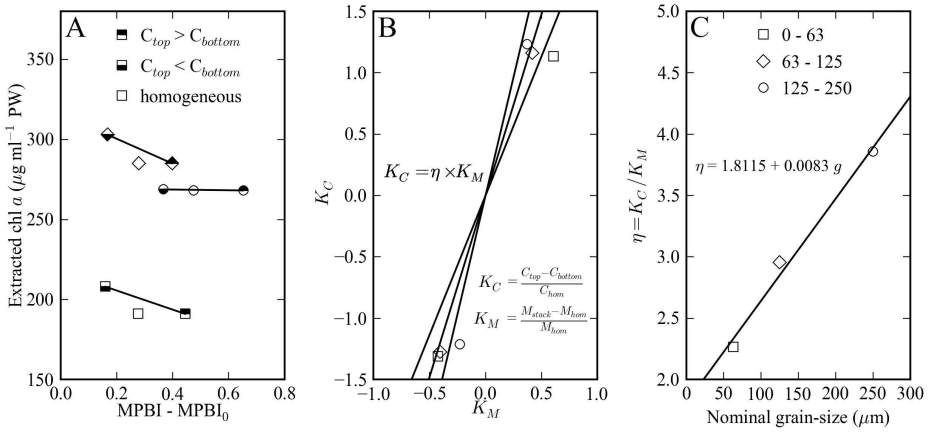

Figure 2.5: The effect of the vertical distribution of Chlorophyll *a* in a 1 mm thick MPB biofilm on the MPBI signal. (A) MPBI values for "high-low;; and "low-high" stacked biofilms (half-filled symbols) and for homogeneous biofilms (unfilled symbols), plotted against the corresponding depth-integrated Chl *a* content in the biofilms. (B) Relationships between the MPBI contrast (K_M; 2–iii) and the chlorophyll contrast (K_C; 2–iv), as derived from data shown in panel A. (C) Slope of the relationship $K_C = \eta \times K_M$ as a function of the nominal sediment grain-size.

2.4.2 *Effects of vertical distribution of Chl a*

The effects of a sub-millimeter scale vertical distribution of surficial Chlorophyll *a* on hyperspectral measurements were studied by imaging stacked biofilms. First, homogeneous biofilms were prepared similarly as for the calibration (see above) but with a thickness of 0.5 mm instead of 1 mm. The Chl *a* concentrations in these biofilms were in the ratio of 1:4. Subsequently, a biofilm with a higher Chl *a* concentration was placed on top of one with a lower Chl *a* concentration, or vice versa, resulting in 1 mm thick biofilms with a well defined (two-layer) vertical distribution of Chl *a*. After imaging the stacked biofilms with Hypersub, the Chl *a* concentration in each 0.5 mm layer was separately quantified through extraction and spectrophotometry.

In general, MPBI values determined for stacked biofilms with a larger Chl *a* concentration on top ("high-low" biofilms) were larger than those with the reversed Chl *a* distribution ("low-high" biofilms), although the depth-integrated Chl *a* content in both biofilm types were similar (Figure 2.5A). The difference depended on the grain size and ranged from 2-fold for the coarse-grained (125–250 µm) to about 3–fold for the fine-grained (<63 µm) sediment. This shows that the hyperspectral imaging method is sensitive not only to the amount of Chl *a* in a specific region of sediment where light penetrates, but also to its vertical distribution within that region. On the one hand, this is an important drawback of the hyperspectral imaging method, as it cannot distinguish whether an apparent lateral variability in a MPB distribution is due to a truly variable MPB

biomass concentration or due to a lateral variability in its vertical distribution. On the other hand, this phenomenon can be advantageously used for monitoring changes in vertical Chl *a* distribution in time, such as those due to vertical migration of MPB in sediments.

To assess this possibility, we analyzed in detail the relationship between the offset-corrected MPBIs for stacked biofilms (denoted as M_{HL} and M_{LH} for the high-low and low-high biofilms, respectively), the offset-corrected MPBIs for homogeneous biofilms with an equivalent depth-integrated Chl *a* amount in the top 1 mm (denoted as M_{hom}), the relative deviation of M from M_{hom}, defined as

$$K_M = \frac{M - M_{hom}}{M_{hom}} \tag{2–iii}$$

and the contrasts in Chl *a* concentrations in the stacked biofilms, defined as

$$K_C = \frac{C_{top} - C_{bottom}}{C_{hom}} \tag{2–iv}$$

where C_{top} and C_{bottom} are Chl *a* concentrations in the top and bottom half of the stacked biofilm, respectively, and $C_{hom} = (C_{top} + C_{bottom})/2$. We found that, irrespective of the grain-size, the MPB indices were with good accuracy related as $M_{hom} = (M_{HL} + M_{LH})/2$ (Figure 2.5A). Furthermore, K_C depended on K_M by a linear relationship (Figure 2.5B),

$$K_C = \eta \times K_M \tag{2–v}$$

where the proportionality constant η depended on the nominal sediment grain-size g approximately linearly as $\eta = 1.8115 + 0.0083\times$ g (Figure 2.5C). Based on the definition, K_C represents the fraction of total Chlorophyll *a* in the 1 mm thick stacked biofilm that "moved" from the bottom half to the top half (or vice versa if $K_C < 0$) in comparison to the biofilm with a homogeneously distributed Chl *a* of equal total amount. Thus, assuming that the vertical Chl *a* distribution in natural MPB biofilms is approximated by a similar two-step function as in the stacked biofilms, equations 2–iii–2–v allow estimation of the MPB fraction that vertically migrates within the top millimeter of the sediment from the measurement of temporal variations in MPBI (see Mapping of Chl *a* dynamics).

2.4.3 *In situ microscale distribution of Chl a*

For the assessment of Hypersub in the field, we deployed it on an intertidal sandflat near the island of Sylt in the German North Sea (54.9°N, 8.3°E) and imaged in-situ distributions of MPB on rippled and bioturbated sediments. Hyperspectral scans were performed using ambient sunlight, and spanned an area of approximately 80×20 cm in about 7–10 minutes. The

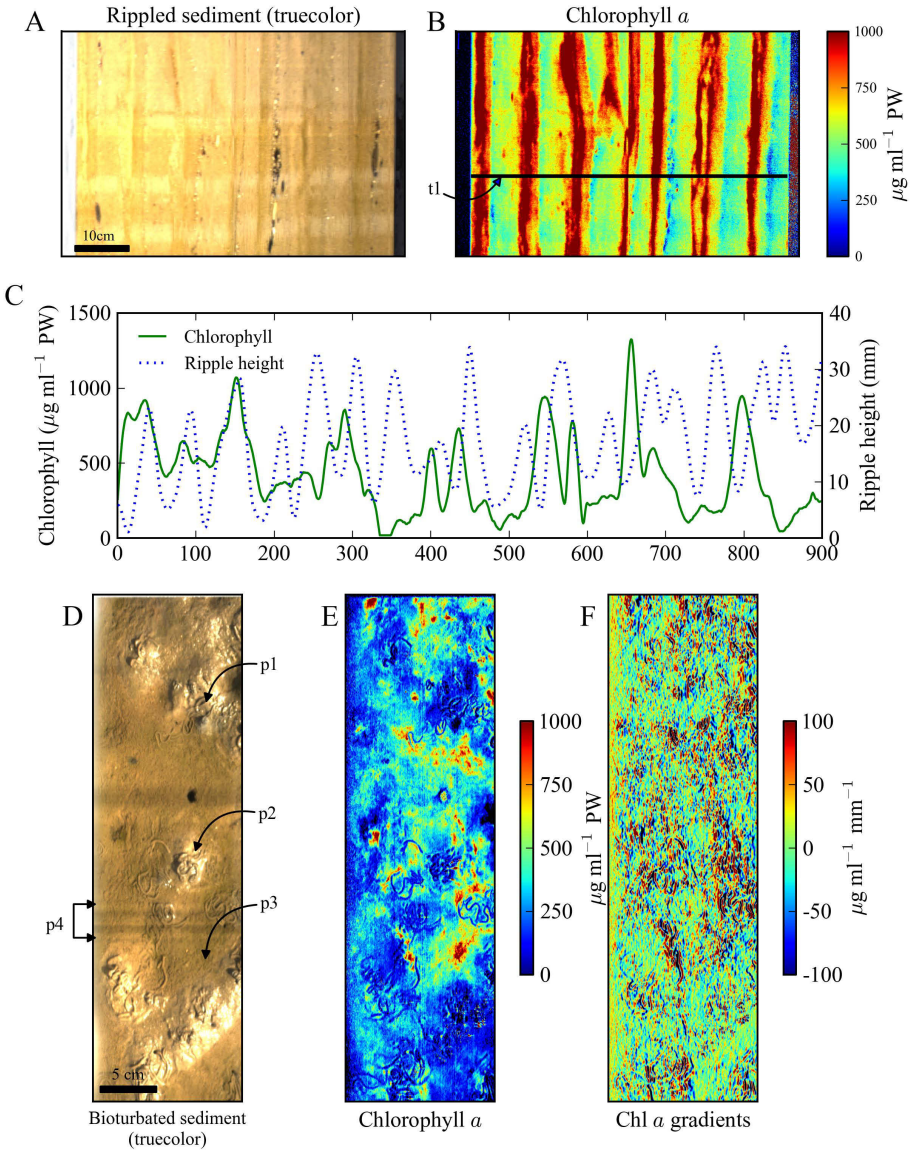

Figure 2.6: *in situ* imaging of MPB biofilms on intertidal sediments using Hypersub. Shown are the true-color images and the corresponding Chl a maps of a rippled sea-bed (A, B) and of sediments affected by the bioturbation activity of lugworms A. marina (D, E). Features of the lugworm habitat such as fecal mounds (p1, p2) and inter-burrow sediment (p3) are annotated. Panel C shows an example of a lateral Chl a profile along a transect line t1 shown in B, overlaid with the corresponding profile of the ripple topography (height). Panel F shows 2D gradients of Chl a concentrations derived from the Chl a map in E. Note that due to the normalized nature of the MPBI calculation, the darker bands in panel D (p4), which are due to fluctuations in the illumination intensity during the scan caused by a passing cloud, are not visible in the Chl a map in panel E. Also note that the Chl a concentrations, given in µg Chl *a* ml^{-1}PW, can easily be converted to µg g^{-1} or mg m^{-2} using formulae given in Materials and Procedures.

obtained MPBI values were converted to Chl *a* concentrations in µg Chl *a* ml^{-1}PW assuming that the measured grain-size (125–250 µm) was constant across the imaged area (i. e., using the corresponding values for S and $MPBI_0$ given in Table 2.2). Additionally, using the measured sediment porosity (0.40), bulk density (1.55 g ml^{-1}), and the formula above, the values were also converted to µg g^{-1} to allow easier comparison with values available in the literature.

In the rippled sediment, the MPB distribution was remarkably variable, ranging from about 150 to 1620 µg Chl *a* ml^{-1}PW (38–418 µg g^{-1}) with a mean value of 710 µg Chl *a* ml^{-1}PW (183 µg g^{-1}), and clearly linked to the sediment topography (Figure 2.6A–B). The gradients of Chl *a* concentrations were perpendicular to the ripple contour, and also remarkably steep, reaching up to 240 µg Chl *a* ml^{-1}PW mm^{-1} (62 µg g^{-1} mm^{-1}), which corresponds to a change of about 330% of the average Chl *a* concentration over a distance of 1 cm. A closer inspection of the Chl *a* concentration and the ripple height along randomly selected transects revealed that local minima in the MPB biomass were typically found on ripple troughs, while local maxima were located on ripple shoulders close to ripple crests (Figure 2.6C). A possible explanation of this pattern could lie in the distribution of the shear force induced by the viscous drag of the water flow during the incoming and outgoing tide; during unidirectional tidal flow, the shear force would be highest on ripple crests, making it more difficult for MPB to accumulate there in high abundance, whereas the lowest shear stress would be at locations around the ripple shoulders (Bhaganagar and Hsu, 2009).

The MPB distribution on the surface of sediments bioturbated by the lugworm Arenicola marina was also remarkably variable (20–1160 µg ml^{-1} PW or 5–300 µg g^{-1}), with an average around 300 µg ml^{-1} PW (77 µg g^{-1}). However, in contrast to the rippled sediment, the distribution was much more irregular (Figure 2.6E). For example, the freshly-defecated fecal mounds (p1, p2; Figure 2.6D) had rather low Chl *a* concentrations, indicating efficient but not complete removal of the MPB cells by lugworm feeding. In contrast, sediments between the fecal mounds (p3; Figure 2.6D) showed elevated Chl *a* concentrations, possibly indicating an enhanced growth rate of MPB, potentially due to an increased supply of nutrients from below driven by bioadvection (Chennu et al., in preparation), which is associated with the hydraulic activity of the lugworm (Rasmussen et al., 1998; Volkenborn et al., 2010). Spatial gradients of the MPB biomass in the bioturbated sediment were also remarkably high and comparable to those found for the rippled sediment. Maximal gradient values reached up to 250 µg ml^{-1} PW mm^{-1} (65 µg g^{-1} mm^{-1}), and more than 5% of pixel-locations had gradients above 110 µg ml^{-1} PW mm^{-1} (28 µg g^{-1} mm^{-1}) (Figure 2.6F). The latter gradient corresponds to a change of about 400% of the average Chl *a* concentration over a distance of 1 cm, which highlights the profound microscale heterogeneity in the MPB distribution in bioturbated sediments.

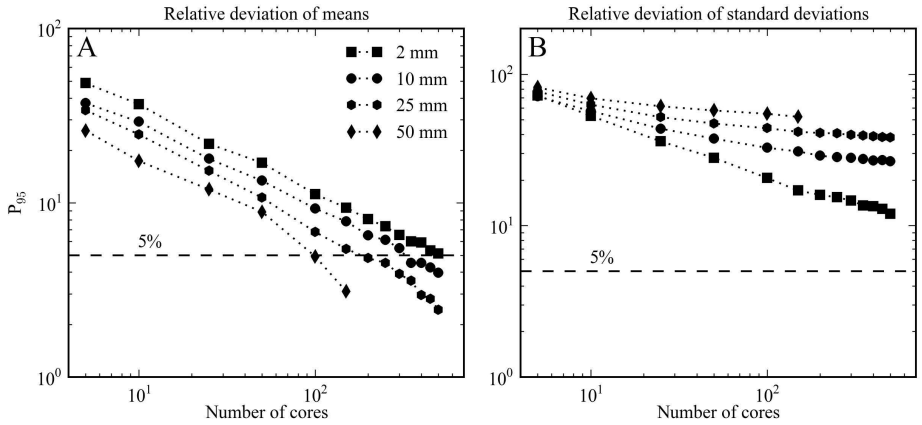

Figure 2.7: Deviations between the true and estimated values of the mean (A) and the standard deviation (B) of Chl a concentrations in a bioturbated intertidal sediment. Shown are 95 percentiles derived from 500 random sampling attempts with N cores of different diameters (see legend), plotted as a function of the sample size N.

In addition to the characterization of spatial patterns in sedimentary Chl *a* distributions, the high-resolution Chl *a* maps obtained by the Hypersub system can be used to assess sampling strategies for estimating the mean and variability of Chl *a* standing stocks in marine sediments. For this assessment we used as an example the complete Chl *a* map obtained for the bioturbated sediment (Figure 2.6E). This map contains 544000 measurements of Chl *a* concentrations over an area of 68 × 20 cm, and the true mean and standard deviation are M_t = 295 µg Chl *a* ml^{-1}PW and SD_t = 180 µg Chl *a* ml^{-1}PW, respectively, i. e., the coefficient of variation is $SD_t/M_t \times 100 = 61$. The Chl *a* map was randomly sampled with N cores (N ranging from 5 to 500) of different diameters (ranging from 2 to 50 mm). This random sampling was repeated 500 times, and for each sampling the relative difference between the obtained mean M_o and the true mean M_t, and between the obtained standard deviation SD_o and the true standard deviation SD_t was calculated as $|M_i - M_t|/M_t$ and $|SD_i - SD_t|/SD_t$, i=1, 2, ..., 500 respectively. Subsequently, the accuracy of the estimate was defined as the 95 percentile of these 500 relative deviations between the estimated and true values.

For a random sampling with N cores of 1 cm in diameter, the accuracy of the estimated mean decreased with N, reaching about 30% at N=10 and 5% at N=350 (Figure 2.7). This means that the estimated mean by random sampling can differ by >30% from the true mean when sampling with <10 replicate cores, and only with >350 randomly distributed cores there is a >95% certainty that the estimated mean deviates by <5% from the true mean. The number of replicates required for a 5% accuracy of the estimated mean drops if the sampling is done with larger cores (e.g., N=100 for the core diameter of 5 cm; Figure 2.7A). Clearly, this is because sampling with larger cores 'averages out' the small-scale variability that is

detected when sampling with smaller cores. With respect to the variability of Chl *a* concentrations within the map, it was not possible to achieve <5% difference between the estimated and true SD with 95% confidence even if the number of randomly sampled 1-cm diameter cores reached N=500 (Figure 2.7B). This is clearly because the sampling core diameter was larger than the distance over which the Chl *a* distribution exhibited significant variations. Overall, this analysis demonstrates that sampling of a low number (5–10) of replicates is inadequate for accurate quantification of Chl *a* concentrations in highly heterogeneous systems such as bioturbated marine sediments. A similar conclusion was drawn in a recent study by Spilmont et al. (2011).

An interesting feature of the analysis of field data is that the 'shadow' regions in the true-color images, caused either by passing clouds or shadows of the frame of Hypersub during the hyperspectral scan, are eliminated in the final Chlorophyll *a* maps (compare Figure 2.6D and 2.6E, region p4). This is because the MPBI value is derived from the ratio of light intensities at essentially two wavelengths, one corresponding to the Chl *a* absorption maximum and the other in the NIR region where Chl *a* does not preferentially absorb (see 2–i and Figure 2.2). This approach provides an intrinsic correction against variations in incident light intensities within the dynamic range of the sensor during the scan, provided that during these variations the spectrum of the incident light remains unchanged.

2.4.4 *Mapping of Chl a dynamics*

To assess the suitability of the method for studying vertical migration of MPB, 3 round buckets (diameter 16 cm; depth 20 cm) were filled with freshly collected and sieved (0.5 cm mesh) surficial sediments from an intertidal flat near the Baruch Marine Field Laboratory in South Carolina (April; 33.3°N, 79.2°W), and incubated in a large tank with continuous flow-through of natural seawater. The sediments were inundated at all times and exposed to shaded natural light. Hyperspectral scans in about 1–2 hour intervals were performed during daylight for 4 days and during the last night of the incubation. Overhead halogen lamps provided supplementary illumination during all scans. MPBI maps at the different time-points were aligned and analyzed with respect to spatial as well as temporal variability.

The MPBI values showed clear diel oscillations in every pixel of the sediment surface, with maximal values occurring shortly after midday and minimal values lasting from about 2 hours after the sunset until shortly before sunrise (Figure 2.8A). Based on the previous work on diel vertical migration of MPB (Consalvey et al., 2004; Palmer and Round, 1967) and the fact that the amplitude of the MPBI oscillations as well as the maximal daily values did not change significantly during the measuring days, we

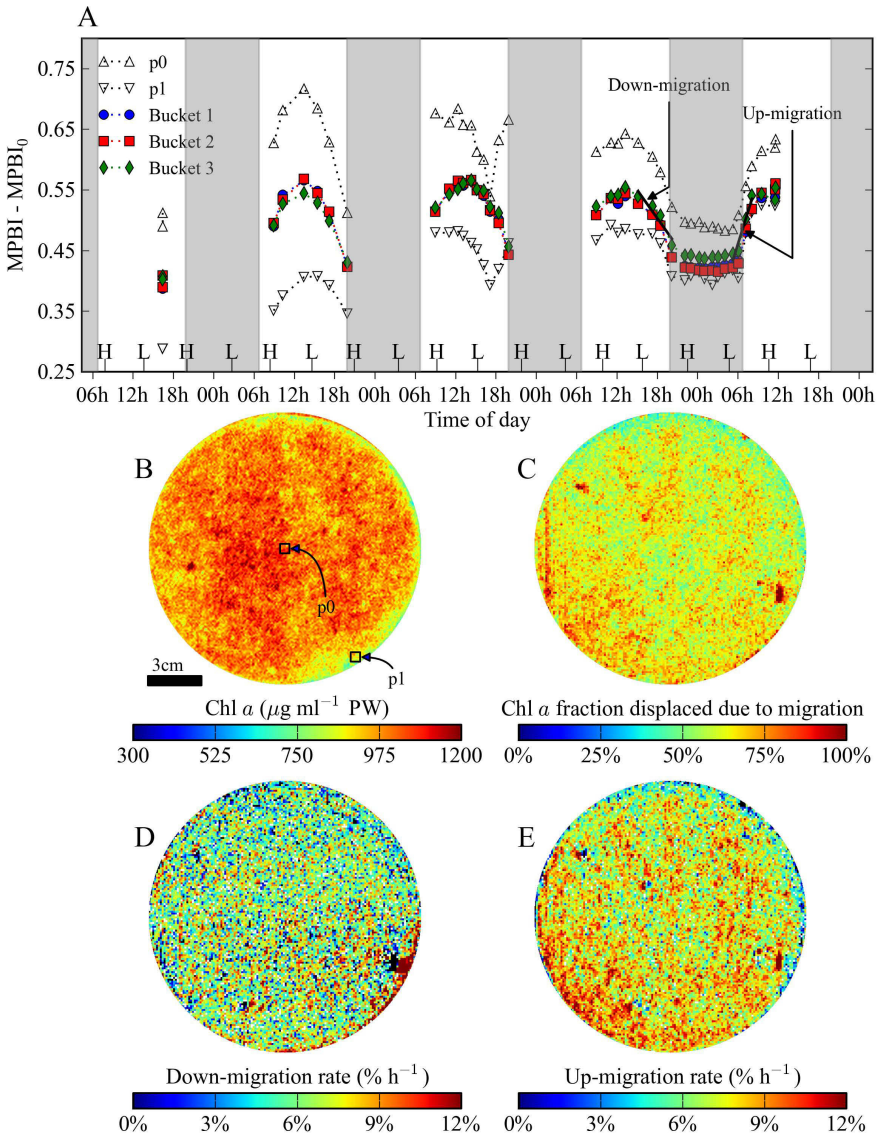

Figure 2.8: Visualization of the spatio-temporal patterns in the distribution of Chl *a* in intertidal sediments associated with vertical migration of MPB. (A) MPBI index as a function of time over the course of 5 days, showing values in selected 5×5 mm areas (p0 and p1) and values averaged over the entire sediment surface in the experimental buckets. The gray and white areas correspond to nighttime and daytime, respectively, with the boundaries indicating the time of sunrise and sunset. Markers H and L indicate high and low tides, respectively. (B) Example of the Chl *a* distribution measured during midday. (C) Image of the fraction of MPB that migrated daily within the top millimeter of the sediment. (D-E) Images of the rates of downward (D) and upward (E) migration of MPB in the top millimeter of the sediment. The migrating fraction and rates are expressed in terms of a percentage of the Chl *a* standing stock in the top millimeter layer of the sediment. The rate maps provide a compact and quantitative visualization of the spatio-temporal dynamics of the chlorophyll distribution.

assumed that the observed MPBI oscillations did not reflect changes in the total MPB biomass but were due to vertical migration of MPB.

To estimate the amount of migrating MPB, we used the daily MPBI minima and maxima observed in each pixel to calculate M_{hom} and the corresponding MPBI contrast K_M (2–ii). By assuming that the vertical Chl *a* distribution in the natural biofilms was well approximated by a two-layer model, we could use 2–iv to calculate the Chl *a* contrast K_C, which represents the fraction of the MPB that migrated daily within the top millimeter of the sediment. The migrating MPB fraction varied between 40% and 80% across the sediment surface (Figure 2.8C), with the median averaged over the 3 replicate buckets of about 66%. A similar fraction of migrating MPB (40-50%) was obtained by direct cell counts in a previous study by Joint et al. (1982). Thus, although our measurements were indirect and based on several arguably crude approximations, they gave comparable results to those obtained by direct but considerably more labor-intensive measurements.

In addition to the mapping of the migrating MPB fraction, the non-invasive character of the hyperspectral imaging method also enabled mapping of the migration rate. To achieve this, the aligned MPBI images were subdivided into windows of 1×1 mm and the MPBI values averaged over these windows at time-points between the daily extrema were fitted as a function of time with a 3rd order polynomial. Subsequently, by combining equations (2–iii)–(2–v), the rate of MPB migration normalized to the total MPB content in the top 1 mm layer was calculated as

$$R_{migration} = \frac{dK_C}{dt} = \frac{\eta}{M_{hom}} \times \frac{dM(t)}{dt} \qquad (2\text{–vi})$$

This calculation revealed that the maximal rates of downward migration, observed shortly before the sunset, ranged from 2 to 12% h^{-1} (average median of buckets about 7% h^{-1}; Figure 2.8D). That is, in the simplified two-layer approximation, 2–12% of the Chl *a* contained in the top 1 mm of the MPB biofilm migrated from the upper 0.5 mm to the lower 0.5 mm in 1 hour. The upward migration, observed shortly before the sunrise, was somewhat faster, ranging from about 4 to 14% h^{-1} (median 9% h^{-1}; Figure 2.8E). Furthermore, no spatial patterns were apparent in the migration rate maps (Figure 2.8D–E), suggesting that MPB cells across the sediment surface in the buckets responded equally to the stimulus (incident light) that drives their vertical migration.

2.5 DISCUSSION

Hypersub is a field instrument for quantification of Chlorophyll *a* in surficial sediments. The main attributes that make it an attractive tool for benthic studies are its spectral, spatial and temporal resolutions, as well as the relatively large areas that can be imaged rapidly. For example, Chlorophyll *a* maps of about 1 m^2 with a lateral resolution of about 1 mm or

better can be typically acquired in 5–10 minutes. The design of the system additionally allows underwater measurements (Figure 2.1B), and this function is currently being tested and will be reported in greater detail elsewhere.

Chlorophyll *a* quantification is based on the measurement of spectral reflectance, derived from the detection of light back-scattered from the studied sediment surface. It is therefore minimally invasive and thus applicable for the study of spatio-temporal dynamics of Chlorophyll *a* distributions. The measurements can be performed under ambient natural illumination or, if not available, under artificial illumination from lamps that emit broadband light in the visible and near-infrared regions.

The instrument can be operated interactively or in a stand-alone automated mode, with the only external dependencies being a 12 V power supply (e.g., a battery or power line) and an ethernet connection. When powered solely by the built-in battery pack, the active measurement time is typically about 3–4 hours, which is sufficient for the acquisition of about 15–20 hyperspectral scans. Through the implementation of a stand-by mode, these scans can be distributed over a total deployment time of about one week. The measurement control is done through a simple set of text-based commands, which are executed by the Sinkraft software on the Linux operating system that controls the on-board computer.

When quantifying the sedimentary Chlorophyll *a* concentrations from the measurement of spectral reflectance, an important question arises: what is the actual quantity that the measurement captures? A short answer to this question is that the reflectance measurement gives information about the concentration of Chlorophyll *a* in the sediment volume, specifically the interstitial porespaces, that interacts with the probing light and is therefore a measure of the biomass of MPB cells that contribute to benthic primary production through their photosynthetic activity. However, as shown by our investigations and discussed in the following, several issues need to be considered in this context.

First, the exact depth of probing cannot be easily estimated or generalized for different sediment types. According to the Beer-Lambert law, the intensity of light traveling through a scatter-free absorbing medium depends exponentially on the concentration of the absorbers, their absorbing strength (which usually strongly depends on the wavelength), and the effective optical path length. The problem is that in a complex media such as marine sediments, the effective optical path length is difficult to quantify as it is affected by absorption as well as by a high degree of multiple scattering on sediment grains, MPB cells and other particles. The latter effect is especially important, as it can substantially prolong the effective path length of light within the sediment matrix and thus influence the absorption imprint of the pigments present (Kühl and Jørgensen, 1994; Yang and Miklavcic, 2005). Since the scattering-induced path variations are generally unknown, it is methodologically impossible to determine two unknown entities — the true euphotic depth and the concentration

of the absorbers (Chlorophyll *a*) within that depth — from a single reflectance measurement. Nevertheless, if the depth of optical probing is critical, it can be determined separately using light microprobes (Fenchel and Straarup, 1971; Lassen et al., 1992). Previous measurements with this technique showed that although variable depending on factors such as the Chlorophyll *a* concentration, sediment grain-size or wavelength, the light penetration depth in MPB biofilms is in the range 0.2–3 mm (Kühl et al., 1994; Lassen et al., 1992; MacIntyre et al., 1996). Since 1 mm can be considered a reasonable intermediate light penetration depth in natural marine sediments, we used artificial biofilms of 1 mm thickness to conduct our calibration, validation and stacked-biofilm measurements.

Second, the spectral reflectance-based method of Chl *a* quantification is sensitive not only to the amount of Chl *a* in the layer of sediment where the probing light penetrates, but also to its vertical distribution within that layer. When the vertical distribution is homogeneous, our calibration measurements showed that the relationship between the sedimentary Chl *a* concentration derived from traditional extraction-based spectrophotometric measurements and the microphytobenthic index (MPBI) derived from the spectral reflectance measurement is linear, with the sensitivity monotonously decreasing with the nominal sediment grain-size (Figure 2.3). On the other hand, our measurements with stacked biofilms showed that MPBI can substantially change if the vertical Chl *a* distribution is not homogeneous (Figure 2.5). More research is required to understand this relationship. With respect to natural sediments, epipelic diatoms such as *Amphora Coffeaeformis* form biofilms in the very top layers of the sediment surface (Mitbavkar and Anil, 2004), while epipsammic species are more homogeneously distributed in the top centimeter or two of the sediment surface (Fenchel and Straarup, 1971). Therefore, although the artificial biofilms used in our experiments are not structurally representative of natural biofilms, we suggest that unless the true vertical Chl *a* distribution and the calibration function corresponding to this distribution are known, Chl *a* concentrations derived from the MPBI index must be reported under the assumption that the distribution is vertically homogeneous within the probing depth. One should bear in mind that if this assumption does not hold, the reported Chlorophyll *a* concentrations derived from the spectral-reflectance based measurements may be erroneous by up to 200-300% (see Effects of vertical distribution of Chl *a*). Clearly, this is a major limitation of the spectral reflectance-based method with respect to absolute quantification of Chl *a* in sediments. On the other hand, this drawback can advantageously be used to monitor changes in the vertical Chl *a* distribution, e.g., due to vertical MPB migration, in a non-disruptive way and with a high spatial and temporal resolution. Moreover, if a two-layer distribution is an acceptable approximation for the description of the vertical Chl *a* distribution in the sediment, then quantification of the MPBI maxima and minima over the course of a day allows estimation of the migratory fraction of the Chl *a* standing stock (Figure 2.8).

Third, the spectral reflectance-based method is unable to distinguish between Chlorophyll *a* and its degradation products in bulk natural sediments, as these have virtually identical absorption characteristics in the wavelength region utilized for the calculation of the MPB index (or any other spectral index used for MPB quantification in the literature). Therefore, hyperspectral imaging cannot replace methods, such as liquid chromatography, based on extraction and separation of the various Chlorophyll *a* forms, but can be used as a valuable supplement with benefits that the extraction-based methods lack (e.g., non-invasiveness) or can achieve only with an unreasonably large effort (high spatial resolution).

The hyperspectral imaging method presented here can provide useful insights in studies of microphytobenthos distribution and dynamics. Through its sub-millimeter spatial resolution, the method enables measurements of MPB distribution with an unprecedented level of detail and may thus alleviate the problem of chronic under-sampling of benthic habitats (Spilmont et al., 2011). By allowing minimally invasive *in situ* measurements of spatial and temporal patterns in the MPB distribution on a local scale, it allows studying mechanisms and processes by which they are regulated, such as physical forcing (Figure 2.6A–C), bioturbation and grazing (Figure 2.6D-F), or diel variations in light (Figure 2.8), which is required to improve our understanding of the ecological role and functions of MPB and its response to environmental changes (Miller et al., 1996; Seuront and Leterme, 2006). Last but not least, it can bridge airborne remote sensing measurements with field-based ground-truthing, the latter traditionally done through sediment sampling, and thus enable critical analyses of patterns in benthic ecosystems that integrate effects from the scale of the organisms (microscale) to regional scales (Chapman et al., 2010; Levin, 1992).

2.6 COMMENTS AND RECOMMENDATIONS

Chlorophyll *a* quantification by the hyperspectral imaging method is based on the detection of spectral reflectance. Thus, measurements from a spectrally flat reference board are required to account for incident light spectrum and to convert the electronic signal measured by the imaging detector to reflectance. Ideally, these should be part of each scan, e. g., to account for possible changes in the spectrum of the incident light that may occur if scans are done at ambient illumination over extended periods of the day or during different days. If these changes are negligible, it is sufficient to scan the reference board separately and only once. The potential heterogeneity in the incident light intensity along the line-of-view detected by the imager, such as that occurring when artificial illumination by a lamp is used, are corrected for during data processing, where each captured spatial line in the scan is referenced against the corresponding (averaged) spatial line from the reference board (see also Bachar et al. (2008)). In contrast, minor variability in the incident light intensity during the scan, such

as that induced by a passing cloud when using ambient illumination, are automatically corrected for through the nature of the MPBI index, as long as the incident light field is similarly diffused and has the same shape of the spectrum. However, because this latter variability can be substantial, potentially leading to an over- or under-saturated signal by the imaging detector, it is recommended to conduct field measurements on a cloudless or overcast day, when such fluctuations are minimal.

Many of the spectral correction problems that are critical in hyperspectral imaging at remote-sensing scales are not relevant for imaging at the microscale. This is chiefly due to the comparatively short optical path length through the atmosphere. While this obviates the need for atmospheric corrections, albedo, etc., some attention has to be paid to the optical properties of the water column during field-based hyperspectral scans. Furthermore, microscale events that occur faster than the duration of scanning, such as lateral motion of the surficial sediment due to water flow, could be a source of spatial blurring or misinformation in the Chlorophyll *a* maps. Variations in the topography of the sediment surface could be larger than the depth of focus of the objective lens, leading to spectral mixing in neighboring points due to spatial blurring. This problem can be, however, minimized by using suitable optics with a longer depth of focus. Although not shown here, it is possible to use the grayscale imager to capture deformations of a laser line projected on the sediment surface to reconstruct the topography of the scanned sediment surface at a resolution similar to the hyperspectral image, in a similar manner as previously shown (Cook et al., 2007; Røy et al., 2005). This information could then be used to identify regions of the scanned area that are beyond the depth of focus and should therefore be excluded in subsequent analysis.

The spatial resolution of the hyperspectral maps is determined by the optical magnification of the objective, scanning speed of the line-of-view across the sediment, frame acquisition rate and the imager-to-sediment distance. While these can be configured in several combinations, the resolution is ultimately limited by the intensity of the detected light and the sensitivity and signal-to-noise ratio of the imaging detector. The intensity of the back-scattered light can be increased by increasing the intensity of the incident irradiance, which can be achieved artificially, e.g., through lamps. However, to avoid potentially harmful effects of excessive light exposure, this additional illumination should not substantially exceed the typical ambient intensities to which the studied biofilms are exposed. Artificial illumination is essential when measuring at night, i.e., when the ambient illumination is negligibly low. Under such circumstances, spectral imaging cannot be considered as a fully non-invasive technique, as the artificial illumination could trigger vertical migration in the MPB community. However, due to the rather brief duration of the measurement (10–15 min), our experience is that the artificial illumination will not have significant effects for that particular measurement. Whether or not it would cause significant migration that would be detectable in a subsequent measurement (e. g.in the next hour) is unknown and requires further investigation, al-

though our results obtained during the last night of the vertical migration experiment (Figure 2.8A) indicate that this is unlikely.

Owing to its modular design, the Hypersub system can be adapted for other applications than those presented in this report. For example, by attaching it to a submersible vehicle, the system can be used for rapid and more specific large-scale surveys of the sea-floor, e.g., in coral reef ecosystems, many of which are presently threatened by harmful microalgal colonization (McCook, 2001). By adding a diver interface for viewing the imaged area and controlling the measurement, the system could be operated by a SCUBA diver in a similar interactive way as a regular underwater video recorder. Alternatively, by improving the water depth rating of the underwater housing, the system could be implemented as part of underwater observatories (Barnes et al., 2013) for long-term, remotely operated or autonomous monitoring of the sea-floor.

2.7 ACKNOWLEDGMENTS

We thank the laboratory technicians of the Microsensor group and the electronic and mechanical workshops at the Max Planck Institute for Marine Microbiology for their invaluable assistance throughout the implementation of this project. We thank Michael Kühl from University of Copenhagen for fruitful discussions and experimental suggestions. We also thank Justus van Beusekom, Karsten Reise, and Elisabeth Herre from the Alfred Wegener Institute for Polar and Marine Research, and George Matsui, Sarah Woodin and David Wethey from the University of South Carolina for their support during field campaigns. This work was funded by the Marie Curie Initial Training Network "SENSEnet" (grant 237868), the National Science Foundation (OCE 0928002), and the Max Planck Society of Germany.

2.8 AUTHOR CONTRIBUTIONS

Return to start

Arjun Chennu and Lubos Polerecky designed the project. Arjun Chennu and Paul Färber designed and constructed the Hypersub hardware. Arjun Chennu designed and built the hardware control (SinKraft) and hyperspectral analysis (Hypurveyor) softwares. Arjun Chennu and Mohammad Al-Najjar prepared and measured the calibration biofilms. Nils Volkenborn prepared the field experiments and measured sediment properties. Felix Janssen helped with field instrumentation and field measurements were conducted by Arjun Chennu, Nils Volkenborn and Lubos Polerecky. Data analysis and method development was done by Arjun Chennu and Lubos Polerecky. Manuscript was prepared by Arjun Chennu, Lubos Polerecky, Dirk de Beer, Felix Janssen and Nils Volkenborn.

2.9 REFERENCES

Azovsky, A., E. Chertoprood, M. Saburova, and I. Polikarpov (2004). "Spatio-temporal variability of micro- and meiobenthic communities in a White Sea intertidal sandflat." In: *Estuarine, Coastal and Shelf Science* 60.4, pp. 663–671. DOI: 10.1016/j.ecss.2004.03.005 (cited on page 48).

Bachar, A., L. Polerecky, J. P. Fischer, K. Vamvakopoulos, D. de Beer, and H. M. Jonkers (2008). "Two-dimensional mapping of photopigment distribution and activity of *Chloroflexus*-like bacteria in a hypersaline microbial mat." In: *FEMS microbiology ecology* 65.3, pp. 434–48. DOI: 10.1111/j.1574-6941.2008.00534.x (cited on pages 50, 71).

Bale, A. J. and A. J. Kenny (2007). "Sediment Analysis and Seabed Characterization." In: *Methods for the Study of Marine Benthos*. Third. Blackwell Science Ltd. Chap. 2, pp. 43–86. DOI: 10.1002/9780470995129.ch2 (cited on page 48).

Barillé, L., J.-L. Mouget, V. Méléder, P. Rosa, and B. Jesus (2011). "Spectral response of benthic diatoms with different sediment backgrounds." In: *Remote sensing of Environment* 115.4, pp. 1034–1042. DOI: 10.1016/j.rse.2010.12.008 (cited on pages 49, 55 sq.).

Barnes, C., M. Best, F. Johnson, L. Pautet, and B. Pirenne (2013). "Challenges, Benefits, and Opportunities in Installing and Operating Cabled Ocean Observatories: Perspectives From NEPTUNE Canada." In: *IEEE Journal of Ocean Engineering* 38.1, pp. 144–157. DOI: 10.1109/JOE.2012.2212751 (cited on page 73).

Bhaganagar, K. and T.-J. Hsu (2009). "Direct numerical simulations of flow over two-dimensional and three-dimensional ripples and implication to sediment transport: Steady flow." In: *Coastal Engineering* 56.3, pp. 320–331. DOI: 10.1016/j.coastaleng.2008.09.010 (cited on page 64).

Brito, A., A. Newton, P. Tett, and T. Fernandes (2009a). "Development of an optimal methodology for the extraction of microphytobenthic chlorophyll." In: *Journal of International Environmental Application and Science* 4.1, pp. 42–54 (cited on page 49).

Brito, A., A. Newton, P. Tett, and T. F. Fernandes (2009b). "Temporal and spatial variability of microphytobenthos in a shallow lagoon: Ria Formosa (Portugal)." In: *Estuarine, Coastal and Shelf Science* 83.1, pp. 67–76. DOI: 10.1016/j.ecss.2009.03.023 (cited on page 49).

Carrère, V., N. Spilmont, and D. Davoult (2004). "Comparison of simple techniques for estimating Chlorophyll *a* concentration in the intertidal zone using high spectral-resolution field-spectrometer data." In: *Marine Ecology Progress Series* 274, pp. 31–40. DOI: 10.3354/meps274031 (cited on pages 56, 60).

Chapman, M., T. Tolhurst, R. Murphy, and A. Underwood (2010). "Complex and inconsistent patterns of variation in benthos, micro-algae and sediment over multiple spatial scales." In: *Marine Ecology Progress Series* 398, pp. 33–47. DOI: 10.3354/meps08328 (cited on page 71).

Chennu, A., P. Färber, N. Volkenborn, M. A. A. Al-Najjar, F. Janssen, D. de Beer, and L. Polerecky (2013). "Hyperspectral imaging of the microscale distribution and dynamics of microphytobenthos in intertidal sediments." In: *Limnology and Oceanography: Methods* 11, pp. 511–528. DOI: 10.4319/lom.2013.11.511 (cited on page 47).

Clark, R. N. and T. L. Roush (1984). "Reflectance spectroscopy: Quantitative analysis techniques for remote sensing applications." In: *Journal of Geophysical Research* 89.B7, p. 6329. DOI: 10.1029/JB089iB07p06329 (cited on page 56).

Consalvey, M., D. Paterson, and G. Underwood (2004). "The ups and downs of life in a benthic biofilm: migration of benthic diatoms." In: *Diatom Research* 18, pp. 181–202. DOI: 10.1080/0269249X.2004.9705870 (cited on page 66).

Cook, P. L. M., F. Wenzhöfer, R. N. Glud, F. Janssen, and M. Huettel (2007). "Benthic solute exchange and carbon mineralization in two shallow subtidal sandy sediments: Effect of advective pore-water exchange." In: *Limnology and Oceanography* 52.5, pp. 1943–1963. DOI: 10.4319/lo.2007.52.5.1943 (cited on page 72).

Farías, M. E., N. Rascovan, D. M. Toneatti, V. H. Albarracín, M. R. Flores, D. G. Poiré, M. M. Collavino, O. M. Aguilar, M. P. Vazquez, and L. Polerecky (2013). "The discovery of stromatolites developing at 3570 m above sea level in a high-altitude volcanic lake Socompa, Argentinean Andes." In: *PloS one* 8.1, e53497. DOI: 10.1371/journal.pone.0053497 (cited on page 50).

Fenchel, T. and B. J. B. Straarup (1971). "Vertical distribution of photosynthetic pigments and the penetration of light in marine sediments." In: *Oikos* 22.2, pp. 172–182 (cited on page 70).

Forster, R. and B. Jesus (2006). "Field spectroscopy of estuarine intertidal habitats." In: *International Journal of Remote Sensing* 27.17, pp. 3657–3669. DOI: 10.1080/01431160500500367 (cited on page 49).

Grinham, A. R., T. J. Carruthers, P. L. Fisher, J. W. Udy, and W. C. Dennison (2007). "Accurately measuring the abundance of benthic microalgae in spatially variable habitats." In: *Limnology and Oceanography: Methods* 5, pp. 119–125. DOI: 10.4319/lom.2007.5.119 (cited on page 49).

Guarini, J.-M. and G. Blanchard (1998). "Dynamics of spatial patterns of microphytobenthic biomass: inferences from a geostatistical analysis of two comprehensive surveys in Marennes-Oléron Bay (France)." In: *Marine Ecology Progress Series* 166, pp. 131–141. DOI: 10.3354/meps166131 (cited on page 49).

Hakvoort, H., K. Heymann, C. Stein, and D. Murphy (1997). "In-situ optical measurements of sediment type and phytobenthos of tidal flats: a basis for imaging remote sensing spectroscopy." In: *Ocean Dynamics* 49.2-3, pp. 367–373. DOI: 10.1007/BF02764045 (cited on page 49).

Honeywill, C., D. Paterson, and S. Hagerthey (2002). "Determination of microphytobenthic biomass using pulse-amplitude modulated minimum fluorescence." In: *European Journal of Phycology* 37.4, pp. 485–492. DOI: 10.1017/S0967026202003888 (cited on page 49).

Ionescu, D., C. Siebert, L. Polerecky, Y. Y. Munwes, C. Lott, S. Häusler, M. Bižić-Ionescu, C. Quast, J. Peplies, F. O. Glöckner, A. Ramette, T. Rödiger, T. Dittmar, A. Oren, S. Geyer, H.-J. Stärk, M. Sauter, T. Licha, J. B. Laronne, and D. de Beer (2012). "Microbial and chemical characterization of underwater fresh water springs in the Dead Sea." In: *PloS one* 7.6, e38319. DOI: 10.1371/journal.pone.0038319 (cited on page 50).

Jesus, B., V. Brotas, M. Marani, and D. Paterson (2005). "Spatial dynamics of microphytobenthos determined by PAM fluorescence." In: *Estuarine, Coastal and Shelf Science* 65.1-2, pp. 30–42. DOI: 10.1016/j.ecss.2005.05.005 (cited on page 49).

Jesus, B., R. Perkins, and C. Mendes (2006). "Chlorophyll fluorescence as a proxy for microphytobenthic biomass: alternatives to the current methodology." In: *Marine Biology* 150.1, pp. 17–28. DOI: 10.1007/s00227-006-0324-2 (cited on page 49).

Joint, I., J. Gee, and R. Warwick (1982). "Determination of fine-scale vertical distribution of microbes and meiofauna in an intertidal sediment." In: *Marine Biology* 72.2, pp. 157–164. DOI: 10.1007/BF00396916 (cited on page 68).

Kazemipour, F., V. Méléder, and P. Launeau (2011). "Optical properties of microphytobenthic biofilms (MPBOM): Biomass retrieval implication." In: *Journal of Quantitative Spectroscopy and Radiative Transfer* 112.1, pp. 131–142. DOI: 10.1016/j.jqsrt.2010.08.029 (cited on page 49).

Kohls, K., R. M. M. Abed, L. Polerecky, M. Weber, and D. de Beer (2010). "Halotaxis of cyanobacteria in an intertidal hypersaline microbial mat." In: *Environmental microbiology* 12.3, pp. 567–75. DOI: 10.1111/j.1462-2920.2009.02095.x (cited on page 50).

Kokaly, R. F. and R. N. Clark (1999). "Spectroscopic Determination of Leaf Biochemistry Using Band-Depth Analysis of Absorption Features and Stepwise Multiple Linear Regression." In: *Remote Sensing of Environment* 67.3, pp. 267–287. DOI: 10.1016/S0034-4257(98)00084-4 (cited on page 56).

Krause-Jensen, D. and K. Sand-Jensen (1998). "Light attenuation and photosynthesis of aquatic plant communities." In: *Limnology and Oceanography* 43.3, pp. 396–407. DOI: 10.4319/lo.1998.43.3.0396 (cited on page 59).

Kromkamp, J. C., E. P. Morris, R. M. Forster, C. Honeywill, S. Hagerthey, and D. M. Paterson (2006). "Relationship of intertidal surface sediment chlorophyll concentration to hyperspectral reflectance and chlorophyll fluorescence." In: *Estuaries and Coasts* 29.2, pp. 183–196 (cited on page 49).

Kühl, M. and B. B. Jørgensen (1994). "The light field of microbenthic communities: radiance distribution and microscale optics of sandy coastal sediments." In: *Limnology and Oceanography* 39.6, pp. 1368–1398. DOI: 10.4319/lo.1994.39.6.1368 (cited on page 69).

Kühl, M., C. Lassen, and B. B. Jørgensen (1994). "Light penetration and light intensity in sandy marine sediments measured with irradiance and scalar irradiance fiberoptic microprobes Rid A-1977-2009." In: *Marine Ecology Progress Series* 1.2, pp. 139–148 (cited on page 70).

Kühl, M. and L. Polerecky (2008). "Functional and structural imaging of phototrophic microbial communities and symbioses." In: *Aquatic Microbial Ecology* 53, pp. 99–118. DOI: doi:10.3354/ame01224 (cited on pages 49 sq.).

Lassen, C., H. Ploug, and B. B. Jørgensen (1992). "Microalgal photosynthesis and spectral scalar irradiance in coastal marine sediments of Limfjorden, Denmark." In: *Limnology and Oceanography* 37.4, pp. 760–772. DOI: 10.4319/lo.1992.37.4.0760 (cited on page 70).

Levin, S. (1992). "The problem of pattern and scale in ecology: the Robert H. MacArthur award lecture." In: *Ecology* 73.6, pp. 1943–1967. DOI: 10.2307/1941447 (cited on pages 48, 71).

Lorenzen, C. (1967). "Determination of chlorophyll and pheo-pigments: spectrophotometric equations." In: *Limnology and Oceanography* 12.2, pp. 343–346. DOI: 10.4319/lo.1967.12.2.0343 (cited on page 49).

MacIntyre, H., R. Geider, and D. Miller (1996). "Microphytobenthos: The ecological role of the "secret garden" of unvegetated, shallow-water marine habitats. I. Distribution, abundance and primary production." In: *Estuaries and Coasts* 19.2, pp. 186–201. DOI: 10.2307/1352224 (cited on pages 48, 70).

McCook, L. J. (2001). "Competition between corals and algal turfs along a gradient of terrestrial influence in the nearshore central Great Barrier Reef." In: *Coral Reefs* 19, pp. 419–425. DOI: 10.1007/s003380000119 (cited on page 73).

Miller, D., R. Geider, and H. MacIntyre (1996). "Microphytobenthos: the ecological role of the "secret garden" of unvegetated, shallow-water marine habitats. II. Role in sediment stability and shallow-water food webs." In: *Estuaries and Coasts* 19.2A, pp. 202–212. DOI: 10.2307/1352225 (cited on pages 48, 71).

Mitbavkar, S. and A. C. Anil (2004). "Vertical migratory rhythms of benthic diatoms in a tropical intertidal sand flat: influence of irradiance and

tides." In: *Marine Biology* 145.1, pp. 9–20. DOI: 10.1007/s00227-004-1300-3 (cited on page 70).

Montagna, P., G. Blanchard, and A. Dinet (1995). "Effect of production and biomass of intertidal microphytobenthos on meiofaunal grazing rates." In: *Journal of Experimental Marine Biology and Ecology* 185.2, pp. 149–165. DOI: 10.1016/0022-0981(94)00138-4 (cited on page 48).

Moreno, S. and F. X. Niell (2004). "Scales of variability in the sediment chlorophyll content of the shallow Palmones River Estuary, Spain." In: *Estuarine, Coastal and Shelf Science* 60.1, pp. 49–57. DOI: 10.1016/j.ecss.2003.06.006 (cited on page 48).

Murphy, R. J., T. J. Tolhurst, M. G. Chapman, and A. J. Underwood (2005). "Estimation of surface chlorophyll-a on an emersed mudflat using field spectrometry: accuracy of ratios and derivative-based approaches." In: *International Journal of Remote Sensing* 26.9, pp. 1835–1859. DOI: 10.1080/01431160512331326530 (cited on pages 49, 55, 59).

— (2008). "Spatial variation of chlorophyll on estuarine mudflats determined by field-based remote sensing." In: *Marine Ecology Progress Series* 365, pp. 45–55. DOI: 10.3354/meps07456 (cited on page 48).

Murphy, R. J., A. J. Underwood, and A. C. Jackson (2009). "Field-based remote sensing of intertidal epilithic chlorophyll: Techniques using specialized and conventional digital cameras." In: *Journal of Experimental Marine Biology and Ecology* 380.1-2, pp. 68–76. DOI: 10.1016/j.jembe.2009.09.002 (cited on pages 49, 60).

Al-Najjar, M. A. A., D. de Beer, M. Kühl, and L. Polerecky (2012). "Light utilization efficiency in photosynthetic microbial mats." In: *Environmental Microbiology* 14.4, pp. 982–92. DOI: 10.1111/j.1462-2920.2011.02676.x (cited on page 50).

Nozais, C., R. Perissinotto, and S. Mundree (2001). "Annual cycle of microalgal biomass in a South African temporarily-open estuary: nutrient versus light limitation." In: *Marine Ecology Progress Series* 223, pp. 39–48. DOI: doi:10.3354/meps223039 (cited on page 48).

Palmer, J. D. and F. E. Round (1967). "Persistent, vertical-migration rhythms in benthic microflora. VI. The tidal and diurnal nature of the rhythm in the diatom *Hantzschia virgata*." In: *The Biological Bulletin* 132.1, pp. 44–55. DOI: 10.1017/S0025315400017641 (cited on page 66).

Polerecky, L., A. Bissett, M. Al-Najjar, P. Färber, H. Osmers, P. A. Suci, P. Stoodley, and D. de Beer (2009a). "Modular spectral imaging (MOSI) system for discrimination of pigments in cells and microbial communities." In: *Applied and Environmental Microbiology* 75.3, pp. 1–9. DOI: 10.1128/AEM.00819-08 (cited on pages 49 sq., 55).

Polerecky, L., J. M. Klatt, M. A. A. Al-Najjar, and D. de Beer (2009b). "Hyper-spectral imaging of biofilm growth dynamics." In: *Hyperspectral*

Image and Signal Processing: Evolution in Remote Sensing. WHISPERS '09. Pp. 1–4 (cited on page 50).

Rasmussen, A., G. Banta, and O. Andersen (1998). "Effects of bioturbation by the lugworm *Arenicola marina* on cadmium uptake and distribution in sandy sediments." In: *Marine Ecology Progress Series* 164.Wells 1966, pp. 179–188. DOI: doi:10.3354/meps164179 (cited on page 64).

Røy, H., M. Huettel, and B. B. Jørgensen (2005). "The influence of topography on the functional exchange surface of marine soft sediments, assessed from sediment topography measured in situ." In: *Limnology and Oceanography* 50.1, pp. 106–112. DOI: 10.4319/lo.2005.50.1.0106 (cited on page 72).

Serôdio, J., J. Marques da Silva, and F. Catarino (1997). "Non-destructive tracing of migratory rhythms of intertidal benthic microalgae using in vivo chlorophyll a fluorescence." In: *Journal of Phycology* 33.3, pp. 542–553. DOI: 10.1111/j.0022-3646.1997.00542.x (cited on page 49).

Seuront, L., V. Gentilhomme, and Y. Lagadeuc (2002). "Small-scale nutrient patches in tidally mixed coastal waters." In: *Marine Ecology Progress Series* 232, pp. 29–44. DOI: 10.3354/meps232029 (cited on page 48).

Seuront, L. and S. Leterme (2006). "Microscale patchiness in microphytobenthos distributions: evidence for a critical state." In: *Functioning Of Microphytobenthos In Estuaries*. Ed. by J. C. Kromkamp, J. de Brouwer, G. F. Blanchard, R. M. Forster, and V. Créach. Royal Netherlands Academy of Arts and Sciences, pp. 167–186 (cited on pages 48, 71).

Spilmont, N., D. Davoult, and A. Migné (2006). "Benthic primary production during emersion: In situ measurements and potential primary production in the Seine Estuary (English Channel, France)." In: *Marine pollution bulletin* 53.1-4, pp. 49–55. DOI: 10.1016/j.marpolbul.2005.09.016 (cited on page 48).

Spilmont, N., L. Seuront, T. Meziane, and D. T. Welsh (2011). "There's more to the picture than meets the eye: Sampling microphytobenthos in a heterogeneous environment." In: *Estuarine, Coastal and Shelf Science* 95.4, pp. 470–476. DOI: 10.1016/j.ecss.2011.10.021 (cited on pages 48 sq., 59, 66, 71).

Stal, L. J. (2010). "Microphytobenthos as a biogeomorphological force in intertidal sediment stabilization." In: *Ecological Engineering* 36.2, pp. 236–245. DOI: 10.1016/j.ecoleng.2008.12.032 (cited on page 48).

Sundbäck, K., V. Enoksson, W. Graneli, and K. Pettersson (1991). "Influence of sublittoral microphytobenthos on the oxygen and nutrient flux between sediment and water: a laboratory continuous-flow study." In: *Marine Ecology Progress Series* 74.2, pp. 263–279 (cited on page 48).

Underwood, A. J., M. G. Chapman, and S. D. Connell (2000). "Observations in ecology: you can't make progress on processes without understanding the patterns." In: *Journal of Experimental Marine Biology and*

Ecology 250.1-2, pp. 97–115. DOI: 10.1016/S0022-0981(00)00181-7 (cited on page 48).

Volkenborn, N., L. Polerecky, D. S. Wethey, and S. A. Woodin (2010). "Oscillatory porewater bioadvection in marine sediments induced by hydraulic activities of *Arenicola marina*." In: *Limnology and Oceanography* 55.3, pp. 1231–1247. DOI: 10.4319/lo.2010.55.3.1231 (cited on page 64).

Whitney, D. E. and W. M. Darley (1979). "A method for the determination of chlorophyll a in samples containing degradation products." In: *Limnology and Oceanography* 24.1, pp. 183–186. DOI: 10.4319/lo.1979.24.1.0183 (cited on page 49).

Yang, L. and S. J. Miklavcic (2005). "Revised Kubelka—Munk theory. III. A general theory of light propagation in scattering and absorptive media." In: *Journal of the Optical Society of America A* 22.9, p. 1866. DOI: 10.1364/JOSAA.22.001866 (cited on page 69).

3

THE GARDENING LUGWORM: BIOADVECTION BY *ARENICOLA MARINA* AND ITS FERTILIZING EFFECT ON MICROPHYTOBENTHOS AT THE SEDIMENT SURFACE

Arjun Chennu[1], Nils Volkenborn[2,3], Dirk de Beer[1], David S. Wethey[2], Sarah A. Woodin[2] and Lubos Polerecky[1,4]

See Author contributions

MANUSCRIPT STATUS

Submitted to *Limnology and Oceanography* on 20.11.2013, pending review.

3.1 ABSTRACT

We investigated the effect of bioturbation by lugworms (*Arenicola marina*) on the standing stock of microphytobenthos (MPB) biomass in surficial permeable marine sediments. We hypothesized that despite their feeding on MPB, lugworms increase the overall MPB biomass at the sediment surface through enhanced nutrient supply by porewater bioadvection. We used hyperspectral imaging to record surficial Chlorophyll *a* distributions in the presence and absence of lugworms, both in the field and in the laboratory. We found that in a period of days to weeks, the surficial MPB biomass was 1.5–2.5–fold higher in the presence of lugworms as compared to sediments without lugworms. This enhancement comprised a 2.2–3.3–fold higher biomass in the bioadvected (but non-reworked) areas and a reduced (1.4–fold higher) biomass in reworked areas relative to the MPB biomass in the sediment without worms. Experiments with artificial lugworm-mimics confirmed that porewater advection is sufficient to explain the increase in the surficial MPB biomass observed with real lugworms. Additionally, modeling results indicated that the increased nutrient flux across the sediment-water interface results not only from enhanced porewater transport linked to bioadvection but also from stimulation of nutrient remineralization in the sediment induced by input of electron acceptors (e. g., oxygen) by lugworm pumping. Our results indicate that the injection of water at depth leads to the fertilization of the

1 Max Planck Institute for Marine Microbiology, Celsiusstrasse 1, Bremen 28359, Germany
2 Dept. of Biological Sciences, University of South Carolina, Columbia SC 29208, USA
3 IFREMER, Laboratory of Benthic Ecology, Technopole Brest BP70, Plouzane, France
4 Dept. of Earth Sciences - Geochemistry, Utrecht University, Budapestlaan 4, 3584 CD Utrecht, The Netherlands

microphytobenthic 'garden' at the sediment surface, and thus increases the overall primary productivity of the lugworms' habitat.

3.2 INTRODUCTION

The function and structure of benthic ecosystems emerge from a tight interplay between the physics of the sediment environment and the biology of the bottom-dwelling organisms (Herman et al., 1999; Reise, 2002). The physical parameters of the sediment, such as grain-size and permeability, constrain the distribution and abundance of benthic macrofauna. On the other hand, large burrowing macroinfauna, such as arenicolid polychaetes or thalassinid crustaceans, significantly alter the physical state of the environment (Krantzberg, 1985). They thereby may improve their own living conditions and also affect those of other organisms, a concept known as 'ecosystem engineering' (Levinton, 1995).

In intertidal sediments, e. g., in the Wadden Sea, the lugworm *Arenicola marina* is a dominant ecosystem engineer that reworks and irrigates immense volumes of sediment (Beukema and De Vlas, 1979; Reise, 1985). Lugworms live in 20 to 40 cm deep J-shaped blind-ending burrows (reviewed by Riisgård and Banta (1998) and Wells (1966)). The sediment above the blind end is funneled down and selectively ingested by the lugworm. After partial digestion of organic matter the sediment is defecated at the surface above the tail shaft in characteristic mounds of coiled fecal strings. In addition to sediment reworking, lugworms ventilate their burrows thro-ugh peristalsis from tail to head. This not only fulfills the most critical function of satisfying the lugworm's metabolic demand for oxygen, but also leads to enhanced transport of oxygen and other solutes from the overlying water into the sediment. The sediment reworking and bioirrigation activities by the lugworms bioturbate the sediment into a significantly altered state in terms of sediment stratification, porewater solute distributions (Hüttel, 1990; Volkenborn et al., 2007) and diversity and activity of microbial populations (Kristensen, 2001; Nielsen et al., 2003; Reichardt, 1988). The requirement to ventilate the blind-ending burrow restricts lugworms from colonizing cohesive muddy sediments, as the pressure required to force a flow of water through such sediments would be beyond the physiological limits of the "lugworm pump" (Meysman et al., 2006; Riisgård et al., 1996). On the other hand, muddy-sand to sandy sediments are permeable enough to allow such porewater percolation, which makes them the primary habitat for *Arenicola marina* (Meysman et al., 2005).

Sandy sediments, which span 70% of the coastal area in the North Sea, display microbial activity and organic remineralization that is commensurate with nutrient-rich muddy sediments despite containing lower levels of organic matter and microbial cells (de Beer et al., 2005). This occurs due to greater transport efficiency of advection, which is the dominant mode of solute transport in permeable sediments (Hüttel, 1990; Malcolm

and Sivyer, 1997). Porewater advection occurs when pressure gradients are induced within the sediment. A physical driver for advection is the interaction between the hydrodynamics of the overlying water (i. e. currents and waves) and the sediment topography, which cause significant porewater flow within the upper 5 cm of the sediment (Precht et al., 2004; Precht and Huettel, 2003). A biotic driver of advection is the pumping of water into the sediment by organisms with incomplete burrow linings such as arenicolid polychaetes (Volkenborn et al., 2010; Wethey et al., 2008) and some thalassinid crustaceans and bivalves (Volkenborn et al., 2012a; Volkenborn et al., 2012b). This process, referred to as *bioadvection*, can generate porewater flows much deeper in the sediment than those from physical forcing. The consequent changes in the steepness of diffusional gradients (Kristensen, 1985; Rasmussen et al., 1998) and non-local mixing of surrounding porewater with overlying and burrow waters (Boudreau, 1984; Hüttel, 1990) are important factors that affect the geochemistry of permeable sediments (Aller, 2001; Kristensen, 2000; Volkenborn et al., 2010).

Bioadvection also has an important role in the nutritional regimen of lugworms. The ability of lugworms to derive sustenance from surprisingly low-nutrient sediment has elicited considerable discussion (Riisgård and Banta, 1998). Several possible sources of nutrition have been considered: detritus, surficial diatoms, funnel microbes and meiofauna. Hylleberg (1975) introduced the concept of "gardening" as the process of stimulating growth of meiofauna in the headshaft of the burrow and their subsequent use as food. Subsequently, Grossmann and Reichardt (1991) considered any growth-promoting effect of macroinfauna on sedimentary bacteria as gardening, while Plante et al. (1990) postulated that the nutritional benefit must be from direct consumption of the stimulated bacteria and not mediated through the food-web. There is evidence that the direct consumption of bacteria and (subducted) diatoms comprise the primary diet of lugworms (Retraubun et al., 1996), but the effects of sediment reworking and bioirrigation by lugworms have been primarily studied with respect to the bacterial and meiofaunal biomass within the burrow. As such, little information is available on the effects of bioirrigation on surficial microphytobenthos (MPB), comprising diatoms, dinoflagellates and cyanobacteria, which is a major compartment of the lugworm's microbenthic garden (MacIntyre et al., 1996; Retraubun et al., 1996).

In this study, we explore whether gardening by *Arenicola marina* extends to driving MPB growth at the sediment surface above burrows. Our conceived mechanism was that the ventilation current induced by lugworm pumping pressurizes the porewater in the (permeable) sediment (Wethey and Woodin, 2005) surrounding the feeding pocket in the blind-end of the burrow. Since the transported water contains oxygen, this results in an upward as well as lateral percolation of partially oxygenated porewater (Meysman et al., 2005; Volkenborn et al., 2010; Wethey et al., 2008) through deeper, anoxic sediment regions, which stimulates diagenetic nutrient remineralization (Kristensen, 2000). These nutrients are then transported by porewater bioadvection towards the sediment surface, where

they aid fertilization and thus increase the MPB biomass. Given that porewater pressure fluctuations can be measured >30 cm away from lugworms (Wethey et al., 2008), we expected that the area of influence would reach far beyond the immediate surroundings of the feeding pocket.

To understand the cumulative effect of these opposing forces of lugworm bioturbation, i. e. depletion by feeding or fecal deposition versus fertilization by bioadvection of nutrient-rich porewater, we measured the surficial MPB biomass concentrations in the presence and absence of lugworms in three experimental settings: 1) *in situ* experimental plots with and without lugworms, where the MPB growth occurred under natural conditions, but was potentially affected by factors other than the presence or absence of lugworms, such as grazing or physical disturbance by waves or currents; 2) laboratory experimental containers with and without lugworms, which allowed us to isolate the effects of the lugworm bioturbation and separately quantify the effects of reworking (due to feeding and defecation) and bioadvection (due to burrow ventilation) on the MPB concentrations; and 3) laboratory experimental containers with and without mechanical lugworm-mimics, which allowed us to isolate the effect of bioadvection from all other perturbations. Additionally, we used numerical modeling to explore the mechanism by which bioadvection could generate higher nutrient fluxes across the sediment-water interface, and whether this enhancement would conform to an increased fertilization of MPB at the surface.

3.3 METHODS

3.3.1 *Hyperspectral imaging of MPB biomass*

MPB biomass in surficial sediments, measured as Chlorophyll *a* (Chl *a*) concentrations in the porewater, was quantified using the hyperspectral imaging system hypersub and experimental protocols described by Chennu et al. (2013). Briefly, the system captures back-scattered light from the sediment and, using a spectral reference, converts the detected signal into reflectance spectra (wavelength range 400–900 nm, spectral resolution about 1 nm). These spectra are used to calculate a microphytobenthos index (MPBI) at each location in the spectral image, from which Chl *a* concentrations in the top millimeter of the sediment are estimated by using a linear calibration (Chennu et al., 2013). The non-destructive character of the imaging method allows monitoring of the spatial patterns of Chl *a* concentrations over the same sediment region with high spatial and temporal resolutions.

During this study, the hypersub system was positioned 0.8–1.0 m above the sediment surface and the scanning parameters were adjusted to obtain hyperspectral images with a spatial resolution of 1×1 mm per pixel. *In situ* measurements were made with ambient sunlight, whereas

measurements in experimental tanks (see below) used partially shaded ambient light together with a supplemental illumination from overhead halogen lamps. Measurements conducted during the night involved illumination of the sediment surface only by the halogen lamps, which was restricted to the duration of the scan. Since each scan took about 10 min and subsequent scans were separated by at least 1 hour, the effects of the artificial illumination on vertical migration of MPB within the surficial sediment layer, which could affect interpretation of the results (Chennu et al., 2013), were negligible. In all measurements, a gray plastic board with a matte surface finish was used as a spectrally flat reference.

Chlorophyll *a* concentrations (µg Chl *a* ml^{-1}PW) were calculated from the MPBI as Chl $a = S \times (\text{MPBI} - \text{MPBI}_0)$, where S = 1776 µg Chl *a* ml^{-1}PW and MPBI_0 = 0.030. These calibration values correspond to the measured grain-size of the studied sediment (125–250 µm), which was assumed not to vary significantly over the scanned sediment regions (Chennu et al., 2013). In addition to Chl *a* maps, which are presented here as false-color images, true-color images of the scanned sediment regions were generated by using reflectance values at specific wavelengths as intensities of the red (640 nm), green (550 nm) and blue (460 nm) channels in composite RGB images.

3.3.2 *Experimental design*

The spatio-temporal variations of Chl *a* were studied in natural sediments with and without lugworms. For all experiments in this study, sediments were collected from an intertidal flat, sieved through a coarse mesh (5 mm) to exclude large infauna and other objects, and subsequently homogenized. The sediments from the deeper anoxic layers and the surficial oxic layer were processed separately. Subsequently, they were recomposed in a similar way as the original oxic and anoxic layers, and left to settle for at least 24 hours before the commencement of experiments.

3.3.2.1 *In situ experiment in the presence and absence of lugworms*

To study the effect of lugworm activity on MPB distributions under natural conditions, experimental plots with and without lugworms were established in the intertidal zone near the island of Sylt, Germany (55.04°N, 8.41°E) in summer 2010. The site contained abundant natural population of lugworms and was close to the area investigated previously by Volkenborn et al. (2007). Replicate plots were established by burying open-top mesh bags (diameter 18 cm, 25 cm deep, mesh size 1 mm) into the sediment and surrounding them by a horizontal exclusion mesh (50×50 cm with 1 mm mesh) placed at a depth of 10 cm. The mesh bags contained recomposed sediment from the site (permeable sandy sediment, grain-size 125–250 µm and porosity 0.39). Three days after the establishment of the

plots, 4 small lugworms (per lugworm wet weight: 1.46 ± 0.30 g; total length: 7.5 ± 0.8 cm) were added to three of the six mesh bags. This corresponded to a lugworm abundance of 16 ind. m^{-2}, which is within the typical natural lugworm abundances found in this area (10-30 ind m^{-2}; Volkenborn and Reise, 2006). Occasional counts of fecal mounds within the plots and the collection of worms at the end of the experiment confirmed that all lugworms remained active within the mesh bags over the course of the experiment. Hyperspectral scans of the plots were made 5 weeks after the introduction of the lugworms into the mesh bags.

3.3.2.2 *Laboratory experiment in the presence and absence of lugworms*

To study the effect of lugworm activity on the growth of MPB under more controlled conditions and in isolation from other natural perturbations, incubation experiments were conducted in a greenhouse laboratory at the Wadden Sea Station Sylt (Germany) in summer 2010. Sediment from the site of the *in situ* experiment was collected and recomposed (as described above) into six containers (area 18.5×18.5 cm, 20 cm height). Incubation was performed with the containers submerged in a large tank with continuously recirculating seawater maintained at 18 °C. After one day, single lugworms (wet weight 4.33 ± 0.4 g) were added to three of the six containers. The sediment surface was exposed to natural illumination shaded by the roof of the greenhouse. Hyperspectral scans of the sediment surfaces were made 1, 4 and 11 days after the lugworms were added.

3.3.2.3 *Laboratory experiment in the presence and absence of a lugworm-mimic*

To test whether porewater transport that mimics lugworm pumping could yield increased MPB stock at the sediment surface, similar incubation experiments were conducted as described above but using a mechanical lugworm-mimic instead of real lugworms. This was done in an open-air laboratory at the Baruch Marine Field Laboratory of the University of South Carolina in summer 2011. Sediment was collected from an intertidal flat at Oyster Landing, North Inlet, Winyah Bay, South Carolina, USA (33.35°N, 79.19°W), and processed and recomposed into six round containers (diameter 15 cm, height 18.5 cm).

The biomimetic porewater flow was administered through the use of the "robolug" system (Matsui et al., 2011), which allows realistic imitation of porewater advection produced by lugworms. The robolug system consisted of a thin (1.6 mm inner diameter) tube, with one end connected to a peristaltic pump and the other end entering the buckets from the side and buried (14 cm deep) within the sediment at the central axis of the container. The use of pulsed unidirectional pumping that delivered 0.25 ml pulses of seawater at a frequency of 6 pulses per minute through the tube outlet (2.5 mm diameter) ensured that the average pumping rate (1.5 ml min^{-1}) as well as the source pressures resembled those induced by

real "lugworm pumps" (Matsui et al., 2011; Riisgård et al., 1996; Wethey et al., 2008). Additionally, to mimic the oxygen concentration in the water pumped by real lugworms, which is reduced due to lugworm's respiration (Timmermann et al., 2006; Volkenborn et al., 2010), the water pumped by the lugworm-mimic was maintained at approximately 30% air saturation by bubbling with N_2 gas. The robolug outlets were set up in three of the six containers; the remaining three containers had no active porewater flow within the sediment. Incubation of the containers was performed in a large tank filled with continuously circulating seawater at 25 °C. Sediment surface was exposed to natural illumination shaded by the roof of the open-air laboratory to 90–150 µmol photons $m^{-2}s^{-1}$. Hyperspectral scans of the sediment surfaces were made in about 1 h intervals over 4 days using halogen lamp illumination as described above.

3.3.3 *Modeling of nutrient flux in the containers with a lugworm-mimic*

To interpret the spatial patterns of MPB growth observed in the containers of the robolug lugworm-mimic experiment, dynamic transport of nutrients across the sediment-water interface (SWI) was modeled using the Comsol software (v4.3a from www.comsol.com). The no-flow containers were modeled with the "Transport of dilute species" module and the robolug containers with the "Reacting flow in porous media" module of the software. Both simulations were done in 3D under stationary and time-dependent conditions.

The geometry consisted of two sub-domains: a porous medium with the same porosity (0.39), permeability (2.95×10^{-12} m^2) and geometry (see above) as the sediment in the experimental containers, and a thin layer of water above. The latter domain was introduced to be able to fix the nutrient concentration at some distance above the SWI to that in the overlying water (see below). For the situation with no porewater flow, this distance corresponds to the thickness of the diffusive boundary layer (DBL), which ranges between 0.1 mm and 1 mm depending on the velocity of the laminar flow above the SWI (Boudreau and Jørgensen, 2001). Therefore, the thickness of the thin water layer in our model was set to 0.5 mm in both modeled scenarios (with and without porewater flow). This numerical choice did not influence significantly the modeled results.

The robolug outlet was approximated by a sphere with a radius of 2.5 mm, which was chosen to simplify numerical simulations. Although this choice did not match the shape of the real robolug outlet, the distance of the outlet to the SWI (14 cm) was large enough that the modeling results at the SWI were not significantly affected. This geometrical arrangement was similar to that employed in the "pocket injection" model of Meysman et al. (2006) and Meysman et al. (2005), where it was demonstrated that the hydraulic forces exerted by ventilating lugworms in permeable sediments can be adequately abstracted as emanating from a sphere located at the

depth of the feeding pocket. Water injection through the robolug outlet at the experimental value of 1.5 ml min^{-1} was achieved by setting a constant flow-velocity of 0.816 mm s^{-1} across the surface of the injection sphere, which accounted for the porosity of the medium. Boundary conditions for the porewater flow were set to zero-flow (i. e., no slip) at the outer and lower boundaries of the domain (corresponding to the container walls) and to zero pressure at the upper domain boundary (corresponding to the top of the water layer above the SWI).

The initial concentration of nutrients in the sediment sub-domain was set to zero, which was in line with the porewater replacement by the initial sediment processing (homogenization and recomposition). Since the overlying water in the experimental tank had no significant nutrients and was well-mixed, the concentration of nutrients in the injected water (when modeling the robolug containers) as well as at the top of the thin water layer above the SWI was set to zero. The latter boundary condition allowed differentiation between the diffusive and advective contributions to the total nutrient flux across the SWI, which is in contrast to models of Meysman et al. (2006) and Meysman et al. (2005), where such distinction is not possible. Nutrient generation was assumed to occur at a constant rate throughout the sediment sub-domain for both the no-flow and robolug containers. The choice of the nutrient generation rate (1 μmol $m^{-3}s^{-1}$) was not important since the aim of the model was to obtain the relative spatial distribution and not the absolute values of nutrient fluxes across the SWI.

3.4 RESULTS

3.4.1 *In situ chlorophyll distribution in the presence and absence of lugworms*

The true-color and Chl *a* maps from the *in situ* experiment showed a clear difference between the experimental plots with and without lugworms (Figure 3.1A–D). The presence of lugworms was manifested by biogenic structures such as fecal mounds or feeding funnels visible at the sediment surface (p1 and p2 in Figure 3.1A). Freshly defecated sediment was characterized by very low Chl *a* concentrations, indicating effective removal of chlorophyll by the lugworms (Figure 3.1E: reworked). In contrast, sediment that was not visibly affected by reworking (sediment excluding feeding funnels and fecal mounds) showed greatly enhanced Chl *a* content, indicating an increased MPB standing stock in these regions (Figure 3.1E: bioadvected).

The overall surficial MPB stock, measured as the Chl *a* mean over the scanned area, was about 2.5–fold higher in the sediment with lugworms as compared with the lugworm-free sediment (Figure 3.1E). While the Chl *a* standard deviation over the scanned area was about 2.5–fold higher in the presence of lugworms as well (Figure 3.1E), the coefficient of variation

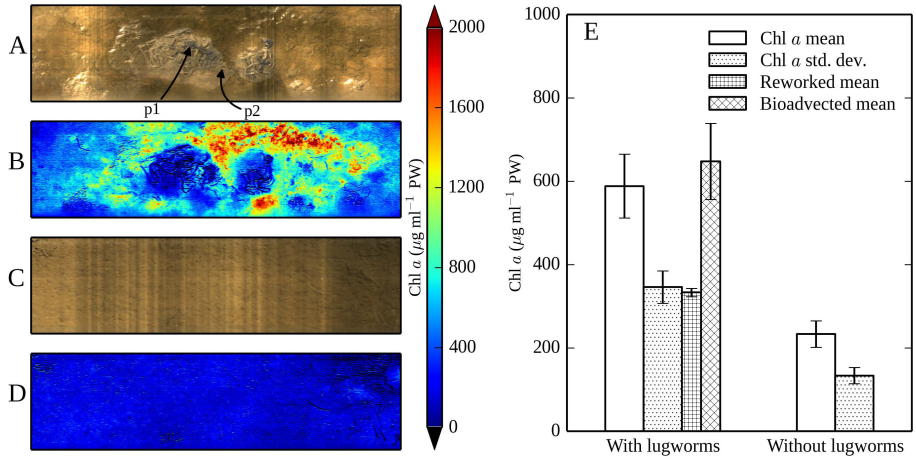

Figure 3.1: Examples of Chlorophyll *a* maps at the surface of permeable intertidal sediments with (B) and without (D) lugworms, shown together with the corresponding true color images of the sediment surface (A and C). Measurements were done *in situ*, around noon, five weeks after the establishment of the experimental plots, using the hyperspectral imaging system Hypersub. The true-color image A shows biogenic structures characteristic for lugworms, such as fecal mounds (p1) and feeding funnels (p2). Panel E shows averages and standard deviations of the surficial Chl *a* concentrations, as derived from hyperspectral scans of 3 replicate plots. For the lugworm plots, sediment areas that were undisturbed (bioadvected) and affected by reworking were averaged separately. Error bars represent standard errors.

was about the same (58%) for both treatments. Based on the true-color images of the sediment surface, the maps of the sediment with lugworms were sectioned qualitatively into regions affected by reworking and those that were visibly undisturbed. This qualitative sectioning revealed that the sediment regions undisturbed by reworking contained up to 3.3–fold higher Chl *a* content than the sediment without lugworms, whereas Chl *a* concentrations in the reworked sediment were on average only 1.4–fold higher (Figure 3.1E).

3.4.2 *Chlorophyll distribution in laboratory containers in the presence and absence of lugworms*

The Chl *a* maps of containers with and without a lugworm (Figure 3.2A) showed that the same constrained area of sediment experienced an increased MPB growth in the presence of lugworms, despite the evident signs of MPB depletion in the defecated sediment (Figure 3.2A: day 4, 11). The average Chl *a* concentration increased by roughly the same amount (~65%) in containers of both treatments over the first 4 days of incubation, possibly due to migration of MPB towards the sediment surface at the start. However, at the end of 11 days of incubation, the Chl *a* concentration of the treatment with lugworms was on average about 1.5–fold higher than

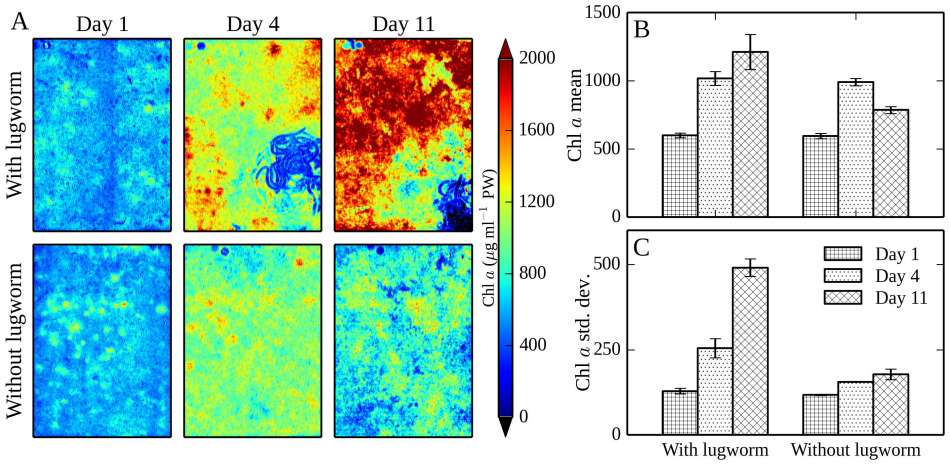

Figure 3.2: Chlorophyll *a* maps at the surface of permeable intertidal sediments in experimental containers with and without lugworms (A). Shown are examples from the same containers taken at the beginning, after 4 days and after 11 days of incubation. Panels B and C show the corresponding averages and standard deviations of the surficial chl a concentrations, as derived from 3 replicate containers. Error bars represent standard errors.

that without lugworms (Figure 3.2B). The spatial variability of MPB in the containers with lugworms monotonically increased 3–fold during the incubation, with the final standard deviation about 2.8–fold higher than that without lugworms (Figure 3.2C).

Due to the opposing effects of sediment reworking and bioadvection on MPB biomass, plus some changes in the spatial position of fecal mounds over time (Figure 3.2A: day 4, 11), the Chl *a* concentration in a given pixel at the sediment surface did not change monotonically with time (data not shown). Therefore, the increase or decrease in the MPB biomass measured at a given time-point may not represent the full range of MPB variation during a given time interval. To depict this full range during the 11 day incubation, the Chl *a* maps obtained at various time points for each container were compiled into a spatially aligned time-stack. From these time-stacks two maps were created, one containing in each pixel the minimal Chl *a* value measured over the incubation period, and the other one containing the maximal Chl *a* values. These minimum and maximum Chl *a* maps were subsequently combined into a single map of maximal Chl *a* heterogeneity. Specifically, pixels where the minimal Chl *a* value was less than the initial value of the time-series were assigned the minimum-map value, else they were assigned the corresponding value for the pixel from the maximum-map. Finally, this composite image was normalized by the values of the initial Chl *a* image from the time-series to create a spatial representation of the greatest extent of relative changes, positive or negative, of the surficial chlorophyll concentrations over the duration of the experiment. These composite maps for the treatments with lugworms consisted of regions with negative values, which correspond to sediment reworking features such as fecal mounds or feeding funnels, and positive

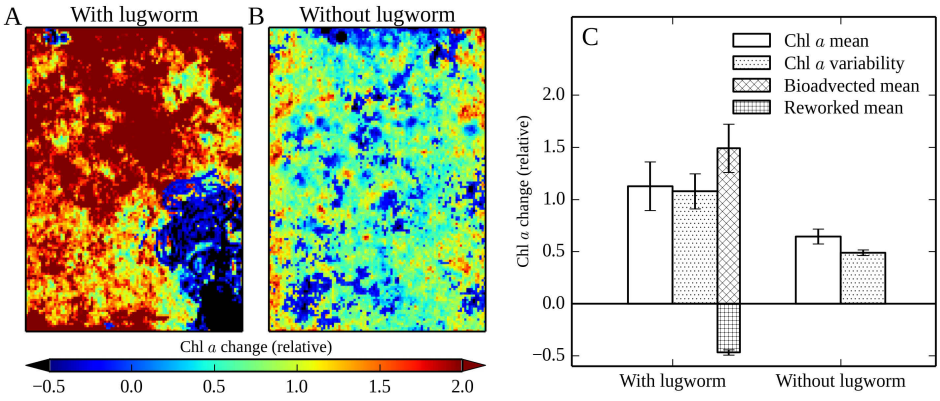

Figure 3.3: Examples of maximum heterogeneity maps of Chl *a* concentrations at the surface of permeable intertidal sediments in experimental containers with (A) and without (B) lugworms. Maps show the maximal changes in chl a concentrations encountered during 11 days of incubation relative to the initial Chl *a* concentration. In map A, regions with negative values correspond to reworked sediment (e. g., fecal mounds) while the large positive values depict areas affected by bioadvection. Panel C shows the corresponding averages and standard deviations of the maximum heterogeneity maps, as derived from 3 replicate containers. For maps with lugworms the values are given separately for the areas affected by reworking and bioadvection. Error bars represent standard errors.

values, which correspond to non-reworked sediment affected by bioadvection (Figure 3.3A).

The maximum-heterogeneity maps revealed that the maximal increase in the surficial MPB biomass during the 11 days of incubation was about 0.7–fold in the containers without lugworms, whereas the maximal increase during the same interval in the lugworm containers was about 1.1–fold (Figure 3.3C). Both values correspond to a net relative increase over the entire sediment surface. However, the maximum-heterogeneity maps made it also possible to express the net value in the containers with lugworms as a sum of two components: a 1.5–fold increase over the sediment surface affected by bioadvection, which covered 80 ± 5 % of the total sediment surface area, and a 0.5–fold decrease over the sediment surface affected by reworking, which covered 20 ± 5 % of the total surface area (Figure 3.3C). These values correspond to the average effect of one lugworm over a total sediment surface area of 15×15 cm^2 during 11 days of incubation, derived from measurements in 3 replicate sediment containers.

3.4.3 *Chlorophyll distribution in the presence and absence of a lugworm-mimic*

To obtain a simplified view of the temporal variability of the surficial MPB biomass in the experimental containers with and without the lugworm-mimic, the spectral index used for the quantification of MPB biomass (MPBI) was averaged over the entire sediment surface for each replicate container and plotted as a function of time (Figure 3.4A). In general, the

MPBI signal for both types of containers exhibited diel oscillations, with maxima reached each day around noon and minima lasting during most of the night. This MPBI dynamic was due to the vertical migration of MPB (Chennu et al., 2013).

As argued by Chennu et al. (2013), the maximal values of the MPBI measured each day correspond to the maximal concentrations of the light-exposed MPB at the sediment surface for that day. Our data showed that over the 4 day incubation period the daily MPBI maxima (averaged over the entire sediment surface) remained approximately constant in the no-flow containers but increased by about 60% in the containers with lugworm-mimics (Figure 3.4A). This means that within 4 days the MPB community responded to the lugworm-mimic treatment by enhanced growth, whereas it did not respond with significant net growth in the no-flow treatment.

Using the daily MPBI maxima, we calculated for each pixel the relative change in the MPB biomass between the first and last day of incubation (examples shown in Figure 3.4B–C). Additionally, we averaged these relative changes over annuli of increasing radius and plotted the averages as a function of the radial distance from the center of the container (Figure 3.4D). The results revealed that in the lugworm-mimic treatment the MPB biomass was progressively higher towards the edges of the containers, while it was slightly decreased in the central region of the containers. In contrast, the no-flow containers showed no net growth or a slight decrease in the MPB biomass overall. A two-way ANOVA revealed that the flow regime was a significant factor in the observed MPB growth irrespective of the radial coordinate ($p<10^{-6}$), while the effect of the radial distance was definitely significant for the lugworm-mimic treatment ($p<10^{-6}$) and not significant for the no-flow treatment ($p=0.2$).

3.4.4 *Modeling of nutrient fluxes in the presence and absence of a lugworm-mimic*

To interpret the observed MPB growth patterns in the lugworm-mimic experiment, the total upward nutrient flux across the SWI was calculated for both treatments. First, the steady-state solutions revealed that the radial profile of the upward nutrient flux in the no-flow container was largely flat, whereas it increased towards the edge in the container with the lugworm-mimic (Figure 3.5A). However, the total amount of nutrients transported through the SWI, calculated by integrating the areal flux distribution over the entire sediment surface, was the same for both treatments. This is consistent with the fact that the amount of nutrients generated per unit time within the entire sediment volume, which must be transported through the SWI under steady state conditions, was the same in both modeled scenarios. Thus, if the MPB at the sediment surface responded to the nutrient flux from the underlying sediment under steady state conditions, the expected radial distributions of the MPB growth would be flat for the no-

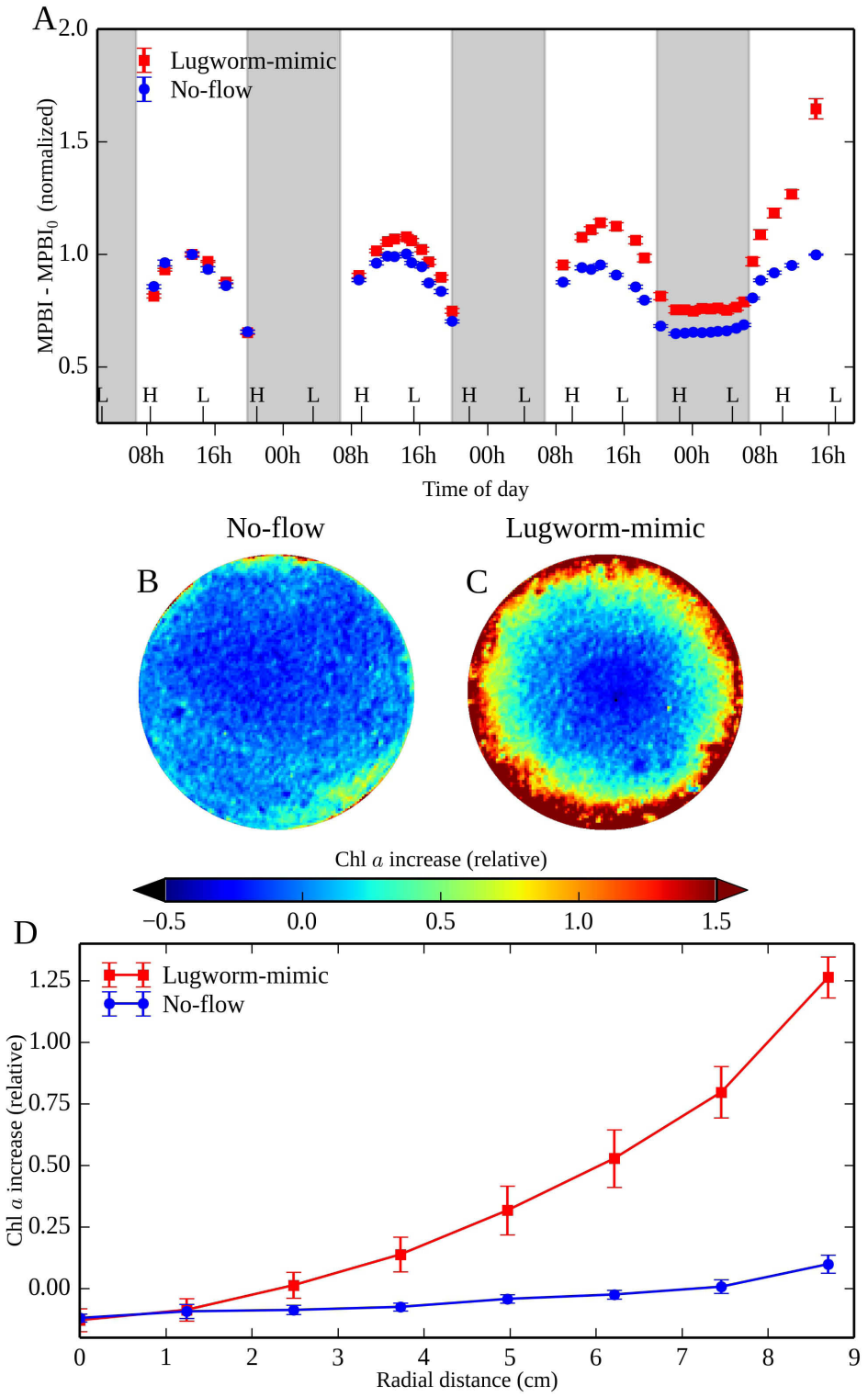

Figure 3.4: Dynamics of Chl *a* concentrations at the surface of permeable sediments incubated in containers with and without a lugworm-mimic. (A) The normalized mean and standard deviation of the MPBI values averaged over the entire sediment surface in the containers, as derived from 3 replicates for each treatment. (B–D) Relative changes in the surficial chl a concentrations between day 1 and day 4 of the incubation, shown as example images (B, C) and as radial profiles averaged over annular sections derived from 3 replicate measurements for each treatment (D).

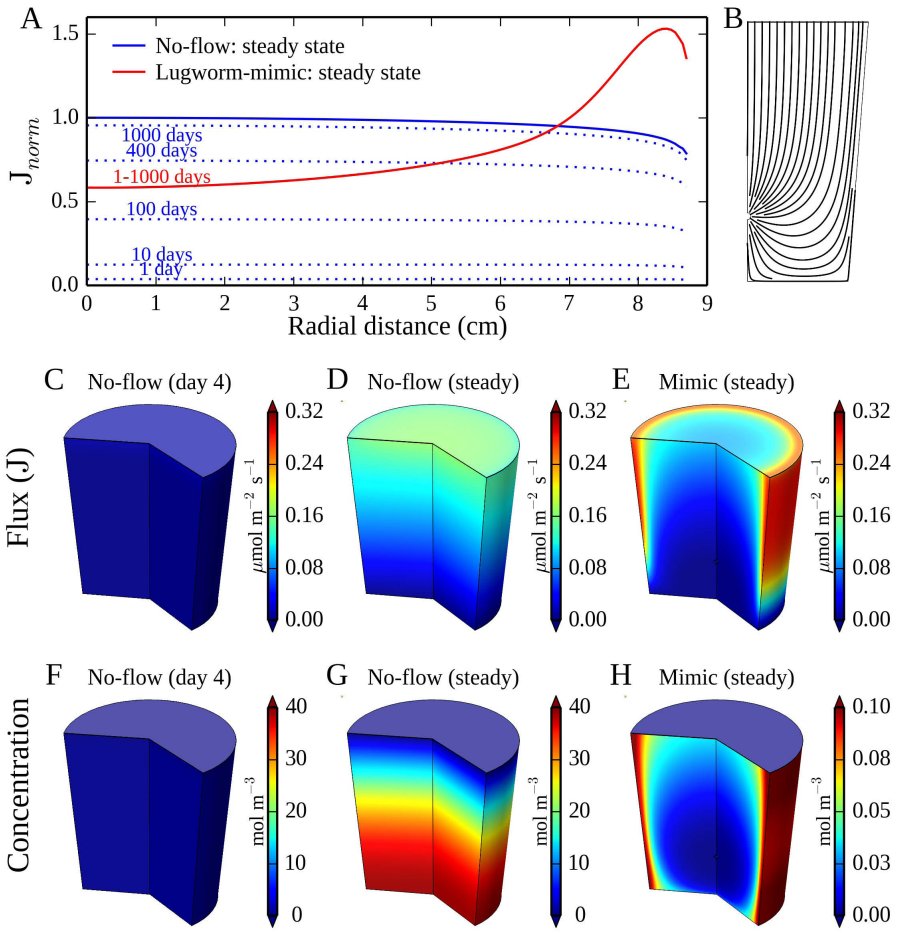

Figure 3.5: Modeling results of the total upward flux of nutrients, J, through the sediment-water interface (SWI) in the experimental containers with and without a lugworm-mimic. (A) Radial distributions of J (normalized) at different time-points (see annotations) from the beginning of the experiment and under steady-state conditions (see legend). (B) Modeled streamlines of the porewater flow induced by the lugworm-mimic in the experimental container. (C–H) Modeled distributions of the total upward flux of nutrients and of the nutrient concentrations in the experimental containers with and without a lugworm-mimic. Shown are examples at day 4 and in a steady state. Note the difference between the concentration color bars.

flow treatment and radially increasing for the lugworm-mimic treatment, but the integral over the entire sediment area should not change. In other words, under steady-state conditions, the effect of the lugworm-mimic in a constrained sediment volume should lead only to a spatial redistribution of the MPB growth but not to its overall increase. This is not, however, what was observed, since there was an overall increase in surficial Chl *a* in the lugworm-mimic experiment (compare Figure 3.4D and 3.5A).

To correctly interpret the results of the lugworm-mimic experiment, it is necessary to compare the temporal evolution of the upward nutrient flux across the SWI. Our simulations revealed that, in the lugworm-mimic treatment the steady-state flux distribution was reached after a day, which was due to the rapid advective transport of porewater within the sediment volume (Figure 3.5A). Although the steady-state nutrient concentrations were low (Figure 3.5H), the nutrient flux across the SWI remained high and radially increased towards the edge of the container (Figure 3.5E), which was consistent with the computed streamlines of porewater flow (Figure 3.5 B). In contrast, starting from zero, the nutrient distribution and the corresponding upward flux in the no-flow treatment would take >1000 days to reach a steady-state (Figure 3.5A), which is clearly due to the substantially lower rates of diffusive transport. For the duration of the experiment, the nutrient fluxes across the SWI remained very low (<5% of the potential maximum) and radially flat (Figure 3.5A and C). Thus, assuming that the MPB population was able to respond within days to an increase in the nutrient supply, which would be consistent with the short turnover times (1–3 days) of benthic microalgae (Admiraal et al., 1982), the numerical simulations predict results consistent with our observations shown in Figure 3.4D, i. e., a radially increasing MPB growth in the lugworm-mimic container and negligible MPB growth in the no-flow container.

3.5 DISCUSSION

Lugworms are a classic example of hydraulic ecosystem engineers (Woodin et al., 2010), which assiduously rework the marine sediments they inhabit and as sedentary upward-conveyors they transport impressive amounts of sediment from depth to the sediment surface (Kristensen et al., 2012). Feeding by lugworms causes subduction of surficial sediment into the burrow gallery through the feeding funnel at the blind-end of the J-shaped burrow. The microorganisms, including MPB, in the subducted sediment are (partially) digested and the sediment is ejected at the other end of the burrow in characteristic fecal castings on the surface. Therefore, through ingestion and burial under defecated sediment, we expected the sediment reworking activity of lugworms to decrease the standing stock, and to increase the spatial heterogeneity, of MPB at the sediment surface. On the other hand, based on porewater pressure gradients generated by peristalsis of arenicolid polychaetes (Wethey et al., 2008) and planar optode imagery of porewater exiting the sediment surface as a result (Volkenborn et al., 2010),

we expected bioadvective enhancement of nutrient supply to the surface (Rasmussen et al., 1998) to increase the surficial MPB biomass. In the case of lugworms, the effects of bioturbation (sediment reworking and bioadvection) on the surficial MPB oppose each other, and our investigations were designed to resolve the interplay between them.

Both our expectations were satisfied in the experiments with real lugworms: we observed that the MPB biomass at the surface was depleted due to sediment reworking (fecal casts) and enhanced due to bioadvection (surrounding regions), as seen in Figures 3.1B, 3.2A and 3.3A. The combined effect of these opposing forces of bioturbation of lugworms was a net increase in the MPB stock at the surface (Figures 3.2B and 3.3C) in both natural and artificially-constrained sediments. This enhancement of the MPB stock, related to the presence of lugworms, resulted in a 1.5–2.5 fold higher biomass in both experimental conditions as compared to the sediment without lugworms (Figure 3.2B).

Another consequence of the opposing effects of sediment reworking and bioadvection was a higher spatial variability (2.6–2.8 fold) of the resulting MPB stock compared to the situation without lugworms (Figures 3.1E and 3.2C). The spatial variance in the MPB biomass was a reflection of whether a particular pixel was from a reworked (fecal mounds, feeding funnel) location or an area of potential bioadvection and thus subjected to nutrient enhancement through porewater expulsion by the lugworm (Figures 1B and 2A). However, the positions of the lugworm's feeding funnels and fecal mounds are not static (Figure 3.2A: days 4, 11; Krager and Woodin, 1993), which allows a particular location on the surface to be categorized both as bioadvected and as reworked at different points of time. The composite maps of maximum-heterogeneity (Figure 3.3A–B), derived through simplistic categorization, represent a fuller range of the spatio-temporal variability of the surficial Chl *a* during the incubation period. This categorization revealed that bioadvection induces significant growth (1.5–fold) of MPB over a large area (80%) of the sediment surface, whereas reworking causes sharp depletion (0.5–fold) over a much smaller area (20%) (Figure 3.3A–C).

Although the MPB biomass and variability was enhanced due to the presence of lugworms in both the *in situ* and laboratory experiment, it must be noted that under *in situ* conditions several other factors possibly affect the surficial MPB stock. Tidal flushing causes porewater advection into surface layers of sediment (Precht and Huettel, 2003), which may deplete nutrients, and also causes surficial erosion which may alter rates of recolonization of depleted areas such as fecal castings. The laboratory experiments reduced the different drivers of MPB biomass change between treatments to the effects of bioadvection and reworking by the lugworm. These experiments resulted in an enhancement of the MPB biomass similar to that seen in the field experiments (Figures 3.1, 3.2 & 3.3). Overall, both experimental results are consistent with our hypothesis of increased MPB stock in the sediment affected by lugworm bioadvection.

To test whether our conceived mechanism that an enhanced upward flux of nutrients induced by bioadvection is the proximate and sufficient cause of the elevated MPB biomass, we eliminated all other physical and biological factors that have an impact on MPB growth except the hydraulic forces exerted during burrow ventilation by using mechanical lugworm-mimics. By considering the daily maximum MPBI during the incubation (Figure 3.4A), the temporal variability due to vertical migration of MPB was eliminated; thus the changes between subsequent daily maxima represent net growth or decline of the surface MPB biomass (Figure 3.4B–C). After 4 days, the MPB biomass increased 1.25–fold at the edge of the containers of the lugworm-mimic treatment (Figure 3.4D), which is similar to the level of MPB growth produced in the laboratory containers with real lugworms (Figure 3.3C). The experiment with the robotic lugworms confirm that bioadvection, and the associated enhancement of nutrient flux, is a sufficient cause for the enhanced biomass in surficial MPB (Figure 3.4D). The elemental cycling of the worm itself, or the supply of nutrients through its defecation, are not necessary to explain the observed increase in MPB stock in permeable sediments.

To understand the mechanism through which the hydraulic activity of the lugworm at feeding depth and associated bioadvection of porewater could render elevated MPB stock at the surface, we modeled the nutrient transport through the sediment porewater in the geometry of the lugworm-mimic (robolug) containers. The modeling results show that, given the extremely slow (>1000 days) approach to steady state of the no-flow condition and the 1 day to steady state of the lugworm-mimic, a greater amount of nutrient reaches the SWI in the lugworm-mimic model during the incubation period of 4 days (Figure 3.5) and this is reflected in the net increase of surficial MPB biomass during the mechanical lugworm-mimic experiment (Figure 3.4A). This is consistent with an increase in the volume-specific nutrient generation rate. That such an increase occurred during our experiment is expected as a result of an increased diagenetic remineralization induced by the introduction of oxic water into the anoxic sediment (Aller, 1994; Kristensen, 2000). Therefore, bioadvection renders elevated nutrient flux at the SWI through the stimulation of remineralization at depth as well as through the rapid transport of released solutes to the surface. The combination of these effects allows ventilating infauna such as lugworms to maintain geochemical conditions in the sediment characterized by concomitantly low concentration and high flux of nutrients (Figure 3.5 E, H). Additionally, the rapid transport from the feeding depth to the surface limits the residence time of solutes to a time-scale of 1–2 days, which is commensurate with the doubling-time of MPB cells and results in an increase of the sustainable biomass at the surface (Guarini et al., 2000), which suggests an ecological grounding to the idea of MPB gardening by lugworms.

The predicted steady-state radial profile of upward nutrient flux in the lugworm-mimic setting qualitatively matched the spatial pattern of MPB growth in the robolug containers (compare Figures 3.4D and 3.5A

and 3.5B). The increasing radial profile of upward flux in the lugworm-mimic container derives from the patterns of porewater flow at steady-state within the container geometry. In contrast to the radially flat profile for the no-flow setting (due to the isotropic diffusive transport), in the lugworm-mimic setting the radial variation in flux arises due to two different zones of flow: 1) a lower "radiation zone", where the flow streamlines radiate away in all directions from the injection sphere (modeled feeding pocket) and 2) an upper "percolation zone" where the flow streamlines align parallel to the vertical boundary of the container towards the SWI (Figure 3.5B; Meysman et al., 2006). Since the flow along the longer streamlines delivers higher concentration of nutrients to the SWI because of a longer passage time through the sediment volume where nutrients are generated, the flux at the radial edge of the container is higher than at the center (Figure 3.5B, E & H). This spatial pattern of upward flow also occurs in unconstrained sediments due the pressure head at depth, as has been shown previously by Wethey et al. (2008).

Previous studies/models in permeable sediments have been used to estimate the 'advective footprint' of an individual lugworm with respect to various solutes, with values ranging from 5 to 30 cm^2 (Meysman et al., 2006; Meysman et al., 2005; Riisgård et al., 1996; Timmermann et al., 2003). Given that we observed MPB growth till the radial edge of the experimental containers (Figures 3.3A & 3.4B), the area of the advective footprint of a single lugworm is likely larger than 15 cm in diameter (~700 cm^2). Wethey et al. (2008) determined the diameter of an area with a complete daily porewater replacement to be 12–14 cm, which corresponds with our modeled values of the time-to-steady-state and radial profile for the flux in the lugworm-mimic setting. Thus, with neighboring worms at densities of 50 m^{-2}, it is expected that overlapping flow-fields of neighboring worms yields a sediment bed that is flushed on a daily basis to the feeding depth of the worms. Our measurements are consistent with the interpretation that, without specific attention to any particular solute, in dense flats of arenicolids the sandflats seep nutrient-rich porewater out of the sediment nearly everywhere. The effect of lugworms on both the nutrient flux across the sediment-water interface and its chemical signature could play an important role in various ecosystem functions such as primary productivity or chemical signaling for colonization or predation (Marinelli and Woodin, 2002).

Our data show that in sandflats with lugworms, biological advection is the primary driver of solute transport from deeper sediment layers to the surface and forms a "nutrient pump" that leads to increased MBP fertilization. Through the exercise of frequent hydraulic activity, lugworms maintain a low-capital high-throughput economy of nutrients in the vicinity of their burrows, by which they likely replenish a primary component of their diet (MPB). Thus, despite the low standing stock of nutrients, tidal flats inhabited by lugworms are highly productive systems where the lugworms themselves play a significant role in sustaining their habitat. Overall, we conclude that the depletion of MPB due to feeding or defecation

per lugworm is much smaller than the stimulation of MPB growth due to the bioadvective enhancement of the upward nutrient flux (Figures 3.1–3.4). This implies that lugworms enhance the MPB biomass more than they consume, leading to an increased MPB availability for other ecosystem players such as hydrobii snails and harpacticoid copepods, which are an important food supply for fish and birds. Thus, the hydraulic activity of lugworms leads to an increased fertility of the microphytobenthic garden, and essentially boosts the productivity of intertidal ecosystems.

3.6 ACKNOWLEDGMENTS

We thank the the electronic and mechanical workshops at the Max Planck Institute for Marine Microbiology for the technical support. We also thank Justus van Beusekom, Karsten Reise, and Elisabeth Herre from the Alfred Wegener Institute for Polar and Marine Research, and George Matsui from the University of South Carolina for their support during field campaigns. The Alfred Wegener Institute for Polar and Marine Research Wadden Sea Station at Sylt and the Baruch Field Laboratory of the University of South Carolina provided facilities during field campaigns. This work was funded by the Marie Curie Initial Training Network "SENSEnet" (grant number: 237868), the National Science Foundation (OCE 0928002), and the Max Planck Society of Germany.

3.7 AUTHOR CONTRIBUTIONS

The project was designed by Arjun Chennu, Lubos Polerecky and Nils Volkenborn. The field work at the Wadden Sea Station, Sylt were conducted by Arjun Chennu, Lubos Polerecky and Nils Volkenborn. The field work at Baruch Marine Field Laboratory, South Carolina were conducted by Arjun Chennu, Lubos Polerecky, Nils Volkenborn, David Wethey and Sarah Woodin. The data analysis was performed by Arjun Chennu, Lubos Polerecky, Nils Volkenborn and David Wethey. The manuscript was prepared by Arjun Chennu with considerable input from all co-authors.

Return to start

3.8 REFERENCES

Admiraal, W., H. Peletier, and H. Zomer (1982). "Observations and experiments on the population dynamics of epipelic diatoms from an estuarine mudflat." In: *Estuarine, Coastal and Shelf Science* 14, pp. 471–487. DOI: 10.1016/S0302-3524(82)80071-6 (cited on page 95).

Aller, R. C. (1994). "Bioturbation and remineralization of sedimentary organic matter: effects of redox oscillation." In: *Chemical Geology* 114.3-4, pp. 331–345. DOI: 10.1016/0009-2541(94)90062-0 (cited on page 97).

Aller, R. C. (2001). "Transport and reactions in the bioirrigated zone." In: *The benthic boundary layer: Transport processes and biogeochemistry*, pp. 269–301 (cited on page 83).

Beukema, J. and J. De Vlas (1979). "Population parameters of the lugworm, *Arenicola marina*, living on tidal flats in the Dutch Wadden Sea." In: *Netherlands Journal of Sea Research* 13.3-4, pp. 331–353. DOI: 10.1016/0077-7579(79)90010-3 (cited on page 82).

Boudreau, B. P. and B. B. Jørgensen (2001). *The Benthic Boundary Layer: Transport Processes and Biogeochemistry*. Oxford University Press (cited on page 87).

Boudreau, B. (1984). "On the equivalence of nonlocal and radial-diffusion models for porewater irrigation." In: *Journal of Marine Research* 42, pp. 731–735 (cited on page 83).

Chennu, A., P. Färber, N. Volkenborn, M. A. A. Al-Najjar, F. Janssen, D. de Beer, and L. Polerecky (2013). "Hyperspectral imaging of the microscale distribution and dynamics of microphytobenthos in intertidal sediments." In: *Limnology and Oceanography: Methods* 11, pp. 511–528. DOI: 10.4319/lom.2013.11.511 (cited on pages 84 sq., 92).

de Beer, D., F. Wenzhöfer, T. G. Ferdelman, S. E. Boehme, M. Huettel, J. E. E. van Beusekom, M. E. Böttcher, N. Musat, and N. Dubilier (2005). "Transport and mineralization rates in north sea sandy intertidal sediments, Sylt-Rømøbasin, Wadden sea." In: *Limnology and Oceanography* 50.1, pp. 113–127. DOI: 10.4319/lo.2005.50.1.0113 (cited on page 82).

Grossmann, S. and W. Reichardt (1991). "Impact of *Arenicola marina* on bacteria in intertidal sediments." In: *Marine Ecology Progress Series* 77.Reise 1985, pp. 85–93 (cited on page 83).

Guarini, J.-M., G. F. Blanchard, P. H. Gros, D. Gouleau, and C. Bacher (2000). "Dynamic model of the short-term variability of microphytobenthic biomass on temperate intertidal mudflats." In: *Marine Ecology-Progress Series* 195, pp. 291–303. DOI: 10.3354/meps195291 (cited on page 97).

Herman, P. M. J., J. J. Middelburg, J. van de Koppel, and C. H. R. Heip (1999). "Ecology of Estuarine Macrobenthos." In: *Estuaries*. Ed. by D. B. Nedwell and D. G. Raffaelli. Vol. 29. Advances in Ecological Research. Academic Press, pp. 195–240. DOI: http://dx.doi.org/10.1016/S0065-2504(08)60194-4 (cited on page 82).

Hüttel, M. (1990). "Influence of the lugworm *Arenicola marina* on porewater nutrient profiles of sand flat sediments." In: *Marine Ecology Progress Series* 62, pp. 241–248 (cited on pages 82 sq.).

Hylleberg, J. (1975). "Selective feeding by *Abarenicola pacifica* with notes on *Abarenicola vagabunda* and a concept of gardening in lugworms." In: *Ophelia* 14.1-2, pp. 113–137. DOI: 10.1080/00785236.1975.10421972 (cited on page 83).

Krager, C. D. and S. A. Woodin (1993). "Spatial persistence and sediment disturbance of an arenicolid polychaete." In: *Limnology and Oceanography* 38.3, pp. 509–520. DOI: 10.4319/lo.1993.38.3.0509 (cited on page 96).

Krantzberg, G. (1985). "The influence of bioturbation on physical, chemical and biological parameters in aquatic environments: A review." In: *Environmental Pollution Series A, Ecological and Biological* 39.2, pp. 99–122. DOI: 10.1016/0143-1471(85)90009-1 (cited on page 82).

Kristensen, E., G. Penha-Lopes, M. Delefosse, T. Valdemarsen, C. Quintana, and G. Banta (2012). "What is bioturbation? The need for a precise definition for fauna in aquatic sciences." In: *Marine Ecology Progress Series* 446, pp. 285–302. DOI: 10.3354/meps09506 (cited on page 95).

Kristensen, E. (1985). "Oxygen and Inorganic Nitrogen Exchange in a *Nereis virens* (Polychaeta) Bioturbated Sediment-Water System." In: *Journal of Coastal Research* 1.2, pp. 109–116 (cited on page 83).

— (2000). "Organic matter diagenesis at the oxic/anoxic interface in coastal marine sediments, with emphasis on the role of burrowing animals." In: *Hydrobiologia* 426.1, pp. 1–24. DOI: 10.1023/A:1003980226194 (cited on pages 83, 97).

— (2001). "Impact of polychaetes (*Nereis spp.* and *Arenicola marina*) on carbon biogeochemistry in coastal marine sediments." In: *Geochemical Transactions* 2.12, p. 92. DOI: 10.1039/b108114d (cited on page 82).

Levinton, J. (1995). "Bioturbators as ecosystem engineers: Control of the sediment fabric, inter-individual interactions, and material fluxes." English. In: *Linking Species & Ecosystems*. Ed. by C. G. Jones and J. H. Lawton. Springer US, pp. 29–36. DOI: 10.1007/978-1-4615-1773-3_3 (cited on page 82).

MacIntyre, H., R. Geider, and D. Miller (1996). "Microphytobenthos: The ecological role of the "secret garden" of unvegetated, shallow-water marine habitats. I. Distribution, abundance and primary production." In: *Estuaries and Coasts* 19.2, pp. 186–201. DOI: 10.2307/1352224 (cited on page 83).

Malcolm, S. and D. Sivyer (1997). "Biogeochemistry of Intertidal Sediments." In: ed. by Jickells, Tim D and Rae, Joy E. Cambridge University Press. Chap. Nutrient recycling in intertidal sediments, pp. 84–98 (cited on page 82).

Marinelli, R. L. and S. A. Woodin (2002). "Experimental evidence for linkages between infaunal recruitment, disturbance, and sediment surface chemistry." In: *Limnology and Oceanography* 47.1, pp. 221–229. DOI: 10.4319/lo.2002.47.1.0221 (cited on page 98).

Matsui, G. Y., N. Volkenborn, L. Polerecky, U. Henne, D. S. Wethey, C. R. Lovell, and S. Woodin (2011). "Mechanical imitation of bidirectional bioadvection in aquatic sediments." In: *Limnology and Oceanography:*

Methods 9, pp. 84–96. DOI: 10.4319/lom.2011.9.84 (cited on pages 86 sq.).

Meysman, F. J. R., O. S. Galaktionov, B. Gribsholt, and J. J. Middelburg (2006). "Bioirrigation in permeable sediments: Advective pore-water transport induced by burrow ventilation." In: *Limnology and Oceanography* 51.1, pp. 142–156. DOI: 10.4319/lo.2006.51.1.0142 (cited on pages 82, 87 sq., 98).

Meysman, F., O. Galaktionov, and J. Middelburg (2005). "Irrigation patterns in permeable sediments induced by burrow ventilation: a case study of *Arenicola marina*." In: *Marine Ecology Progress Series* 303, pp. 195–212. DOI: 10.3354/meps303195 (cited on pages 82 sq., 87 sq., 98).

Nielsen, O., E. Kristensen, and M. Holmer (2003). "Impact of *Arenicola marina* (Polychaeta) on sediment sulfur dynamics." In: *Aquatic Microbial Ecology* 33, pp. 95–105. DOI: 10.3354/ame033095 (cited on page 82).

Plante, C., P. Jumars, and J. Baross (1990). "Digestive associations between marine detritivores and bacteria." In: *Annual Review of Ecology and Systematics* 21, pp. 93–127. DOI: 10.1146/annurev.es.21.110190.000521 (cited on page 83).

Precht, E., U. Franke, L. Polerecky, and M. Huettel (2004). "Oxygen dynamics in permeable sediments with wave-driven pore water exchange." In: *Limnology and Oceanography* 49.3, pp. 693–705. DOI: 10.4319/lo.2004.49.3.0693 (cited on page 83).

Precht, E. and M. Huettel (2003). "Advective pore-water exchange driven by surface gravity waves and its ecological implications." In: *Limnology and Oceanography* 48.4, pp. 1674–1684. DOI: 10.4319/lo.2003.48.4.1674 (cited on pages 83, 96).

Rasmussen, A., G. Banta, and O. Andersen (1998). "Effects of bioturbation by the lugworm *Arenicola marina* on cadmium uptake and distribution in sandy sediments." In: *Marine Ecology Progress Series* 164.Wells 1966, pp. 179–188. DOI: doi:10.3354/meps164179 (cited on pages 83, 96).

Reichardt, W. (1988). "Impact of bioturbation by *Arenicola marina* on microbiological parameters in intertidal sediments." In: *Marine Ecology Progress Series* 44, pp. 149–158. DOI: 10.3354/meps044149 (cited on page 82).

Reise, K. (1985). *Tidal flat ecology : an experimental approach to species interactions*. Ecological studies. Berlin: Springer (cited on page 82).

— (2002). "Sediment mediated species interactions in coastal waters." In: *Journal of Sea Research* 48, pp. 127–141. DOI: 10.1016/S1385-1101(02)00150-8 (cited on page 82).

Retraubun, A., M. Dawson, and S. Evans (1996). "The role of the burrow funnel in feeding processes in the lugworm *Arenicola marina* (L.)" In:

Journal of Experimental Marine Biology and Ecology 202.2, pp. 107–118. DOI: 10.1016/0022-0981(96)00017-2 (cited on page 83).

Riisgård, H. U. and G. T. Banta (1998). "Irrigation and deposit feeding by the lugworm *Arenicola marina*, characteristics and secondary effects on the environment. A review of current knowledge." In: *Vie et milieu* 48.4, pp. 243–257 (cited on pages 82 sq.).

Riisgård, H. U., I. Berntsen, and B. Tarp (1996). "The lugworm (*Arenicola marina*) pump:characteristics, modelling and energy cost." In: *Marine Ecology Progress Series* 138, pp. 149–156. DOI: 10.3354/meps138149 (cited on pages 82, 87, 98).

Timmermann, K., G. T. Banta, J. Larsen, and O. Andersen (2003). "Modelling particle and solute transport in sediments inhabited by *Arenicola marina*. Effects of pyrene on transport processes." In: *Vie et milieu* 53.4, pp. 187–200 (cited on page 98).

Timmermann, K., G. T. Banta, and R. N. Glud (2006). "Linking *Arenicola marina* irrigation behavior to oxygen transport and dynamics in sandy sediments." In: *Journal of Marine Research* 64.6, pp. 915–938. DOI: 10.1357/002224006779698378 (cited on page 87).

Volkenborn, N., S. Hedtkamp, J. van Beusekom, and K. Reise (2007). "Effects of bioturbation and bioirrigation by lugworms (*Arenicola marina*) on physical and chemical sediment properties and implications for intertidal habitat succession." In: *Estuarine, Coastal and Shelf Science* 74.1-2, pp. 331–343. DOI: 10.1016/j.ecss.2007.05.001 (cited on pages 82, 85).

Volkenborn, N., L. Polerecky, D. Wethey, T. DeWitt, and S. Woodin (2012a). "Hydraulic activities by ghost shrimp *Neotrypaea californiensis* induce oxic–anoxic oscillations in sediments." In: *Marine Ecology Progress Series* 455.3, pp. 141–156. DOI: 10.3354/meps09645 (cited on page 83).

Volkenborn, N., C. Meile, L. Polerecky, C. A. Pilditch, A. Norkko, J. Norkko, J. E. Hewitt, S. F. Thrush, D. S. Wethey, and S. A. Woodin (2012b). "Intermittent bioirrigation and oxygen dynamics in permeable sediments: An experimental and modeling study of three tellinid bivalves." In: *Journal of Marine Research* 70.6, pp. 794–823. DOI: 10.1357/002224012806770955 (cited on page 83).

Volkenborn, N., L. Polerecky, D. S. Wethey, and S. A. Woodin (2010). "Oscillatory porewater bioadvection in marine sediments induced by hydraulic activities of *Arenicola marina*." In: *Limnology and Oceanography* 55.3, pp. 1231–1247. DOI: 10.4319/lo.2010.55.3.1231 (cited on pages 83, 87, 95).

Volkenborn, N. and K. Reise (2006). "Lugworm exclusion experiment: Responses by deposit feeding worms to biogenic habitat transformations." In: *Journal of Experimental Marine Biology and Ecology* 330.1, pp. 169–179. DOI: 10.1016/j.jembe.2005.12.025 (cited on page 86).

Wells, G. (1966). "The lugworm (*Arenicola*) - a study in adaptation." In: *Netherlands Journal of Sea Research* 3.2, pp. 294–313 (cited on page 82).

Wethey, D. S., S. A. Woodin, N. Volkenborn, and K. Reise (2008). "Porewater advection by hydraulic activities of lugworms, *Arenicola marina*: A field, laboratory and modeling study." In: *Journal of Marine Research* 66.2, pp. 255–273. DOI: 10.1357/002224008785837121 (cited on pages 83 sq., 87, 95, 98).

Wethey, D. S. and S. A. Woodin (2005). "Infaunal hydraulics generate porewater pressure signals." In: *The Biological Bulletin* 209.2, pp. 139–145 (cited on page 83).

Woodin, S. A., D. S. Wethey, and N. Volkenborn (2010). "Infaunal hydraulic ecosystem engineers: cast of characters and impacts." In: *Integrative and Comparative Biology* 50.2, pp. 176–87. DOI: 10.1093/icb/icq031 (cited on page 95).

4

CYANOBACTERIA RESURRECTED: RAPID REACTIVATION OF PHOTOSYNTHESIS UPON REHYDRATION OF DESICCATED MICROBIAL MATS

Arjun Chennu[1], Alistair Grinham[2] and Mohammad A. A. Al-Najjar[1][3]

See Author contributions

MANUSCRIPT STATUS

Prepared for submission to *Environmental Microbiology*.

4.1 ABSTRACT

Desiccated cyanobacterial microbial mats are the dominant biological feature in the arid zone of Exmouth Gulf, Australia. Despite prolonged periods of desiccation, these sediments develop a bright green color on the surface soon after rehydration. We studied the rehydration response of these mats to understand the process of rapid resurrection of the desiccated cyanobacteria (family *Oscillatoriales*). Based on field observations, we hypothesized that the resurrection occurs through rapid resynthesis of Chlorophyll *a* (Chl *a*) in the subsurface layer of dormant cyanobacteria, followed by reactivation of photosynthesis and subsequent vertical migration towards the mat surface. We used high-resolution hyperspectral imaging to simultaneously monitor the Chl *a* concentration in the surface and subsurface layers of the mats, and found signs of Chl *a* resynthesis within minutes of rehydration followed by migration to the surface over 48 hours. Confocal laser scanning microscopy was used to confirm the vertical displacement of the cyanobacteria. Measurements with oxygen microsensors and pulsed-amplitude modulation fluorometer provided evidence of photosynthetic activity in the mats 10–15 minutes after rehydration. We found that the resynthesis of Chl *a* and the migratory response of the resurrected cyanobacteria occurred both in the light and in the dark, with the availability of water being the sole trigger. We reject the idea that the migratory behavior to the upper surface is hydrotaxis, and the drivers for the migration remain unclear. We hypothesize that the rapid response to rehydration is mediated through an innate behavioral adaptation of the cyanobacteria that enables sequestration of Chl *a* in a precursor state during desiccation.

1 Max Planck Institute for Marine Microbiology, Celsiusstrasse 1, Bremen, Germany
2 School of Civil Engineering, The University of Queensland, St. Lucia, Australia
3 Red Sea Research Center, King Abdullah University of Science and Technology, Saudi Arabia

4.2 INTRODUCTION

Microbial mats are dense benthic communities of very diverse species of bacteria, archaea and eukaryotes. They are generally complete, self-sustaining ecosystems as they contain photoautotrophic, photoheterotrophic, chemoautotrophic and heterotrophic populations, and as a result contain nearly all the microbial elements and biogeochemical process that exist in any aquatic ecosystem (Canfield and Des Marais, 1993). Geochemical and fossil evidence indicates the existence of microbial mats in the early stages (3.5 Ga) of the evolution of life on Earth (Walter et al., 1980), and modern microbial mats are considered extant representatives of the ecosystems of the ancient Earth. Therefore, living microbial mats, which represent an invaluable repository of biogeochemical and genetic information about the evolution of our planet and the only known biosphere, are studied for their paleo- and astro-biological significance (Bebout et al., 2002; Des Marais, 2003). Photosynthetic microbial mats typically contain cyanobacteria, which convert the solar light energy into chemical form, and thus forms the autotrophic base upon which the other microorganisms depend for trophic sustenance. The intricate associations between the metabolisms of the various species regulates the catalytic transformation of oxygen, carbon, sulfur, nitrogen, phosphorus and various metals (Van Gemerden, 1993) and engenders spatially distinct and temporally dynamic microbial and geochemical zones of sub-millimeter and millimeter scales (Jørgensen et al., 1979; Revsbech and Jørgensen, 1986; Revsbech et al., 1983). Details about the structure and functions of microbial mats can be found in several reviews (Franks and Stolz, 2009; Stal, 1995; Van Gemerden, 1993).

Microbial mats are laminated structures with microbial and chemical zonations on millimeter or sub-millimeter scales (Franks and Stolz, 2009). They are generally rich in organic content (compared to mineral content) due to the prominence of cyanobacterial primary production, and hence most of the organic material is autochthonous (Canfield and Des Marais, 1993; Stolz, 2000). The primary carbon production occurs within 0.2–3 mm deep within the mat, resulting in very steep vertical gradients of oxygen, pH and sulfide (Revsbech et al., 1983). This is accompanied by equally steep vertical gradients of light availability due to intense attenuation through light scattering in the dense sediment matrix (Kühl et al., 1994; Al-Najjar et al., 2012). These steep light and chemical gradients, which change dramatically with diel periodicity (Garcia-Pichel et al., 1994; Jørgensen et al., 1979), create chemically distinct micro-environments within the mat, which are the primary organizational control of the structure and distribution of the microbial communities.

In nature, photosynthetic microbial mats are the dominant biological feature in harsh environments characterized by high salinity, temperature or aridity, where higher organisms cannot flourish and compete for the limited resources available (Garrett, 1970). Cyanobacterial populations,

typically filamentous, are found in hypersaline lakes (Bauld, 1981; Des Marais, 2003), thermal and iron springs (Ward et al., 1998), caves, lagoons, Arctic dry valleys (Franks and Stolz, 2009), and in the arid and mesic zones, both terrestrial and marine, of the tropical, temperate and polar regions (Decho, 2000). The formation of photosynthetic microbial mats has significant consequences for these ecosystems. Cryptobiotic desert crusts, reviewed by Eldridge and Greene (1994) markedly change the physicochemical and geochemical properties of the sediment surface, such as increased water infiltration and retention, resistance against erosion, albedo, nitrogen fixation and eventual establishment of lichens and fungi (Belnap and Eldridge, 2001; Johansen, 1993). Marine microbial mats, reviewed by Decho (2000), can also develop in arid peritidal and intertidal zones, often landward of mangroves where the combination of infrequent inundation (only during high spring tides) and extremely high evaporative load results in conditions that are unsuitable for mangrove or salt marsh growth (Smith III and Duke, 1987). These mats, despite being active only during sporadic events of water availability, display high rates of carbon and nitrogen fixation, photosynthesis and growth (Lovelock et al., 2010; Stal, 1995) and provide nutrient subsidies to surrounding habitats (Polis et al., 1997).

Cyanobacteria and the other members of mat ecosystems have developed complex adaptations to cope with the dynamic boundaries of the micro environments (Franks and Stolz, 2009; Stal, 1995), a primary example being the ability to vertically migrate within the mat. Due to their critical dependence on light for photosynthesis, cyanobacteria migrate to optimize their position within the light field (Castenholz et al., 1991; Jørgensen and Des Marais, 1988; Al-Najjar et al., 2009), which can vary dramatically due to factors such as self-shading or sedimentation at the surface (Stal, 1995), or onset of strong ultraviolet radiation (Castenholz and Garcia-Pichel, 2002). The diel light and oxygen-sulfide cycle are generally considered to be the key drivers for the motility of cyanobacteria in mats, although other factors such as salinity gradient (Kohls et al., 2010), community composition (Bebout et al., 2002) or desiccation state (Pringault and Garcia-Pichel, 2004) have been shown to play a role.

However, in arid regions, where cyanobacteria face prolonged conditions of drought such as in desert crusts or dry peritidal mats, the availability of water (and not light) is the primary control of migration and activity (Garcia-Pichel and Belnap, 1996; Garcia-Pichel et al., 2001). This is often evidenced by the appearance of a green coloration when the cyanobacteria, which take refuge deeper in the mat during desiccation, migrate and reach the surface. Pringault and Garcia-Pichel (2004) demonstrated that cyanobacteria migrate up and down in desert crusts to follow the rise and fall of a "water potential" over cycles of hydration and desiccation, which they termed hydrotaxis. The migratory response occurred under both dark and light conditions. The rapidity of the migratory response to rehydration is remarkable since the cyanobacteria generally remain in a desiccated state for the greater part of each year. Although it is known that oxygen production resumes within minutes of rehydration (Garcia-

Pichel and Belnap, 1996), no information is yet available about how this rapid response is possible, especially with respect to reactivation of the photosynthetic apparatus of the desiccated cells upon rehydration.

In this study, we studied the rehydration response of a desiccated peritidal microbial mat from Exmouth gulf in Australia with the aims 1) to test if rapid resynthesis of Chl *a* is involved in the resurrection of desiccated cyanobacteria, 2) to study the short-term dynamics of Chl *a* resynthesis, 3) to analyze the interplay between rapidly reactivated photosynthesis and vertical migration and 4) to measure the primary productivity immediately after rehydration. To study these, we monitored with high spatial and temporal resolutions the Chl *a* content and distribution, both lateral and vertical, in the rehydrated mats over time-scales of minutes to days. Our focus was on the changes that occur immediately after rehydration, which could provide evidence of rapid resynthesis of Chl *a* in the mat before subsequent migration to the surface, concomitant with resumption of photosynthetic activity. Based on our observations, we hypothesize the presence of an innate adaptation in cyanobacteria that enables them, upon desiccation, to sequester their Chl *a* in a precursor state which allows rapid resynthesis when the cyanobacteria are resurrected. The ecological implications of such an adaptation are discussed.

4.3 MATERIALS AND METHODS

The aim of our measurements was to study the dynamics of the rehydration response of the desiccated mats over two temporal scales: 1) in the minutes immediately after rehydration and 2) over a period of 1-2 days after rehydration. To assess the rapid reactivation of photosynthesis and subsequent migration after rehydration, we studied the Chl a distribution and dynamics in the mat with specific attention to the subsurface layer where the desiccated cyanobacteria are, and to the surface of the mat. Firstly, hyperspectral imaging was used as a non-invasive method of monitoring the Chl *a* content simultaneously at the surface and in the subsurface cyanobacterial layer. Secondly, the total Chl a content was measured using high-performance liquid chromatography, with a temporal resolution of minutes to days. Thirdly, confocal laser scanning microscopy was employed to determine the fine-scale vertical distribution of the cyanobacterial filaments within the mat. Finally, to confirm that the resurrected cyanobacteria in the mats were photosynthetically active soon after rehydration and during migration, we measured the oxygen productivity and the photosynthetic potential within the mat. We used a microsensor to quantify the oxygen productivity using light-dark shift measurements (Revsbech et al., 1983). The photosynthetic potential was measured using pulsed-amplitude modulation fluorometry (Schreiber, 2004).

4.3.1 *Site description*

The Exmouth Gulf in Australia, which is one of the largest unmodified arid zone estuaries in the world, has thick carpet-like desiccated cyanobacterial mats at the outer edge of the peritidal zone landward of the mangroves (see Discussion). The mats cover approximately 80 km^2 in the eastern section of the Gulf, with an additional 20 km^2 in the southern and western parts of the Gulf (Lovelock et al., 2010). The cyanobacterial mats were sampled, by excising the intact sediment surface with a pocket knife, at various points along a 200m transect within Giralia Bay (22.437°S, 114.34°E). Microscopic inspection revealed that the mats were dominated by cyanobacteria from the families *Chroococcaceae* and *Oscillatoriaceae*. Within the *Oscillatoriaceae* family, species from the highly cosmopolitan taxon *Microcoleus chthonoplastes* (Garcia-Pichel et al., 1996) were dominant, with minor contributions of *Oscillatoria* (Lovelock et al., 2010). It was also possible to visually notice a dark olive-brown layer just below the top surface that corresponded to the cyanobacterial community. The excised mats were placed on sand and allowed to dry naturally in full sunlight over 2 days. They were then wrapped in bubble wrap and packaged for transporting to the laboratory, where they were placed in dry-air rooms maintained at 25° C for several weeks to allow complete desiccation before measurements commenced. The desiccated mats were cut into approximately 1×1 cm pieces and inspected to verify that the subsurface brown layer of cyanobacteria were not damaged in the process. These mat pieces were used in measurements described below.

4.3.2 *Hyperspectral imaging (HSI)*

We used hyperspectral imaging to study the immediate and extended response of the cyanobacteria to rehydration, by using protocols described in Chennu et al. (2013). Briefly, the system captures back-scattered light from the sediment and, using a spectral reference, converts the detected signal into reflectance spectra (wavelength range 400–900 nm, spectral resolution about 1 nm). These spectra were used to calculate a microphytobenthos index (MPBI) at each location in the spectral image. MPBI is a spectral index that is sensitive to the Chl *a* concentration, as well as its vertical distribution, in the euphotic zone of the sediment. A calibration between MPBI and absolute Chl *a* concentration was not attempted here due to the heterogeneity of the mat substrate with respect to the surficial crust, the laminar desiccated cyanobacteria, and the underlying grain sizes (Chennu et al., 2013).

Twelve mat pieces (see above) were fixed using modeler's clay to a gray plastic board, which served as a spectrally flat reference material, such that the top-surface of nine of the mat pieces were parallel to the reference board. The other three pieces were fixed with their top-surfaces

perpendicular to the reference board, such that a view of the mat's deeper layers was visible from above (Figure 4.1A). Additionally, three of the nine horizontal mat pieces had the top crust scratched off over half of the surface area, in order to expose the subsurface cyanobacterial layer. The scratched surfaces and the edges of the vertical mat pieces, offered a simultaneous view of the surface and the subsurface layers of the mat. The reference board with the attached mat pieces was then placed in a large petri dish.

The HSI system was mounted about 50 cm above the petri dish on a linear motor such that the area of the reference board (5×5 cm) could be scanned in one minute with a high spatial resolution (100×100 µm per pixel). The desiccated mats were scanned once. Then, to mimic rehydration of the mats due to tidal action in the field, filtered seawater was added to the petri dish until a thin (5–10 mm) overlying layer of water formed above the mats. A minute after rehydration, the mats were scanned again, after which they were scanned periodically every 10 minutes for the first 1.5 hours and thereafter every 2 hours for a period of two days. Separate time series of the rehydrated mat pieces were captured both under light and dark conditions. Illumination was provided by a halogen lamp attached to the imager, which was switched off between scans for the dark treatment.

The spectral images at each time point were used to generate true-color and Chl *a* (MPBI) maps. The regions of the Chl *a* map corresponding to the surface and subsurface layers of each mat were sectioned into separate regions-of-interest. For every time-point, the values within each region were averaged and then compiled into a time-series for the subsurface and surface regions.

4.3.3 *High-performance liquid chromatography (HPLC)*

In order to determine the total Chl *a* content of the mats during rehydration response, we sampled the mat pieces after various durations of rehydration and quantified the pigment contents using HPLC. During the HSI monitoring of the mat pieces, we collected three mat pieces each time at the start, after 15 minutes, after 24 hours and at the end (2 days) of the time-series for measurement with HPLC. Additionally, to record the short-term changes in Chl *a* content immediately after rehydration, several small mat pieces (1×1 cm) were soaked in filtered seawater. Two of them were sampled each time in intervals of 2 minutes over a period of 20 minutes, in addition to 2 dry mat pieces to measure Chl *a* content in the dry mat. In both cases, the sampled mat pieces were crushed, added to 2 ml of 100% cold acetone, sonicated and placed for 24 hours at -20°C to facilitate pigment extraction. Subsequently, the supernatant was filtrated through a 0.45 µm syringe filter (Acrodiscs CR 4 mm; Pall Gelman laboratory, USA) and the filtrates were injected into a reverse-phase HPLC consisting of a photodiode array detector (Waters 996) and a Waters 2695

separation module (Waters Corp., USA). Pigments were separated using a 125×4.6 mm vertex column packed with Eurospher100 C18 particles of 5 mm in diameter (Knauer GmbH, Berlin, Germany). The Chl *a* in the filtrates were quantified by comparing the retention time and spectrum of the eluents with respect to those of a Chl *a* standard (DHI Water and Environment, Denmark), and normalized with respect to the volume (for the hyperspectral series samples) and to the weight (for the short-term series) of the mat pieces. The samples were kept on ice and under dim light during the measurement procedure.

4.3.4 *Confocal laser scanning microscopy (CLSM)*

To quantify the changes in the vertical distribution of the Chl *a* in the mat in response to rehydration, a mat piece was measured using a CLSM (Zeiss LSM 510), which consisted of an inverted microscope, a He-Ne (633 nm) photodiode laser, confocal scanner with photomultiplier tube and a computer to automate the measurements. The technique is based on measuring the autofluorsescent response of the phycobilin within the cyanobacterial filaments (Vermaas et al., 2008). With the initial focus of the optics leveled to the top surface of the mat and illumination at 633 nm provided by the He-Ne laser, a stack of Z-profile (up to a depth of 400 µm) images were collected over an area of over 1.2×1.2 mm with a fine voxel size (2.5×2.5×20 µm) within the desiccated mat. The light collected by the microscope was in two separate channels: one through a 650 nm long-pass filter which measures the autofluorescence response of phycobilin, and the other unfiltered to capture light reflected from the sediment matrix. Then, the mat was rehydrated with filtered seawater and the measurement scan repeated after 1 minute. Thereafter, the mat was allowed to remain untouched under the CLSM for a period of 24 hours in the dark before being scanned again to a depth of 400 µm.

The extent of cell cover within the layers of the Z-stack was estimated by filtering the autofluorescence channel against a certain threshold (1.001) such that only pixels with filaments of cyanobacteria, and no detrital or noise pixels, were selected. The extent and intensity of the filtered pixels were considered proportional to the (pigmented) cyanobacterial biomass at those locations, irrespective of the depth within the mat (Vermaas et al., 2008). By summing the fluorescent intensity in each layer of the Z-stack, the density of pigmented biomass was determined (with a depth resolution of 20 µm) and was normalized and plotted against depth within the mat.

4.3.5 *Oxygen microsensor*

A desiccated microbial mat sample was placed in a small flow-through cell (11×5×5 cm) placed under a vertically-incident collimated light beam

from a tungsten-halogen lamp (KL 2500, Schott). The tip of a fast response Clark-type microelectrode (tip diameter ~10-20 µm; Revsbech, 1989) was positioned just above (200 µm) the surface of the dried mat using a microscope. Then, circulation of filtered seawater (3.5% salinity) was started within the flow-cell. We waited about 5 minutes before making measurements in the mat. This was to allow the hard crust of the mat to soften enough to allow the microsensor tip to penetrate it without damage.

Volumetric rates of gross photosynthesis (GP in µmol O_2 m^{-3} s^{-1}) were measured using the light-dark shift method (Revsbech et al., 1983), at incident irradiance of 320 µmol photon $m^{-2}s^{-1}$. GP measurements were conducted in vertical depth intervals of 100 µm, with 3 replicates at each depth, up to a depth of 600 µm. Vertical profiles of GP were obtained approximately every 15 minutes during the first hour of rehydration and every hour thereafter for a total of 12 hours.

4.3.6 *Pulsed-amplitude modulation (PAM) fluorometry*

Photosynthetic potential within the mats were investigated using a PAM fluorometer (Walz GmbH, Germany) positioned 12 mm above the mat. Three different conditions of the mat were monitored: 1) the dry mat illuminated, 2) a rehydrated mat under illumination and 3) a rehydrated mat in the dark. The photosynthetic potential was measured using the pulse-saturation method (Kromkamp and Forster, 2003; Schreiber et al., 1995) with a pulse intensity of 2400 µmol photons $m^{-2}s^{-1}$ and duration of 0.8 s. The measured variable fluorescence response, which represents the yield of photosystem II, was sampled repeatedly in three replicate mat pieces over a period of 3 hours after rehydration under the three treatment conditions.

4.4 RESULTS

In all our measurements, a stark green color was observed in both the surface and subsurface layers of the mat between 12–48 hours after rehydration, under both light and dark treatments. Example images from the HSI time-series are provided (Figure 4.1 A-B). This provided a general confirmation that the addition of filtered seawater led to the resurrection of the desiccated cyanobacteria and subsequent migration to the surface.

4.4.1 *Evidence for rapid resynthesis of Chlorophyll a*

The average Chl *a* signal from the HSI time-series for the surface and subsurface regions of the three replicate mats revealed that the Chl *a* values in the subsurface layer, increased steeply within 10 minutes after rehydration, by about 3.9–fold under light treatment and by about 1.2–fold under

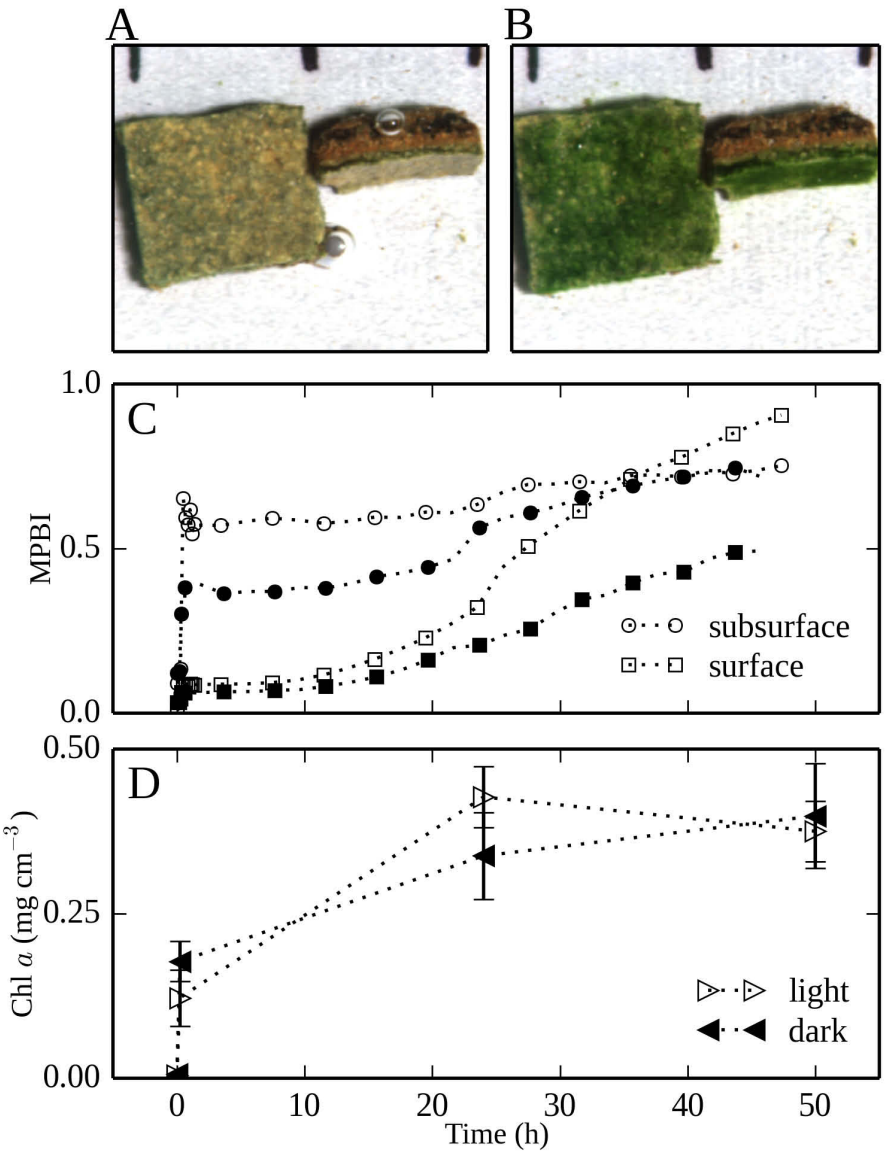

Figure 4.1: Comparison of the true-color maps derived from hyperspectral images of a microbial mat piece (A) immediately after and (B) 24 hours after rehydration (at t=0h) revealed the development of a bright green color in the surface and subsurface layers, along with evolution of air bubbles immediately after rehydration. The time-series of the chl a signal, determined as MPBI, averaged separately over the surface and subsurface layers of (N=3–9) replicate mat pieces are shown in panel B for measurements in the dark (solid symbols) and in the light (empty symbols). Panel C shows the total chl a content of a subset (N=3) of the same mat pieces determined using HPLC. Error bars represent standard error.

dark treatment (Figure 4.1C). During the same time period, the average Chl *a* signal for the top surface of the mats only registered a moderate 1–fold increase for both the light and the dark treatments. Over the course of the subsequent 48 hours of rehydration, the subsurface Chl *a* signal only gradually increased to a slightly higher final level of 4.5–fold in both treatments, whereas the surface Chl *a* signal increased gradually but by a large extent (see below for migration results). This showed that the primary response to rehydration occurred in the subsurface layer, where the desiccated cyanobacteria were located initially, and led to resynthesis of Chl *a* within minutes in that layer. Furthermore, the slow and marginal increase of the subsurface Chl *a* values in the subsequent 48 hours indicated that the resynthesis of Chl *a* was very rapid and nearly most of it occurred in the minutes after rehydration. The increase in Chl *a* signal due to cellular duplication of the cyanobacteria is unexpected as generation time of *Microcoleus* is ~84h (Tiwari et al., 2001).

The dynamics of the total Chl *a* content during the HSI time-series, as measured by HPLC, revealed similar characteristics with a rapid and substantial increase (by 27–fold) during the first 15 minutes of rehydration (Figure 4.1D). Separate HPLC measurements of the short-term (1–20 minutes) dynamics of the total Chl *a* content qualitatively matched the rates and scales of increase in the Chl *a* content of the subsurface layer measured by HSI (Figure 4.2). Furthermore, the rate of Chl *a* resynthesis, as inferred from the three time-points after hydration in the HSI time-series, under light was about 4–fold higher than in the dark (Figure 4.2). Interestingly, the HPLC measurement could not detect Chl *a* in the desiccated state, but up to 8 mg $l^{-1}g^{-1}$ d.w. was detected two minutes after rehydration, with similar results obtained from CLSM data (Figure 4.4). This provides grounds for the inference of rapid resynthesis of chlorophyll in the desiccated mats upon rehydration, both in the light and in the dark.

4.4.2 *Evidence for rapid reactivation of photosynthesis*

Depth profiles of the gross photosynthetic rate were repeatedly measured in the mat using an oxygen microsensor. The resulting values, calibrated to mmol O_2 $m^{-3}s^{-1}$, were compiled into an array and visualized through a false-color image (Figure 4.3A). The first record of oxygen production occurred at a depth of 500 µm about 13 minutes after rehydration. Thereafter, a 'band' of oxygen productivity, ostensibly the resurrected cyanobacteria, gradually moved upwards towards the surface for the entire 12 hours of the measurements. This band was about 200 µm wide initially and expanded to about 500 µm wide by the end (Figure 4.3A). The vertical displacement of the band over the course of the measurements was determined to be approximately 300 µm, and provided further evidence of vertical migration (see below). As this band overlapped with the euphotic zone of the mat (~250–400 µm; data not shown), the maximum oxygen productivity was recorded 8 hours after rehydration to be 9.2 mmol

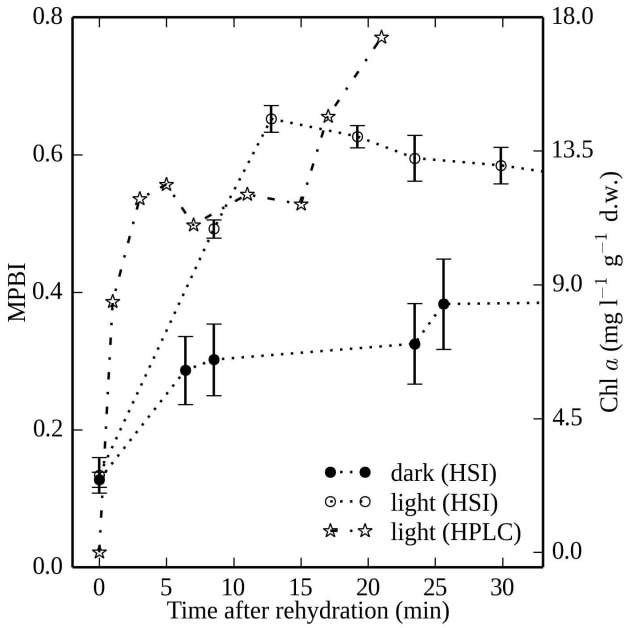

Figure 4.2: Short-term changes in the total Chl *a* content (star symbol), as determined by HPLC, of (N=2) different mats rehydrated (at t=0h) and maintained in the light is compared against the average subsurface chl a signal (MPBI) from the HSI time-series in Figure 4.1 for both light (empty circles) and dark (solid circles) treatments. Error bars represent standard errors.

O_2 $m^{-3}s^{-1}$ at 100 µm depth (Figure 4.3A). The depth-integrated oxygen production increased steadily after rehydration with time and reached a maximum of about 25 mmol O_2 m^{-2} s^{-1} (Figure 4.3B). Overall, these results indicate that the resurrected cyanobacteria engaged in photosynthesis within 15 minutes of rehydration and as they migrated towards the surface.

The measurements from the PAM fluorometer showed no signs of pigment photoactivity (variable fluorescence) in light-exposed desiccated mats for the entire duration of the experiment (Figure 4.3C). On the other hand, the measured variable fluorescence (quantum yield of photosystem II) increased within 10 minutes after rehydration, under both light and dark conditions, and continued to rise monotonically for 2.5 hours. The variable fluorescence of cyanobacteria in the mats in the dark was initially significantly higher than the mats in the light, but after 2.5 hours of monotonic increase, mats from both conditions exhibited equal quantum yields (20%). The inference from these results is that the cyanobacteria rapidly transition from photo-inactive while desiccated, to photo-active (w.r.t Chl *a*) shortly after rehydration as they reactivate their photosystem II for primary production.

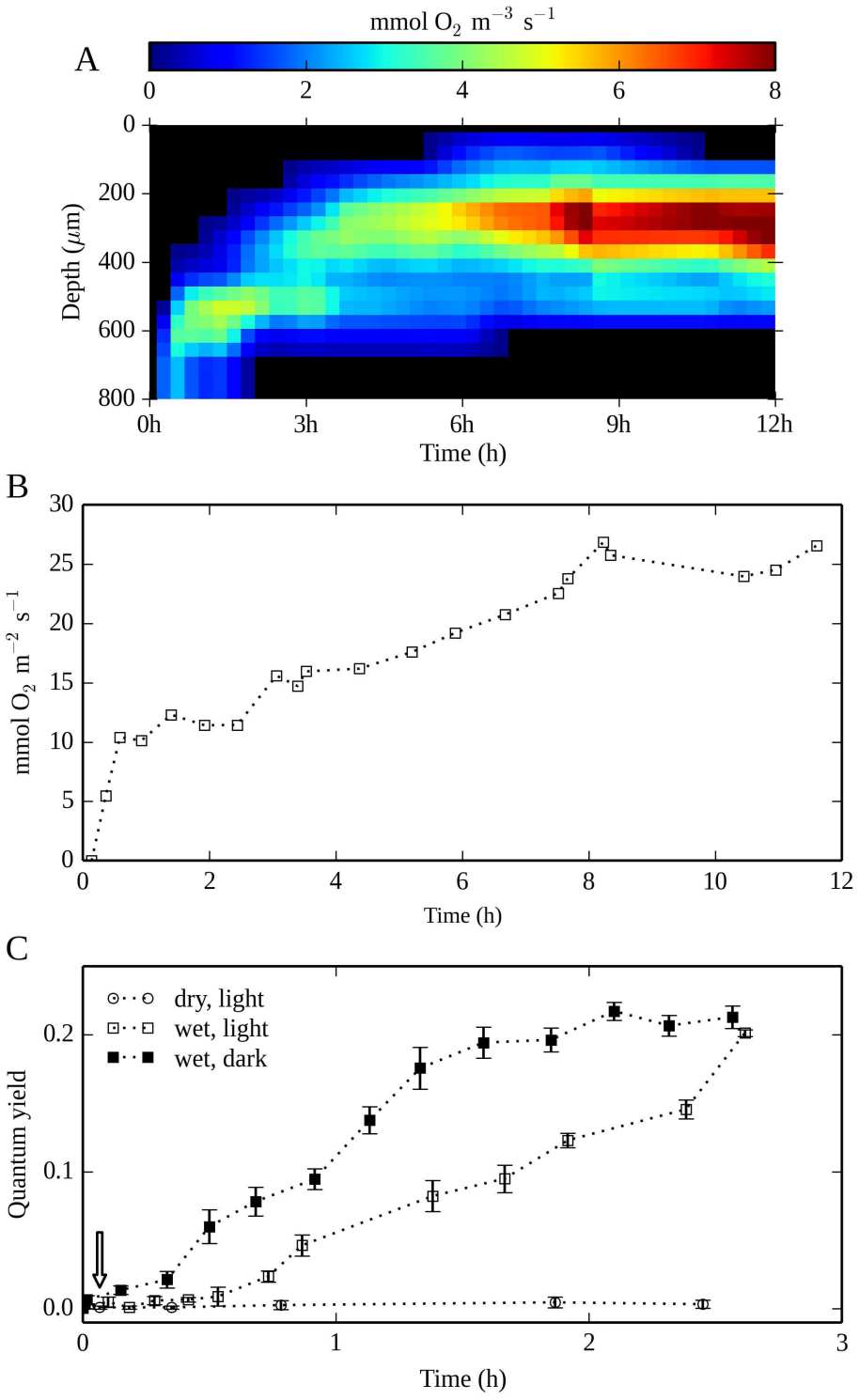

Figure 4.3: (A) Color-coded visualization of the time-series of depth profiles of the gross photosynthetic production within a rehydrated (at t=0h) mat piece as measured by the light-dark shift technique using oxygen microsensors. (B) Depth-integrated oxygen production for the profiles shown in panel A. (C) Time-series of the average quantum yield of photosystem II measured using a PAM fluorometer of (N=3) mat pieces maintained dry and illuminated (empty circles), wet and illuminated (empty squares) and wet and unilluminated (solid squares). Arrow indicates the time-point of hydration. Error bars represent standard errors.

4.4.3 *Evidence for vertical migration after resurrection*

The change in the color of the mat (Figure 4.1A-B) due to rehydration was an indication of emergence of the resurrected cyanobacteria at the surface. Although the subsurface Chl *a* signal showed signs of rapid (minutes) and steep increase upon rehydration, the surface Chl *a* signal hardly increased (~1.2–fold) over first 10 hours of rehydration for both light and dark treatments (Figure 4.1B). However, after 10 hours the surface Chl *a* signal increased faster, till 24 hours (2.2–fold and 1.9–fold for light and dark treatments), reaching the maximum increase of 8–fold for the light and 5.9–fold for dark treatment between 24–48 hours. The surface Chl *a* signal in the light treatment exceeded the maximum subsurface Chl *a* signal, which is probably indicative of a dense accumulation of cyanobacteria at the surface. The final Chl *a* signals were 20–fold and 14–fold higher than the start for the light and dark treatments respectively. The fact that the increase of the Chl *a* signal at the surface lags by about 24 hours the (almost immediate) emergence in the subsurface indicates that while chlorophyll is resynthesized rapidly within the rehydrated mat, the migration of the cyanobacterial filaments to the surface is slower and takes about a day.

The Z-stack images from the CLSM also provided evidence of both rapid resynthesis of chlorophyll and subsequent vertical migration. Images from the desiccated mat showed no cyanobacterial filaments and threshold filtering of the autofluorescence channel produced no structure of filaments. However, in the Z-stack obtained immediately after rehydration, cyanobacterial filaments were visible in the autofluorescence channel. Visual confirmation of the migration of the cyanobacterial filaments was possible by comparing the composite images obtained just after and 24 hours after rehydration in the CLSM Z-stack. Images from the 120µm depth layer are shown for two time-points (Figure 4.4A–B). The depth profile of the pigmented biomass in the dry mat was flat indicating that although a dark brown layer of cyanobacteria was visible (to the eye) under the surface, no active (fluorescent) photopigments was present within this layer. However, the depth profile obtained immediately after rehydration showed a clear peak of active pigments centered around a depth of 200 µm (Figure 4.3C), which supports our findings with HPLC measurements. Furthermore, the depth profile after 24 hours of hydration had a biomass maximum around 100 µm (Figure 4.3C), which implies that the active pigments were displaced upwards due to the migration of the cyanobacteria. The profiles also corroborate the observation of a 'band' of productivity migrating upwards in the oxygen microsensor data (Figure 4.3A), as a layer of Chl a centered around 200–250 µm depth was found displaced upwards by about 100 µm after 24 hours of rehydration (Figure 4.4C).

The rate of vertical migration of the resurrected cyanobacteria was estimated by comparing the dynamics from three datasets: CLSM, HSI and gross photosynthesis profiles. The vertical displacement in the peak of pigmented biomass and oxygen productivity was 100 µm over 24 hours

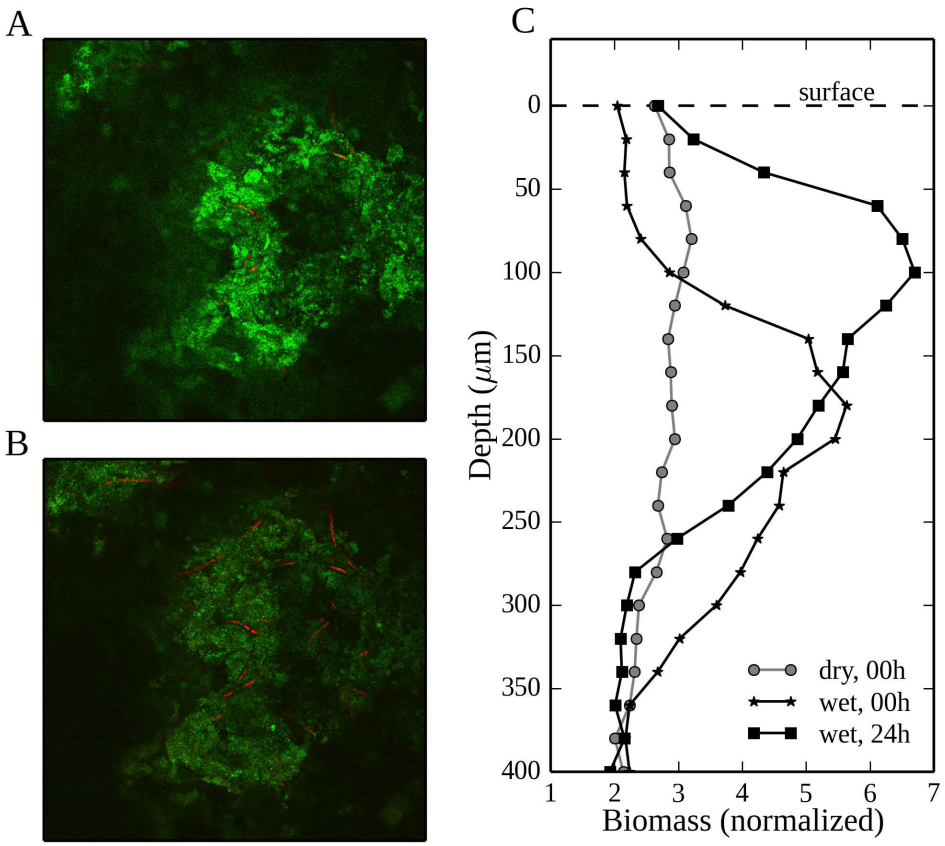

Figure 4.4: Composite images at the same depth (120 µm) of the sediment reflection (green) and cyanobacterial autofluorescence (red) channels measured using a CLSM of a mat piece (A) immediately after and (B) 24 hours after rehydration show increased density of cyanobacterial filaments in the latter image. Depth profiles of the normalized (pigmented) biomass of cyanobacteria before, immediately after and 24 hours after rehydration in panel C shows evidence of rapid resynthesis of chl a and subsequent vertical migration of the resurrected cyanobacteria.

in the dark and 300 µm over 12 hours in the light respectively (Figure 4.3A and Figure 4.4C). This provides an estimate of the speed of migration as 7 µm/h in the dark and 25 µm/h in the light. From the HSI time-series, we ascertained the periods of linear increase (10–24 and 24–48 hours) of the surface Chl *a* signal in the HSI time-series (Figure 4.1C), and estimated the best-fit slope as a simplistic indicator of the migration speed. This provided a proportionality between the migration speeds in the light and in the dark during both periods of migration. Combined with the speeds of migration from the CLSM and oxygen microsensor data, we estimated 7–35 µm/h as the range of conservatively-estimated vertical migration speeds.

4.5 DISCUSSION

The cyanobacterial mats from the arid estuary of Giralia Bay remain desiccated, on an average, for 280 days per year and receive water only sporadically due to unusually high tides or from rainfall. The high average temperature range (24–38 °C), low rainfall (262 mm annually) and topographical elevation of the area combine towards a high evaporative load, leaving only short periods when water is available in the sediments for biological activity (Lovelock et al., 2010). This implies that, in essence, for a majority of the year these marine mats face meteorological conditions that are akin to those faced by terrestrial desert crusts. To cope with the desiccation, cyanobacteria are able to minimize damage by down-regulating their metabolism to protect themselves against reactive oxide species (Wolfe-Simon et al., 2005), and secrete extra-cellular polymeric substances to regulate the loss of water and reduce damage to cell membranes (Potts, 1999). Primary production by the resident cyanobacteria, upon which the entire mat ecosystem depends, is therefore limited to the short windows of opportunity (~1 week) that brings together the necessary components: water, light, nutrients and physiological ability. Shortly after rewetting, cyanobacteria become active and they are found to be distributed within the photic zone in the mat to optimally harvest light. During inundation, they exhibit very efficient photosynthetic production (Al-Najjar et al., 2012), with production rates that are commensurate with other ecosystems (Lovelock et al., 2010). This suggests the action of specific adaptations in the cyanobacteria that facilitate an opportunistic lifestyle with respect to water availability.

Another vital behavioral adaptation is that the cyanobacteria migrate vertically in the mat, as has been observed in desert crusts (Pringault and Garcia-Pichel, 2004) as well as microbial mats (Garcia-Pichel et al., 1994; Kohls et al., 2010). They adopt such behavior in order to take refuge in the layers below the surficial crust to avoid extreme conditions of heat, light or salinity. We observed a dark olive-brown subsurface layer (but no greenness), up to a depth of 0.5–2 mm in the desiccated mats. This suggests that when the mat is rehydrated, the cyanobacteria are underneath

the very thin euphotic zone (250–600 µm; data not shown) and need to migrate upwards, and rapidly, into the euphotic zone in order to utilize the opportunity of available water to perform photosynthesis. Signs of emergence of the cyanobacteria to the surface within a few hours have been observed in the field. Therefore, upon rehydration of desiccated mats we expected to observe signs of resynthesis of chlorophyll in the subsurface layer, followed by the migration towards the surface (euphotic zone). Our investigations attempted to document and understand the mechanisms of this rehydration response.

The general observation among all the mats we studied was the appearance of a greenish tint at the surface some hours after rehydration, and accumulating to a bright green layer one day later (Figure 4.1A-B). This confirmed that the storage and processing of the microbial mats in the laboratory had maintained the viability of the migratory response of the dormant cyanobacteria. We observed that air bubbles (Figure 4.1B) formed and escaped the surfaces of the mat pieces in the initial 2–3 minutes after the addition of water, but none thereafter, which provides an indication of the time taken for the porespaces in the mat to be filled by porewater. This has implications for adopting the concept of hydrotaxis, as discussed below. Additionally, in some cases rehydration caused the mats to slightly expand (40–80 µm), which was taken into account in our data analysis.

Rapid resynthesis of Chlorophyll a

The hyperspectral imager, due to its high spatial range and resolution, provided a synoptic measurement of the Chl *a* signal in the surface and subsurface layers of the mat. The time-series measurement showed that rehydration resulted in a very steep (1.2– to 4–fold in 2 minutes) increase in the Chl *a* signal in the subsurface layer, but no increase in values at the surface (Figures 4.1C & 4.2). The HPLC time-series, which measured the total Chl *a* content within the mat pieces, also showed a large increase in the Chl *a* content within minutes of hydration (Figures 4.1D & 4.2). The increase in the first 15 minutes was roughly 50% of total Chl *a* content measured after days 1 and 2. Importantly, no evidence of Chl *a* was found in the desiccated mat from the HPLC (Figures 4.1C & 4.2), but we consider it unlikely to be due a methodological problem of extracting pigment from the dry mat because of the corroborating evidence from the CLSM depth profiles (Figure 4.4C). We concluded that the build-up of Chl *a* in the rehydrated mats was rapid (~15–20 minutes), and also that once the desiccated chlorophyll was resynthesized in the mats, no significant production of new chlorophyll occurred during our measurements. Interestingly, these observations show that the chlorophyll resynthesis upon rehydration is very rapid and occurs in the subsurface layer corresponding to the layer of dormant cyanobacteria. This is much faster than the time required (8–24 hours) for complete synthesis of Chl *a* (Beale and Appleman, 1971), which suggests that cyanobacteria in the dehydrated mats might sequester one

or more of the intermediates or precursors of Chl *a* to enable rapid resynthesis (see below).

Rapid reactivation of photosynthesis

Our measurements with the PAM fluorometer, the CLSM and oxygen microsensors confirmed that pigment photoactivity and photosynthetic production could be detected in the mat within 10–15 minutes after rehydration (Figures 4.3 & 4.4). As a larger fraction of the cyanobacterial filaments migrated into the euphotic zone, the cumulative oxygen productivity gradually increased over this period (Figure 4.3B). It was not possible to measure with microsensors in the desiccated mat due to the hard surface crust and the fragility of the sensors, or in the dark due to the use of light for the light-dark shift method. However, no oxygen production is expected to occur in the desiccated or dark state as both water and light are required components for photosynthesis. We did measure the dry mats with a PAM fluorometer and could not detect any variable fluorescence in them (Figure 4.4C). The detection of variable fluorescence within minutes of rehydration led us to infer the rapid reactivation of the photosynthetic apparatus of the cyanobacteria. The higher quantum yields of mats incubated in the dark is expected as the plastoquinon pool of the photosystem is less occupied by electrons than for the cells incubated under light.

The rapidity of the reactivation of the photosynthetic apparatus is remarkable given the extended periods of desiccated dormancy that precede it. We postulate that this is possible through an evolutionary adaptation of the cyanobacteria that allows them, during desiccation, to sequester their Chlorophyll *a* in a precursor state, most likely protoporphyrin IX. This would involve knocking out the magnesium ion from the ring structure of Chl a, a quick and low-energy step, which renders the molecule photoinactive and relatively stable, and which is also easily reversed upon rehydration. There is evidence that this occurs in the field, as (Lovelock et al., 2010) reported that the magnesium concentration in the mat sediments was two–fold higher than the surrounding marine or terrestrial soils. Further investigations are underway towards confirming the precursor sequestration hypothesis and detailed results will be reported elsewhere.

Vertical migration to the surface

Given that the subsurface Chl *a* signal and the HPLC measurements indicated no increase in the total Chl *a* content between the two days (Figure 4.1C–D), the gradually increasing Chl *a* signal at the surface is indicative of the slower process of migration of the cells towards the surface. The presence or absence of light did not change the mechanism of the migratory response to rehydration, but the rates of migration were slower in the dark than in the light (Figure 4.1B). Vertical migration of the cyano-

bacteria was visually confirmed from the Z-stack images from a similar rehydration protocol in the dark. The density of cyanobacterial cells at a given depth was interpreted from the measured fluorescent emission intensity, which is considered to indicate the presence of physiologically active chlorophyll (Schreiber et al., 1995). Comparison of the depth profiles of Chl *a* just after and 24 hours after rehydration provided quantitative confirmation of the upward migration of the filaments, by up to 100 µm in dark (Figure 4.4C). The time-series of gross photosynthesis depth profiles (Figure 4.3A) showed characteristics that are consistent with the CLSM depth profiles and the HSI time-series, i.e. a zone of oxygen productivity roughly 300–400 µm broad that moves continuously from the depth towards the surface up to 48 hours after rehydration.

The probing depth of the hyperspectral imager is closely related with the depth of light penetration in the mat, and the spectrally derived Chl *a* signal (MPBI) is sensitive to the concentration and vertical distribution of the Chl *a* pigmented cells within the probing depth (Chennu et al., 2013). A potential variability in our interpretation of the MPBI as a quantitative measure of the Chl *a* content within the probing depth arises from the highly heterogeneous vertical structure of the mats, which also changed temporally due to migration. This might result in an overestimation of the Chl *a* signal at the surface when the euphotic zone is densely populated by cyanobacteria.

With the reasonable assumption that we observed the same phenomenon of cyanobacterial migration through the three methods, we made inter-comparisons of the dynamics to estimate the range of speeds of vertical migration of the ~300-µm-broad cyanobacterial layer to be 7–35 µm h^{-1}. Migration speeds 25–250 times faster have been reported in hypersaline mats (Garcia-Pichel et al., 1994), but in the context of diel rhythms where the primary driver (light) of migration changes rapidly. In addition, cyanobacteria cells in that case were already hydrated, active, and energetically equipped for migration. On the other hand, during desiccation, the cells are dormant and their metabolism is at the minimum; thus, it presumably requires longer to reacquire necessary energy reserves. Our estimates are the first report, to our knowledge, of the speed of migration of cyanobacteria upon recovery from desiccation, where crucially light is not the driver. We postulate that the observed migration rate is characteristic of the adaptation in desiccated cyanobacteria that triggers vertical migration towards the photic zone upon the availability of water and before the establishment of a diel migratory rhythm as is commonly observed in microphytobenthos (Guarini et al., 2000; MacIntyre et al., 1996). Furthermore, we harbor reservations about adopting the paradigm of "hydrotaxis" for this migratory response, as nominated by Pringault and Garcia-Pichel (2004). Our understanding of the effect of addition of water suggests that the inundation of the sediment porespaces occurs within several minutes (while air bubbles escaped the mats), after which water is available to the cells in nearly the whole volume of the mat. While the availability of water is the necessary trigger for the resynthesis of chlorophyll, the subsequent

migration continues for at least 24 hours. During this extended period of unidirectional migration, there is likely no gradient of a "water potential" in the vertical direction as proposed by Pringault and Garcia-Pichel (2004) and therefore, the term hydrotaxis would be a misnomer as it generally implies the movement driven along a gradient, as is implied in the term related term "halotaxis" (Kohls et al., 2010). One possible gradient related to the available water is the hydrostatic pressure due to gravity which might be a driver for the migrational direction. However the direction of the rehydration migratory response of the cyanobacteria was unaltered upon inverting the gravitational axis of the mat (personal observation). Although the observed migrational response after rehydration qualifies for the phraseology of the Greek *taxis* (i.e. an innate behavioral response in an organism to a directional stimulus or gradient), the exact nature of the driving stimulus remains to be identified.

To summarize, using a variety of techniques we showed that upon rehydration of desiccated marine microbial mats, the dormant cyanobacteria within are resurrected through the mechanisms of 1) rapid resynthesis of chlorophyll occurring within minutes, 2) rapid reactivation of photosynthesis using the resynthesized chlorophyll, and 3) the onset of an innate behavioral response that involves migration towards the surface at speeds of 7–35 µm h^{-1} irrespective of light gradients.

The ability to sequester and rapidly reactivate the photosynthetic apparatus, combined with the ability to vertically migrate in the sediment, are likely crucial adaptations that enable cyanobacteria to thrive in arid environments with sporadic water availability. The migratory response upon resurrection being uninhibited by light conditions of the mat suggests that this behavior is an innate *festina lente* response that drives the cyanobacteria towards the photic zone when conducive conditions for photosynthesis (i.e. water and nutrients) are available. This behavioral disregard for the light and chemical gradients that typically regulate spatial distributions within perennially hydrated microbial mats can be understood as an overriding priority of the opportunistic lifestyle of desiccated cyanobacteria to capitalize on the infrequent chance to engage in productive phototrophy. Additionally, the exclusion of many higher trophic levels in these harsh environments reduces greatly the risks of predation that the cyanobacteria face at the sediment surface (Garrett, 1970), compared to intertidal microphytobenthos that adhere to strongly diurnal and/or tidal rhythms to cope with the dynamics of predators (Buffan-Dubau and Carman, 2000). It is yet unknown whether cyanobacterial species in arid environments develop such periodic rhythms of activity upon prolonged availability of water, although it is known that they exhibit primary productivity for up to a week after a single inundation event (Lovelock et al., 2010). Nevertheless, through their sensitively triggered rehydration response and rapid reactivation of primary production, they provide sustenance to the co-dependent microbial communities and play a pivotal role in resurrecting the function of desiccated microbial mat ecosystems. Further investigation of the controls and functions of modern microbial

mats promises to engender a greater understanding of the influence of cyanobacterial mats on the evolution of the early Earth biosphere as well as modern ecosystems.

4.6 ACKNOWLEDGMENTS

We thank the technicians of the microsensor group and the electronic workshop at the Max Planck Institute for Marine Microbiology for their assistance with instrumentation. We also thank Martin Beutler (Bionsys GmbH) for assistance with microscopy and Lubos Polerecky (Utrecht University) for experimental discussions. This work was funded by the Marie Curie Initial Training Network "SENSEnet" (grant number: 237868) and the Max Planck Society of Germany.

4.7 AUTHOR CONTRIBUTIONS

Return to start

Arjun Chennu and Mohammad Al-Najjar designed the project, and analyzed the data. Hyperspectral and confocal microscopy measurements were performed by Arjun Chennu and Mohammad Al-Najjar. HPLC and microsensor measurements were performed by Mohammad Al-Najjar. PAM fluorometry and field work were conducted by Alistair Grinham. Manuscript text was prepared by Arjun Chennu, with assistance from Mohammad Al-Najjar and Alistair Grinham.

4.8 REFERENCES

Bauld, J. (1981). "Occurrence of benthic microbial mats in saline lakes." In: *Salt Lakes*. Ed. by W. D. Wiliams. Springer-Verlag, pp. 87–111. DOI: 10.1007/978-94-009-8665-7_8 (cited on page 107).

Beale, S. I. and D. Appleman (1971). "Chlorophyll Synthesis in Chlorella: Regulation by Degree of Light Limitation of Growth." In: *Plant Physiology* 47.2, pp. 230–235. DOI: 10.1104/pp.47.2.230 (cited on page 120).

Bebout, B. M., S. P. Carpenter, D. J. Des Marais, M. Discipulo, T. Embaye, F. Garcia-Pichel, T. M. Hoehler, M. Hogan, L. L. Jahnke, R. M. Keller, S. R. Miller, L. E. Prufert-Bebout, C. Raleigh, M. Rothrock, and K. Turk (2002). "Long-term manipulations of intact microbial mat communities in a greenhouse collaboratory: simulating earth's present and past field environments." In: *Astrobiology* 2.4, pp. 383–402. DOI: 10.1089/153110702762470491 (cited on pages 106 sq.).

Belnap, J. and D. Eldridge (2001). "Disturbance and recovery of biological soil crusts." In: *Biological soil crusts: structure, function, and management*, pp. 363–383. DOI: 10.1007/978-3-642-56475-8_27 (cited on page 107).

Buffan-Dubau, E. and K. R. Carman (2000). "Diel feeding behavior of meiofauna and their relationships with microalgal resources." In: *Limnology and Oceanography* 45.2, pp. 381–395. DOI: 10.4319/lo.2000.45.2.0381 (cited on page 123).

Canfield, D. E. and D. J. Des Marais (1993). "Biogeochemical cycles of carbon, sulfur, and free oxygen in a microbial mat." In: *Geochimica et Cosmochimica Acta* 57.16, pp. 3971–3984. DOI: 10.1016/0016-7037(93)90347-Y (cited on page 106).

Castenholz, R. W. and F. Garcia-Pichel (2002). "Cyanobacterial responses to UV-radiation." In: *The ecology of cyanobacteria*. Springer, pp. 591–611. DOI: 10.1007/0-306-46855-7_21 (cited on page 107).

Castenholz, R., B. Jørgensen, E. D'Amelio, and J. Bauld (1991). "Photosynthetic and behavioral versatility of the cyanobacterium *Oscillatoria boryana* in a sulfide-rich microbial mat." In: *FEMS Microbiology Ecology* 9.1, pp. 43–57. DOI: 10.1111/j.1574-6941.1991.tb01737.x (cited on page 107).

Chennu, A., P. Färber, N. Volkenborn, M. A. A. Al-Najjar, F. Janssen, D. de Beer, and L. Polerecky (2013). "Hyperspectral imaging of the microscale distribution and dynamics of microphytobenthos in intertidal sediments." In: *Limnology and Oceanography: Methods* 11, pp. 511–528. DOI: 10.4319/lom.2013.11.511 (cited on pages 109, 122).

Decho, A. (2000). "Microbial biofilms in intertidal systems: an overview." In: *Continental Shelf Research* 20, pp. 1257–1273 (cited on page 107).

Des Marais, D. J. (2003). "Biogeochemistry of hypersaline microbial mats illustrates the dynamics of modern microbial ecosystems and the early evolution of the biosphere." In: *The Biological Bulletin* 204.2, pp. 160–167 (cited on pages 106 sq.).

Eldridge, D. and R. Greene (1994). "Microbiotic soil crusts — a review of their roles in soil and ecological processes in the rangelands of Australia." In: *Soil Research* 32.West 1990, pp. 389–415. DOI: 10.1071/SR9940389 (cited on page 107).

Franks, J. and J. F. Stolz (2009). "Flat laminated microbial mat communities." In: *Earth-Science Reviews* 96.3, pp. 163–172. DOI: 10.1016/j.earscirev.2008.10.004 (cited on pages 106 sq.).

Garcia-Pichel, F. and J. Belnap (1996). "Microenvironments and microscale productivity of cyanobacterial desert crusts." In: *Journal of Phycology* 32, pp. 774–782. DOI: 10.1111/j.0022-3646.1996.00774.x (cited on page 107).

Garcia-Pichel, F., A. López-Cortés, and U. Nübel (2001). "Phylogenetic and morphological diversity of cyanobacteria in soil desert crusts from the Colorado Plateau." In: *Applied and Environmental Microbiology* 67.4, pp. 1902–1910 (cited on page 107).

Garcia-Pichel, F., M. Mechling, and R. W. Castenholz (1994). "Diel migrations of microorganisms within a benthic, hypersaline mat community." In: *Applied and environmental microbiology* 60.5, pp. 1500–1511 (cited on pages 106, 119, 122).

Garcia-Pichel, F., L. Prufert-Bebout, and G. Muyzer (1996). "Phenotypic and phylogenetic analyses show *Microcoleus chthonoplastes* to be a cosmopolitan cyanobacterium." In: *Applied and Environmental Microbiology* 62.9, pp. 3284–3291 (cited on page 109).

Garrett, P. (1970). "Phanerozoic stromatolites: Noncompetitive ecologic restriction by grazing and burrowing animals." In: *Science* 169.3941, pp. 171–173. DOI: 10.1126/science.169.3941.171 (cited on pages 106, 123).

Guarini, J.-M., G. F. Blanchard, P. H. Gros, D. Gouleau, and C. Bacher (2000). "Dynamic model of the short-term variability of microphytobenthic biomass on temperate intertidal mudflats." In: *Marine Ecology-Progress Series* 195, pp. 291–303. DOI: 10.3354/meps195291 (cited on page 122).

Johansen, J. R. (1993). "Cryptogamic crusts of semiarid and arid lands of North America." In: *Journal of Phycology* 29.2, pp. 140–147. DOI: 10.1111/j.0022-3646.1993.00140.x (cited on page 107).

Jørgensen, B. B. and D. J. Des Marais (1988). "Optical properties of benthic photosynthetic communities: Fiber-optic studies of cyanobacterial mats." In: *Limnology and Oceanography* 33.1, pp. 99–113. DOI: 10.4319/lo.1988.33.1.0099 (cited on page 107).

Jørgensen, B. B., N. P. Revsbech, T. H. Blackburn, and Y. Cohen (1979). "Diurnal cycle of oxygen and sulfide microgradients and microbial photosynthesis in a cyanobacterial mat sediment." In: *Applied and Environmental Microbiology* 38.1, pp. 46–58 (cited on page 106).

Kohls, K., R. M. M. Abed, L. Polerecky, M. Weber, and D. de Beer (2010). "Halotaxis of cyanobacteria in an intertidal hypersaline microbial mat." In: *Environmental microbiology* 12.3, pp. 567–75. DOI: 10.1111/j.1462-2920.2009.02095.x (cited on pages 107, 119, 123).

Kromkamp, J. C. and R. M. Forster (2003). "The use of variable fluorescence measurements in aquatic ecosystems: differences between multiple and single turnover measuring protocols and suggested terminology." In: *European Journal of Phycology* 38.2, pp. 103–112. DOI: 10.1080/0967026031000094094 (cited on page 112).

Kühl, M., C. Lassen, and B. B. Jørgensen (1994). "Light penetration and light intensity in sandy marine sediments measured with irradiance and scalar irradiance fiberoptic microprobes Rid A-1977-2009." In: *Marine Ecology Progress Series* 1.2, pp. 139–148 (cited on page 106).

Lovelock, C. E., A. Grinham, M. F. Adame, and H. M. Penrose (2010). "Elemental composition and productivity of cyanobacterial mats in an

arid zone estuary in north Western Australia." In: *Wetlands Ecology and Management* 18.1, pp. 37–47. DOI: 10.1007/s11273-009-9146-6 (cited on pages 107, 109, 119, 121, 123).

MacIntyre, H., R. Geider, and D. Miller (1996). "Microphytobenthos: The ecological role of the "secret garden" of unvegetated, shallow-water marine habitats. I. Distribution, abundance and primary production." In: *Estuaries and Coasts* 19.2, pp. 186–201. DOI: 10.2307/1352224 (cited on page 122).

Al-Najjar, M. A. A., D. de Beer, B. B. Jørgensen, M. Kuhl, and L. Polerecky (2009). "Conversion and conservation of light energy in a photosynthetic microbial mat ecosystem." In: *ISME J* 4.3, pp. 440–449. DOI: 10.1038/ismej.2009.121 (cited on page 107).

Al-Najjar, M. A. A., D. de Beer, M. Kühl, and L. Polerecky (2012). "Light utilization efficiency in photosynthetic microbial mats." In: *Environmental Microbiology* 14.4, pp. 982–92. DOI: 10.1111/j.1462-2920.2011.02676.x (cited on pages 106, 119).

Polis, G. A., W. B. Anderson, and R. D. Holt (1997). "Toward an integration of landscape and food web ecology: the dynamics of spatially subsidized food webs." In: *Annual review of ecology and systematics*, pp. 289–316. DOI: 10.1146/annurev.ecolsys.28.1.289 (cited on page 107).

Potts, M. (1999). "Mechanisms of desiccation tolerance in cyanobacteria." In: *European Journal of Phycology* 34.4, pp. 319–328. DOI: 10.1080/09670269910001736382 (cited on page 119).

Pringault, O. and F. Garcia-Pichel (2004). "Hydrotaxis of cyanobacteria in desert crusts." In: *Microbial ecology* 47.4, pp. 366–73. DOI: 10.1007/s00248-002-0107-3 (cited on pages 107, 119, 122 sq.).

Revsbech, N. P. (1989). "An oxygen microsensor with a guard cathode." In: *Limnology and Oceanography* 34.2, pp. 474–478. DOI: 10.4319/lo.1989.34.2.0474 (cited on page 112).

Revsbech, N. P. and B. B. Jørgensen (1986). "Microelectrodes: their use in microbial ecology." In: *Advances in Microbial Ecology* 9, pp. 293–352. DOI: 10.1007/978-1-4757-0611-6_7 (cited on page 106).

Revsbech, N. P., B. B. Jørgensen, T. H. Blackburn, and Y. Cohen (1983). "Microelectrode studies of the photosynthesis and O_2, H_2S, and pH profiles of a microbial mat." In: *Limnology and Oceanography* 28.6, pp. 1062–1074. DOI: 10.4319/lo.1983.28.6.1062 (cited on pages 106, 108, 112).

Schreiber, U., H. Hormann, C. Neubauer, and C. Klughammer (1995). "Assessment of photosystem II photochemical quantum yield by chlorophyll fluorescence quenching analysis." In: *Functional Plant Biology* 22.2, pp. 209–220. DOI: 10.1071/PP9950209 (cited on pages 112, 122).

Schreiber, U. (2004). "Pulse-amplitude-modulation (PAM)) fluorometry and saturation pulse method: an overview." In: *Chlorophyll a Fluores-*

cence. Ed. by G. Papageorgiou and Govindjee. Vol. 19. Advances in Photosynthesis and Respiration. Springer Netherlands, pp. 279–319. DOI: 10.1007/978-1-4020-3218-9_11 (cited on page 108).

Smith III, T. J. and N. C. Duke (1987). "Physical determinants of inter-estuary variation in mangrove species richness around the tropical coastline of Australia." In: *Journal of Biogeography* 14, pp. 9–19. DOI: 10.2307/2844783 (cited on page 107).

Stal, L. J. (1995). "Physiological ecology of cyanobacteria in microbial mats and other communities." In: *New Phytologist* 131, pp. 1–32. DOI: 10.1111/j.1469-8137.1995.tb03051.x (cited on pages 106 sq.).

Stolz, J. F. (2000). "Structure of Microbial Mats and Biofilms." English. In: *Microbial Sediments*. Ed. by R. E. Riding and S. M. Awramik. Springer Berlin Heidelberg, pp. 1–8. DOI: 10.1007/978-3-662-04036-2_1 (cited on page 106).

Tiwari, O., R. Prasanna, A. Yadav, W. Dhar, and P. Singh (2001). "Growth potential and biocide tolerance of non-heterocystous filamentous cyanobacterial isolates from rice fields of Uttar Pradesh, India." English. In: *Biology and Fertility of Soils* 34.4, pp. 291–295. DOI: 10.1007/s003740100402 (cited on page 114).

Van Gemerden, H. (1993). "Microbial mats: a joint venture." In: *Marine Geology* 113.1, pp. 3–25. DOI: 10.1016/0025-3227(93)90146-M (cited on page 106).

Vermaas, W. F., J. A. Timlin, H. D. Jones, M. B. Sinclair, L. T. Nieman, S. W. Hamad, D. K. Melgaard, and D. M. Haaland (2008). "*In vivo* hyperspectral confocal fluorescence imaging to determine pigment localization and distribution in cyanobacterial cells." In: *Proceedings of the National Academy of Sciences* 105.10, pp. 4050–4055. DOI: 10.1073/pnas.0708090105 (cited on page 111).

Walter, M. R., R. Buick, and J. S. R. Dunlop (1980). "Stromatolites 3,400–3,500 Myr old from the North Pole area, Western Australia." In: *Nature* 284.5755, pp. 443–445. DOI: 10.1038/284443a0 (cited on page 106).

Ward, D. M., M. J. Ferris, S. C. Nold, and M. M. Bateson (1998). "A natural view of microbial biodiversity within hot spring cyanobacterial mat communities." In: *Microbiology and Molecular Biology Reviews* 62.4, pp. 1353–1370 (cited on page 107).

Wolfe-Simon, F., D. Grzebyk, O. Schofield, and P. G. Falkowski (2005). "The role and evolution of superoxide dismutases in algae." In: *Journal of Phycology* 41.3, pp. 453–465. DOI: 10.1111/j.1529-8817.2005.00086.x (cited on page 119).

5

GROWTH OF SUBTIDAL MICROPHYTOBENTHOS

The following is the abstract of a (co-authored) study with the use of hyperspectral imaging to monitor the growth of MPB assemblages from subtidal sites under controlled light and nutrient conditions.

WILL AN UPWARD SHIFT OF THE TEMPERATURE BASELINE CHANGE BIOMASS GROWTH OF SUB-ARCTIC (SVALBARD, KONGSFJORDEN) AND TEMPERATE (NORTH SEA, HELGOLAND) MICROPHYTOBENTHOS COMMUNITIES? A QUANTITATIVE PILOT-STUDY

Duygu S. Sevilgen[1,2], Arjun Chennu[2] and Tom Brey[1]

See Author contributions

MANUSCRIPT STATUS

In preparation for submission to *Polar Biology*.

5.1 ABSTRACT

Subtidal microphytobenthic (MPB) communities from a temperate (Helgoland, Germany) and a sub-arctic site (Svalbard, Norway) were incubated in the laboratory at different temperatures, under mimicked *in situ* light cycles and under nutrient-enriched conditions. Our general aim was to study the response of the MPB to an increase in the baseline temperature, which is expected to occur in these regions due to global climate change. We applied treatments of temperatures that spanned the extreme range of *in situ* temperatures for each site (5°, 10° & 20°C and 0°, 5° & 10°C for Helgoland and Svalbard), coupled with non-limiting nutrient load. We monitored the dynamics of Chlorophyll *a* content using hyperspectral imaging to calculate growth rates and doubling times. Additionally we used high-performance liquid chromotography to study potential changes in the composition of major MPB pigments. Compared to previously known values, growth rates were low and maximum final biomasses were found at the intermediate temperatures in both sites. The growth rates did not differ significantly between sites nor between the intermediate and high temperatures applied (0.34 ± 0.16/0.33 d^{-1} and 0.24 ± 0.05/0.22 ± 0.07

1 Alfred-Wegener Institute, PO Box 120161, Bremerhaven, Germany
2 Max Planck Institute for Marine Microbiology, Celsiusstr. 1, Bremen, Germany

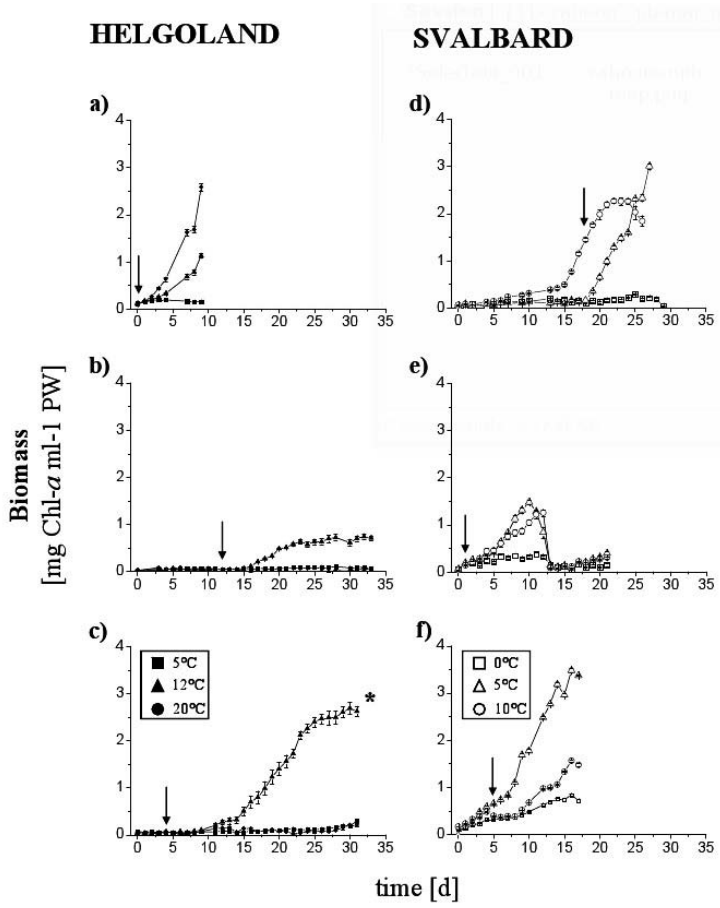

Figure 5.1: Growth curves of MPB biomass measured as Chl *a* concentration in the top 1 mm of temperate (Helgoland) and sub-arctic (Svalbard) subtidal sandy sediments during controlled incubation. Three replicate growth series at three experimental temperatures (5°, 12° and 20°C for Helgoland and 0°, 5° and 10°C for Svalbard) are shown for each site. Each data point in the growth series represents the average ± SD of (n=3) pseudoreplicate temperature incubations. Arrows indicate the day of nutrient addition; * indicates incubation with n = 2 replicates.

d^{-1} for intermediate/high temperatures in Helgoland and Svalbard respectively). No growth was detectable at low temperatures in Helgoland and low-temperature growth in Svalbard was very low within the duration of our studies. Analyses of MPB pigments indicated diatom dominance in the communities but were very heterogeneous in all treatments. Fucoxanthin:Chlorophyll *a* ratios were too heterogeneous to derive general trends of community changes at different temperatures. Based on our observations, we expect that no net change in the growth rates will occur with an upward shift of the temperature baseline and speculate that the overall biomass may decrease due to potential differences in species and size classes forming the temperature-'specific communities. Based on the little data available for the temperature response of entire communities, we encourage further long-term community-wide studies under natural conditions from different seasons.

5.2 AUTHOR CONTRIBUTIONS

Return to start

Duygu Sevilgen designed the study and performed the field sampling. Hyperspectral analyses were performed by Arjun Chennu and Duygu Sevilgen. HPLC analyses were performed by Duygu Sevilgen. Manuscript was prepared by all authors.

Part III

PERPSECTIVE

6

DISCUSSION AND OUTLOOK

6.1 DISCUSSION

Microphytobenthos are microbial benthic phototrophs that form assemblages with very dense concentration of cells in the top layers of benthic sediment substrates. These sub-millimeter scale assemblages are cryptic ecological zones in terms of form, function and control, which are regulated by the dynamic and complex interactions that characterize the microbenthic environment (Boudreau and Jørgensen, 2001). This makes their study a technical challenge and has partly been responsible for the latent recognition of its status as a "secret garden" that exerts significant influence over the ecological functions of coastal ecosystems (MacIntyre et al., 1996; Miller et al., 1996). Despite the relative dearth of global or long-term datasets about neritic MPB communities, it is clear that they are disproportionately fertile and form the fundament of the trophic food web in coastal environments with a significant annual contribution to the global primary production (Cahoon, 1999).

Investigations into the spatio-temporal distribution of MPB communities on seasonal or regional scales have revealed perplexing or contradictory results (Chapman et al., 2010; Underwood et al., 2000), indicative of systematic errors in assessing their abundance (MacIntyre et al., 1996; Spilmont et al., 2011). This has underscored the need to record the small-scale heterogeneity in the distributions of MPB communities, both for interpreting large-scale patterns and for understanding the operant controls on the structure and function of these communities (Levin, 1992; Miller et al., 1996). The use of microsensors has provided great insights into the geochemical drivers of the organization of MPB communities, especially microbial mats, but it has proved difficult to extrapolate results over larger areas due to the limited lateral resolution of microsensors (Glud, 2006; Revsbech and Jørgensen, 1986). Remote sensing measurements with hyperspectral imagers has the potential to provide regular records of the distribution of MPB and multifarious ecological parameters over large areas with relative ease (Méléder et al., 2010). However, a methodological gap exists for the *in situ* measurement of microscale distribution and dynamics of MPB in natural sediments, both under and above water. The primary goals of this doctoral thesis were to fill this methodological void by developing a suitable *in situ* hyperspectral imaging system and apply it towards the study of microbenthic ecology.

6.1.1 *Technical design and capabilities*

The *in situ* hyperspectral imaging system, called Hypersub, developed as a part of this doctoral project is capable of measuring an area of 1×1 m with a lateral resolution of 0.5–2 mm/pixel within 10–15 minutes. This range:resolution ratio of 1000 is similar to the high-resolution imager planned for the EnMap satellite mission (Kaufmann et al., 2012), and represents the degree of spatial detail relative to the span of the imager's field-of-view. The spectral resolution of the imager is about 1 nm over the visible and near-infrared range, which enables a range of spectrometric analyses useful for the assessment of *in situ* MPB distributions. Hypersub is an adaptation of a laboratory system developed for high-resolution imaging of samples using magnifying objectives or a microscope (Polerecky et al., 2009), and is geared towards making field measurements (Chapter 2).

The design motivation for Hypersub was to enable *in situ* measurements of intertidal and subtidal habitats with an extended scanning range, high resolution and the possibility to deploy the system for long-term measurements. The design specifications for the hardware and software of Hypersub were derived directly from the necessities of the measurements planned for ecological studies. This resulted in a synergistic coupling between the design and the deployment phases of the method development. The hardware of Hypersub consists of commercially available imagers, optics, miniature computer and a suite of custom-built electronic and mechanical assemblies that were designed for modular and autonomous operation. The primary criterion for the hardware was ease and flexibility of assembly, transport, reconfiguration and disassembly of the system with commonly available field tools. A light-weight frame (Figure 2.1) was built that allowed the handling of the system by one or two persons on an intertidal flat. The underwater housings for the electronics and the motor, constructed from light but robust plastic, were pressure-rated to a depth of 80 meters and equipped with wet-mateable electronic connectors. An on-board battery pack was included to enable autonomous operation for limited periods. The modular construction enabled the assembly to be performed on-site or on-shore before deployment.

A control software, called SinKraft, was developed to enable hierarchical operation of the components of Hypersub on a common network platform. The design of the software reflected the modularity and inter-operability of the hardware, such that the operation of each device was independent and could be interactively controlled, or integrated into a system-level measurement protocol. The modular architecture allowed components to be added, modified or replaced with ease, which enables SinKraft to adaptively incorporate new devices into Hypersub as required for measurements, such as light and temperature loggers, cameras, microsensor profilers, etc. For example, an additional camera and a line laser were integrated to make topographical measurements of the sediment. Overall, this architectural scalability means that Hypersub can be oper-

ated as the control center of a remotely-operable observatory, or as a node in larger observatory infrastructure. Such integration is aided by the fact that the only external dependencies of Hypersub are a 12V power supply and networked access, which are common standards in modern ocean observation platforms. Hypersub was successfully operated over the course of the doctoral project in laboratories, outdoor greenhouses, on intertidal sand flats and in a subtidal site with cabled network access. The flexible software design allowed the system operation to be interactive (for preliminary investigation), autonomous (for capturing time-series) or networked (for field or underwater work).

6.1.2 *Ecological insights*

The Chl *a* signal, represented as a spectral-index (MPBI), in the reflected light from sediment was calibrated to quantify the Chl *a* content of the top layer of sediment. The index performed linearly and was valid for Chl *a* quantification over a wide range of naturally found Chl *a* concentrations (Chapter 2). The high-resolution hyperspectral images were used to generate Chl *a* maps of unprecedented detail, which revealed that natural intertidal sediments host a remarkable degree of spatial heterogeneity of MPB distribution at the millimeter to centimeter scale, with spatial variability of up to 400% over 1 cm consisting of small patches of a range of sizes (Figure 2.6). Preliminary analyses of these 'snapshot' maps of MPB distribution were indicative of ecological forces, such as sediment topography, tidal action, or bioturbation by lugworms that shaped the observed distribution of the MPB communities. Availability of spatially dense samples of Chl *a* concentration enabled us to compare the statistical effectiveness of estimating MPB biomass by the traditional method of sediment sampling. Our analysis revealed that a very large number (> 300) of samples are necessary to accurately estimate the average MPB biomass in a natural sediments with bioturbating macrofauna (Figure 2.7). Moreover, it revealed that sediment sampling with cores might be unable to access the spatial resolutions required to capture the microscale variability of the MPB distribution, or would be an inordinately arduous task unsuited for regular assessments. This degree of microscale heterogeneity implies a systematic under-sampling in many previous field studies and invites a careful re-evaluation of sampling and measurement strategies employed in the assessment of MPB biomass (Grinham et al., 2007; Spilmont et al., 2011). With the development of robust protocols for ground-truthing MPB biomass estimations in a variety of substrates, hyperspectral imaging has the potential to become a standard method for recording the MPB distributions with sufficient spatial detail and span to reveal small-scale patterns that can be integrated into large-scale analyses of ecosystems. The possibility to easily record the surficial microscale distribution of MPB in natural sediments opens up the field of "micro-landscape ecology", which analyzes spatial patterns involved in the interplay of resources, producers

and consumers within a microbenthic region (Sandulli and Pinckney, 1999; Sundbäck and McGlathery, 2013). A suite of techniques, such as fractal geometry, patch size analysis, correlograms, etc. borrowed from landscape ecology (Cullinan and Thomas, 1992; Li, 2000) can be applied to reveal hidden patterns and causalities in the small-scale spatio-temporal structure of MPB distributions. Such analyses provide the foundation for the natural scales of variability and comparison to "emerge from the data" (Chapman et al., 2010; Levin, 1992).

However, the true advantage of hyperspectral imaging derives from non-invasive assessment of the combined information about spatial structure and functional entities (pigments) of a habitat (Figure 1.5). This makes microscale hyperspectral imaging an incisive tool for the study of ecological *processes* at the scale of the organism/habitat that underlie the development of observed spatio-temporal patterns. The non-invasive mode of hyperspectral imaging allowed us to repeatedly measure the same region of sediment in order to compile a high-resolution spatio-temporal profile of the Chl *a* dynamics in the region. The knowledge of pigment concentration at each spatial location at each time-point of a dense time-series was used to validate relevant temporal models (e.g. growth or migration) at each location of the spatial map. The fit parameters of such models marked at each pixel was used to generate "rate maps", which provide an elegant and rich representation of the dynamics of the microscale Chl *a* distribution at the surface. The inherent spatial patterns in the rate maps were indicative of the underlying ecological processes that generate the structure of MPB distributions.

The temporal dynamics of surficial Chl *a* revealed the variability over an area that is attributable to the vertical migration of the MPB, suggesting that the time of sampling MPB in the field must be carefully chosen (Chapter 2). By monitoring the surficial Chl *a* in lugworm-inhabited sediments, we proved that the growth and distribution of the MPB at the surface are intimately linked to the activity of lugworms living deeper in the sediment (Chapter 3). The spatio-temporal profiles of Chl *a* guided our experimental and modeling efforts, which led us to the conclusion that only the bioadvection associated with the burrow ventilation of lugworms is a sufficient cause for the observed fertilization of surficial MPB. Thus, we were able to establish the case for a "gardening lugworm", which promotes the fertility of the microphytobenthic garden upon which it feeds as a significant ecological control of the structure of natural MPB communities in intertidal sediments. In the case of desiccated cyanobacteria mats (Chapter 4), the spatial span and detailed resolution of hyperspectral imaging provided a synoptic view over the surface and subsurface regions of the microbial mat which allowed us to follow the dynamics of Chl *a* simultaneously in both regions. The temporal profile of Chl *a* led us to infer and estimate the speed of the rehydration-triggered vertical migration, which seems to be an adaptation of cyanobacteria to be able to thrive in desiccated environments. In our studies the ability of Hypersub measurements to be automated greatly alleviated the effort involved in recording sufficiently

dense time-series of hyperspectral images. Ultimately, it was the combination of the spatial span at the operant scales of variation and the temporal density of Chl *a* measurements from Hypersub that were crucial towards developing a conceptual understanding of the functional relationships and first-order ecological interactions that shaped the 'microphytobenthic landscape' — one of the steps necessary for a reductionist understanding of microbenthic ecology (Miller et al., 1996).

6.1.3 *Methodological features and limitations*

The quantification of surficial Chl *a* concentration in sediments was performed by the development of a new spectral index named microphytobenthic index (MPBI). Through the inclusion of a logarithmic transformation of the spectral data, MPBI accounts for the exponentially decreasing light intensity in a MPB biofilm and thereby provides a linear correlation with the Chl *a* concentration. This is in contrast to most spectral indices with simple arithmetic ratios, which hold a saturating-exponential relationship to Chl *a* (Barillé et al., 2011; Carrère et al., 2004). In order to derive an empirically useful calibration that includes the effect of the sediment substrate, the calibration of MPBI was performed against the Chl *a* content of the porewater of millimeter-thick artificial biofilms consisting of sediment grains and diatom cells instead of pure culture calibrations used for optical modeling of MPB biofilms (Kazemipour et al., 2011). Normalization against the porewater volume was used as it represents the volume within the sediment substrate occupied by MPB cells and thereby probed by the incident light. The calibrations derived for different sediment-types were found to be linear over nearly the entire range of Chl *a* concentrations found in natural MPB biofilms (Chapter 2). A universal calibration for all sediment types was not possible despite the continuum correction included in the MPBI calculation. This, along with the empirical relationship of the calibration parameters to the grain-size of the sediment, were indicative of the strong effect of light scattering by the sediment substrate (Kühl and Jørgensen, 1994). A consequence of the non-linear nature of the scattering of sediments was that the MPBI was found to be sensitive not only to the Chl *a* content of the porewater in the top millimeter, but also to the vertical distribution of Chl *a* within this depth. This is a potential drawback of the method, due to possibly confounding variations between lateral and depth distributions, but can be applied to advantage in assessing the fraction of Chl *a* that is displaced due to vertical migrations of MPB.

An important limitation of current optical methods, both fluorescent and spectroscopic, of assessing MPB biomass in sediments is that the exact probing depth cannot be easily estimated or generalized for different sediment types. This limitation arises due to the high degree of optical scattering within the sediment matrix, which bears a complex and non-linear effect on the optical path through the substrate. Since the scattering-

induced optical path variations are generally unknown, it is methodologically impossible to determine two unknown entities — the true photic depth and the concentration of absorbers within that depth — from a single physical measurement. For studies where knowledge of the photic depth is critical, separate measurements with light microsensors are recommended. Another limitation of optical methods is the inaccuracy in the absolute quantification of photopigment concentrations, which arises in fluorometry due to issues related to photochemistry of chlorophylls (Consalvey et al., 2005; Perkins et al., 2010), and in spectral imaging due to the spectral mixing of the various absorption and scattering imprints superimposed in the reflected spectrum. One implication for hyperspectral images of marine sediments is that Chl *a* is virtually indistinguishable from its degradation products through its spectral signature over the visible range, and necessitates sophisticated analyses to resolve them. The sensitivity of MPBI to the vertical distribution of Chl *a* provides an indication of the presence of active Chl *a* since this is the fraction of the chlorophyll pool that is expected to show signs of diel migration. More work is necessary to determine the impact of degradation products, which is known to be a seasonal factor in the measurement of MPB biomass (Sun et al., 1994), on using MPBI for biomass estimation. Therefore, while Hypersub provides a detailed synoptic view of the momentary distribution of Chl *a* over a region of the sediment surface, it is recommended to perform pigment extraction measurements in studies where the absolute pigment concentrations are of critical importance.

The high spectral resolution of hyperspectral measurements is amenable to the identification and quantification of multiple pigments in the scanned samples. Different pigment groups, which are usually taxonomical markers, generally have characteristic spectral signatures that are possibly mixed or superimposed in the spectrum of the light reflected from the sample. However, a large set of spectrometric techniques are available for spectral unmixing, peak resolution and end-member decomposition of similar signals of constituent pigments. Derivative analysis provides increases sensitivity in resolving nearby spectral features, but at the cost of robust quantification across samples. Additionally, the spectral span (400–900 nm) of the hyperspectral imager allows for the use of fluorescence imaging as has been demonstrated previously for microscopic measurements (Bachar et al., 2008; Kühl and Polerecky, 2008; Polerecky et al., 2009). Adaptation of the technique to field measurements are theoretically possible, if incorporated with the use of appropriate filters and illumination protocols.

In field measurements of hyperspectral reflectance, the short optical path-length between the Hypersub imager and the sediment surface obviates the need for the complex corrections for influences of the atmosphere, water-column, mixed pixels, etc. that are necessary for analyzing reflectance data obtained from airborne or spaceborne imagers. However, the imager in Hypersub was not radiometrically calibrated and therefore a spectral reference board was placed within the field-of-view to convert

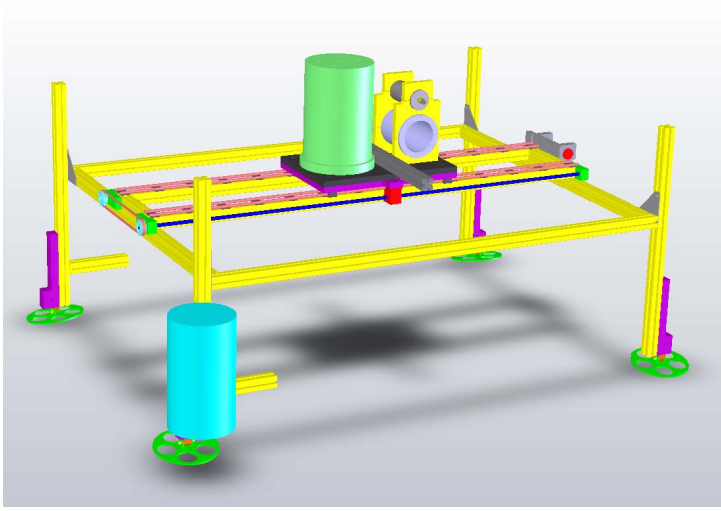

Figure 6.1: A 3D schematic of Hypersub adapted for long-term deployment as a subtidal cabled observatory.

the captured optical data into reflectance. This is a potential limitation for long-term deployments in eutrophic settings where biofouling of the spectral reference board is expected, but can be delayed by including some cleaning or anti-biofouling mechanisms for the reference board.

6.2 OUTLOOK

6.2.1 *Future adaptations*

The modular architecture of Hypersub lends itself to several adaptations that extend the range of benthic habitats that it is capable of measuring.

6.2.1.1 *Hypersub as an observatory*

The infrastructure of ocean observatories has greatly improved in recent years, with the addition of new cabled observatories such as NEPTUNEcanada and COSYNA, and plans for several more. As mentioned earlier, the scalable architecture and limited external dependencies of Hypersub allow it to be operated as the control center of a remotely-operable observatory, or as a node in larger observatory infrastructure. A prototype of Hypersub as a standalone observatory was successfully tested in Banyuls-sur-mer, France and further development is underway to construct a robust frame (Figure 6.1) that can host a variety of instruments for long-term deployment on the COSYNA network in Svalbard. A planned over-winter deployment, if successful, could provide valuable information about the insofar sparse record of subtidal phototrophs in shallow Arctic ecosystems, especially during the harsh and inaccessible Arctic winter.

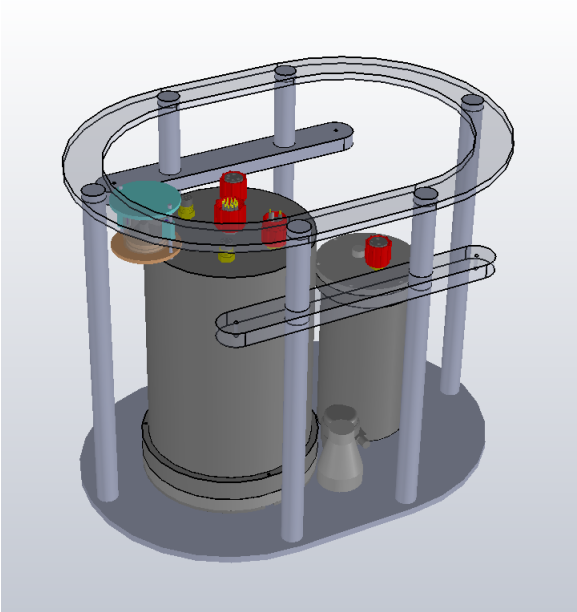

Figure 6.2: A 3D schematic of the Hypersub system adapted for operation by SCUBA divers.

6.2.1.2 *Hypersub as a surveying imager*

With the construction of a deep-sea housing, it should be possible to directly integrate Hypersub as a part of the imaging infrastructure that is common on deep-sea roving observatories or on modern marine vehicles such as ROVs and submarines. Integration of hyperspectral imaging would enhance the surveying capabilities of these vehicles for geochemical and biological parameters of interest in the deep-sea, such as algal biomass export (Boetius et al., 2013) or pigmentation of organisms in deep-sea corals and hydrothermal vents (Beatty et al., 2005). Additionally, integration with shallow-water ROVs could be used to study the rarely documented abundance and distribution of sea-ice algae, which is generally inaccessible because of the logistics of measurements under thick ice-sheets.

6.2.1.3 *Hypersub as a diving imager*

An adaptation of Hypersub for interactive operations by SCUBA divers is also planned (Figure 6.2). The aim of this adaptation is to provide maximal flexibility for hand-held operations, and thus enable the use of Hypersub as a surveying and mapping tool in shallow subtidal ecosystems, which host a variety of benthic phototrophs. This is particularly useful in areas with difficult and uneven terrain, such as on coral reefs or rocky shores with macroalgal coverage. Diver-operated hyperspectral imaging has the potential to be an incisive tool in monitoring changes in communities and structure of such habitats in response to ocean acidification.

6.2.2 *Future research*

This doctoral project has attempted to establish a method for studying the microscale distribution and dynamics of microphytobenthic communities in natural sediments, and demonstrate a few applications of the method in studies of benthic ecology. Naturally, there remains great scope for improvements in the methodology of microscale hyperspectral imaging for studying microphytobenthic communities. A particularly ripe avenue of study would be the relationship between the internal structure of sediment substrates and the emergent macroscopic spectral properties. There has been some effort in this direction (Barillé et al., 2007; Barillé et al., 2011), but the intense multiple-scattering of sediments necessitates complex optical models (Kühl and Jørgensen, 1994). A simpler alternative might be to apply macroscopic optical theories such as Kubelka-Munk formulations, which have undergone much improvement in recent years (Yang and Kruse, 2004; Yang et al., 2004; Yang and Miklavcic, 2005), which are able to include the effect of scattering and absorption in predicting the spectral properties of textured surfaces based on their internal structure. Such models developed for coastal sediments would greatly inform the current efforts in modeling the optical properties of microphytobenthic biofilms for large-scale mapping by airborne hyperspectral imagers (Combe et al., 2005; Kazemipour et al., 2012). Microscale hyperspectral imaging of sediments could be used to assess the near-field properties of *in situ* sediment reflectance under varying conditions and provide empirical input for the models oriented towards remote-sensing. This would be particularly relevant for underwater hyperspectral imaging, which could eliminate the air-water interface in the optical path and help compare the effectiveness of remote-sensing algorithms in quantifying subtidal MPB distributions. The development of such analyses and models for hyperspectral imaging, with the relevant scale-dependent corrections, could provide a seamless and scalable view of the microphytobenthic abundance in coastal sediments.

The focus of the studies presented in this thesis have been the role of various ecological processes in determining the spatio-temporal microstructure of MPB communities. As such, the spectral analysis was limited to estimating MPB biomass through quantification of the Chl *a* signal, which is only a basic descriptor of the MPB community. A range of photopigments, which serve as markers for various taxa in the composition of a MPB community, can be identified and quantified using hyperspectral imaging. Such analyses are particularly useful to analyze the spatial patterns that delineate the interaction zones of a heterogeneous microbial ecosystem, such as microbial mats or corals (Figure 1.5). Therefore, hyperspectral imaging would potentially serve as a useful tool in the study of systems with multifarious pigmented players with complex spatio-temporal interactions: coral-algal phase shifts (Barott et al., 2009), horizontally migrating mats such as black-band disease of corals (Kuta and Richardson, 2002), ocean acidification effects on reefs (Fabricius et

al., 2011), vertical migration of Arctic communities during the polar night (Berge et al., 2009).

In conclusion, microbenthic ecology and hyperspectral imaging are both extensive topics of active research, with the potential for concomitant and mutualistic development. Improvements in the field instrumentation for hyperspectral imaging will aid in the much-needed and urgent effort to compile *in situ* datasets, which could be integrated with large-scale remote sensing efforts, about global microphytobenthic distributions. This will enable empirical grounding of our understanding of the role of the under-studied secret garden of microphytobenthos, with the potential to develop global models of primary production that include the effect of ecological interactions that operate on scale of microbial habitats. The scalable analysis of structure and function that hyperspectral imaging enables in a variety of settings, such as coral reefs, estuaries, coastal wetlands and polar seas, promises to further our understanding of the processes, both natural and anthropogenic, that influence these threatened but crucial ecosystems in a rapidly changing global climate.

6.3 REFERENCES

Bachar, A., L. Polerecky, J. P. Fischer, K. Vamvakopoulos, D. de Beer, and H. M. Jonkers (2008). "Two-dimensional mapping of photopigment distribution and activity of *Chloroflexus*-like bacteria in a hypersaline microbial mat." In: *FEMS microbiology ecology* 65.3, pp. 434–48. DOI: 10.1111/j.1574-6941.2008.00534.x (cited on page 140).

Barillé, L., V. Méléder, and J. Combe (2007). "Comparative analysis of field and laboratory spectral reflectances of benthic diatoms with a modified Gaussian model approach." In: *Journal of Experimental Marine Biology and Ecology* 343.2, pp. 197–209. DOI: 10.1016/j.jembe.2006.11.013 (cited on page 143).

Barillé, L., J.-L. Mouget, V. Méléder, P. Rosa, and B. Jesus (2011). "Spectral response of benthic diatoms with different sediment backgrounds." In: *Remote sensing of Environment* 115.4, pp. 1034–1042. DOI: 10.1016/j.rse.2010.12.008 (cited on pages 139, 143).

Barott, K., J. Smith, E. Dinsdale, and M. Hatay (2009). "Hyperspectral and physiological analyses of coral-algal interactions." In: *PLoS One* 4.11, e8043. DOI: 10.1371/journal.pone.0008043 (cited on page 143).

Beatty, J. T., J. Overmann, M. T. Lince, A. K. Manske, A. S. Lang, R. E. Blankenship, C. L. Van Dover, T. A. Martinson, and F. G. Plumley (2005). "An obligately photosynthetic bacterial anaerobe from a deep-sea hydrothermal vent." In: *Proceedings of the National Academy of Sciences* 102.26, pp. 9306–9310. DOI: 10.1073/pnas.0503674102 (cited on page 142).

Berge, J., F. Cottier, K. S. Last, O. Varpe, E. Leu, J. Soreide, K. Eiane, S. Falk-Petersen, K. Willis, H. Nygard, and et al. (2009). "Diel vertical migration of Arctic zooplankton during the polar night." In: *Biology Letters* 5.1, pp. 69–72. DOI: 10.1098/rsbl.2008.0484 (cited on page 144).

Boetius, A., S. Albrecht, K. Bakker, C. Bienhold, J. Felden, M. Fernández-Méndez, S. Hendricks, C. Katlein, C. Lalande, T. Krumpen, M. Nicolaus, I. Peeken, B. Rabe, A. Rogacheva, E. Rybakova, R. Somavilla, F. Wenzhöfer, and R. P. A.-3.-S. S. Party (2013). "Export of Algal Biomass from the Melting Arctic Sea Ice." In: *Science* 339.6126, pp. 1430–1432. DOI: 10.1126/science.1231346 (cited on page 142).

Boudreau, B. P. and B. B. Jørgensen (2001). *The Benthic Boundary Layer: Transport Processes and Biogeochemistry*. Oxford University Press (cited on page 135).

Cahoon, L. B. (1999). "The role of benthic microalgae in neritic ecosystems." In: *Oceanography and Marine Biology, An Annual Review*. Ed. by A. Ansell, R. Gibson, and M. Barnes. Vol. 37. Aberdeen University Press, pp. 47–86 (cited on page 135).

Carrère, V., N. Spilmont, and D. Davoult (2004). "Comparison of simple techniques for estimating Chlorophyll *a* concentration in the intertidal zone using high spectral-resolution field-spectrometer data." In: *Marine Ecology Progress Series* 274, pp. 31–40. DOI: 10.3354/meps274031 (cited on page 139).

Chapman, M., T. Tolhurst, R. Murphy, and A. Underwood (2010). "Complex and inconsistent patterns of variation in benthos, micro-algae and sediment over multiple spatial scales." In: *Marine Ecology Progress Series* 398, pp. 33–47. DOI: 10.3354/meps08328 (cited on pages 135, 138).

Combe, J. P., P. Launeau, V. Carrere, D. Despan, V. Meleder, L. Barille, and C. Sotin (2005). "Mapping microphytobenthos biomass by non-linear inversion of visible-infrared hyperspectral images." In: *Remote sensing of Environment* 98.4, pp. 371–387. DOI: 10.1016/j.rse.2005.07.010 (cited on page 143).

Consalvey, M., R. G. Perkins, and D. M. Paterson (2005). "PAM fluorescence: a beginners guide for benthic diatomists." In: *Diatom Research* 20.1, pp. 1–22. DOI: 10.1080/0269249X.2005.9705619 (cited on page 140).

Cullinan, V. I. and J. M. Thomas (1992). "A comparison of quantitative methods for examining landscape pattern and scale." In: *Landscape Ecology* 7.3, pp. 211–227 (cited on page 138).

Fabricius, K. E., C. Langdon, S. Uthicke, C. Humphrey, S. Noonan, G. De'ath, R. Okazaki, N. Muehllehner, M. S. Glas, and J. M. Lough (2011). "Losers and winners in coral reefs acclimatized to elevated carbon dioxide concentrations." In: *Nature Clim. Change* 1.3, pp. 165–169 (cited on page 143).

Glud, R. N. (2006). "Microscale techniques to measure photosynthesis: A mini-review." In: *Functioning of microphytobenthos in estuaries: Proceedings of the Colloquium, Amsterdam, 21-23 August 2003*. Ed. by J. C. Kromkamp. Vol. 103. Royal Netherlands Academy of Arts and Sciences, pp. 123–140 (cited on page 135).

Grinham, A. R., T. J. Carruthers, P. L. Fisher, J. W. Udy, and W. C. Dennison (2007). "Accurately measuring the abundance of benthic microalgae in spatially variable habitats." In: *Limnology and Oceanography: Methods* 5, pp. 119–125. DOI: 10.4319/lom.2007.5.119 (cited on page 137).

Kaufmann, H., S. Förster, H. Wulf, K. Segl, L. Guanter, M. Bochow, U. Heiden, A. Müller, W. Heldens, T. Schneiderhan, P. Leitão, S. van der Linden, P. Hostert, J. Hill, H. Buddenbaum, W. Mauser, T. Hank, H. Krasemann, R. Röttgers, N. Oppelt, and B. Heim (2012). *Science Plan of the Environmental Mapping and Analysis Program (EnMAP)*. Tech. rep. Potsdam: Deutsches GeoForschungsZentrum GFZ (cited on page 136).

Kazemipour, F., P. Launeau, and V. Méléder (2012). "Microphytobenthos biomass mapping using the optical model of diatom biofilms: Application to hyperspectral images of Bourgneuf Bay." In: *Remote Sensing of Environment* 127, pp. 1–13. DOI: 10.1016/j.rse.2012.08.016 (cited on page 143).

Kazemipour, F., V. Méléder, and P. Launeau (2011). "Optical properties of microphytobenthic biofilms (MPBOM): Biomass retrieval implication." In: *Journal of Quantitative Spectroscopy and Radiative Transfer* 112.1, pp. 131–142. DOI: 10.1016/j.jqsrt.2010.08.029 (cited on page 139).

Kühl, M. and B. B. Jørgensen (1994). "The light field of microbenthic communities: radiance distribution and microscale optics of sandy coastal sediments." In: *Limnology and Oceanography* 39.6, pp. 1368–1398. DOI: 10.4319/lo.1994.39.6.1368 (cited on pages 139, 143).

Kühl, M. and L. Polerecky (2008). "Functional and structural imaging of phototrophic microbial communities and symbioses." In: *Aquatic Microbial Ecology* 53, pp. 99–118. DOI: doi:10.3354/ame01224 (cited on page 140).

Kuta, K. and L. Richardson (2002). "Ecological aspects of black band disease of corals: relationships between disease incidence and environmental factors." English. In: *Coral Reefs* 21.4, pp. 393–398. DOI: 10.1007/s00338-002-0261-6 (cited on page 143).

Levin, S. (1992). "The problem of pattern and scale in ecology: the Robert H. MacArthur award lecture." In: *Ecology* 73.6, pp. 1943–1967. DOI: 10.2307/1941447 (cited on pages 135, 138).

Li, B.-L. (2000). "Fractal geometry applications in description and analysis of patch patterns and patch dynamics." In: *Ecological Modelling* 132.1-2, pp. 33–50. DOI: 10.1016/S0304-3800(00)00303-3 (cited on page 138).

MacIntyre, H., R. Geider, and D. Miller (1996). "Microphytobenthos: The ecological role of the "secret garden" of unvegetated, shallow-water marine habitats. I. Distribution, abundance and primary production." In: *Estuaries and Coasts* 19.2, pp. 186–201. DOI: 10.2307/1352224 (cited on page 135).

Méléder, V., P. Launeau, L. Barillé, and J.-P. Combe (2010). "Hyperspectral imaging for mapping microphytobenthos in coastal areas." In: *Geomatic Solutions For Coastal Environments*. Ed. by M. Maanan and M. Robin. Nova Science Publishers Inc., pp. 71–139 (cited on page 135).

Miller, D., R. Geider, and H. MacIntyre (1996). "Microphytobenthos: the ecological role of the "secret garden" of unvegetated, shallow-water marine habitats. II. Role in sediment stability and shallow-water food webs." In: *Estuaries and Coasts* 19.2A, pp. 202–212. DOI: 10.2307/1352225 (cited on pages 135, 139).

Perkins, R., J. Kromkamp, J. Serôdio, J. Lavaud, B. Jesus, J. Mouget, S. Lefebvre, and R. Forster (2010). "The application of variable chlorophyll fluorescence to microphytobenthic biofilms." English. In: *Chlorophyll a Fluorescence in Aquatic Sciences: Methods and Applications*. Ed. by D. J. Suggett, O. Prášil, and M. A. Borowitzka. Vol. 4. Developments in Applied Phycology. Springer Netherlands, pp. 237–275. DOI: 10.1007/978-90-481-9268-7_12 (cited on page 140).

Polerecky, L., A. Bissett, M. Al-Najjar, P. Färber, H. Osmers, P. A. Suci, P. Stoodley, and D. de Beer (2009). "Modular spectral imaging (MOSI) system for discrimination of pigments in cells and microbial communities." In: *Applied and Environmental Microbiology* 75.3, pp. 1–9. DOI: 10.1128/AEM.00819-08 (cited on pages 136, 140).

Revsbech, N. P. and B. B. Jørgensen (1986). "Microelectrodes: their use in microbial ecology." In: *Advances in Microbial Ecology* 9, pp. 293–352. DOI: 10.1007/978-1-4757-0611-6_7 (cited on page 135).

Sandulli, R. and J. Pinckney (1999). "Patch sizes and spatial patterns of meiobenthic copepods and benthic microalgae in sandy sediments: a microscale approach." In: *Journal of Sea Research* 41.3, pp. 179–187. DOI: 10.1016/S1385-1101(98)00048-3 (cited on page 138).

Spilmont, N., L. Seuront, T. Meziane, and D. T. Welsh (2011). "There's more to the picture than meets the eye: Sampling microphytobenthos in a heterogeneous environment." In: *Estuarine, Coastal and Shelf Science* 95.4, pp. 470–476. DOI: 10.1016/j.ecss.2011.10.021 (cited on pages 135, 137).

Sun, M.-Y., R. Aller, and C. Lee (1994). "Spatial and temporal distributions of sedimentary chloropigments as indicators of benthic processes in Long Island Sound." In: *Journal of Marine Research* 52, pp. 149–176. DOI: 10.1357/0022240943076768 (cited on page 140).

Sundbäck, K. and K. McGlathery (2013). "Interactions between benthic macroalgal and microalgal mats." In: *Interactions Between Macro- and Microorganisms in Marine Sediments*. American Geophysical Union, pp. 7–29. DOI: 10.1029/CE060p0007 (cited on page 138).

Underwood, A. J., M. G. Chapman, and S. D. Connell (2000). "Observations in ecology: you can't make progress on processes without understanding the patterns." In: *Journal of Experimental Marine Biology and Ecology* 250.1-2, pp. 97–115. DOI: 10.1016/S0022-0981(00)00181-7 (cited on page 135).

Yang, L. and B. Kruse (2004). "Revised Kubelka—Munk theory. I. Theory and application." In: *Journal of the Optical Society of America A* 21.10, p. 1933. DOI: 10.1364/JOSAA.21.001933 (cited on page 143).

Yang, L., B. Kruse, and S. J. Miklavcic (2004). "Revised Kubelka—Munk theory. II. Unified framework for homogeneous and inhomogeneous optical media." In: *Journal of the Optical Society of America A* 21.10, p. 1942. DOI: 10.1364/JOSAA.21.001942 (cited on page 143).

Yang, L. and S. J. Miklavcic (2005). "Revised Kubelka—Munk theory. III. A general theory of light propagation in scattering and absorptive media." In: *Journal of the Optical Society of America A* 22.9, p. 1866. DOI: 10.1364/JOSAA.22.001866 (cited on page 143).

Part IV

APPENDIX

A

SPECTRAL IMAGING

Electromagnetic radiation is a form of energy that propagates through space, and the energy is characterized by its frequency or wavelength. The region of the electromagnetic spectrum that the human eye is responsive to is what we generally call the light spectrum, extending from the ultraviolet to the infrared. The light reflected by, scattered from, transmitted through, or emitted by an object contains information about the object through characteristic signatures in the spectrum. These signatures inform us about the physical or chemical properties of the object, which provides us with vital clues about its function, composition, chemical identity or physical state.

To understand the details of spectral imaging, it is useful to consider the two components of optical imaging and radiative spectroscopy separately.

A.1 OPTICAL IMAGING

Optical imaging involves capturing light coming from an object and recording spatial and temporal information to create a consistent representation of the features of the object, with respect to scale, configuration or shape. This is an effort with a long history that has used, tested and developed various media for capturing light. The most modern technique is to use digital cameras that have electronic light sensors. Imaging systems are extremely varied in design and function, however a few parameters can be commonly used in characterizing different imaging systems which have an impact on quality and quantity of information in the captured images:

Modern electronic light sensors are generally of two kinds: a charge-coupled-device (CCD) or a complementary metal-oxide semiconductor (CMOS) array. They enable rapid recording of images by converting the captured light field into an electronic signal.

SPATIAL RESOLUTION determines the closest distinguishable features in the object. It depends primarily on numerical aperture of the imaging lens, wavelength, magnification and pixel size of the array detector. The latter two are the constraints upon the spatial frequency that can be sampled to achieve full resolution.

FOCAL RANGE is the possible range of distances of the objective lens from the object. The state of full focus is an instrumental feature of acquiring images, although it is not a fundamental property of the system. This follows from the principles of refractive optics, and determines the clarity or sharpness of the focused image depending on the configuration of the internals of the imaging system.

SIGNAL LIMIT is the lowest detectable signal level that can be imaged. This depends on the quantum efficiency of the sensor, the quality and

numerical aperture of the objective. This becomes a critical parameter in ultra-low light level imaging necessitating the use of electron-multiplying CCDs, or in a highly time-constrained measurement window involved in fluorescent quenching or time-gated imaging.

DYNAMIC RANGE refers to the range of intensity levels that the system can capture or reproduce. It is essentially the ratio of the maximum number of measurable electrons at each pixel and the lowest detectable signal. This ratio is the maximum capable range, but the system might be configured to lower values if the light intensity is low and does not saturate the pixel with electrons.

DEPTH OF FOCUS is a spatial measure along the imaging axis of the region around the focal plane, where the image can yet be considered to be 'in focus'. It is characterized by the confocal volume around the plane of focus, and is controlled by the size of the effective aperture of the imaging lens, where the smaller aperture produces a greater depth of focus.

FIELD OF VIEW (FOV) is the maximum area that can be imaged by the combination of sensor and optical objectives, and is usually determined as a solid angle (steradians) or converted to a spatial area.

EXPOSURE TIME is the amount of time the shutter exposes the sensor to the incident light. For ambient light situations this relates closely with the dynamic range and the quantum efficiency of the sensor, and must be optimized to avoid bleaching or over-exposure in the image. It is of critical importance in time-gated imaging and there are now devices available that provide up to picoseconds resolution.

A.2 RADIATIVE SPECTROSCOPY

The science of radiative spectroscopy, which deals with acquisition and analysis of spectra of electromagnetic radiation such as light, is an old and highly instructive science[1]. While spectroscopy is a term that finds very diverse use, the focus here will be on optical spectroscopy, in and around the visible range of light. In the domain of optics, a spectrum is a collection of light intensities at various wavelengths. The spectrum is a direct measure of the electronic energy structure of the probed object. This is because the structure of molecules and atoms have specific and discrete energy levels between which electrons can transition. This allows molecules to absorb or emit light energy. Since the electronic band structure is an intrinsic property of any molecule, the interactions of light with its band structure leaves precise 'fingerprints' in the spectrum.

1 I. Newton (1671). "A Letter of Mr. Isaac Newton, Professor of the Mathematicks in the University of Cambridge; Containing His New Theory about Light and Colors: Sent by the Author to the Publisher from Cambridge, Febr. 6. 1671/72; In Order to be Communicated to the R. Society." English. In: *Philosophical Transactions (1665-1678)* 6, pages

The interaction of light with matter often induces one or more of the photonic processes of absorption, emission or fluorescence, which are different forms of electronic transitions induced by the interaction. Absorption occurs due to the electron capturing light energy and transitioning to higher energy states, while emission is a transition in the reverse direction. Since the energy difference between the states is constant, the spectral response is centered strongly around a specific wavelength; that is it always occurs around the same wavelength for the same transitions. Near-infrared (NIR) light is often used for measuring absorption through the vibrational modes of molecules. These vibrational modes are characteristic of the interatomic bonds and the NIR absorption renders an informative imprint of the molecular structure. Fluorescence is the emission of light energy by an electron by transitioning through a meta-stable state, which causes the emitted light to be at a different wavelength than the excitation light. Ultra-violet (UV) light has shorter wavelengths and higher energy than infrared (IR) light. This means that UV light can provide higher excitation energy for electron transitions for fluorescence. The fluorescent object or molecule is itself the source of light, and often there is a direct functional relationship between the concentration of fluorescent molecules and the fluorescent intensity. At low concentrations, the relationship is linear which allows us to make quantitative analyses. Fluorescence detection requires a critical discrimination between the strong excitation light and the usually weaker emitted light, leading to the prolific use of color filters and dichroic mirrors.

Characterizing a spectrum essentially involves dispersing the light into its constituent wavelength (or color) components, and measuring the intensity of each of those components. There are different ways of dispersing the light, and nearly every one of them finds use in the various systems available. The quality of a spectral measurement is dependent on the following:

SPECTRAL RESOLUTION is determined by the bandwidth and sampling density of the channels of the spectrometer and is a measure of the closest wavelengths that can be distinguished and measured. The narrower the spectral bandwidth, the finer the absorption feature the spectrometer can measure accurately, if enough spectral samples are recorded.

SPECTRAL RANGE is the range of wavelengths that can be accurately measured. It is important that this range encompasses enough diagnostic spectral absorptions to solve the desired problem. The general ranges of wavelengths of interest are UV, Visible, NIR and far infrared.

DYNAMIC RANGE and the lowest detectable signal measure the number of distinguishable intensity levels in a given measurement, and determine the signal-to-noise ratio in measured spectra.

SHAPE of the spectrum affects the other parameters because of the range of wavelengths over which the energy is distributed. This is why

laser light has a sharp, clear line in its spectrum, as compared to a broadband spectrum which has energy distributed over a large spectral range.

The various spectrometric systems differ mainly in their spectral resolution and range. Typically the spectrum is split into several 'bands', each of which is then measured. Measurement systems range from those that capture a single band to those systems that simultaneously measure hundreds of bands. The spectrometers that were able to capture several bands distributed across the spectral range were termed multi-spectral systems. However, the development of the diffraction grating as a precise, yet compact, dispersion element has led to the emergence of hyperspectral systems that measure several hundred contiguous bands across the spectrum, effectively covering more than the entire visual span.

A.3 HYPERSPECTRAL IMAGING

Hyperspectral refers to spectroscopic systems that capture the spectral information in contiguous bands over a certain range, and therefore provide a much denser sampling of the optical spectrum at each imaged location of the target. Hyperspectral images, sometimes referred to as hypercubes, are rich datasets that provide a greater scope for spectral analysis than multispectral datasets. The speed and mode of capturing a hyperspectral images depends on the dimensionality of the imaging sensor. If the capture sensor is only a two-dimensional array, then the entire spectral image cannot be captured in one shot. One dimension of the array can be mapped spatially, and the spectrum captured along the other. Use of a lower dimensional detector, such as a line detector or a point detector, implies a higher acquisition time for the same imaged area. This instrumental trade-off in data acquisition between the spectrum and the image intensity leads to different paradigms of hyperspectral imaging:

WAVELENGTH-SCAN methods capture the intensity for one wavelength (or band) at a time. Using a set of narrow-band color filters is suitable for multi-spectral imaging, but not for the demands of hyperspectral imaging. However, use of a liquid-crystal tunable filter (LCTF) or acousto-optic tunable filter (AOTF) allows one to tune the passband of the filter and thus variably pass different wavelengths through. These filters capture images one wavelength at a time, with a flexibility of the choice of the wavelengths. However, the spectral resolution and range depends on the capabilities of the particular set of filters used.

SPATIAL-SCAN methods measure the entire spectrum of a region of the image at a time. The dispersive element in such systems is usually a prism or a diffraction grating. For an imaging system, only one line of the object, that is, $I(x, \lambda)$ is recorded in each acquisition run. Repeated acquisitions along the y-axis produces a hypercube. This

method of capture provides a high spectral resolution, with a tunable spatial resolution. A disadvantage could be that a scanning mechanism is always necessary to image an area, but this paradigm provides access to scales within micrometers by imaging through a microscope.

TIME-SCAN methods measure a set of images which form a superposition of spectral and spatial information. This implies that the data has to be transformed in order to arrive at the spectral image. For example, using Fourier spectroscopy one can use interferometers without any filters to arrive at the spectral information, by applying a Fourier transform on the measured interferogram. This method, like the spatial scan, also has the advantage that the intensity at every measured wavelength is available throughout the measurement. The disadvantages are that a full spectrum has to be recorded always to perform an effective Fourier transform, and also that interferometers need fairly intricate optical alignment.

While there are also methods that achieve a compromise or synthesis of these various paradigms, it is significant that the *systemic speed* of the measurement is essentially limited by the number of detector elements in the system that collect information at any given time. This speed along with the quality of the optical adjustment and spectral signal determines the overall quality of the hyperspectral image.